ERRATA

ABSTRACT

Line 11 - Correct '28.5%' to '28.5% of column area'

CHAPTER 1

Page 5, line 2 - Correct '8cm' to '8cm in width'

CHAPTER 2

Page 30, equation (19) - ϕ_1 = Fractional free area of plate

Page 54 - Add $Re = \rho_L v d_B / \eta$ as equation (62a)

Page 54 - Add $v_B = 2\dot{V}_g / A_H$ as equation (62b)

Page 64, line 6, Correct 'strem' to 'stream'

Page 69, line 11, Correct 'measurments' to 'measurements'

Page 73, line 14, Correct 'I_o/I' to '$ln(I_o/I)$'

CHAPTER 3

Page 78, line 14, Correct 'chracterize' to 'characterize'

Page 80 - Correct 'crosssectional area' to 'Area available for liquid'

Page 86 - Correct '$t_p = L/u$' to '$t_p = \epsilon_L L/u$'

Page 103, line 2, Correct 'to resort' to 'to resort to'

CHAPTER 5

Page 172, line 3 , Correct 'This due' to 'This is due'

FOAMING IN DISTILLATION AND ABSORPTION COLUMNS

BY

INI JOHNSON URUA

B.Sc(Ife), M.Sc(Lond.), D.I.C

Department of Chemical Engineering and Chemical Technology

Imperial College of Science and Technology

London SW7

Thesis submitted in fulfilment of the requirements for the award of the degree of Doctor of Philosophy (Ph.D) of the University of London.

JANUARY 1988

ACKNOWLEDGEMENT

I wish to express my sincere gratitude to my supervisor Dr. M. C. G. del Cerro and also to Prof. G. F. Hewitt for guidance, advice and help throughout the period of study.

My sincere thanks also to the Technical Staff of the department without whose support the experimental work would not have gone smoothly. Many thanks to the departmental Librarians who had been extremely helpful and very friendly.

The encouragement and support of my colleagues, Ceasar Savastano, David Boey, Ania Grobicski, Zaki El Hassan, Maria, Louise, and a host of others is greatly acknowledged.

I wish also to thank the Federal Government of Nigeria for some financial support during the research work.

Finally, I wish to express my sincere gratitude to my fiancee, Rita, for all the help and understanding throughout the research work.

DEDICATION

Dedicated to my niece Miss Nsikak Ekanem, my parents and to the memory of my late uncle Mr. Esenubong Obot.

REFLECTIONS

That Which is Easy is

Not Worth The

Trouble

CONTENTS

ABSTRACT

Experimental and theoretical studies of the flow behaviour of foam and/or froth on plates and in downcomers of a sieve plate column have been carried out. Experimental studies consisted of measurements of liquid residence time in the downcomer, measurements of liquid fraction and Sauter mean diameter of bubbles on the plate and in the downcomer and measurement of dry and wet pressure drops on the plate. Three plates with the same free area of 11% of the total active area of the plate, hole and pitch sizes of 3.5mm, 4.75mm, 6.0mm and 10.0mm, 13.0mm, 16.0mm respectively were studied. Two downcomer sizes representing 23.1% and 28.5% were investigated.

Liquid fraction measurements were carried out using the Gamma ray absorption technique. Sauter mean diameter measurements were carried out using the light transmission technique. A tracer injection technique was employed to determine liquid residence times in the downcomer.

Analysis of the results of these measurements show that downcomer limitations due to flooding (effect of foams) are pronounced when operating in the frothing or mixed froth regime of plate operation. Analysis of liquid residence time data reveals that the recommended residence time of liquid in the downcomer is not adequate for complete gas/vapour disengagement for foaming systems.

Plate pressure drop measurements and experimentally obtained height of clear liquid in the downcomer are consistent with recommended values.

Theoretical equations for, residence time distribution in the downcomer, prediction of foam/froth heights in the downcomer and simulation of froth profile/behaviour on the plate have been proposed. The residence time distribution model proposed shows that liquid is not in plug flow in the downcomer but rather follows the dispersion model for all the systems studied. Excellent agreement between experimental information and theoretical descriptions developed here have been demonstrated for the prediction of foam/froth heights in the downcomer and simulation of froth properties/profiles on the plate.

CHAPTER 1

INTRODUCTION

Distillation and absorption operations are amongst the most widely used separation techniques in the chemical and process industries. The general principles governing these operations are well documented in the literature[65].

Most distillation and absorption operations are usually carried out with the use of either packed or plate columns. Generally, plate columns are prefered, and widely used in large scale operations, as against packed columns. This is primarily due to the fact that large throughputs can be handled easily and also because they have a wider operating range.

Plate columns are classified into two broad classes, namely those which operate with dual flow of liquid and gas, and those which are fitted with downcomers. The dual flow plate systems are typified by pure countercurrent flow of liquid and gas on the plate while plate systems fitted with downcomers are characterized by crossflow of liquid and gas on the plate. Here, liquid is delivered from one plate to the other with the aid of downcomers. Bubblecap, sieve and valve plates are good examples of the crossflow plates while turbogrid plates are typical examples of the dual flow plates. In most industrial applications, the crossflow plates are

often used in preference to the dual flow plates because of separation efficiency advantages and also because they have a wider operating range. The effective and safe operation of crossflow plates depends on the specifications of the column with respect to plate area and characteristics. It also depends on downcomer dimensions and characteristics. Distillation, absorption and other forms of separation, normally conducted in plate columns employing crossflow plates, are often based on a specified degree of separation and hence, on proper operation of any column used.

The capacity and separation efficiency of plate columns with crossflow of liquid and gas are always limited by a hydrodynamic phenomenon known as flooding. There exits two types of flooding namely, entrainment and downcomer flooding. Entrainment flooding occurs when the gas rate is very high, so that excessive liquid is carried from one plate to the other by the gas. This has been widely studied, and useful data abound in the literature[65].

Downcomer flooding is closely associated with the hydraulic conditions on the plate and in the downcomer, and also on the foamability of the liquid used. This phenomenon is usually associated with the level of froth in the downcomer and, for foaming systems, the conditions are usually very adverse, whereby, the entire downcomer volume may be completely filled by the foam or, in more general terms, with a gas-liquid mixture. In most industrial applications, the problem of foaming is usually solved by the introduction of de-foamers to depress

the amount of foam generated, or use of anti-foaming agents to prevent the formation of foam. This approach does not in general terms give satisfactory results as it requires firstly large amounts of defoamers or anti foaming agents to arrest the situation . Secondly, it requires extra separation equipment to remove the de-foamer or anti-foaming agent. These factors may inhibit economical operation. Also the eventual contamination of the final product can be closely associated with the use of these chemicals. In most distillation and absorption processes, the provision of large interfacial areas for mass transfer is usually associated with the attainment of a high degree of separation. Hence, the operation of most columns is conducted in the foaming or frothing regime of plate operation. Much as the provision of large interfacial area is recognised as the basis for a high degree of separation, the generation of unwanted foams poses a difficult problem to the process engineer, as this leads to complications in the separation process undertaken.

Current design practice is inadequate. This is because, traditionally, most columns are designed on the assumption of a foaming system with high foaming factors†. Undoubtedly, these columns are usually oversized with gross consequences in capital cost. Where foaming factors are not used, and presently, where raw materials for separation may be of varied source and quality, the column may be undersized thereby leading to

† *See Chapter 2, Section 2.4*

high running cost as the shut down frequency of such units may be high.

This work seeks to find solutions to the problem of downcomer flooding with a view to recommending new tecniques for an economical design of plate columns. The studies undertaken is reported under two broad classes, namely, experimental and theoretical studies. In the experimental work, the behaviour of gas-liquid mixtures in the downcomer was studied for foaming and non-foaming systems with sieve plates of different hole sizes and also with different downcomer areas. It was also necessary to investigate the behaviour of the gas-liquid dispersion on the plate to aid the complete characterisation of the system under study. Since one of the problems associated with downcomer flooding is the liquid residence time in the downcomer, it was necessary to investigate this experimentally. The characterisation of the gas-liquid dispersion in the downcomer and on the plate is based primarily on the measurement of dispersion densities and Sauter mean diameters along the entire height of the dispersion. Dispersion density measurements were carried out using the gamma ray absorption technique while Sauter mean diameters were determined using the light transmission technique. The foaming systems studied are n-pentanol in water (1.3% vol. n-pentanol) and n-butanol in water (3% vol. n-butanol) with air as the gaseous phase. The non-foaming system is air-water. Three plates with the same free area (11%) were studied. The major difference between these plates is in the hole diameter and hole pitch. Plates with hole diameters of 3.5mm,

4.75mm, 6.0mm, and hole pitch of 10mm, 13mm, 16mm, respectively were studied. Two downcomer sizes, $6cm$ and $8cm$ representing 23.1% and 28.5% of total column area respectively were studied.

The theoretical work focusses mainly on modelling of the downcomer and froth behaviour on the plate. Also some theoretical work based on fitting theoretical models of residence time distributions in the downcomer is carried out. These are discussed in chapter 3 .

A survey of literature on foams, design and operation of sieve plates and measurements is given in chapter 2. In chapter 4, the experimental work carried out in this study is outlined and discussed. The general results obtained from the experimental and theoretical work are presented and discussed in chapter 5.

CHAPTER 2

LITERATURE SURVEY

2.0 Introduction

In this chapter, a survey of the literature relevant to the scope of the work reported in this thesis is presented and discussed. In Section 2.1, general concepts on foams are presented . The main thrust here, is focussed on current methods used for the prevention and breakage of foams. Section 2.2 examines the dependence of formation and flow of foams on the physical properties of the liquid used in view of its importance in the design and operation of separation columns. Theoretical models proposed to date to describe the formation and flow of foams are presented in Section 2.3. In Section 2.4 the extensive literature available on the design of sieve tray columns is reviewed, with special emphasis on the design of downcomers. Section 2.5 deals with the different regimes of fluid flow observed on sieve plate. The material covered in this section, as it shall be seen later, is necessary so as to provide a better understanding of the phenomenon of foaming in distillation and absorption columns. Since the flow regime is controlled mainly by the formation and flow of bubbles and/or liquid drops on the plate, the mechanisms of bubble formation on sieve plates are examined and discussed in section 2.6. In Section 2.7, a review of literature on the analysis of residence

time in downcomers, a critical parameter in determining the performance of columns and also envisaged as a crucial factor in the ability of the downcomer to cope with foams is presented. Since this is one of the areas of study undertaken, the literature presented will give a good overview of the approach used in determining downcomer residence time from experimental data.

2.1 General Concepts on Foams

Foams are examples of disperse systems which are usually classified according to their constituents. According to this classification, foams are gases dispersed in liquids. Theoretical aspects of foams covered in the literature usually revolves around the following

(a) Theory of thin films

(b) Foam drainage

(c) Foam Collapse

These concepts are properly documented in standard texts[3] and hence, will not be discussed further.

2.1.1 Foam Prevention Methods

Since one of the aims of the present work lies in finding alternative means of coping with foams in separation columns, a brief survey of traditional methods for prevention or elimination of foam is presented and discussed here.

Chemical Methods

Chemical methods of breaking foams involve the use of chemical defoamers or anti-foaming agents. Chemicals that expedite the disintegration or destruction of foams, when they are added to a gas-liquid dispersion, are called defoamers. Commercial defoamers normally cause rapid disintegration of the foam to which they are added, and, are usually added in relatively small amounts often in parts per million. Chemical defoamers fall into two categories, those which are soluble in the liquid phase of the foam and those which are insoluble. Soluble agents are similar to aqueous surfactants; they may be the very agents that under other conditions will promote foams. Hence, the concentration range in which they are effective is critical. This fact obviously restricts their use in most commercial units. Insoluble defoamers usually combine the characteristics of low volatility, ease of dispersion, strong spreading power, surface activity, as well as their orientation at the interface. Low volatility prevents the stripping of the defoamer before it becomes effective, while dispersibility and spreading power account for the effectiveness of small quantities of the material used. Much of the function of defoamers lies in their ability to concentrate in the thin film regions of the foam, and thus altering the nature of the films in the direction of reduced stability. The general disadvantage of defoamers is basically that they constitute an addition of a contaminant to the process stream, and subsequently to the product stream. They are also relatively expensive to use and recycle.

Certain specific agents which prevent the formation of foams on addition to the process stream are known as anti-foaming agents. Chemically, they are in the same class as defoamers, but may differ in composition and use. Anti-foaming agents generally act against the various factors which promote foam stability. Since the capacity of modern plants is usually very large, the addition of even a few parts per million of the anti-foaming agent becomes very expensive. Futhermore, the products must pass through many other processing units before reaching their final destination, hence, problems in later stages of production or processing may be encountered due to the pressence of these chemicals in the flow stream. For the reasons given above, it would be better (*if feasible*) to design or modify the hardware , either to handle the foam or prevent its formation, rather than to resort to the use of chemical methods.

Physical Methods

Physical methods of breaking or preventing the formation of foams include: **Thermal methods, Electrical methods, Mechanical methods and Acoustic vibrations.**

Mechanical Methods

These involve the use of mechanical barriers to aid foam destruction. Static or rotating bars are often used with variable success to destroy or control the foam level. In distillation and/or absorption columns,

this approach leads to an increase in pressure drop and therefore, to an increase in pump and/or compressor duty. As a result, the overall operating cost of the total operation is increased. Also, a shift in the pressure drop of the system leads to a shift in the hydrodynamic behaviour of the fluid stream processed, and subsequently of the separation efficiency of the column.

Thermal Methods

A hot surface in contact with, or near, a foam usually destroys it. Foam breaking results from evaporation and changes in the surface properties of the foam. For distillation and absorption processes/operations, the degree of separation is based on the degree of approach to equilibrium, which is highly temperature dependent. However, an increase in temperature, though it might break foams, will invariably bring about a marked decrease in separation efficiency of the column and consequently an increase in separation and processing cost.

Electrical Methods

Although there is evidence that an electric field will weaken or destroy foams[65], the underlying mechanisms are poorly understood. The introduction of an electric field may lead to the disintegration or decomposition of desired components into other forms. This is indeed a disadvantage in situations where sensitive materials are being separated.

Acoustic Vibrations

High frequency impulses are found to break the froth generated in coal flotation, and high frequency air pulses are used to control the foam generated in sugar syrup evaporators[65]. Distillation and absorption columns are usually very tall and mechanically designed to withstand specified mechanical perturbations. The introduction of extra vibrations may undermine the safety of such equipment and consequently disrupt smooth operation.

Summary

In this section, the mode of formation (*see reference 3*) of foams and ways of preventing or destroying them have been examined. It is clear from here that an alternative means of coping with the problem of foaming in process units is desirable. The ability of foams to form depends basically on the stability of the thin films separating bubbles, and hence, on the pysical properties of the liquid used. The next section examines the effect of physical properties on the formation and flow of foams clearly with special emphasis on work done on distillation and absorption columns.

2.2 Foams and Fluid Physical Properties

In any mass transfer operation, the primary objective is the provision of large interfacial areas for transfer of desired components of a mixture. The nature and extent of this interfacial area is dependent on the stability of liquid films in between bubbles and/or drops formed. This stability, in turn, depends on the surface tension difference between that on the film and that existing in the bulk liquid. In mass transfer operations such as distillation, a temperature gradient is always associated with a concentration gradient. Both of these gradients affect the surface tension of the system and hence, the stability of the bubbles or drops formed. The net effect depends on the combination of the individual effects.

Zuiderweg and Harmens[12], in their study of the effect of surface phenomena on the performance of distillation columns, showed that three types of systems can be distinguished with respect to changes in surface tension. These are the **Negative, Positive and Neutral** systems. In a positive system, the surface tension of the more volatile component is lower than that of the less volatile component. During distillation or stripping, depletion of the more volatile component, leads to higher surface tension in the thin film, than at the surrounding points (bulk). The resultant surface tension gradient along the surface sets up a surface-energy driving force causing liquid to flow from regions of low surface tension to regions of high surface tension. This flow is energetically

favoured because of the resulting reduction in the total surface energy. As a result of this flow, thin regions which would otherwise break, are thickened and reinforced, and thus foam/froth stability is promoted. In a system where the more volatile component has a higher surface tension **(Negative System)**, the phenomenon is the reverse of that observed in the positive system. Here, thin regions will exhibit lower surface tension than the bulk solution, consequently, the resulting flow will be away from thin regions leading to increased film thinning and rupture. Any foam or froth formed from this type of system tend to be unstable . In a neutral system, there is no marked difference in surface tension between the less and more volatile components, and hence, foam or froth is not promoted. Zuiderweg and Harmens[12], showed experimentally that the efficiency of separation in binary distillation is higher in the frothing regime† for the positive systems. Bainbridge and Sawistowski[11] found higher stage efficiencies for the negative system as against the positive system for sieve plates operating in the spray regime.†

Considerable work has been carried out to study the behaviour of foams/froths on sieve plates. For example, Gardner and Macleans[43] studied three systems namely, **air-water, air- carbontetrachloride,**

† *See Chapter 2, Section 2.5*

air-decahydronaphthalene. They found that the dispersion characteristics were different in each case and concluded that fluid properties had a significant effect on the behaviour of the dispersion. The gas-liquid transition was studied in detail by Rennie and Evans[20] who discussed it in terms of plate geometry and the orifice Reynolds number. De Goederen[45] showed that foam heights in any system increased with a decrease in the viscosity of the liquid used. Thomas and Shah[23] studied the behaviour of frothing liquid systems on sieve plates and in downcomers using a water-glycerol/air system. They concluded that the height of froth in the downcomer is affected by liquid and air flowrates, width of the downcomer and the surface tension of the liquid. It was also concluded that downcomer flooding by froth does not lead to flooding of the entire column. This however, differs from the conclusion of Huang and Hudson[27], Bolles[28], Kirkbridge[29], Davies[30], Leibson,Kelley and Bullington[31], and Hughmark and O'Connell[32], that if the aerated liquid in the downcomer reaches the top of the outlet weir, then, the column will flood. On the other hand, Thomas and Shah[23] concluded instead that flooding in any column is much more dependent on vapour or gas carry-under from the downcomer, entrainment on the plate and froth height on the plate. Foss and Gerstner[47], analysed the effect of gas velocity on foam heights and concluded that gas superficial velocity was a fundamental variable in the behaviour of foams in any process unit. Thomas and Campbell[21] predicted the heights of air/glycerol-water dispersions on a distillation plate in terms of the gas superficial velocity, liquid flowrate, gas density and weir height according to the expression

$$H_F = 2.45F_G + 0.53L_A + 1.24H_W \quad (1)$$

Where

H_F = Froth height (inches)

F_G = F-factor for gas = $u_g\sqrt{\rho_g}$, $(lb^{\frac{1}{2}} ft^{\frac{-1}{2}} s^{-1})$

L_A = Liquid flowrate (gal/min - ft weir width)

H_W = Weir height (inches)

u_g = Superficial gas velocity (ft/sec)

ρ_g = Gas density (lb/ft^3)

All the works presented suggest that the generation, stability and flow of foams in any process unit can be described in terms of the physical properties of the system and the dimensions and configuration of the equipment used. To be able to understand the effect of foams in any process system, it is necessary to study the combined effect of system physical properties and equipment dimension and configuration.

Summary

In this section, a survey of literature on the effect of the physical properties of the system on the generation and flow of foams has been made. Most of the literature presented in this section has been mainly concerned with qualitative effects of different parameters on the behaviour of foams. The next section examines theoretical models for use in a quantitative analysis of formation and flow of foams.

2.3 Models of Foams and Foaming in Downcomers

Most studies of foams and froths are usually concerned with the development of a model for the prediction of film thickness, liquid holdup fraction and foam height, from a knowledge of the physical properties of the liquid and the gas superficial velocity. However, since most of the models, as shall be shown later, are usually based on static foams (i.e where gas is bubbled through a pool of liquid), their extension to dynamic systems becomes difficult. Ho and Prince[41] described the behaviour of foams on a sieve plate by equating the flow of liquid carried upwards by the bubbles to the downward flow through the plateau borders. They derived an equation containing an empirical constant which relates the liquid holdup fraction to the gas velocity, the bulk physical properties of the liquid and the bubble size according to equation (2).

$$u_g = \frac{3.1}{k}\left[d_B^2 \epsilon(1-\epsilon)\right] \tag{2}$$

Where

d_B = Volume average bubble diameter (cm)

k = Ratio liquid holdup in the foam to
Liquid holdup in plateau borders

u_g = Gas superficial velocity (m/s)

ϵ = Gas holdup fraction (-)

Barber and Hartland[7] derived a model for cellular foams. In their model derivation, it is proposed that foams may be represented by a tesselated structure of pentagonal dodecahedra in which liquid is carried upwards by the films forming the faces of the dodecahedra and returns to the bulk by gravitational forces in the plateau borders. Here, the films drain into the plateau borders because of reduced pressure relative to the gas in the bubbles. When the liquid surfaces are rendered immobile, the foam height is related to the film thickness in terms of the physical properties of the fluids and the bubble diameter by the expression

$$H_F/d_B = \frac{0.55(\eta u_g d_B)^{5/4}}{(\rho_L g)^{0.25}\sigma\delta^{0.25}} \tag{3}$$

Barber and Hartland[7] futher predicted the variation of liquid holdup fraction with the height of the dispersion and fluid physical properties and gas superficial velocity according to equation (4).

$$1-\epsilon = \frac{2.34(\eta u_g)^{5/7} d_B^{2/7}}{(\rho_L g)^{1/7}(\sigma H_F)^{4/7}} + \frac{52(\eta u_g)^{6/7}}{(\rho_L g)^{4/7}(\sigma H_F)^{2/7} d_B^{6/7}} \tag{4}$$

Nomenclature for equations 3 and 4

d_B = Bubble diameter (m)

g = Acceleration due to gravity (m/s^2)

H_F = Foam height (m)

u_g = Superficial Gas velocity (m/s)

ρ_L = Liquid density (Kg/m^3)

η = Liquid viscosity (Ns/m^2)

δ = Film thickness (m)

σ = Surface tension (N/m)

ϵ = Gas holdup fraction (-)

Equations (3) and (4) have been found to adequately describe the behaviour of foams[7] but cannot be used to predict foam heights in industrial columns because the film thickness has to be determined experimentally. Also, they do not take into account the liquid momentum on the plate or in the downcomer.

The rate of collapse of cellular foams as a function of the initial foam height, liquid viscosity, bubble diameter, surface tension, critical film thickness and liquid density was predicted by Barber and Hartland[8] according to the relation

$$t = \frac{0.55\eta d_B^{9/5} H_{F_o}^{1/5}}{(\rho_L g)^{1/5}\sigma^{4/5}\delta_c^{7/5}}\left[\left(H_F/H_{F_o}\right)^{-1/7} - H_F/H_{F_o}\right] \qquad (5)$$

H_{F_o} = Initial foam height (m)

δ_c = Critical film thickness (m)

Other parameters are as defined for equations (3) and (4)

It should be pointed out that equations (3) – (5) may hardly be used when dealing with normal plate operations for the same reasons as stated earlier. Also, and most importantly, the hardware of the equipment is not taken into consideration. However, they do give an insight into the behavioural patterns of foams which may be incorporated into modelling of dynamic systems.

Barber and Wijn[9], in their study of foaming in the flash vessels of crude a crude oil distillation unit, derived a model for foam height. This model was also extended to the prediction of foam heights in downcomers. The model proposed was reported[9] to be in good agreement with experimental data. From their conclusions, it follows that the amount of surface active material present in crude units is sufficient to stabilize the bubbles generated. Therefore, foam heights are generally only functions of hydrodynamic conditions. The equation for foam heights proposed by the authors[9] is

$$H_F = \frac{1.7 \times 10^{12} \nu u_L 3.67}{g^2 v_i^{0.67} (1-\epsilon)^{6.32}} \left(\frac{\rho_L}{\Delta\rho}\right)^{1.33} \tag{6}$$

In the application of their theory to downcomers[9], it was assumed that the downcomer is completely filled by foam (i.e Foam height equals the downcomer height). Their expression for downcomers predicts the liquid superficial velocity in a downcomer according to the relation

$$u_d = \frac{8.0 \times 10^{-5} g^{0.67} (1-\epsilon)^{2.1} H_F^{0.33}}{\nu^{0.33}} \left(\frac{\rho_L}{\Delta\rho}\right)^{0.44} \tag{7}$$

Where

g = Acceleration due to gravity (m/s^2)

H_F = Foam height in equation (6) (m)

= Downcomer depth in equation (7) (m)

u_L = Liquid superficial velocity (m/s)

v_i = Velocity of two phase mixture at inlet (m/s)

ν = Liquid kinematic viscosity (m^2/s)

ρ_L = Liquid density (Kg/m^3)

$\Delta\rho$ = Liquid - gas density difference (Kg/m^3)

Each of the models presented further the belief that foaming is solely a function of the physical properties of the systems involved and the operating conditions.† To be able to make a critical analysis of the be-

† *Operating conditions refer to gas/liquid rates and geometry of the unit*

haviour of foams in any plate-downcomer system, it is worthwhile to review current design methods used to size downcomers. This is necessary so as to be able to ascertain if current design criteria for downcomers are adequate in view of the presence of foams. This critical review and assessment is given in the next section.

2.4 DOWNCOMER DESIGN

2.4.1 Criteria for Downcomer Design

Conventionally, downcomers are designed to meet the following criteria

(a) Downcomer area should be between 5 – 14% of the column cross-sectional area and the downcomers should be of segmental type. For most atmospheric columns a convenient downcomer area of 10% of the column cross-sectional area is usually recommended

(b) The froth height in the downcomer should not reach the weir of the tray above. This criterion deals with downcomer flooding, since, it is the belief that if the froth in the downcomer reaches the weir above, an unstable condition results, which eventually leads to flooding.

(c) It is suggested[65] that the minimum residence time of liquid in the downcomer should be 3 seconds. In most designs, a residence time of 5 seconds is usually recommended and used. This criterion basically states that the residence time of the liquid in the downcomer should be long enough for practically complete vapour/gas disengagement.

(d) In most cases, an equivalent criterion to criterion (c) is based on liquid velocity in the downcomer. It is recommended that the superficial liquid velocity in the downcomer should be low enough to allow vapour/gas disengagement for clear liquid to be delivered to the next tray. Liquid velocities between 0.03 and 0.21 m/sec for non-foaming systems are usually recomended for design purposes, depending on the tray spacing[23,32].

(e) In the past, a limitation used to be imposed on the liquid throw over the weir. It was generally recommended that the liquid throw over the weir shold be smaller than the widest part of the downcomer since if the liquid from the plate above strikes the column wall, an unstable condition is obtained whereby the mouth of the downcomer is blocked, thereby preventing the escape of disengaged gas. Bolles[28,65] recommends that the liquid throw sholud not exceed 60% of the widest downcomer width. More recently, it has been shown that this criterion is not a limiting factor in downcomer design[12,13,19].

2.4.2 Downcomer Area

Downcomer area is normally calculated as a fraction of total column area. Plate areas are usually calculated using the Souders-Brown equation.

$$V_F = C_F \left(\frac{\rho_L - \rho_g}{\rho_g} \right)^{0.5} \tag{8}$$

Where

V_F = Flooding gas velocity (m/s)

ρ_L = Liquid density (Kg/m^3)

ρ_g = Gas density (Kg/m^3)

C_F = Capacity factor (m/s)

From equation (8), it can be seen that the flooding gas velocity, V_F, is calculated using only vapour/gas and liquid densities. The effect of other system properties is introduced through a system derating factor, S_F, according to the relation

$$V_F = S_F C_F \left(\frac{\rho_L - \rho_g}{\rho_g} \right)^{0.5} \tag{9}$$

Fair[70] related the system derating factor, S_F, to a phase property - liquid surface tension - through the relation

$$S_F = \left(\frac{\sigma}{0.02}\right)^{0.2} \tag{10}$$

where σ = Surface tension of liquid (N/m)

Treybal[66], gives a correlation for the calculation of C_F values from available data on flooding of sieve trays according to the relation

$$S_F C_F = \left[\alpha_1 \log \left[\frac{1}{L'/G' \left(\frac{\rho_g}{\rho_L}\right)^{0.5}} \right] + \beta_1 \right] \left[\frac{\sigma}{0.02} \right]^{0.2} \tag{11}$$

Where

$$\alpha_1 = 0.0744T_p + 0.01173 \tag{12}$$

$$\beta_1 = 0.0304T_p + 0.015 \tag{13}$$

L' = Liquid mass flowrate (Kg/m^3)

G' = Gas mass flowrate (Kg/m^3)

T_p = Tray Spacing (m)

The effect of hole diameter is taken into account by a ratio of the hole area to active area A_o/A_a. Equation (9) for C_F values from equation (11) is only valid for $A_o/A_a \geq 0.1$. If the ratio of hole area to active area is less than 0.1 then

$$V_F = C_F\left(\frac{\rho_L - \rho_g}{\rho_g}\right)^{0.5}\left[\frac{5A_o}{A_a} + 0.5\right] \tag{14}$$

Values of plate cross-sectional area from equations due to Treybal[66] are limited to hole diameters not greater than 6mm, and also to cases where the weir height does not exceed 15% of the tray spacing, and most importantly, to non-foaming systems. Seader[67] makes use of a foaming factor to predict the actual corrections for C_F in equation (9). The corrected C_F values, C'_F, is given as

$$C'_F = F_{ST}F_{HA}F_FC_F \tag{15}$$

Where

F_{ST} = Surface tension correction factor $(\frac{\sigma}{0.02})^{0.2}$

F_{HA} = Hole factor correction factor

$= 1.0$ for $A_o/A_a \geq 0.1$

$= 5(A_o/A_a) + 0.5$ for $A_o/A_a < 0.1$

F_F = Foaming factor

For non-foaming systems, $F_F = 1.0$. For foaming systems, F_F is usually in the range $0.3 - 0.8$ depending on the degree of foaming envisaged. Another method of calculating column cross-sectional area is given by Sawistowski[75]. Here use is made of Souders-Brown equation to calculate the column diameter by assuming a plate spacing, T_p, and a dynamic liquid seal, S,. Tabulations of C_F values for different plate spacings and liquid seals are given in table 2.1. However, before C_F values from table 1 can be used, they have to be corrected for foaming using a foaming factor F_F.

Table 2.1 :- C_F Values $\times 10^{-3}$ (m/s)

T_p (m)	S (mm)			
	12.5	25.0	50.0	75.0
0.15	6 - 12	-	-	-
0.39	27-34	21-27	15-21	-
0.45	46	43	37	27
0.60	56	52	49	46
0.75	59	56	55	53
0.90	62	59	58	56

The correlations given so far are based on the assumption that the froth/spray transition is the limit of tray operation. This limit is no longer the case since some industrial columns do operate in the spray regime. The spray regime can be taken into account by the determination of a maximum gas flow parameter $(F_G)_{max}$ in the following manner.

Consider entrainment of a drop and balance the gravitational, drag and buoyancy forces giving

$$\frac{\pi d^2}{4} C_D \frac{\rho_g}{2} u_g^2 = \frac{\pi d^3}{6} [\rho_L - \rho_g] g \tag{16}$$

Solving for d (where d = drop diameter), and noting that the F-factor is given as $F_G = u_g \sqrt{\rho_g}$,

$$d = \frac{3 C_D}{4(\rho_L - \rho_g) g} F_G^2 \tag{17}$$

Where C_D = Drag Coefficient

Since the plate operation is in the spray regime, the Reynolds number is high hence, C_D becomes constant at 0.44. A graphical representation of equation (17) is shown in figure 2.1

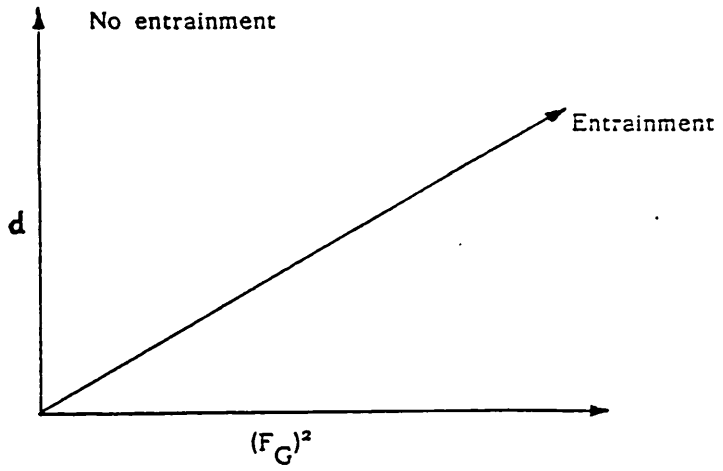

Figure 2.1 :- Plot of $(F_G)^2$ against d for entrainment considerations

Now, consider the jetting effects and drop breakup on sieve plates. Assume that there is jetting at a hole, as shown in figure 2.2, and that the diameter of the jet is approximately equal to the diameter of the hole on the plate. Consider a drop coming into the path of the jet and also the stability of the drop being subjected to the jet velocity. For drop breakup, the critical Weber number equals 12.

$$We_c = \frac{u^2 d \rho_g}{\sigma} = 12 \tag{18}$$

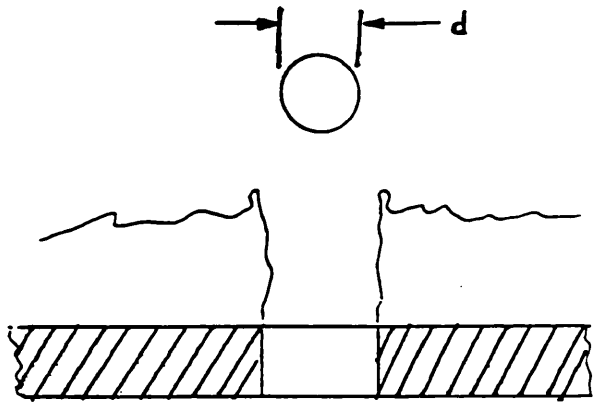

Figure 2.2 :- Jetting at a single hole on a sieve plate

In the spray regime, for a drop above the hole, $u = u_H$, where u_H is the hole gas velocity. Hence,

$$We_c = \frac{u_H^2 d \rho_g}{\sigma} = \frac{F_G^2 d}{\phi_1^2 \sigma} \tag{19}$$

Where ϕ_1 = fractional area of the plate

From equation (19), an expression for the drop diameter, d, is obtained as

$$d = \frac{We_c \phi_1^2 \sigma}{F_G^2} \tag{20}$$

The critical drop diameter can be obtained by equating values of d from equations (17) and (20). This also defines the critical F-factor. That is,

$$\frac{3C_D}{4(\rho_L - \rho_g)g} F_G^2 = \frac{We_c \phi_1^2 \sigma}{F_G^2} \tag{21}$$

$$\Rightarrow \quad F_{Gc} = F_{Gmax} = \left[\frac{4We_c \phi_1^2 g(\rho_L - \rho_g)}{3C_D}\right]^{1/4} \tag{22}$$

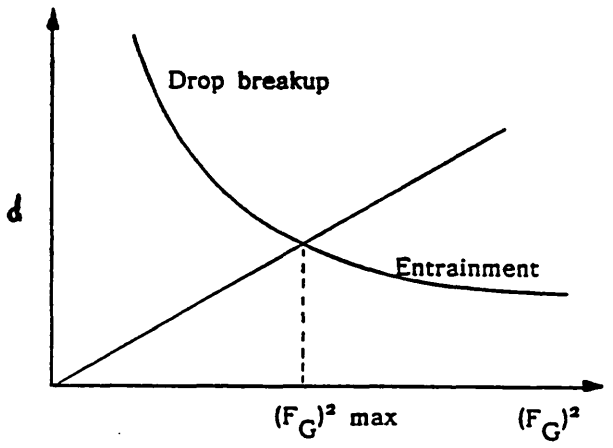

Figure 2.3 :- Plot showing determination of F_{Gc}

Noting that $F_G = C_F(\rho_L - \rho_g)^{0.5}$ gives

$$C_{Fc} = \left(\frac{4We_c}{3C_D}\right)^{1/4} \left[\frac{\phi_1^2 \sigma g}{\rho_L - \rho_g}\right]^{1/4} \tag{23}$$

For $We_c = 12$ and $C_D = 0.44$ we obtain

$$C_{Fc} = 2.46\left[\frac{\phi_1^2 \sigma g}{\rho_L - \rho_g}\right]^{1/4} \tag{24}$$

The critical capacity factor C_{Fc} can be determined from equation (24) which enables the calculation of F_{Gc} or F_{Gmax}. A plot of F_{Gc} against d is shown in figure 2.3. By a suitable choice of F_G/F_{Gmax} ratio (% or degree of flooding), the diameter of the column can be calculated.

From the analysis given so far, ways of determining the flooding capacity factor and/or flooding velocities have been given. Normal design criteria require that columns should be designed using a certain percentage of the flooding velocity or the capacity factor (say ψ). Note that flooding in this sense refers strictly to entrainment flooding. Percentage flooding ratios of $60 - 80\%$ are normally recommended in practice[66]. Hence,

$$V_d = \frac{\psi}{100} V_F$$
$$or \tag{25}$$
$$(F_G)_d = \frac{\psi}{100} F_{Gmax}$$

Where

V_d = Design velocity (m/s)

$(F_G)_d$ = Design f - factor

Hence, the net column area can be calculated from the relation

$$A = \frac{G'}{v_d \rho_g} = \frac{G' v_d}{F_{Gd}^2} \tag{26}$$

Where

A = Net column area (m^2)

G' = Mass flowrate of gas (Kg/s)

2.4.3 Permissible Height of Liquid in the Downcomer

The height of clear liquid in the downcomer (liquid backup in downcomer) is usually calculated using equation (27) due to Huang and Hudson[27]

$$h_B = h_L + h_t + h_{dc} + h_\Delta \tag{27}$$

Where

h_B = Height of clear liquid in downcomer (mm)

h_L = Height of clear liquid on the plate (mm)

h_t = Total pressure drop on the plate (mm)

h_{dc} = Head loss under the downcomer apron (mm)

h_Δ = Liquid gradient across the plate (mm)

The height of clear liquid on the plate (h_L) is usually calculated[66,68,70] using equations (28) and (29).

$$h_L = h_w + h_{ow} \tag{28}$$

$$h_{ow} = 750\left(\frac{L'}{\rho_L l_w}\right)^{2/3} \tag{29}$$

Where

h_{ow} = Height of liquid over the weir (mm)

h_w = Height of overflow weir (mm)

l_w = Weir length (m)

L' = Liquid mass flowrate (Kg/s)

ρ_L = Liquid density (Kg/m^3)

More recently, Zuiderweg et al[80] noted that values from equations (28) and (29) are usually over estimated since, on the plate there usually

exists a gas-liquid dispersion which flows over the weir as against clear liquid which equations (28) and (29) suggest. From their studies[80], the following are proposed to calculate the clear liquid height on the plate and the height of liquid over the weir.

$$h_L = 0.6 H_w^{0.5} p^{0.25} \Psi^{0.25} \qquad (30)$$

$$25mm < H_w < 100mm$$

$$\begin{aligned} h_{ow} &= 2.4 g^{-0.33} (u_L/b)^{0.67} (\Psi/h_L)^{0.33} \\ &\quad FP < 3-4 \quad (Mixed\ and\ Spray\ Regimes\dagger) \\ &= 1.04 g^{-0.33} (u_L/l_w)^{0.67} \\ &\quad FP > 3-4 \quad (Emulsion\ Regime\dagger) \end{aligned} \qquad (31)$$

Where

b = Weir length per unit active area (m^{-1})

H_w = Weir height (m)

p = Hole pitch (m)

$\Psi = (Q/l_w u_g)\sqrt{\rho_L/\rho_g}$

Q = Volumetric Liquid flowrate (m^3/s)

h_L = Plate liquid holdup (m)

u_L = Superficial liquid velocity (m/s)

u_g = Superficial gas velocity (m/s)

g = Acceleration due to gravity (m/s^2)

ρ_L, ρ_g = Liquid and Gas densities respectively (Kg/m^3)

FP = Flow parameter $= L/G\sqrt{\rho_g/\rho_L}$

L, G = Liquid and Gas mass flowrates respectively (Kg/s)

Dhulesia[77] argued that equation (30) cannot be used to span all the regimes† of plate operation and proposed a modification to equation (30) for use in plate operation in the frothing regime.

This modification was shown[77] to fit data of different workers better and is given as

$$h_L = 0.5 H_w^{0.5} p^{0.17} \Psi^{0.33} \tag{32}$$

The total pressure drop on the plate, h_t, is normally given as[65,66,67,68]

$$h_t = h_d + \beta(h_w + h_{ow}) + h_r \tag{33}$$

$$h_d = 51\left[\frac{u_H}{C_o}\right]^2\left(\frac{\rho_g}{\rho_L}\right) \tag{34}$$

† *See Section 2.5*

$$h_r^* = \frac{6 \times 10^3 \sigma}{\rho_L d_h g} \tag{35}$$

* (*see references* 65, 66, 68)

Where

C_o = Orifice coefficient

d_h = Hole diameter (m)

h_d = Dry pressure drop (mm)

h_r = Residual pressure drop (mm)

g = Acceleration due to gravity (m/s^2)

β = Aeration factor

σ = Liquid surface tension (N/m)

Using the equations put forward by Zuiderweg et al[80] and Dhulesia[77], equation (33) can be put in the form

$$h_t = h_d + 10^3 h_L + h_r \tag{36}$$

which takes care of the aeration factor with the added advantage of proper evaluation of the actual hydrostatic pressure due to liquid on

the plate. The head loss under the downcomer apron can be calculated using the relation[68]

$$h_{dc} = 166\left[\frac{L'_d}{\rho_L A_{da}}\right]^2 \tag{36}$$

Where

L'_d = Liquid mass flowrate in downcomer (Kg/s)

A_{da} = Area under downcomer apron (m^2)

The factor, β, introduced in equation (33), takes into account the aerated form of liquid on the plate. This can be estimated from the value of froth density ϕ_f. Generally, this factor, β, is given as[65]

$$\beta = \frac{\phi_f + 1}{2} \tag{37}$$

The introduction of β into equation (33) compensates for the aeration on the plate and makes equation (28) similar to equations (30) and (32). There has not yet been extensive testing of the use of equations (30) and (32) for design; hence, it cannot be said at this stage which of the forms of the equation best approximates the real hydrostatic pressure of the liquid on the plate. The liquid gradient, h_Δ, represents the head required

to produce aerated liquid crossflow on the plate. This parameter, for sieve plates, is usually very small and negligible. Hence, for most sieve plate designs, the liquid gradient is not normally taken into account.

In equation (27), the liquid backup in the downcomer is expressed in terms of clear liquid. For a frothing system, in practice, the liquid in the downcomer is in an aerated form. As a result, the level of fluid in the downcomer will be higher than that predicted. In most designs, a correction factor for the downcomer backup based on a frothing system is usually employed. Since the liquid in the downcomer is in an aerated form, the actual backup is given as[65]

$$h'_B = \frac{h_B}{\phi_{dc}} \tag{38}$$

$$\phi_{dc} = \frac{h_{Ld}}{h_{fd}} \tag{39}$$

Where

h_{Ld} = Height of clear liquid in downcomer (m)

h_{fd} = Froth height in downcomer (m)

ϕ_{dc} = Downcomer froth density (-)

For design purposes, a value of $\phi_{dc} = 0.5$ is usually recommended for non-foaming systems and a value of $\phi_{dc} = 0.2 - 0.3$ is recommended for foaming systems[56]. For optimum design using equation (38), h'_B is restricted to a value not greater than the tray/plate spacing[65]. The idea of sizing downcomers based on equation (38) is quite reasonable especially for foaming systems. On the other hand, where accurate means of estimating ϕ_{dc} are not available, the dependency on equation (38) for design becomes difficult.

2.4.4 Liquid Residence Time in Downcomers

The liquid residence time in downcomers is usually calculated from the relation[68]

$$t_R = \frac{A_d h_B \rho_L}{L'_d} \tag{40}$$

Where

t_R = Resìdence time ($secs$)

h_B = Clear liquid backup in downcomer (m)

L'_d = Liquid mass flowrate in downcomer (Kg/s)

The liquid residence time calculated from equation (40) may not be representative of the true residence time since it is based primarily on the assumption of pure plug flow of liquid and also on the liquid flowrate only. In nearly all practical conditions, the flow of liquid in the downcomer may not really follow the pure plug flow model, hence, the residence time calculated from this equation may be rather too conservative. Also, and in particular, for foaming systems, in which a highly aerated liquid exists in the downcomer, a value of $3 - 5$ seconds recommended for the residence time may be rather too low for practically complete vapour/gas disengagement. Alternative ways of analysing residence time distributions in downcomers are given in section 2.7. Theoretical models for use in fitting the data from residence time measurements are given in chapter 3. The results of the measurements are presented in chapter 5.

Summary

In this section, available methods for the design of sieve plate columns and the corresponding design equations have been critically reviewed. However, at this stage, the actual behaviour of the gas-liquid mixture on the plate and how it affects the overall performance of the separation process undertaken has not yet been taken into consideration. This phenomenon is examined and reviewed in section 2.5.

2.5 Flow Regimes and Tray/Plate Hydraulics

Introduction

In section 2.4, plate and downcomer design methods were described with a brief mention of flow patterns on the plate. In this section the mode of flow of the two phase mixture on the plate is discussed. The importance of flow regimes shall be seen later in chapter 5 where the results of the present work is presented and discussed.

Two phase flow patterns on perforated plates can be effectively described and characterised by considering the different types of flow behaviour of the dispersion existing on the plate. Traditionally, the operating range of sieve plates is characterised by an upper boundary - the flooding limit, and the lower boundary - the weeping limit. Visual observations have shown that within this range, there exist different regimes of flow in which either the vapour/gas or the liquid is the dominant dispersed phase.

Four principal regimes of plate behaviour can be identified. Different authors describe these regimes by different names, but basically the general characteristics and properties of the regimes are the same. Ho, Muller and Prince[41] recognise the regimes as **BUBBLE, CELLULAR FOAM, FROTHING and SPRAY** regimes, existing in the given order with increasing superficial gas velocity for a fixed liquid loading on

the plate. Hofhuis and Zuiderweg[16] recognise these regimes as **FREE BUBBLING, EMULSION, MIXED FROTH and SPRAY** existing in the order given for a fixed liquid rate and increasing gas velocity. The spray regime of plate operation has been studied by numerous authors[13,41,48]. In this regime, which appears at relatively low liquid loadings and high vapour/gas velocities, the liquid is dispersed almost completely into small droplets by the action of vapour/gas jets issuing from the tray perforations. The transport of liquid over the weir occurs here principally by spraying action. The different studies undertaken of this regime have been used for the identification of the transition into the spray regime. The results of these studies show a large degree of mutual agreement. The onset of the spray regime is mainly influnced by the hole vapour/gas velocity, the vapour/gas density, liquid holdup on the plate and the size of the holes. A number of correlations have been proposed for the transition into the spray regime, namely,

(*a*) **Barber and Wijn**[9]

$$\frac{h_L}{d_h} = 1.35\left[\left(\frac{u_g(\rho_g/\rho_L)^{0.5}}{\phi_1\sqrt{gd_h}}\right)^{0.4} - 0.59\right]\left(\frac{p}{d_h}\right)^{0.33} \tag{41}$$

(*b*) **Lockett**[106]

$$\frac{h_L}{d_h} = \frac{2.777}{\phi_1}\left[u_g\left(\frac{\rho_g}{\rho_L}\right)^{0.5}\right] \tag{42}$$

(c) Hofhuis and Zuiderweg[16]

$$\frac{h_L^{1.5}}{d_h} = \frac{1.053}{g^{0.5}\phi_1}\left[u_g\left(\frac{\rho_g}{\rho_L}\right)^{0.5}\right] \tag{43}$$

Nomenclature for equations (41) - (43)

h_L = Liquid holdup on the plate (m)

d_h = Hole diameter (m)

u_g = Gas superficial velocity (m/s)

ρ_L, ρ_g = Liquid and Gas densities respectively (Kg/m^3)

p = Pitch of the holes (m)

ϕ_1 = Fractional free area of plate (-)

Equations (41) to (43) indicate that the transition into the spray regime can occur freely over the range of vacuum distillation and atmospheric distillation by changing the hole size, tray free area, weir height and length (the last two parameters influnce h_L).

The next important regime of plate operation exists at high liquid loadings and average vapour/gas rates. By shearing action of the liquid due to its high velocity, the vapour/gas jets are uniformly dispersed into bubbles. The transport over the weir is now mainly by continuous flow of liquid, containing the uniformly dispersed gas/vapour. This regime has been called the emulsion flow regime by Hofhuis and Zuiderweg[16] and

the cellular foam regime by Ho et al[41]. Hofhuis and Zuiderweg[16] showed that the transition into this regime is controlled mainly by the ratio of the horizontal momentum of the liquid and the vertical momentum due to the vapour/gas, given by

$$\frac{u_L}{u_g}\left(\frac{\rho_L}{\rho_g}\right)^{0.5} > 3.0 \qquad (44)$$

Similarly, by variation of the weir height and length, the transition into this regime can be made to occur freely over the range of atmospheric and pressure distillation. The next regime of plate operation is the mixed froth or froth regime which lies between the emulsion and spray regimes. The existence of this regime depends on how large the transition range between the emulsion and spray regimes is, which is a strong function of flowrates, physical properties and tray design. It is characterised by jetting action which causes both bubbles and drops to form in the two phase mixture. In general, this regime is representative of atmospheric distillation or operations.

The last regime, the bubbling or free bubbling regime, is characterised by bubble formation at the sieve plate orifices. This regime occurs close to the weeping point. From the view-point of commercial scale operations, the free bubbling regime is of little significance.

A good representation of all the flow regimes is given in the form of a flow regime diagram due to Hofhuis and Zuiderweg[16] and is shown in figure 2.4.

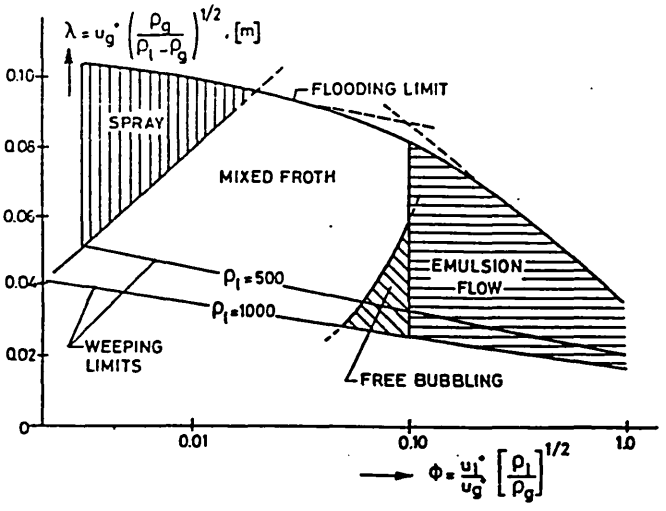

Figure 2.4 :- Flow Regime Diagram[16]

Since the hydrodynamic conditions in the downcomer are a function of those prevalent on the plate, then, as a first approximation, it can be assumed that each of the above regimes will exhibit certain properties in the downcomer. That is, the dispersion in the downcomer behaves differently for each of the flow regimes on the plate.

2.5.1 Dispersion Density on Sieve Plates

Hofhuis and Zuiderweg[16] found that the average gas fraction on the plate varies with the tray Froude number according to the relation

$$\frac{1}{1-\bar{\epsilon}} = c_1 \left[\frac{u_g}{(gh_L)^{0.5}} \left(\frac{\rho_g}{\rho_L} \right)^{0.5} \right]^n + 1 \qquad (45)$$

with c_1 and n different for the spray regime and the mixed/emulsion regimes.

Where

c_1 = Constant

n = Constant

$\bar{\epsilon}$ = Average gas fraction on the plate (-)

h_L = Plate liquid holdup (m)

g = Acceleration due to gravity (m/s^2)

ρ_g = Gas density (Kg/m^3)

ρ_L = Liquid density (Kg/m^3)

The values of c_1 and n are

$$\begin{aligned} &\textit{Spray Regime} : \quad c_1 = 265 \qquad n = 1.7 \\ &\textit{Mixed/Emulsion Regime} : \quad c_1 = 40.0 \qquad n = 0.8 \end{aligned} \qquad (46)$$

Summary

In this section the different regimes of flow of the two phase mixture on plates have been reviewed and critically examined. However, the modes of formation of bubbles may have a significant effect on the existence of these regimes of flow. Bubble formation on sieve plates is reviewed and examined in section 2.6.

2.6 Formation and Flow of Bubbles on Sieve Plates

A review of current literature on the formation and flow of bubbles on sieve plates provides a proper insight into the different regimes of plate operation discussed in section 2.5. Two main bubble formation mechanisms are of interest for sieve plate operation. At very low gas flowrates, the volume of the bubbles generated is a function of surface tension, buoyancy force and the orifice diameter only. The gas flowrate and the volume of the chamber beneath the orifice have no influence on the volume of bubbles generated. Here, the bubble volume is given as

$$\dot{V}_b = \frac{\pi d_h \sigma}{(\rho_L - \rho_g) g} \tag{47}$$

Where

d_h = Orifice diameter $(m\ )$

g = Acceleration due to gravity (m/s^2)

$\dot{V}_b$ = Bubble volume (m^3)

σ = Surface tension (N/m)

ρ_L = Liquid density (Kg/m^3)

ρ_g = Gas density (Kg/m^3)

At higher gas flowrates, the bubble formation frequency approaches a constant value, hence, the bubble volume, $\dot{V}_b$, becomes dependent on the gas flowrate. Davidson and Schüler[82,107] derived from first principles a relation between bubble volume and the gas flowrate. This relation is given by

$$\dot{V}_b = 1.378 g^{-3/5} \dot{V}_g^{6/5} \tag{48}$$

$$\Rightarrow \quad d_B = 1.38 g^{-1/5} \dot{V}_g^{2/5} \tag{49}$$

For a sieve plate with holes drilled on a triangular pitch, p, the ratio of the hole to active area is given by,

$$\frac{A_o}{A_a} = 0.907 \left(\frac{d_h}{p} \right)^2 \tag{50}$$

and the hole velocity given by,

$$\begin{aligned} u_H &= \frac{u_g A_a}{A_o} \\ &= 1.1 u_g \left(\frac{p}{d_h}\right)^2 \end{aligned} \tag{51}$$

Hence, the volumetric gas flowrate,$\dot{V}_g$ through one hole is given by

$$\begin{aligned} \dot{V}_g &= \frac{\pi d_h^2}{4} \times 1.1 u_g \left(\frac{p}{d_h}\right)^2 \\ &= 0.866 u_g p^2 \end{aligned} \tag{52}$$

Replacing (52) in (49) the following relation is obtained for diameter of bubbles formed on sieve plates.

$$d_B = 1.3 g^{-1/5} p^{4/5} u_g^{2/5} \tag{53}$$

· Where

d_B = Bubble diameter (m)

A_o = Hole area (total) on plate (m^2)

A_a = Active area of plate (m^2)

g = Acceleration due to gravity (m/s^2)

u_g = Superficial gas velocity (m/s)

$\dot{V}_b$ = Bubble volume (m^3)

$\dot{V}_g$ = Gas volumetric flowrate (m^3/s)

u_H = Hole gas velocity (m/s)

If it assumed that bubble growth on adjacent holes occurs simultaneously, then as the gas velocity is increased, the maximum possible attainable bubble diameter equals the hole pitch. From the Davidson - Schüler relation (equation (53), it follows that for this limit, the gas velocity is given by

$$u_g(d_B = p) = 0.52\sqrt{gp} \tag{54}$$

Above this velocity, the diameter of the single bubbles cannot increase futher. It has been shown[108] that there are three mechanisms which may account for the transition of flow regimes on the plate above this velocity.

(a) Coalescence of Bubbles on top of each Other

Here, bubbles on top of each other coalesce and a gas channel is formed which results in a transition from the free bubbling regime to the frothing regime as shown in figure 2.6.

(*b*) Formation of Cylindrical Bubbles

Here, the bubbles become cylindrical, with diameter equal to the hole pitch and length, l, as shown in figure 2.7. Above a certain gas velocity, these bubbles also coalesce and again a gas channel is formed. The coalescence of cylindrical bubbles will occur only when the bubbles have reached a maximum length, l_m, and hence, a maximum length to diameter ratio, l_m/d_B. This ratio depends on the surface tension, gas momentum and the dispersion height. If the Davidson - Schüler equation is used, it can be shown that for this limit, the gas velocity is given by (by defining a sphere with same volume as the cylindrical bubble)

$$u_g(l = l_m, d_B = p) = 0.52\left[\frac{3}{2}\frac{l_m}{p}\right]^{5/6}\sqrt{gp} \qquad (55)$$

Above this velocity, free bubbling of gas is no longer possible and a mixed froth develops.

(*c*) Coalescence of Adjacent Bubbles

Here, bubbles on adjacent holes coalesce. Hence, steric hinderance disappears and a new larger bubble is formed (see figrue 2.8). It has been shown[108] that steric hinderance occurs at a gas velocity given by

$$u_g(d_B = 2p) = 0.86\sqrt{pg} \tag{56}$$

When these bubbles coalesce to form a cylindrical bubble, the gas velocity at which l_m is reached is given by

$$u_g(d_B = 2p, l = l_m) = 0.86\left[\frac{3}{2}\frac{l_m}{p}\right]^{5/6}\sqrt{gp} \tag{57}$$

Also, as in the previous cases, a mixed froth or emulsion flow develops when this gas velocity is exceeded, depending on the conditions of operation.

The above review deals primarily with bubbles formed in stagnant fluids. Hence, it is of little consequence when dealing with industrial units. It only gives indications of the different types of flow patterns that may develop on the plate for different gas/liquid loadings. An elaborate analysis of bubble formation mechanisms in stagnant and flowing liquids has been carried out by Räbiger and Vogelpohl[78,79]. According to this analysis, the balance of forces acting on a bubble forming at an orifice and immersed in a flowing liquid is given by

$$\frac{g\Delta\rho d_B^3\pi}{12}\left[2-3\left(\frac{d_h}{d_B}\right)^2\right]=d_h\sigma\pi+c_w\rho_L K\frac{d_B^2\pi}{8}\times \left[2\left(\frac{\dot{V}_g}{A_H}-v_L\right)\left(\frac{d_h}{2d_B}\right)+v_{Bo}\right]^2 \tag{58}$$

$$v_{Bo}=\sqrt{\frac{4gd_B}{3c_{w1}}} \tag{59}$$

$$c_w=\frac{24}{Re}+\frac{4}{Re^{0.5}}+0.4 \tag{60}$$

Nomenclature for equations 58 - 63

$$v_R=2v_E+v_{Bo} \tag{62}$$

$$v_E=\left(\frac{\dot{V}_g}{A_H}-v_L\right)\left(\frac{d_h}{2d_B}\right)^2 \tag{63}$$

A_H = Hole area (m^2)

v_L = Imposed liquid flowrate (m/s)

d_B = Bubble diameter (m)

d_h = Hole diameter (m)

c_w = Drag coefficient (-)

$\dot{V}_g$ = Volumetric gas flowrate through a hole (m^3/s)

g = Acceleration due to gravity (m/s^2)

v_B = Velocity of bubble base (m/s)

v_{Bo} = Velocity of bubble base in stagnant fluid (m/s)

v_E = Expansion velocity of bubble (m/s)

v_R = Relative velocity of bubble (m/s)

$\Delta\rho = \rho_L - \rho_g$

ρ_L, ρ_g = Liquid and gas densities respectively (Kg/m^3)

K = Constant

σ = Surface tension (N/m)

The solution of equation (58) is by iteration with the following conditions.

(1) c_{w_1} in equation (59) is calculated by substituting the velocity of the bubble base, v_B, in equation (60).

(2) c_w in equation (58) is calculated by substituting the relative velocity, v_r, for Reynolds number in equation (60).

Räbiger and Vogelpohl[78,79] found that a K value of 1.5 fitted their data very well and K values of 0.45 to 1.1 were used to reproduce results of Davidson and Schüler[82,107] to within acceptable limits. Equation (58) should be very useful in predicting bubble diameters on plates which in

turn, should give an indication of the type of flow obtainable. However, the analysis in references 78 and 79 was based on pure co-current or countercurrent flow of gas and liquid and its applicability to plate columns of the crossflow type may be difficult. This difficulty, may make these equations unsuitable for use in predicting primary bubble diameters obtainable on plates.

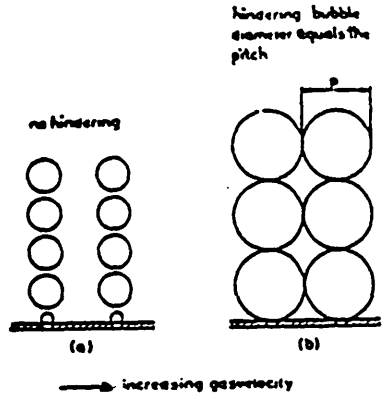

Fig. 2.5

Hindering at Simultaneous Bubble Growth

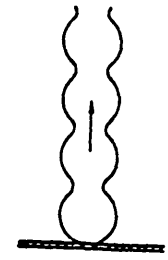

Fig 2.6

Formation of a Gas Channel

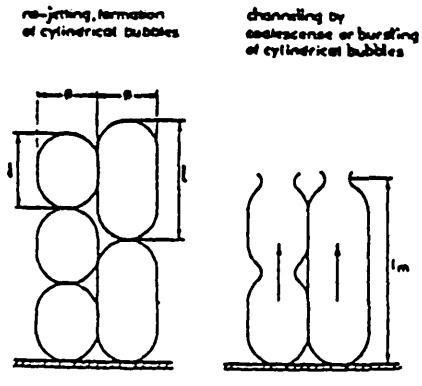

Fig. 2.7

Formation and Coalescence of Cylindrical Bubbles

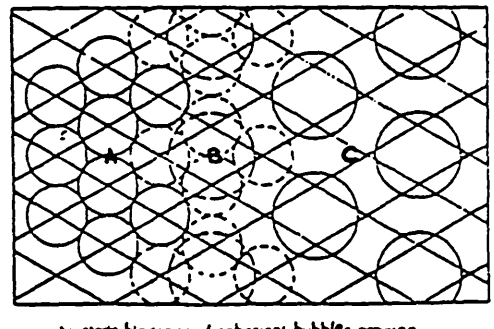

A: steric hindering of spherical bubbles growing on adjacent holes.

B: coalescence of 4 bubbles.

C: one bubble fed by 4 orifices: the hindering has disappeared.

Fig 2.8

Coalescence of Adjacent Spherical Bubbles

2.7 Analysis of Residence Time in Downcomers

Introduction

In this section, a review of literature on measurement and analysis of liquid residence time in downcomers is presented. A critical analysis of analytical methods for the evaluation of data obtained from measurements is also presented. This is used later in chapter 5 where results of the present work on liquid residence time in downcomers is presented and discussed.

When a stream of material flows steadily through a vessel such as a pipe or tank where it takes part in some process, such as a chemical reaction, heat or mass transfer or simply mixing, it is usual prctice to assume one of the following

(a) The fluid in the vessel is completely mixed, so that its properties are uniform and identical with those of the exiting stream. This assumption forms the basis of calculations on stirred tanks.

(b) Elements of fluid entering the vessel at the same time move through it with constant and equal velocity on parallel paths and leave at the same time. This assumption forms the basis of plug or piston flow.

In practice, the actual flow does not usually follow the above idealized patterns. However, the flow pattern in a real system is usually too complex to be determined fully by experiments, or theoretically from either the solution of Navier - Stokes equation or by statistical mechanical considerations. Determination of the actual residence time distribution of fluid elements in the effluent stream provides an indication of the flow and mixing patterns within the vessel. Also, it provides a starting point for the constuction of a mathematical model to simulate the actual behaviour and flow of fluid elements in the system. Thus, the age distribution (residence time distribution) function obtained experimentally serves as a strong guide for the selection of a proper model of flow within the vessel. It basically describes the length of time spent within the vessel by different elements of the inflow material before leaving the system.

Danckwerts[100] advanced the residence time distribution theory, based on the idea of an infinite number of entering streams which reside in the flow system for a certain time, so that a complete distribution of fluid residence times is produced. Taylor[102] formulated the theory of turbulent mixing by the cummulative effect of the action of many small eddy fluctuations. Danckwerts[100], Taylor[102] and Tichacek[103] developed the diffusion model for the analysis of the dispersion of a non - reacting tracer in an agitated flow process.

Recently, much interest has been focussed either on plate mixing or combined plate/downcomer mixing as a single unit. Bell[110] used the fibre optics technique to study the distribution of residence times in a commercial scale sieve plate. This method is based on the use of fibre optic probes to detect the presence of a fluorescent tracer which has a very rapid activation and decay time. From experimental information, Bell[110] concluded that there exists circulating flow near the wall of the column on the plate which may contribute to lower plate efficiencies compared to those calculated from standard equations. Thomas et al[55] used a tracer injection technique to study mixing effects on a sieve plate/downcomer system. The following conclusions were made by Thomas et al[55].

(a) Experimentally determined liquid residence time showed that liquid holdup in the plate - downcomer system increases with increasing liquid rate and also with downcomer area.

(b) Gas flowrate has no significant effect on mixing in the system considered.

(c) Extent of liquid mixing in the system increases with decrease in the height of the overflow weir.

(d) Mixing patterns are characterized by eddy diffusivities, D_E, between $1.068 \times 10^{-3} - 2.83 \times 10^{-3}\ m^2/s$.

The main criticism that can be raised against the conclusions of Thomas et al[55] centers on conclusion (b). This view may apply to either a particular regime of plate operation, or to low-foaming to non-foaming systems as is the case in their work. Also, measurement of liquid residence time on a combined plate/downcomer system may not reveal much about degrees of mixing either on the plate or in the downcomer. Before any definite conclusions can be made in this regard, it is therefore important to focus attention on the downcomer and the plate, in isolation of each other . A positive step towards the characterisation of mixing in downcomers was initiated by Welch et al[105]. They concluded that for a particular liquid flowrate, neither the gas flowrate nor the liquid physical properties had a significant effect on mixing in the downcomer. This view is in agreement with that of Thomas et al[55]. However, some short comings are apparent in their work. In their experiments, the tracer was injected on the plate near the inlet weir. Hence, it can be argued that mixing of tracer on the plate will completely obscure mixing effects in the downcomer. Their analysis of the resulting data was based on the dispersion model as it gave both physical representation of mixing and a convenient means of data analysis. Baker and Self[111] determined mixing patterns on a sieve plate and correlated their results in terms of gas rate and plate liquid holdup according to the relation

$$D_E = 0.01298 u_g^{1.44} + 0.3024 h_L - 0.0605 \qquad (64)$$

Where

D_E = Eddy diffusivity (ft^2/s)

u_g = Gas superficial velocity (ft/s)

h_L = Plate liquid holdup (ft)

Equation (64) is valid for plate liquid holdups between $0.75 - 3.5\ ft$ and gas superficial velocities between $1.0 - 4.0\ ft/sec$. The results of Baker and Self[111] is at variance with other studies[55,105] and shows a dependence of plate mixing on both liquid and gas rates.

In the present work, these effects on mixing in downcomers for foaming and non-foaming systems are investigated. Also, the work on liquid residence time is set out to develop an appropriate way of studying mixing or determining liquid residence times in downcomers in isolation of the plate. This and other aspects of measurement of liquid residence time in the downcomer is presented and discussed in chapter 4.

2.7.1 Probabilistic Representation of Residence Time Distribution Functions

In treating residence time distributions in any system, it is often easy to represent the distribution functions as probability density functions. Consider figure 2.9 which shows the response of the exit concentration of a tracer to an impulse input $\delta(t)$.

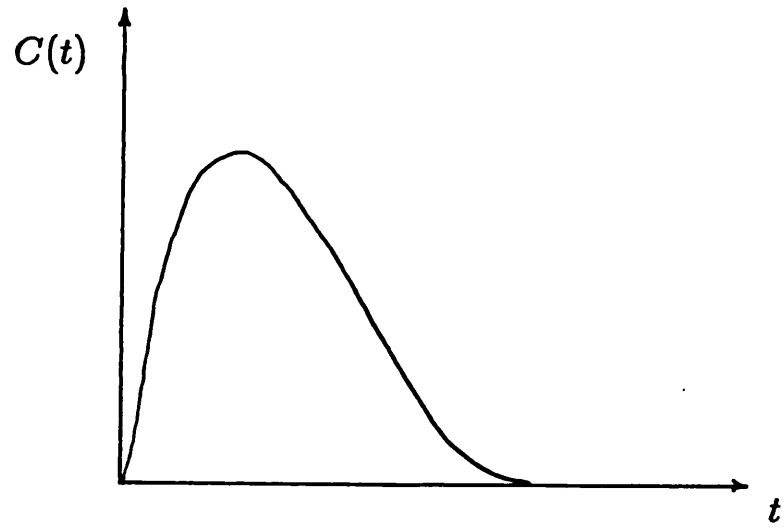

Figure 2.9 :- Typical Response to an Impulse Input

The total area under the curve is given by

$$E' = \int_0^\infty C dt \tag{65}$$

Hence the exit density function (E-function) can be defined for any time, t, as

$$E(t) = \int_0^t C dt \tag{66}$$

The probability density function requires that

$$\int_0^\infty E(t)dt = 1.0 \tag{67}$$

With respect to the condition of equation (67), the exit distribution function can be scaled to conform to this condition. Thus $E(t)$ becomes

$$E(t) = \frac{\int_0^t C(t)dt}{\int_0^\infty C(t)dt} \tag{68}$$

which gives the probability, $E(t)$, of an element of fluid in the exit strem having a residence time between t and $t + \Delta t$. This is represented diagramatically in figure 2.10.

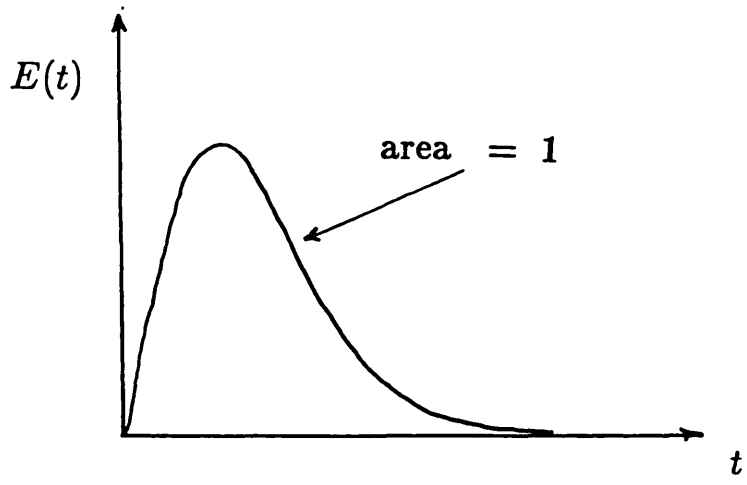

Figure 2.10 :- Probability Representation of Exit Density Function

2.7.2 Comparison of Age Distribution Curves

As mentioned in Section 2.7, the age distribution function may be used as supporting evidence to the selection and validity of any proposed model. In comparing the age distribution of a synthetic flow system with experimental data, the moments of the distribution curve may be matched. Since any probability distribution function may be completely defined by its moments, it is often convenient to compare the moments of the distributions rather than matching the spread of the entire distribution curve. The n^{th} moment, M_n, of the probability density distribution, $E(t)$, with respect to a point α, for non-negative values of t is defined as

$$M_{n\alpha} = \int_0^\infty \left(t - \alpha\right)^n E(t)dt \tag{69}$$

$$Where \quad n = 0,\ 1,\ 2 \ldots N$$

The first moment about the origin is commonly called the mean of the distribution, μ_1, given as

$$\mu_1 = \int_0^\infty t\, E(t)\, dt \tag{70}$$

The second moment about the mean is normally refered to as the variance, σ_1^2, defined as

$$\sigma_1^2 = \int_0^\infty \left(t - \mu_1\right)^2 E(t)\, dt \tag{71}$$

The third moment about the mean is normally called the skewness and defined as

$$\gamma^3 = \int_0^\infty \left(t - \mu_1\right)^3 E(t)\, dt \tag{72}$$

In general, in order to completely characterize an arbitrary probability density function, all moments are required. However, it is sufficient for all practical purposes to employ the first three moments in any tracer analysis.

Summary

The concepts introduced and the equations presented in this section are used to analyse experimental residence time data obtained in this work. The results of these analysis are presented and discussed in chapter 5.

2.8 Experimental and Analytical Techniques

Introduction

In this section attention is given to methods of measuring dispersion density and bubble diameter in any gas - liquid dispersion. This will give an insight into the different measurements undertaken in this work to characterize the two phase mixture either in the downcomer or on the plate. Different methods of measuring dispersion density exist of which the most widely used ones are pressure drop measurements and gamma densitometry. The gamma densitometry method which is used in this work, is more accurate than the other methods and very easy to use, hence most of the discussion is based on this method.The principles underlying this method is discussed in Section 2.8.1. Methods available for the measurement of bubble diameters are presented and discussed in Section 2.8.2. The underlying principles behind the method used in this work, **Light Transmission Technique** , are presented and discussed in Section 2.8.2.1. The results of the use of these methods of measurements are presented in chapter 5.

2.8.1 Gamma Ray Densitometry

The use of gamma rays to detect changes in level and the position of an interface is a well known technique. Abundant literature on the

use of gamma rays is available and many workers have used this technique for the determination of liquid holdup and density of gas - liquid dispersions[54]

2.8.1.1 Principle of Gamma Ray Densitometry

The technique is based on the principle that the absorption of a parallel mono-energetic beam of gamma radiation by a homogeneous medium of density, ρ_m, and thickness, x, is described by an exponential law similar to Lambert's law for parallel monochromatic light.

$$I = I_o e^{-\rho_m \mu x} \tag{73}$$

Where

I_o = Intensity of incident radiation

I = Intensity of transmited radiation

x = Thickness of the medium

ρ_m = Density of the homogeneous medium

μ = Mass absorption coefficient of the medium

The mass absorption coefficient, μ, depends on the radiation energy, the atomic number of the absorbing medium, and its capture cross-

section per unit mass. When applying equation (73) to the measurements in gas-liquid dispersions, it is essential that large fluctuations in density do not occur during the period of measurment to avoid the detector recording the mean of several exponential fluctuations and not the exponential density. The number of counts, N, recorded in a fixed time, or the time, t, taken to record a fixed number of counts gives a measure of the intensity of the transmitted beam. Thus, the intensity of the transmitted beam is directly proportional to the number of counts in a fixed time and inversely proportional to the time taken to record a fixed number of counts. In most cases, it is always better to use the time measurments (i.e time taken to record a fixed number of counts). Now since $I \propto 1/t$, then,

$$\frac{1}{t} = \frac{1}{t_o} e^{-\rho_m \mu x} \tag{74}$$

$$\Rightarrow \quad ln\, I = ln\, I_o + \mu \rho_m\, x \tag{75}$$

This analysis leads to a simple experimental procedure for measurement of dispersion density. The intensity of the transmitted radiation is measured as the time taken to to record a fixed number of counts. This time is measured for both the empty column (filled with gas), (t_o) and

filled with liquid (t_1). A straight calibration line is then drawn on a semi-logarithmic paper through these points ($ln\, t_o,\ \rho_m = 0\ and\ ln\, t_1,\ \rho_m = 1$). The liquid fraction is then determined by measuring the time taken to record the fixed number of counts and reading the dispersion density directly from the calibration chart.

2.8.2 Measurment of Bubble Diameters

Introduction

Bubble/drop sizing in gas-liquid and liquid-liquid dispersions is important for the evaluation of mass transfer coefficients. It also provides better understanding of mass transfer and interfacial phenomena in most systems where two different phases (gas and/or liquid) are being contacted. Different techniques exist by which bubbles/drops can be sized, namely, the **Photographic, Light Transmission, Drop Stabilisation, Conductivity, Chemical, Scintillation and Light Scattering** techniques. Amongst these techniques, the **Photographic, Chemical and Light Transmission** techniques are the most widely used in drop/bubble sizing. A comprehensive and comparative evaluation of these major techniques is given by Landau et al[61]. The chemical method is still the only one which can yield from a single measurement, an overall average of active interfacial area. It is based solely on the utilization of a chemical reaction between the phases contacted and with a well established kinetics of a certain type[73]. However, it suffers from

the disadvantage that a suitable chemical reacting component has to be used[73] and also that measurements of interfacial area are system specific. Hence, for most gas-liquid or liquid-liquid contacting schemes in which there is no primary chemical reaction between the phases, it requires the introduction of another component. This may not really reflect the conditions considered and therefore may give wide deviations of interfacial areas, and hence, also of mass transfer coefficients from expected or real values.

The photographic technique gives good results for all ranges of interfacial areas measured. Also, it yields bubble/drop size distributions for the system considered. However, it has been shown that the results obtained by this technique are subject to serious uncertainties depending on the properties of the system investigated as well as on the manner of taking photographs[61].

The light transmission technique has shown very attractive qualities for use in bubble/drop sizing in most gas-liquid and liquid-liquid dispersions. Here, only a small amount of time is required per experiment (experimentation and analysis of results) as compared to the photographic technique. Also instrumentation required for experimental setup is quite simple and straightforward. The direct applicability of this technique has until recently been limited to conditions where multiple scattering is negligible.

2.8.2.1 Light Transmission Technique

The most widely used theory for light transmission through liquid-liquid and gas-liquid dispersions was developed by Calderbank[59]. Here a dispersion of uniform drop size was assumed and used in the analysis. An elaborate presentation of the theory is given by Calderbank[59]. This theory for monosize systems was extended to polydisperse systems by McLaughlin and Rushton[60] and the results were in perfect agreement with the work of Calderbank[59]. The relation due to Calderbank[59] is

$$\log\left(\frac{I_o}{I}\right) = \frac{K\,A\,L}{9.21}$$
$$ln\left(\frac{I_o}{I}\right) = \frac{K\,A\,L}{4} \qquad (76)$$

Where

A = Interfacial area per unit volume (m^2/m^3)

L = Path length or thickness of medium (m)

I_o = Intensity of incident light (cd)

I = Intensity of transmited light (cd)

K = Constant (function of ratio of refractive indices of continuos and dispersed phases ≈ 1.0

The use of equation (76) is restricted to the existence of the following conditions.

(a) Transparent continuos phase

(b) Random drop/bubble locations

(c) Drops/bubbles greater than 0.1mm in diameter

(d) The light source emits an incoherent parallel beam

(e) No concave drop/bubble surfaces

(f) The detector receives only parallel light (no multiple scattering)

(g) AL values are less than or equal to 20

(h) The path length should not be too large, presumably not greater than 0.1m.

In most systems considered, conditions (a) – (e) are usually satisfied in practice, but the remaining conditions present most of the problems usually associated with this technique. In a recent study by Lockett and Safekourdi[72], they were able to obtain a linear relationship between I_o/I and AL values up to AL value of 27 for a path length of 0.072m. This indicates that the critical AL value for which equation (76) remains linear is not limited to 20. Al Taweel et al[64] have shown that the critical AL value for which equation (76) remains linear is a linear function of the path length. They arrived at this conclusion through a study of the use of light transmission technique to determine interfacial areas of Kaolin suspensions, using path lengths ranging from 0.0244m to 0.165m. The relation due to Al Taweel et al[64] is

$$AL_{cr} = 27 + 2.1L$$
$$AL_{cr} = Critical\ AL\ value \tag{77}$$

A combination of equations (76) and (77) can be used when the fraction of light scattered is negligibly small compared to that transmitted in the dispersion for drop/bubble sizing. To account for multiple scattering, Landau et al[63] proposed a simple model of the form

$$AL = \frac{4\,ln\left(I_o/I\right)}{1-\phi\,(AL)} \tag{78}$$

which was derived from the two flux solutions of the equation of scattering and absorption. The function, $\phi(AL)$, is the multiple scattering correction parameter. According to Landau et al[63], the following attributes are to be expected of $\phi(AL)$.

(1) The quantity $1-\phi(AL)$ should decrease with increasing AL.

(2) The expression $AL\,(1-\phi(AL))$ should be a continuosly increasing function of AL and should vanish as AL approaches zero.

Hence to satisfy the above conditions, they[63] proposed a model for $\phi(AL)$ according to the relation

$$\phi\,(AL) = 1 - \frac{K_1}{AL}\left[1 - e^{-K_2 AL}\right] \tag{79}$$

Using equation (79) and their experimental data, they obtained the following relation which compensates for multiple scattering.

$$AL = -\,17.1674\,ln\left[1 - \frac{ln(I_o/I)}{6.59}\right] \tag{80}$$

Application of equation (80) to their experimental data gave an error of 5% as reported[63]. On the other hand, application of this equation to the data of Lockett and Safekourdi[62] does not give any meaningful result as the right hand side of equation (80) does not exist†. The same findings follows on application of equation (80) to the data of Al Taweel et al[64].

In their analysis, Al Taweel et al[64] incorporated the effect of path length in the form of equation (79) proposed by Landau et al[63] given as

$$\phi(AL) = 1 - \left[\frac{K_1}{AL^{K_2}}\right]\left[1 - e^{-K_3 AL}\right] \tag{81}$$

† *The logarithm of a negative number does not exist mathematically*

Using equations (81) and (79) and the data obtained from their experimental work, Al Taweel et al[64] obtained the following empirical relations for evaluating large interfacial areas in gas -liquid dispersions.

$$AL = -36.2ln\left[1 - \frac{ln(I_o/I)}{6.795L^{0.12}}\right] \qquad (82)$$
$$32 < AL \leq 280$$

$$AL = -29.9ln\left[1 - \frac{ln(I_o/I)}{6.433L^{0.147}}\right] \qquad (83)$$
$$280 < AL \leq 360$$

The application of equations (82) and (83) was reported[64] to yield an error of less than 5%. However, application of equations (82) and (83) to the data of AL Taweel[64] obtained from their experimental data does not give any meaningful result as the right hand side of equations (82) and (83) does not exist†. Using the data of Al Taweel et al[64] and the the theories of Al Taweel et al[64] and Landau et al[63], Urua and del Cerro[95] proposed the following equation for use when the fraction of light scattered becomes significant.

$$AL = -40.0ln\left[1 - \frac{ln(I_o/I)}{21.4075L^{0.112}}\right] \qquad (84)$$
$$32 < AL \leq 280$$

† *Logarithm of a negative number does not exist mathematically*

Equation (84) was shown to fit the data of Al Taweel et al[64] to within 5%.

From equations (76),(77) and (84) AL values can be calculated which can then be used to obtain values of interfacial area per unit volume, A.

2.8.2.2 Sauter Mean Diameter

The Sauter mean diameter of the bubbles in the dispersion can be calculated by a combination of results of sections 2.8.1 and 2.8.2. This is given by

$$d_{32} = \frac{6\epsilon}{A} \tag{85}$$

Where

$\epsilon = 1 - \epsilon_L$ = gas fraction in the dispersion

d_{32} = Sauter mean diameter (m)

A = Interfacial area per unit volime (m^2/m^3)

CHAPTER 3

FORMULATION OF MODELS

Introduction

In this chapter, the models of liquid residence time in the downcomer, foam/froth behaviour in the downcomer and froth/foam flow and behaviour on the plate are presented and discussed. Section 3.1 deals with the derivation of a model of liquid mixing in the downcomer. Theoretical studies of foam/froth behaviour and/or flow in the downcomer is presented and discussed in section 3.2. Section 3.3 deals with theoretical studies of froth behaviour on the plate. The resulting equation(s) from this chapter are used in chapter 5 and where necessary compared with experimental results.

3.1 Residence Time Distribution Model

A number of models were tested to chracterize the flow pattern in the downcomer. The following are some of the models proposed and tested on the experimental data obtained.

(a) Mixed tank in series with a dead volume.

(b) N-mixed tanks in series.

(c) Mixed tank with bypass, in series with a dead volume.

(d) N-mixed tanks in series with bypass, in series with a dead volume.

(e) Gamma mixing (described by gamma distribution function)

(f) Mixed tanks in series with plug flow

(g) Dispersion model, with axial dispersion only

Amongst all these models, model, (g), fitted the dispersion in the downcomer well. The mathematical description of this model is presented in Section 3.1.1 and the results obtained are tested against experimental data in chapter 5.

3.1.1 The Dispersion Model

Consider a flow system with axial dispersion of fluid elements as shown in figure 3.1.

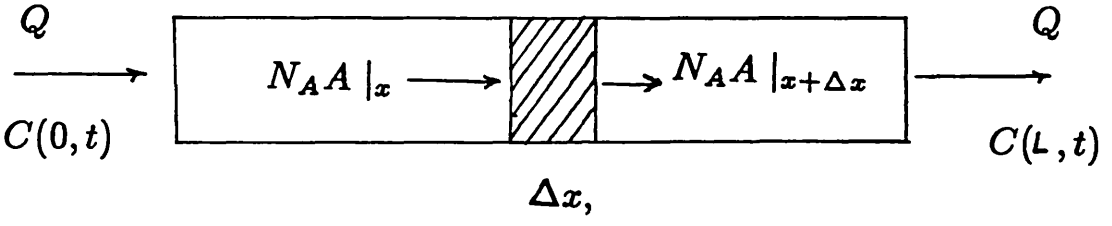

Figure 3.1 Schematic Diagram of Flow System

A material balance on an element of fluid of thickness, Δx, gives

$$QC(x,t) + N_A A\,|_x - QC(x+\Delta x,t) - N_A A\,|_{x+\Delta x} = A\Delta x \frac{\partial C}{\partial t} \quad (86)$$

Where

A = Crossectional area perpendicular to flow (m^2)

$C(x,t)$ = Tracer concentration at any point, x, and time, t, (Kg/m^3)

N_A = Mass flux $= -D_E \partial C/\partial x$ $(Kg/m^2 s)$

D_E = Effective axial dispersion coefficient (m^2/s)

Q = Volumetric liquid flowrate (m^3/s)

Assume perfect mixing of fluid in the y and z directions. This assumption is validated by experimental data reported in chapter 5. Collecting terms in equation (86) and taking limits as Δx tends to zero,

$$\frac{\partial}{\partial x}\left(D_E \frac{\partial C(x,t)}{\partial x}\right) - \frac{Q}{A}\frac{\partial C(x,t)}{\partial x} = \frac{\partial C(x,t)}{\partial t} \quad (87)$$

In this equation, Q/A equals the linear liquid velocity, which in this particular case, is equal to the interstitial liquid velocity. It should be recognised that the formulation of equation (87) is based on average

properties of $D_{\underline{E}}$ and interstitial liquid velocity. Hence it can be transformed into the form

$$D_E \frac{\partial^2 C(x,t)}{\partial x^2} - u \frac{\partial C(x,t)}{\partial x} = \frac{\partial C(x,t)}{\partial t} \tag{88}$$

Equation (88) may be solved for two different sets of boundary conditions, corresponding to

(i) Semi - infinite model

(ii) Infinite model

Semi - Infinite Model

The boundary conditions here, for an impulse tracer input of duration, β, are

$$C(x,0) = 0 \qquad all\ x \tag{a}$$

$$\lim_{x \to \infty} C(x,t) = 0 \tag{b}$$

$$C(0,t) = \frac{A^*}{(Q\beta + V^*)} = A^{**} \qquad 0 < t \leq \beta \tag{c}$$

$$C(0,t) = 0 \qquad t > \beta \tag{d}$$

The parameters A^* and V^* denote the mass and volume of the tracer injected, respectively. For all practical purposes, and for β very small, $Q\beta \gg V^*$ for $0 < \beta \ll 1$. Hence, the boundary condition (c) can be rewritten as

$$C(0,t) = \frac{A^*}{Q\beta} \qquad 0 < t \leq \beta \tag{e}$$

Taking Laplace transforms in equation (88) gives

$$D_E \frac{d^2\overline{C}}{dx^2} - u\frac{d\overline{C}}{dx} = s\overline{C} - C(x,0) \tag{89}$$

Where $\overline{C}$ = Laplace transform of C = $L\{C\}$

Using boundary condition (a), equation (89) becomes

$$D_E \frac{d^2\overline{C}}{dx^2} - u\frac{d\overline{C}}{dx} = s\overline{C} \tag{90}$$

The general solution of equation (90) is of the form

$$\overline{C} = Aexp\left[\frac{\frac{u}{D_E} + \sqrt{\left(\frac{u}{D_E}\right)^2 + \frac{4s}{D_E}}}{2}\right] x + Bexp\left[\frac{\frac{u}{D_E} - \sqrt{\left(\frac{u}{D_E}\right)^2 + \frac{4s}{D_E}}}{2}\right] x \tag{91}$$

with A, B = constants

Boundary condition (b), in Laplace transforms, is of the form,

$$\lim_{x\to\infty} \overline{C}(x,t) = 0$$

$$Similarly,\ L\{C(0,t)\} = \overline{C}(0,s)$$

Incorporating these boundary conditions in equation (91) the constants A and B can be calculated as $A = 0$ and $B = \overline{C}(0,s)$ and hence,

$$\overline{C} = \overline{C}(0,s)exp\left[-\left(\sqrt{\frac{u^2}{4D_E^2} + \frac{s}{D_E}} - \frac{u}{2D_E}\right)\right] x$$

$$= \overline{C}(0,s)\left[exp\left(\frac{ux}{2D_E}\right)exp\left[-x\sqrt{\frac{u^2}{4D_E^2}+\frac{s}{D_E}}\right]\right]$$

$$= exp\left(\frac{ux}{2D_E}\right)\left[\overline{C}(0,s)exp\left(-x\sqrt{\frac{h+s}{D_E}}\right)\right] \tag{92}$$

$$Where\ h = \frac{u^2}{4D_E}$$

Taking inverse Laplace transfom of equation (92),

$$L^{-1}(\overline{C}) = L^{-1}\left[exp\left(\frac{ux}{2D_E}\right)\left[\overline{C}(0,s)\,exp\left(-x\sqrt{\frac{h+s}{D_E}}\right)\right]\right] \tag{93}$$

Note that[130]

$$L^{-1}\left[exp\left(-x\sqrt{\frac{h+s}{D_E}}\right)\right] = \frac{x\,exp\left(-(ht+\frac{x^2}{4D_Et})\right)}{2\sqrt{\pi D_E t^3}} \tag{94}$$

The final solution is found by using a convolution integral as follows[130]

$$C(x,t) = exp(\frac{ux}{2D_E}) \int_0^t g(t)\, f(t-\lambda) d\lambda \qquad (95)$$

$$g(t) = L^{-1}(\overline{C}(0,s)) \;=\; C(0,t) \;=\; A^{**}$$

$$f(t) = equation \quad (94)$$

Equation (95) can be put in the form

$$C(x,t) = exp(\frac{ux}{2D_E}) \int_{t_0}^{t_0+\beta} g(t)\, f(t-\lambda)\, d\lambda$$

By the mean value theorem of integral calculus[131]

$$C(x,t) = A^{**} exp(\frac{ux}{2D_E})\, f[t - (t_0 + \alpha\beta)] \qquad (96)$$
$$0 \leq \alpha \leq 1$$

The response to a perfect pulse or an impulse is defined as

$$\lim_{\beta \to 0} C(x,t) = \lim_{\beta \to 0} A^{**} exp(\frac{ux}{2D_E})\, f[t - (t_0 + \alpha\beta)]$$

$$= A^{**} exp\left(\frac{ux}{2D_E}\right) f(t - t_0)$$

If the time is counted from the instant prior to the introduction of the pulse, the final result is expressed as

$$C(x,t) = \frac{A^{**}x}{2\sqrt{\pi D_E t^3}} exp - \left(\frac{(x-ut)^2}{4D_E t}\right) \tag{97}$$

Defining Peclet number $Pe = \varepsilon_L uL/D_E$, then a parameter, N, may be defined as

$$N = \frac{Pe}{4} \tag{98}$$

Equation (97) then becomes in dimensionless form

$$\phi(x,t) = \sqrt{\frac{N}{\pi\tau^3}} exp\left(\frac{-N(1-\tau)^2}{\tau}\right) \tag{99}$$

Where $\tau = t/t_p, \quad t_p = L/u$

Infinite Model

This is another interpretation of the physical process described by equation (88). Here, the downcomer is considered infinite on each side of $x = 0$, the point at which the impulse is introduced. Also, eddy diffusion is assumed to occur freely in both directions at $x = 0$. The solution using these conditions is given by Levenspiel and Smith[115] in terms of τ and N as

$$\phi(x,\tau) = \sqrt{\frac{N}{\pi\tau}} exp\left(\frac{-N(1-\tau)^2}{\tau}\right) \qquad (100)$$

Equations (99) and 100 shall henceforth be refered to as **dispersion model A** and **dispersion model B** respectively

Summary

In this section a model of liquid flow and mixing in the downcomer has been proposed. The axial dispersion model which is the model of liquid flow and mixing in the downcomer was solved for two boundary conditions given by equations (99) and (100) representing a semi- infinite and finite models respectively. These equations are therefore the final forms of the desired equations to be used in modelling the residence time distributions in the downcomer. The results obtained from these equations are presented and discussed in chapter 5.

3.2 Theoretical Prediction of Foam /Froth Height in Downcomers for Foaming and Non-Foaming Systems

Introduction

In this analysis, an attempt is made to analyse bubble flow in distillation and absorption column downcomers on the basis of an earlier analysis made by Barber and Wijn[9]. However, where necessary, modifications to the assumptions and/or analytical techniques of Barber and Wijn[9] are made to reflect downcomer behaviour more closely.

Assumptions of Barber and Wijn[9]

The following assumptions were made by Barber and Wijn[9].

(1) Bubble coalescence in the system is strictly a binary process.

(2) Liquid fraction in the system does not vary markedly with height of the froth or foam. This is a consequence of experimental information.

(3) The flow of gas through the system is due to bubble motion in the froth or foam only.

(4) Gas and liquid residence times in the system are equal.

(5) The radius of the film separating two bubbles is approximately equal to 30% of the bubble diameter.

The analysis of Barber and Wijn[9] centered on the consideration of the coalescence of bubbles in the dispersion such that a critical diameter is achieved whereby the bubble is just big enough to rise against the downward liquid flow. When this critical bubble diameter is achieved, the bubbles were assumed to leave the dispersion immediately. Under this scenario, it is possible for small bubbles to be entrained in the liquid stream leaving the bottom of the downcomer. The point of disagreement with the assumptions of Barber and Wijn[9] is with assumptions (3) and (4). From the above, it is implicit that at the critical bubble diameter, the velocity of the bubble is zero with reference to a fixed reference frame. Assumption (4) implies

$$\frac{u_{gd}}{\epsilon} = \frac{u_{Ld}}{1-\epsilon} \tag{101}$$

Where

u_{gd} = Gas superficial velocity (m/s)

u_{Ld} = Liquid superficial velocity (m/s)

ϵ = Gas holdup fraction (-)

If assumptions (3) and (4) of Barber and Wijn[9] are combined, then equation (101) cannot hold. Assumption (1) is quite acceptable since any other form of bubble coalesecence can be defined firstly from binary

coalescence data. It has been shown[7] that if foam bubbles are described by the regular dodecahedra model with pentagonal sides, then the radius of the film separating the bubbles is equal to 30% of the equivalent spherical diameter of the bubbles, hence assumption (5).

Formulation of model

Known Conditions

(1) Clear liquid at the bottom of the downcomer.

(2) Gas flow at the top of the downcomer.

These two conditions implies that there is a net upward flow of gas and a net downward flow of liquid in the downcomer. The mode of flow of gas in the downcomer may be in the form of gas bubbles and/or gas.

(3) No gas entrained in the liquid stream.

(4) No liquid entrained in the gas stream.

The above four conditions suggest that the whole operation can be visualised and simulated as countercurrent gas-liquid flow on a net basis.

Present Assumptions

(1) Bubble coalescence in the system is considered strictly as a binary process.

(2) Liquid fraction in the downcomer does not vary appreciably with height of foam or froth.

(3) Gas and liquid residence times in the downcomer are approximately equal.

(4) The radius of the film separating the bubbles can be approximated to 30% of the equivalent spherical bubble diameter.

Analysis

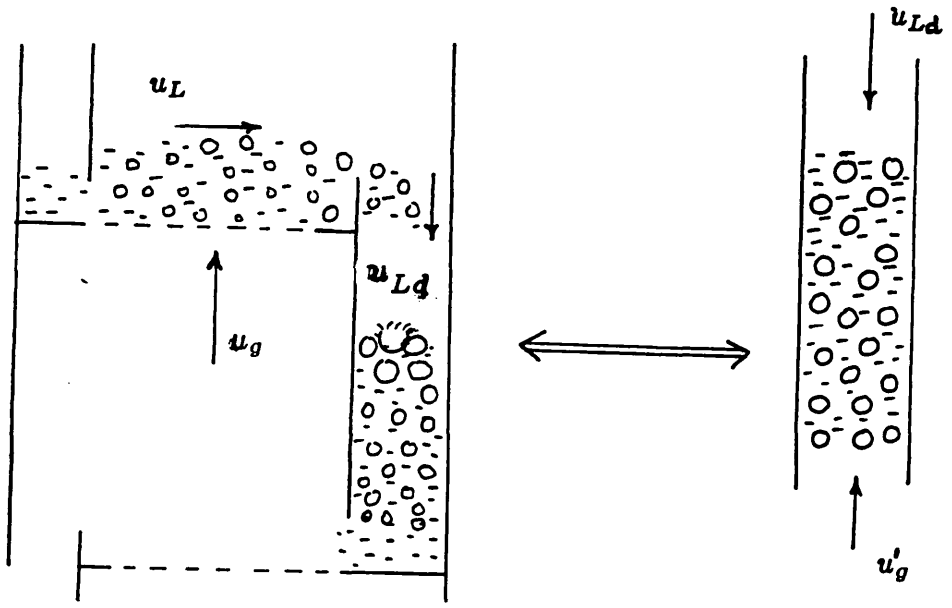

Figure 3.2 Schematic Diagram of Froth Flow in the Downcomer

In this analysis, it shall be futher assumed that gas disengagement in the downcomer is important and occurs only at the top of the froth or foam. This is achieved by bursting or breaking of the bubbles at the gas-liquid interface. For bubbles, generally, there will be a critical diameter above which all bubbles will disengage at the upper interface. In the present case, envisage a bubble impinging on the fluid-gas interface. If the bubble has reached the critical diameter, it will break, else it will be swept into the dispersion to a certain distance whereby buoyancy

compensates the downward momentum of the liquid. Visualize the coalescence of bubbles in the dispersion. As the bubble diameter increases, the bubble rises futher in the dispersion under the prevailing conditions. As coalescence progresses, the bubble keeps rising until it attains the critical diameter at which stage it is then at the top of the dispersion. From the above, the rate limiting step is the coalescence time required by the bubbles to reach the critical diameter. Since we are dealing with a dense dispersion, it shall be further assumed that the probability of a single collision of two bubbles leading to coalescence is unity. Also for this analysis, only coalescence between bubbles of similar diameters shall be considered an important contribution to the total coalescence time required to achieve the critical diameter.

On the basis of the critical diameter, define an average hypothetical velocity of gas due to bubble upward motion that will exactly transform the system into a countercurrent system with the same average holdup fraction, froth height and liquid velocity.

3.2.1 Bubble Escape Diameter

The bubble rise velocity relative to the liquid, u_s, in any dispersion may be related to the actual superficial velocities of the phases contacted through the holdup fraction, (ϵ). In particular, for countercurrent bubbly flow, this relation is given by[121]

$$u_{Ld}\epsilon + (1-\epsilon)u_{gd} = u_s\epsilon(1-\epsilon) \qquad (102)$$

It has been shown by Taitel and Barnea[116] that countercurrent gas-liquid bubbly flow is limited to void fractions not greater than 0.3 for non-foaming systems. For most of the results for the non-foaming system in this work, this condition is fully satisfied †. However for the foaming systems, there are as yet no information as regards limits of occurence of the bubbly flow regime. Hence it shall be assumed that for systems that foam, bubbly flow regime can occur for void fractions greater 0.3. Combining equations (101) and (102) gives

$$u_s = \frac{2u_{Ld}}{(1-\epsilon)} \tag{103}$$

Generally, the relative rise velocity of the bubbles, u_s, is related to the holdup fraction according to the relation

$$u_s = u_0(1-\epsilon)^n \tag{104}$$

Where

u_0 = Bubble free rise velocity (m/s)

n = Index (Generally function of Reynolds number)

† *See Chapter 5*

For air bubbles in the region of 5 to 10mm† in diameter, the free rise velocity is given as[121]

$$u_0 = 0.71\left(\frac{g D \Delta\rho}{\rho_L}\right)^{0.5} \quad (105)$$

Where

D = Bubble diameter (m)

g = Acceleration due to gravity (m/s^2)

ρ_L = Liquid density (Kg/m^3)

ρ_g = Gas density (Kg/m^3)

$\Delta\rho = \rho_L - \rho_g \qquad (kg/m^3)$

Replacing equations (104) with $n = 1$, and (105) into (103) gives

$$D = \frac{8\rho_L u_{Ld}^2}{\Delta\rho g(1-\epsilon)^4} \quad (106)$$

3.2.2 Bubble Residence Time

Assume that bubbles enter the foam or froth with a diameter, d, and that after a single collision, a single bubble of twice the volume of the

† *See chapter* 5

colliding bubbles is formed. If it is futher assumed that the coalescence probability is unity, the number of coalescenes, N, required to increase the bubble diameter from d to D is given as

$$N = \quad 4.33ln\left(\frac{D}{d}\right) \tag{107}$$

The assumption that the coalescence probability is unity is realistic since here we are dealing principally with bubble swarms.

The time, t, for a circular film of radius, r, between two bubbles to drain to its rupture thickness, δ_c, may be calculated using the Reynolds equation[117]

$$t \quad = \quad \frac{3\pi\eta r^4}{2F\delta_c^2} \tag{108}$$

Where

η = Viscosity of liquid (Ns/m^2)

F = Force pressing the bubbles together (N)

δ_c = Critical film thickness (m)

r = Film radius (m)

Incorporating assumption (4) into equation (108) gives

$$t = \frac{0.038\eta d^4}{F\delta_c^2} \tag{109}$$

In reality, equation (109) does not represent the total time required for the film to drain to its rupture thickness as there are dilatational effects especially with the pressence of surfactants. Radöev et al[122] considered the increase in surface tension caused by the expansion of an element of the film surface due to its movement towards the periphery and the compensating effect of diffusion of surfactant molecules from the bulk in an attempt to restore the equilibruim surface concentration and tension. The surface tension gradients set up in this way tend to retard the drainage of the film and consequently stabilize the foam. Ignoring surface diffusion, the authors[122] propose the following equation for the rate of film thinning.

$$\frac{d\delta}{dt} = \left(\frac{d\delta}{dt}\right)_R \left[1 + \frac{3D_s\eta(1+Bc)^2}{RT\Gamma_\infty^2 B^2 c}\right] \tag{110}$$

Where

$\left(\frac{d\delta}{dt}\right)_R$ = Thinning rate given by Reynolds equation

D_s = Surfactant diffusivity in bulk solution (m^2/s)

c = Surfactant concentration $(Kmol/m^3)$

B = Constant derived from Szyskowski's equation

R = Gas constant $(J/Kmol\ K)$

T = Temperature (K)

Γ_∞ = Equilibruim surface concentration of surfactant $(\frac{Kmol}{m^2})$

η = Bulk liquid viscosity (Ns/m^2)

Generally, surfactant adsorption conforms to the Lagmuir isotherm, with the surface excess given by[122]

$$\Gamma = \frac{\Gamma_\infty B c}{1 + Bc} \tag{111}$$

and also the Szyskowski's equation

$$\sigma = \sigma_o - \Gamma_\infty RTln(1 + Bc) \tag{112}$$

Where the parameters of equations (111) and (112) are as defined for equation (110), with σ and σ_o representing surface tension at any concentration and at zero surfactant respectively. Combining equations (109) and (110) gives the time required for the thinning of films to the rupture thickness, δ_c, as

$$t = \frac{0.038\eta d^4}{F\delta_c^2}\left[\frac{RT\Gamma_\infty^2 B^2 c}{RT\Gamma_\infty^2 B^2 c + 3D_s\eta(1+Bc)^2}\right] \qquad (113)$$

Denoting the term in square brackets of equation (113) as B^* gives

$$t = \frac{0.038\eta d^4 B^*}{F\delta_c^2} \qquad (114)$$

In order to apply equation (114) to turbulent dispersions, an expression for F, is needed. Assuming that the eddies responsible for coalescence belong to the inertial subrange, then[117,129]

$$F \approx \rho_L E^{2/3} d^{8/3} \qquad (115)$$

$$\Rightarrow \quad t = \frac{0.038\,\eta\, d^{4/3}\, B^*}{\rho_L\, E^{2/3}\, \delta_c^2} \qquad (116)$$

E = Rate of energy dissipation per unit mass

The total coalescence time, T, in the foam or froth is the sum of the N-coalescence times required to raise the bubble diameter from d to D. The k^{th} coalescence time, t_k, is given as

$$t_k = \frac{0.038\,\eta\,1.36^k\,d^{4/3}\,B^*}{\rho_L\,E^{2/3}\,\delta_c^2} \qquad (117)$$

Summing the series of equation (117) from $k = 0$ to $k = N - 1$ and noting that for N sufficiently large, 1.36^N is much greater 1, the following equation is obtained.

$$T = \frac{0.1056\,\eta\,1.36^N\,d^{4/3}\,B^*}{\rho_L\,E^{2/3}\,\delta_c^2} \qquad (118)$$

Substituting the expression for D (equation 106) and the expression for N (equation 107) in equation (118) gives

$$T = \frac{1.678\,\eta\,u_{Ld}^{2.67}}{\rho_L\,E^{2/3}\,\delta_c^2\,(1-\epsilon)^{5.33}}\left(\frac{\rho_L}{\Delta\rho g}\right)^{1.33} B^* \qquad (119)$$

3.2.3 Foam / Froth Height

Using the residence time assumption of section 3.2 gives

$$H_f = \frac{T \times u_{Ld}}{1-\epsilon} \qquad (120)$$

$$\Rightarrow H_f = \frac{1.678\,\eta\,u_{Ld}^{3.67}}{\rho_L\,E^{2/3}\,\delta_c^2\,(1-\epsilon)^{6.33}}\left(\frac{\rho_L}{\Delta\rho g}\right)^{1.33} B^* \qquad (121)$$

3.2.4 Rate of Energy Dissipation per Unit Mass (E)

In order to be able to use equation (121), a good estimate of the rate of energy dissipation per unit mass, E, must be obtained. For a downcomer system, the only energy input is in the feed stream with a velocity of say, v_i and a kinetic energy per unit mass, $v_i^2/2$. This energy is dissipated mainly in the largest eddies with dimensions similar to the downcomer width, W. The characteristic time of these eddies is given as[129]

$$t^* = \frac{W^{2/3}}{E^{1/3}} \qquad (122)$$

Hence, an estimate of the rate of energy dissipation per unit mass is given as

$$E = \frac{v_i^3}{2.83W} \qquad (123)$$

The crest of liquid over the weir in a plate -downcomer system is given as

$$h_{ow} = 0.75\left(\frac{Q}{lw}\right)^{2/3} \qquad equation(29)$$

with h_{ow} given above in meters

Hence the inlet velocity of the two phase mixture in the downcomer can be expressed as

$$v_i = \frac{Q}{h_{ow} l_w} \qquad (124)$$

Replacing equations (29) and (124) into (123) gives

$$E = 0.84 u_{Ld} \qquad (125)$$

3.2.5 Value of B^*

Recall that B^* is given by the relation

$$B^* = \frac{RT\Gamma_\infty^2 B^2 c}{RT\Gamma_\infty^2 B^2 c + 3D\eta(1 + Bc)^2} \qquad (125a)$$

For water/n-pentanol and water/n-butanol systems, Γ_∞ was found to be 8.33×10^{-9} and 6.25×10^{-9} $Kmols/m^2$ respectively†. The diffusivities of n-pentanol and n-butanol in water are 7.734×10^{-10} and 8.8694×10^{-10} m^2/s respectively.† The values of B for n-pentanol and n-butanol are 30.77 and 22.54 respectively.† For experimental concentrations of 0.1188 $Kmols/m^3$ n-pentanol and 0.322 $Kmols/m^3$ n-butanol, the values of B^* are 0.999 and 0.988 respectively. For pure water, since water does not diffuse in water, $B^* = 1.0$. In reality, it is expected that for dilute aqueous systems, B^* should lie very close to 1.0. For these systems, it is realistic to use the value of $B^* = 1.0$ in all the analysis†. This might not be the case for non-aqueous systems where B^* can take any value between zero and unity ($0 < B^* \leq 1.0$).

3.2.6 Film Thickness

Generally, the critical film thickness is quoted[117] to lie between $10 - 100nm$. This is the case for static systems where a gas is bubbled through a stagnant pool of liquid. For a system in which there is flow of liquid and gas simultaneously, a different picture may be painted. Here, the critical film thickness may lie outside this range due to the effect of liquid flow through the dispersion. Basically, the bubbles in this type of system may actually break before the films drain to their critical thickness. Also, in a dynamic system, it will be unrealistic to assume that the bubbles have enough time to drain to their critical film thicknesses. Since there

† *See Appendix B*

is no simple way of determining this parameter from first principles, it is necessary to resort experimental data to determine the variation of critical film thickness with interstitial liquid velocity, and then test the applicability of this approach to other results.† From the calculations shown in appendix B, it is found that the critical film thickness may be represented as a function of the interstitial liquid velocity according to the relation †

$$\delta_c^2 = A\left(\frac{u_{Ld}}{1-\epsilon}\right)^{B1} \tag{126}$$

Where

ϵ = Gas holdup fraction

A, $B1$ = Constants

The constant $B1$ is found to be 4.0 and A given as ‡

$$A = 2.249 \times 10^{-4}\left(\frac{\sigma}{\sigma_w^+}\right)^{-3} \tag{127}$$

Where

† *See Appendix B*

‡ *See Appendix B*

σ = Surface tension of solution (N/m)

σ_w^+ = Surface tension of pure water = 0.072 (N/m)

3.2.7 General Expression for Foam /Froth Height

By definition, the void fraction in the downcomer is given by ‡

$$1 - \epsilon = \frac{h_L}{H_f} \tag{128}$$

Where

h_L = Liquid holdup (cd)

H_f = Foam/froth height (cd)

ϵ = Gas holdup fraction (-)

This implies that equation (121) becomes

$$H_f = \frac{1.628\,\eta\, u_{Ld}^{3.67}\,(1-\epsilon)^4}{\rho_L\, E^{2/3}\, A\, u_{Ld}^4\,(1-\epsilon)^{6.33}} \left(\frac{\rho_L}{\Delta\rho g}\right)^{1.33} B^*$$

‡ *See Chapter* 5

$$= \frac{1.628\,\eta}{\rho_L\, E^{2/3}\, A\,(1-\epsilon)^{2.33}\, u_{Ld}^{0.33}} \left(\frac{\rho_L}{\Delta\rho g}\right)^{1.33} B^*$$

$$= \frac{(\rho_L A)^{0.75}\, E^{0.5}\, u_{Ld}^{0.25}\, h_L^{1.75}}{1.3869\,\eta^{0.75} B^{*0.75}} \left(\frac{\Delta\rho g}{\rho_L}\right)$$

$$= 0.66 \left(\frac{\rho_l A u_{Ld}}{\eta B^*}\right)^{0.75} h_L^{1.75} \left(\frac{\Delta\rho g}{\rho_L}\right) \qquad (129)$$

Equation (129) proves more useful for practical applications than equation (121), since it is always easier to estimate liquid holdup in downcomers as against void fractions. Methods of determining liquid holdups in downcomers were presented in chapter 2. Results obtained from the use of equation (129) and tested against experimental data are presented and discussed in chapter 5.

3.3 Hydrodynamics of Froth Flow on Sieve Plates

Introduction

In the analysis that follows, close attention is paid to the operation of sieve plates in the frothing or foaming regimes. Fluid mechanically, this regime of plate operation is very difficult to conceptualize and describe by means of simple equations. This then explains why empirical correlations are normally used to describe this regime of plate operation. In this analysis, use is made of the concept of minimum rate of energy dissipation required for steady operation of the plate at different gas - liquid loadings. This concept was introduced by Azbel[76,88] for a theoretical evaluation of gas-liquid dispersions in bubble columns. It was later used by Kolář[97], Takahashi et al[88], Kim[94], and Unno and Inoue[99] to analyse the behaviour of froths on sieve plates. Apart from the results of the analysis by Kolář[97], the results of the analyses of the other workers do not fit experimental data satisfactorily, hence, shall not be considered futher in this section.

Analysis

Consider the froth on a sieve plate as shown in figure 3.3. The forces acting on the two phase mixture are

(1) Body forces

(2) Pressure forces

(3) Forces due to momentum change of the phases

(4) Frictional forces

(5) Surface tension forces

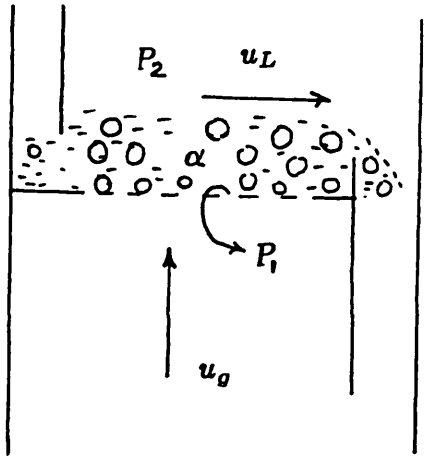

Figure 3.3 :- Schematic Diagram of Froth Flow on a Sieve Plate

Generally, for sieve plates, the area of the wall in contact with the fluid is usually very small compared to the volume of fluid in the control volume. Hence, as a first approximatiom, all forces arising due to friction will be neglected in the analysis. Similarly, because the nature of turbulence in the two phase mixture is not fully understood, all forces arising due to turbulent fluctuations in the control volume shall be neglected. The overall analysis is based on the principle that the fluid on the sieve plate is incompressible. This implies that there are no local changes in gas physical properties as it flows through the dispersion. This, for sieve plate operations, is physically realistic because pressure drop on sieve plates are generally very low and also the residence time of the gas in the two phase mixture on the plate is generally very small. Since the density of the gas is very small compared to that of the liquid, the weight of the

gaseous phase in the control volume shall be neglected. The change in the momentum of the liquid as it flows through the gas-liquid mixture on the plate shall also be neglected. This shall be explained futher through the analysis.

According to Ishii[123] and Drew and Lahey[124], the following conservation equations are valid for the flow of phase, k, in a two phase mixture.

Conservation of Mass

$$\frac{\partial}{\partial t}(\alpha_k \overline{\rho}_k) + \nabla.(\alpha_k \overline{\rho}_k \overline{v}_k) = \Gamma_k \qquad (129a)$$

Conservation of Momentum

$$\frac{\partial}{\partial t}(\alpha_k \overline{\rho}_k \overline{v}_k) + \nabla.(\alpha_k \overline{\rho}_k \overline{v}_k).\overline{v}_k = -\alpha_k \nabla \overline{P}_k + \nabla.\left[\alpha_k(\overline{\tau}_k + \overline{\tau}_k^T)\right] + \alpha_k \overline{\rho}_k \overline{g}_k + M_k \qquad (129.b)$$

Conservation of Energy

$$\frac{\partial}{\partial t}\left[\alpha_k\overline{\rho}_k\left(\overline{\epsilon}_k+\frac{\overline{v}_k^2}{2}\right)\right]+\nabla.\left[\alpha_k\overline{\rho}_k\left(\overline{\epsilon}_k+\frac{\overline{v}_k^2}{2}\right).\overline{v}_k\right]=-\nabla.\left[\alpha_k\left(\overline{q}_k+\overline{q}_k^T\right)\right]$$
$$+\nabla.\left[\alpha_k\left(\overline{\tau}_k+\overline{\tau}_k^T\right).\overline{v}_k\right]$$
$$+\alpha_k\overline{\rho}_k\overline{g}_k\overline{v}_k$$
$$-\nabla.\left(\alpha_k\overline{P}_k\overline{v}_k\right)$$
$$+E_k \qquad (129c)$$

Where

$\overline{\rho}_k$ = Average density of phase, k

α_k = Volume fraction of phase, k

$\overline{v}_k$ = Average velocity of phase, k

$\overline{P}_k$ = Average pressure of phase, k

$\overline{\tau}_k$ $\overline{\tau}_k^T$ = Viscous and turbulent stress tensors of phase, k, respectively

$\overline{g}_k$ = Average acceleration of phase, k

M_k = Rate of momentum generation of phase, k, at the interface

$\overline{q}_k$ $\overline{q}_k^T$ = Conductive and convective (turbulent) heat flux in phase, k, respectively

E_k = Rate of energy generation to phase, k, across the interface

Γ_k = Rate of mass generation due to phase, k, at the interface

$\overline{\epsilon}_k$ = Average internal energy of phase, k

The appropriate jump conditions at the interface are

Interfacial Mass Conservation

$$\sum_{k=1}^{2} \Gamma_k = 0 \tag{129c.1}$$

Interfacial Momentum Conservation

$$\sum_{k=1}^{2} M_k = M_m \tag{129c.2}$$

Where, M_m represents the mixture volumetric momentum source. This results principally from surface tension effects and depends on the geometric state of the interface

Interfacial Energy Conservation

$$\sum_{k=1}^{2} E_k = E_m \tag{129c.3}$$

Where, E_m represents the surface energy source due to surface tension effects.

Ishii[123] and Drew and Lahey[124] have shown that in flow situations where the void fraction does not remain constant over the entire length of the flow unit, the interfacial mixture momentum source, M_m, is given by

$$M_m = 2\overline{H}_{21}\bar{\sigma}\nabla\alpha_2 + M_m^H \qquad (129c.4)$$

Where, $\overline{H}_{21}$ is the average curvature of the interface. M_m^H denotes the forces arising from changes in mean curvature of the interface. $\bar{\sigma}$ is the average surface tension of the liquid phase. Note that in this case, the liquid and gas phases are denoted by phases 1 and 2 respectively. Also Ishii[123] has shown that for most practical applications,

$$E_m \approx 0 \qquad (129c.5)$$

Ishii[123] and Drew and Lahey[124] show that for most practical applications, the force arising from changes in mean curvature of the interface is negligible. Hence for the present, assume

$$M_m^H \approx 0 \qquad (129c.6)$$

Combining equations (129c.1) and (129a), the total mass conservation equation becomes

$$\sum_{k=1}^{2} \frac{\partial}{\partial t}(\alpha_k\bar{\rho}_k) + \sum_{k=1}^{2} \nabla.(\alpha_k\bar{\rho}_k\bar{v}_k) = 0 \qquad (129d.1)$$

Under steady state conditions, equation (129d.1) becomes

$$\sum_{k=1}^{2} \nabla.(\alpha_k \overline{\rho}_k \overline{v}_k) = 0 \qquad (129d.2)$$

Combining equations (129b), (129c.2), (129c.4) and (129c.6), neglecting the viscous and turbulent stresses, the total momentum equation is

$$\sum_{k=1}^{2} \nabla.(\alpha_k \overline{\rho}_k \overline{v}_k).\overline{v}_k = -\nabla P + \sum_{k=1}^{2} \alpha_k \overline{\rho}_k \overline{g}_k + 2\overline{H}_{21}\,\overline{\sigma}\nabla\alpha_2 \qquad (129d.3)$$

Hence, the generalized momentum equation becomes

$$-\nabla P - \sum_{k=1}^{2} \overline{\rho}_k \overline{v}_k^2 \nabla.\alpha_k + \sum_{k=1}^{2} \alpha_k \overline{\rho}_k \overline{g}_k + 2\overline{H}_{21}\,\overline{\sigma}\nabla\alpha_2 = 0 \qquad (129d.4)$$

Rewritting equation (129d.4) in terms of liquid, (L), and gas, (g), properties and noting that $\overline{v}_k = u_k/\alpha_k$ gives in the x-direction

$$\frac{-dP}{dx} - \rho_g\left(\frac{u_g}{\alpha}\right)^2 \frac{d\alpha}{dx} + \rho_L\left(\frac{u_L}{1-\alpha}\right)^2 \frac{d\alpha}{dx} - (1-\alpha)\rho_L g - \alpha\rho_g g - \frac{4\sigma}{d_B}\frac{d\alpha}{dx} = 0 \qquad (129d.5)$$

Where $\sum_{k=1}^{2} \alpha_k = 1$

$\overline{H}_{21}$ = −ve for bubbles and +ve for drops

$\alpha_2 = \alpha$ (Gas void fraction)

Noting that on crossflow sieve plates, there is no net liquid flow in the x-direction, and also neglecting the weight of the gas in the control volume, the generalized momentum equation becomes

$$\frac{-dP}{dx} - \rho_g\left(\frac{u_g}{\alpha}\right)^2\frac{d\alpha}{dx} - (1-\alpha)\rho_L g - \frac{4\sigma}{d_B}\frac{d\alpha}{dx} = 0 \qquad (129e)$$

Combining equations (129c), (129c.3) and (129c.5) the total energy equation for the two phase mixture at any height, x, is

$$\begin{aligned}\sum_{k=1}^{2}\nabla.\left[\alpha_k\overline{\rho}_k\left(\overline{\epsilon}_k+\frac{\overline{v}_k^2}{2}\right).\overline{v}_k\right] = &-\sum_{k=1}^{2}\nabla.\left[\alpha_k\left(\overline{q}_k+\overline{q}_k^T\right)\right]\\ &+\sum_{k=1}^{2}\left(\alpha_k\overline{\rho}_k\overline{g}_k\overline{v}_k\right)\\ &+\sum_{k=1}^{2}\nabla.\left[\alpha_k\left(\overline{\tau}_k+\overline{\tau}_k^T\right).\overline{v}_k\right]\\ &-\sum_{k=1}^{2}\nabla.\left(\alpha_k P_k\overline{v}_k\right)\end{aligned} \qquad (129e.1)$$

When there are no heat effects or in flow systems where these effects are not considered important, the total energy balance becomes

$$\begin{aligned}\sum_{k=1}^{2}\left(\alpha_k\overline{\rho}_k\frac{\overline{v}_k^2}{2}\right).\overline{v}_k = &-\sum_{k=1}^{2}\nabla.\left(\alpha_k\overline{P}_k\overline{v}_k\right)+\sum_{k=1}^{2}\alpha_k\overline{\rho}_k\overline{g}_k\overline{v}_k\\ &+\sum_{k=1}^{2}\nabla.\left[\alpha_k\left(\overline{\tau}_k+\overline{\tau}_k^T\right).\overline{v}_k\right]\end{aligned} \qquad (129e.2)$$

Note that the third term on the right hand side of equation (129e.2) represents the net rate of energy dissipation per unit mass of fluid on

the plate, e_d. This is the term of prime interest in this analysis which is to be minimised. Writting equation (129e.2) in terms of L and g gives

$$\rho_g \left(\frac{u_g}{\alpha}\right)^3 \frac{d\alpha}{dx} - \rho_L \left(\frac{u_L}{1-\alpha}\right)^3 \frac{d\alpha}{dx} = -u_g \frac{dP}{dx} - u_L \frac{dP}{dx} - \rho_L g u_L - \rho_g g u_g + e_d \qquad (129e.3)$$

Neglecting the rate of kinetic energy transfer of the liquid phase, a generalised equation for the rate of energy dissipation per unit mass on any layer of the froth or gas-liquid dispersion is

$$e_d = (u_g + u_L)\frac{dP}{dx} + \rho_g \left(\frac{u_g}{\alpha}\right)^3 \frac{d\alpha}{dx} + (\rho_L u_L + \rho_g u_g) g \qquad (129e.4)$$

On application of equation (129e.4) to countercurrent, co-current or crossflow systems, sign conventions on the velocity of the different phases should be observed.

For a crossflow sieve plate system, where as noted before, the flow of liquid on the plate on a net basis is not in the x-direction, equation (129e.4) becomes

$$e_d = u_g \frac{dP}{dx} + \rho_g \left(\frac{u_g}{\alpha}\right)^3 \frac{d\alpha}{dx} + \rho_g u_g g \qquad (129e.5)$$

The total rate of energy dissipation per unit mass of fluid for the entire froth layer is

$$E = \int_0^{H_f} e_d dx = \int_0^{H_f} \left[u_g \frac{dP}{dx} + \rho_g \left(\frac{u_g}{\alpha}\right)^3 + u_g \rho_g g \right] dx \qquad (130a)$$

Also the total balance of momentum and other forces acting on the froth can be obtained from equation (129e) as

$$\int_0^{H_f} \left[-\frac{dP}{dx} - \rho_g \left(\frac{u_g}{\alpha} \right)^2 \frac{d\alpha}{dx} - (1-\alpha)\rho_L g - \frac{4\sigma}{d_B} \frac{d\alpha}{dx} \right] dx = 0 \qquad (130b)$$

Eversole et al[125] had shown that for the formation of bubbles on sieve plates, the gas bubble grows over a finite time say, Δt, when the gas flows, and by averaging over time it was shown that the pressure loss due to bubble formation becomes

$$\Delta P_R = \frac{6\sigma}{d_B}$$

as against that due to a balance of the internal force in a static bubble required to overcome surface tension given as

$$\Delta P_R = \frac{4\sigma}{d_B}$$

This same argument can be extended to the bubbles in the two phase dispersion on the plate in a different perspective. It was seen earlier that surface tension effects become important in two phase flow systems when there are expanding or contracting bubbles. Since the condition on the plate is very dynamic whereby there is constant formation of secondary bubbles due to the processes of coalescence and breakup, during which time there is passage of gas. The increase or decrease in size of the bubbles by these processes must therefore occur over a finite time say,

Δt_1. Hence the same analysis of Eversole et al[125] can therefore be extended to this case. The final momentum equation becomes

$$\int_0^{H_f} \left[-\frac{dP}{dx} - \rho_g \left(\frac{u_g}{\alpha}\right)^2 \frac{d\alpha}{dx} - (1-\alpha)\rho_L g - \frac{6\sigma}{d_B}\frac{d\alpha}{dx} \right] dx = 0 \quad (130c)$$

The correction to the surface tension term of equation (130b) may be necessary to compensate for the forces due to the changing curvature of the interface, M_m^H, though at this stage it is hard to determine. Equations (130a) and (130c) are the target equations to be used in the analysis of froth behaviour on sieve plates.

In most sieve plate operations, the surface tension effect is usually considered important only near the plate during formation of bubbles and assumed to be constant. In principle, d_B, in equations (129d.5), (129e), (130b) and (130c) which represents the bubble diameter at any distance, x, from the plate surface should vary with position. Since the bubble diameter profile on the plate cannot be defined by means of a simple equation for all possible loadings, and also does not vary drastically with froth height †, it is best to use as a first approximation, the value of the plate hole diameter for this analysis. Hence for all the analysis, $d_B \approx d_o$, with d_o representing the plate hole diameter. Equation (130c) becomes

$$\int_0^{H_f} \left[-\frac{dP}{dx} - \rho_g \left(\frac{u_g}{\alpha}\right)^2 \frac{d\alpha}{dx} - (1-\alpha)\rho_L g - \frac{6\sigma}{d_o}\frac{d\alpha}{dx} \right] dx = 0 \quad (130d)$$

† *See Chapter 5*

A comparison of equation (130d) with equation (36), the conventional equation used for the calculation of total pressure drop on sieve plates, shows a marked resemblance. Note that equation (130d) applies to pressure effects on the froth layer already formed on the plate, hence the pressure loss due to passage of gas through the perforations does apply here. Also observe that the pressure loss due to the resistance of the froth layer to the passage of gas is often neglected in conventional equations for calculation of pressure drop on sieve plates as given by equation (36).

The total weight of material on the plate neglecting the weight of gas is

$$\int_0^{H_f} (1-\alpha) g \rho_L \, dx \;\; = \;\; h_L \rho_L g \tag{131}$$

The boundary conditions of the above equations (130a,130d,131) are

$$\begin{aligned} \alpha \;\; &= \;\; \alpha_o, \qquad x = 0 \\ \alpha \;\; &= \;\; \alpha_h, \qquad x = H_f \end{aligned} \tag{132}$$

If equations (130d) and (131) are valid simultaneously, then the quantity, E, of equation (130a) is given by the boundary conditions and independent of the integration path. To be able to evaluate the dependence of the gas void fraction on the height above the plate, a reasonable assumption or consideration of the physical behaviour of the system under study must be made. Using the same analogy of Kolář[97], where the

froth layer was compared to gas flow through porous beds, the following assumption can be made

$$\frac{dP}{dx} = \xi \frac{\rho_g}{2} \left(\frac{u_g}{\alpha}\right)^2 \tag{133}$$

The coefficient, ξ , normally refered to as the resistance coefficient, is a function of porosity and the local gas fraction, which in turn is a function of porosity. Hence it can be assumed that

$$\xi = \xi(\alpha) \tag{134}$$

To be able to find the final expression, the functionality of ξ with α must be found. This can be achieved by making use of variational calculus. Note that the extremum value of E is not the desired function, but the function $\xi = \xi(\alpha)$, necessary to fit the value of E given by equations (130a), (130d), (131) and the boundary conditions.

The condition for the extremum of a function $F(x, x')$ and a constant $G(x, x')$ to exist is given by the Euler-Lagrange equation.

$$\frac{d}{d\gamma}\left[\frac{d}{dx'}(F + \lambda G)\right] - \frac{d}{dx}[F + \lambda G] = 0 \tag{135}$$

Where λ is a dummy variable of integration. Here, the Euler - Lagrange equation can be written as

$$\frac{d}{dx}\left[\frac{d}{d\alpha'}(F + \lambda G)\right] - \frac{d}{d\alpha}[F + \lambda G] = 0 \tag{136}$$

where $\alpha' = d\alpha/dx$, $\lambda =$ constant coefficient.

The functions $F(\alpha, \alpha')$ and $G(\alpha, \alpha')$ in this case are

$$F(\alpha, \alpha') = u_g \rho_g \left(\frac{u_g}{\alpha}\right)^2 \frac{\xi(\alpha)}{2} + \rho_g \left(\frac{u_g}{\alpha}\right)^3 \alpha' + \rho_g u_g g \tag{137}$$

$$G(\alpha, \alpha') = (1 - \alpha)\rho_L g \tag{138}$$

Since from equations (137) and (138), F and G are not explicit functions of x, then, the differential equation for the calculation of the unknown function $\xi(\alpha)$ (Euler - Lagrange) is given as

$$F(\alpha, \alpha') + \lambda G(\alpha, \alpha') - \alpha' \frac{d}{d\alpha'} [F(\alpha, \alpha') + \lambda G(\alpha, \alpha')] = C \tag{139}$$

Where C is a constant.

Inserting equations (137) and (138) into equation (139) and noting that when $\alpha = 1$, $\xi(\alpha) = 0$, gives

$$C = \rho_g u_g g \tag{140}$$

Hence a relation for $\xi(\alpha)$ is obtained as

$$\xi(\alpha) = \frac{-[2\lambda(1 - \alpha)\rho_L g]}{u_g \rho_g \left(\frac{u_g}{\alpha}\right)^2} \tag{141}$$

The relation for dP/dx becomes

$$\frac{dP}{dx} = \frac{-\lambda[(1-\alpha)\rho_L g]}{u_g \rho_g} \tag{142}$$

Putting the expression for dP/dx from equation (142) into equation (130d) gives

$$\int_0^{H_f} \left[\frac{\lambda(1-\alpha)\rho_L g}{u_g \rho_g} - \rho_g \left(\frac{u_g}{\alpha}\right)^2 \frac{d\alpha}{dx} - (1-\alpha)\rho_L g - \frac{6\sigma}{d_o}\frac{d\alpha}{dx} \right] dx = 0 \tag{143}$$

This implies

$$\frac{\lambda h_L \rho_L g}{u_g \rho_g} - \rho_g u_g^2 \left[\frac{1}{\alpha_o} - \frac{1}{\alpha_h}\right] - h_L \rho_L g - \frac{6\sigma}{d_o}(\alpha_h - \alpha_o) = 0 \tag{144}$$

$$\Rightarrow \quad \lambda = \left[h_L \rho_L g + \rho_g u_g^2 \left(\frac{1}{\alpha_o} - \frac{1}{\alpha_h}\right) + \frac{6\sigma}{d_o}(\alpha_h - \alpha_o) \right] \left[\frac{u_g \rho_g}{h_L \rho_L g}\right] \tag{145}$$

Hence an expression for dP/dx is obtained as

$$\frac{dP}{dx} = -\left[h_L \rho_l g + \rho_g u_g^2 \left(\frac{1}{\alpha_o} - \frac{1}{\alpha_h}\right) + \frac{6\sigma}{d_o}(\alpha_h - \alpha_o) \right] \left[\frac{(1-\alpha)\rho_L g}{h_L \rho_L g}\right] \tag{146}$$

Substituting equation (146) for dP/dx in equation (130d) gives

$$\left[\rho_g u_g^2 \left(\frac{1}{\alpha_o} - \frac{1}{\alpha_h}\right) + \frac{6\sigma}{d_o}(\alpha_h - \alpha_o) \right] \left[\frac{(1-\alpha)\rho_L g}{h_L \rho_L g}\right] = \left[\rho_g \left(\frac{u_g}{\alpha}\right)^2 + \frac{6\sigma}{d_o} \right] \frac{d\alpha}{dx} \tag{147}$$

Rearranging equation (147) and integrating gives

$$\int_0^x \left[\rho_g u_g^2 \left(\frac{1}{\alpha_o} - \frac{1}{\alpha_h}\right) + \frac{6\sigma}{d_o}(\alpha_h - \alpha_o)\right]\frac{dx}{h_L} = \int_{\alpha_o}^{\alpha} \left[\rho_g u_g^2 + \frac{6\sigma\alpha^2}{d_o}\right]\frac{dx}{\alpha^2(1-\alpha)} \tag{148}$$

Integrating the above equation within the given limits gives

$$\frac{x}{h_L} = \frac{\left[\rho_g u_g^2 \left(ln\frac{\alpha(\alpha_h - \alpha_o)}{\alpha_o(\alpha_h - \alpha)} + \frac{\alpha - \alpha_o}{\alpha\alpha_o}\right) + \frac{6\sigma}{d_o} ln\left(\frac{\alpha_h - \alpha_o}{\alpha_h - \alpha}\right)\right]}{\left[\rho_g u_g^2 \left(\frac{\alpha_h - \alpha_o}{\alpha_h\alpha_o}\right) + \frac{6\sigma}{d_o}(\alpha_h - \alpha_o)\right]} \tag{149}$$

If the surface tension effect is neglected in the analysis, the resulting equation from this can be shown to be of the form

$$\frac{x}{h_L} = \frac{\alpha_o\alpha_h}{\alpha_h - \alpha_o}\left[ln\frac{\alpha(\alpha_h - \alpha_o)}{\alpha_o(\alpha_h - \alpha)} + \frac{\alpha - \alpha_o}{\alpha\alpha_o}\right] \tag{150}$$

Equation (150) is of the same form as that derived by Kolář[97]. From equation (149) it can be seen that equation (150) results only if

$$\frac{6\sigma}{d_o} ln\left(\frac{\alpha_h - \alpha_o}{\alpha_h - \alpha}\right) = 0 \tag{150a}$$

and if

$$\frac{6\sigma}{d_o}(\alpha_h - \alpha_o) = 0 \tag{150b}$$

Equations (150a) and (150b) suggest two posibilities, $\sigma = 0$ or $\alpha = \alpha_o = \alpha_h$. Since for real systems, σ is never zero, then the only possibility

is $\alpha = \alpha_o = \alpha_h$. This condition can be obtained only if the gas is flowing alone or for plate operations at very high superficial gas velocities. This, phenomenologically, corresponds to the spray regime of plate operation where there is flow reversal on the plate.

Equation (149) indicates the dependence of the gas fraction, α, at any height, x, above the plate with the liquid holdup, h_L, gas superficial velocity, u_g, gas density, ρ_g, initial gas fraction on the plate, α_o, the gas fraction at the top of the dispersion, α_h, surface tension, σ, and the plate hole diameter, d_o. Equation (150) suggests that the gas fraction, α, at any height, x, above the plate is a function of the initial gas fraction, α_o, the gas fraction at the top of the dispersion, α_h, and the liquid holdup, h_L, only.

Since in most systems, the top of the froth or foam is predominantly gas, then it is reasonable to assume for all practical purposes that $\alpha_h = 1$. Hence equations (149) and (150) transforms into equations (151) and (152) respectively.

$$\frac{x}{h_L} = \frac{\left[\rho_g u_g^2 \left(ln\frac{\alpha(1-\alpha_o)}{\alpha_o(1-\alpha)} + \frac{\alpha-\alpha_o}{\alpha\alpha_o} \right) + \frac{6\sigma}{d_o} ln\left(\frac{1-\alpha_o}{1-\alpha}\right)\right]}{\left[\rho_g u_g^2 \left(\frac{1-\alpha_o}{\alpha_o}\right) + \frac{6\sigma}{d_o}(1-\alpha_o)\right]} \tag{151}$$

$$\frac{x}{h_L} = \frac{\alpha_o}{1-\alpha_o}\left[ln\frac{\alpha(1-\alpha_o)}{\alpha_o(1-\alpha)} + \frac{\alpha-\alpha_o}{\alpha\alpha_o}\right] \tag{152}$$

The use of the final equations (151) and (152) are demonstrated in chapter 5. The degree of fit to available experimental data is shown and discussed also in chapter 5.

CHAPTER 4

EXPERIMENTAL PROCEDURE

4.1 Choice of Suitable Foaming System

To study the behaviour of downcomers for foaming and non-foaming systems, a prudent choice of an appropriate foaming system must be made. The following criteria were used to choose a foaming system.

(a) Foamability and Foam Stability

Systems that give rise to foams which break down almost immediately after formation are not suitable for use in downcomer studies. Neither are those which foam excessively, as this may lead to premature downcomer flooding even in a flow regime where foaming is not anticipated.

(b) Measurement of surface tension at different concentrations of the foaming agent gives information on an appropriate working concentration. The necessity of this particular measurement is to be able to choose a working concentration in regions where changes in surface tension with changes in solution concentration are minimised.

(c) The corrosiveness, toxicity and other forms of hazards usually associated with chemicals. The corrosive nature of the chemical determines how resistant parts of the hardware will be under the influence of

the chemical. The toxicity factor relates to how safe it will be to work within such environments since there is always some degree of stripping of the chemical in question into the surrounding atmosphere.

(d) The volatility of the surfactant is also a parameter that determines its suitability for use in downcomer studies. Highly volatile materials evaporate readily at room temperature and are easily stripped. Here, replication of results will be difficult since solution concentration cannot be guaranteed to remain relatively constant throughout an experiment.

4.1.1 The Bubbling Column Experiment

The bubbling column (figure 4.1) was used to determine the foamability of the system chosen. Here, solutions of the selected surfactant were made at various concentrations in distilled water, and loaded, in turns, into the column. Experiments consisted of passing nitrogen gas through a fixed volume of surfactant solution. The same gas flowrate was used to characterize each solution of a given concentration. Since on the plate and in the downcomer, high shear of bubbles exist, it was necessary to carry out these determinations at a relatively high gas flowrate (see figure 4.1). Previous work on the system n-butanol/water has been reported[6], hence, only results of these measurements for the system n-pentanol/water are reported here. The results obtained are shown in graphical form in figure 4.2.

4.1.2 Surface Tension Determinations

Surface tension was determined using the modified Wilhemy plate method. The results of these measurments are shown graphically in figure 4.2.

4.1.3 Choice of Working Concentration

As mentioned in section 4.1, to avoid excessive fluctuations of solution concentration during the main experiment, and hence inconsistent results, it was necessary to choose a suitable working concentration of the foaming agent. Selection was based on the results of Sections 4.1.1 and 4.1.2. Figure 4.2 shows a plateau region, that is, where there is little or no change in foam height and surface tension with changes in solution concentration. For a surface active agent concentration within this region, changes in solution concentration, either by evaporation or adsorption on the walls of the equipment, will not be expected to affect drastically the corresponding foam heights and surface activity of the solution. A concentration of 1.3% (*vol*) n-pentanol was therefore selected for use in the main experiments. Previous work[6] with the system n-butanol/water gave a good working concentration of 3% (*vol*) n-butanol

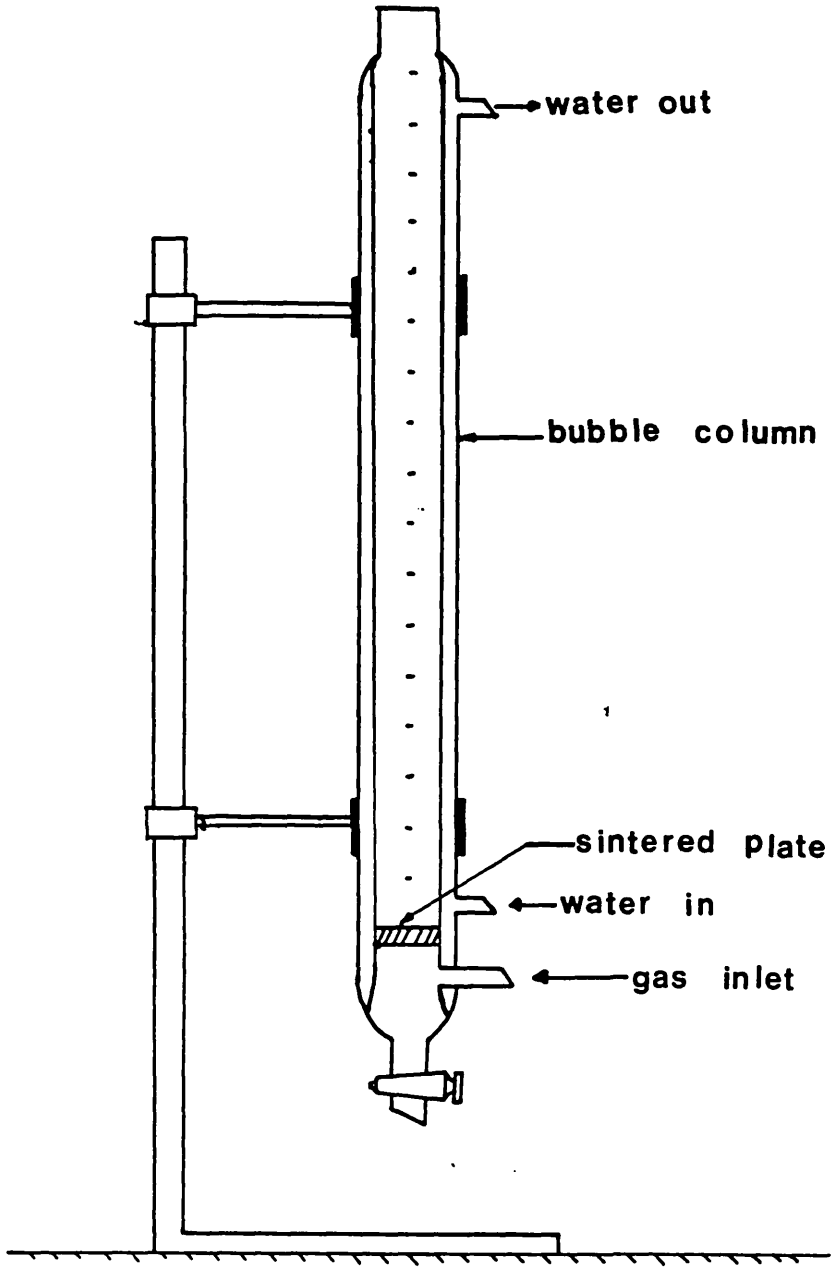

Figure 4.1 :- The Bubble Column

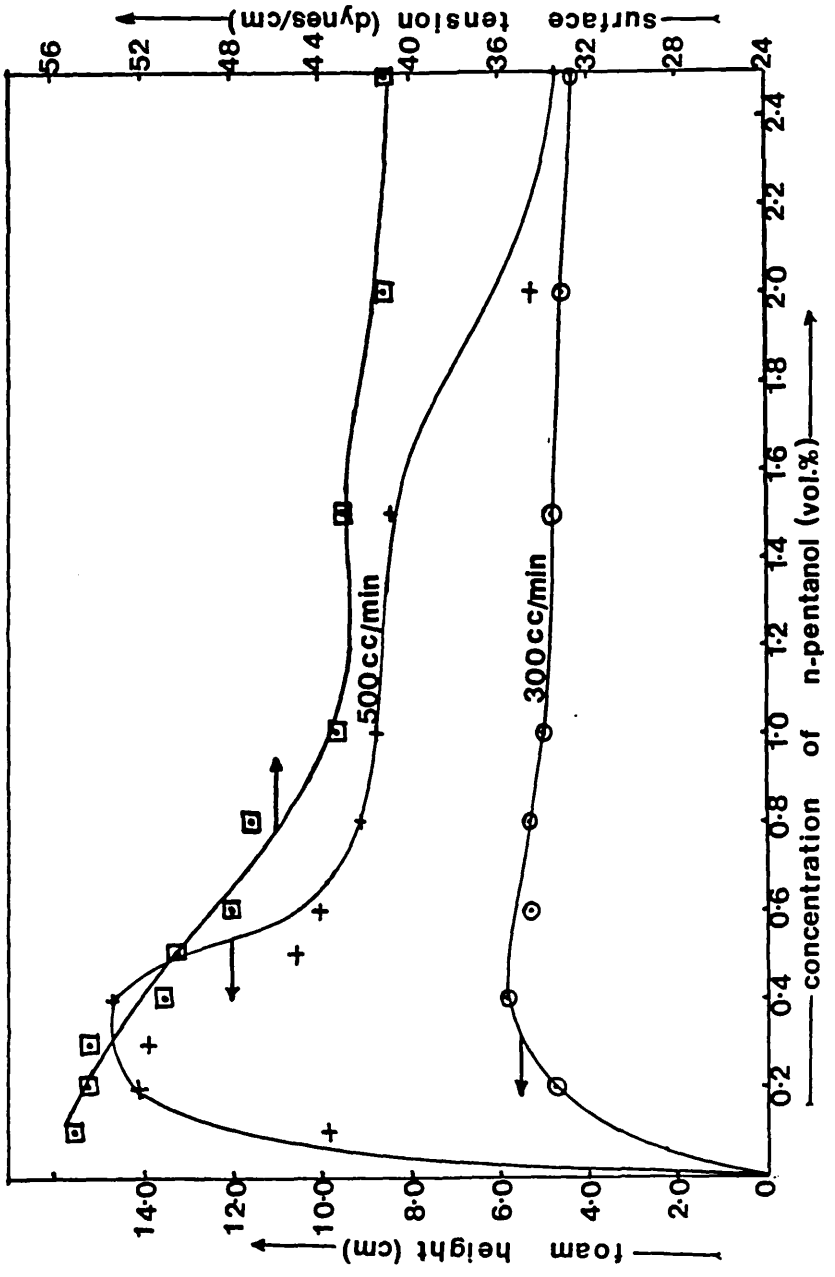

Figure 4.2 :- Plot of Foam Height and Surface Tension against Concentration of n-Pentanol

4.2 Downcomer Studies

4.2.1 General Description of Experimental Unit

A line diagram of the experimental unit used is shown in figure 4.3. The experiments were conducted in three phases :- downcomer studies, residence time studies and plate studies. It was not possible to carry out plate studies with the system n-Pentanol/Water because of hardware difficulties, since this was the first system studied on an existing rig. Results for the system n-Butanol/Water have been reported[6]. However, on replication of data obtained for the widest downcomer studied, namely 6 cm, discrepancies were found. Therefore, it was necessary to repeat the measurements for that system with the 6 cm downcomer. The experiments were carried out with three plates and two downcomer sizes. Details of the plates used are shown in table 4.1. The main measurements carried out in the downcomer are mean dispersion density and Sauter mean diameter. Four liquid flowrates were used. For each of these liquid flowrates, the gas rate was varied from that leading to conditions of incipient weeping to that near the spray regime. The three systems studied are n-Pentanol/Water, n-Butanol/Water, and Water as the non-foaming system. For all the gas - liquid combinations, plate type and system studied, the total plate pressure drop was also measured. The solution under study was stored in tanks T1 and T2 (each of 10 gallons capacity) and was fed into the main experimental unit by a 0.5HP PLP 2117 centrifugal pump (P2). The flowrate of the liquid was varied by means of valves V7 and V8 and measured with A.B.C.M

metric size 18X liquid rotameters (R1 and R2). The gas used for these studies was ordinary air fed into the unit by a Secomak 2.2KW blower unit (C1) and controlled by means of valve (V1). Before the gas was passed into the column, it was pre-saturated in the saturator, S1, so as to eliminate mass and heat transfer effects and therefore reduce surfactant loss through evaporation. The saturator is basically a spray chamber in which the gas is sprayed with the solution or liquid under study. It consists of a spray nozzle supplied with liquid by a Tuscan 0.25HP centrifugal pump, (P1), a spray chamber, S1, and a 70 Watts Stuart Turner centrifugal pump, (P3), used to drain the spray chamber. The gas flowrate was induced by means of a four - inch diameter Airflow Developments Ltd. fan, R3, joined directly to a gas meter from which gas flowrates were read off directly. The whole experimental set - up was operated as a completely closed system, i.e, with total recycle of both gas and liquid. The tanks T1 and T2 were drained by closing valve, V3, and opening valve, V4, using the saturator pump, P1, as the drive. The main column was made of perspex glass, the plates of stainless steel and the pipes were n-PVC pipes. The general dimensions of the main column are shown in figure 4.4.

4.2.2 Dispersion Density Measurments

The two phase density of the dispersion (liquid fraction) in the downcomer and on the plate was measured by means of the gamma ray absorption technique with a 0.3 milli Curie Caesium 137 gamma source.

Figure 4.5 shows the gamma ray traverse system and monitoring devices used in recording dispersion density at any particular level. In this work, only vertical variations of dispersion density in the downcomer and on the plate were investigated. It was found that the horizontal variations of dispersion density in the downcomer and on the plate at any height was negligibly small †. Hence all measurements were taken at the mid - point of the downcomer or plate. Dispersion density measurements were carried out according to the following technique :- the column was flooded (filled) with the liquid solution of interest and the time taken to record 10000 counts taken. A similar measurement was carried out with the column filled with air (empty column). A calibration line was drawn on a semi - logarithmic paper between the two points $(t_o, \rho = 1)$ and $(t_1, \rho = 0)$. For any height in the downcomer or above the test plate, the time taken to record 10000 counts was noted and the corresponding dispersion density read off the calibration line. Alternatively, these results were stored in the computer and the corresponding dispersion density for any measurement computed directly from the calibration. The calibration at the begining of any set of experiments was checked to ensure there was no serious variations of calibration parameters. The gamma ray traverse system was moved up and down the column by means of a hydraulic system to which the gamma ray source and detector were attached. The results of these measurements are presented and discussed in chapter 5 for all the systems studied.

---

† *See Chapter 5*

4.2.3 Measurement of Sauter Mean Diameter

Sauter mean diameters were measured along the entire height of the dispersion in the downcomer, and on the plate, by means of the light transmission technique. The light traverse system and monitoring devices are shown in figure 4.6. The light source is a Helium-Neon (He-Ne) 30 mW class 3B laser powered by a Hughes type 4030F power unit. The laser light generated from the source was passed through the dispersion using a system of optical mirrors fixed at pre-determined angles. A phase sensitive detector unit comprising basically of a chopper and a phase sensitive device was used to synchronise the incident light and the detected light so as to minimize detection of unwanted light (background noise) which might otherwise interfer with desired results. The transmitted light was detected by means of a photodiode. The voltage of the signal obtained from light transmitted through a pure solution was recorded as the reference voltage (that is where Sauter mean diameter is zero since $\epsilon_L = 1.0$) of the system. Subsequent voltages recorded through the dispersion in the downcomer or on the test plate were then refered to this voltage for calculation purposes according to equations 76, 77 and 84. As in Section 4.2.2, Sauter mean diameter variations in the horizontal direction were found to be negligibly small †, hence only the vertical variations were investigated. The light traverse system was moved up and down the entire height of the dispersion in the downcomer and on the test plate by means of a hydraulic system to which they were

† *See chapter 5*

attached. Results of these measurements for all systems studied are presented and discussed in chapter 5.

4.2.4 Measurement of Liquid Residence Time

The experimental technique used in the analysis of liquid residence times in the downcomer was based on the injection of a finite pulse of tracer into the downcomer and monitoring (measuring) the output tracer concentration from the system as a function of time. The tracer used in these experiments was a 1% wt/wt potassium chloride solution and was detected through measurement of the conductivity of the exiting solution with time. The injection time was between 0.2 to 0.3 seconds wherby a pulse of 15-20cm^3 of potassium chloride solution was injected. A schematic diagram of the tracer experimental unit is shown in figure 4.7. The time dependent conductivity of the exiting fluid was recorded by connecting a conductivity cell to a conductivity meter whereby information was transferred to a strip chart recorder. The time constant of the conductivity meter was less than 0.1 milliseconds which allowed effective recording of data without any significant time lag (real time analysis). In each of the measurements, the chart recorder was reset (zeroed) so that only the concentration of the tracer was adequately measured and recorded. Data and results obtained from these experiments were then used in the interpretation of residence time distributions in the downcomer based on the theory of Section 3.1. These are presented and discussed in chapter 5.

Nomenclature for Figure 4.3

C1 = 2.2 KW Secomak gas blower unit

D1 = Experimental Downcomer

F1 = False Wall

P1 = Spray supply pump (0.25HP Tuscan centrifugal pump)

P2 = Main supply pump (0.5HP PLP 2117 Centrifugal pump)

P3 = Spray unit drain (70W Stuart Tunner centrifugal) pump

R1 = Liquid Rotameter (metric size 18 X)

R2 = Rotameter (metric size 18 X)

S1 = Spray Chamber

T1 = Feed Tank

T2 = Feed Tank

V1 = Gas control valve

V2, V3, V4 = Valves

V5, V6, V7, V8 = Liquid flow Control Valves

Table 4.1 :- Description of Plates used for Studies

Plate	Diameter of holes (mm)	pitch (mm)	no of holes	% Free Area	Thicness of plate (mm)
A	3.5	10.0	280	11.0	1.5
B	4.75	12.5	157	11.3	1.5
C	6.0	16.0	100	11.4	1.5

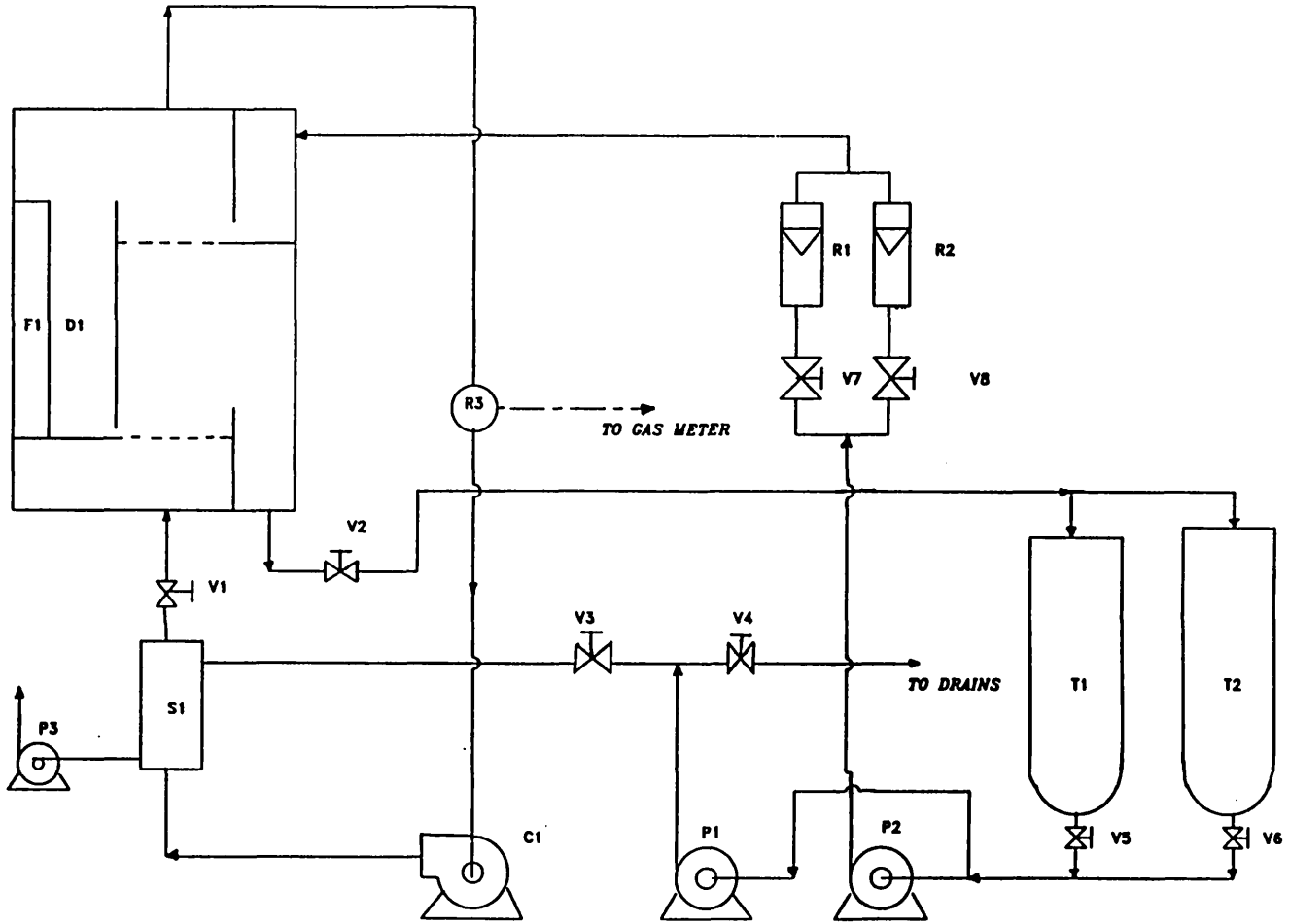

Figure 4.3 :- Line Diagram of Experimental Unit

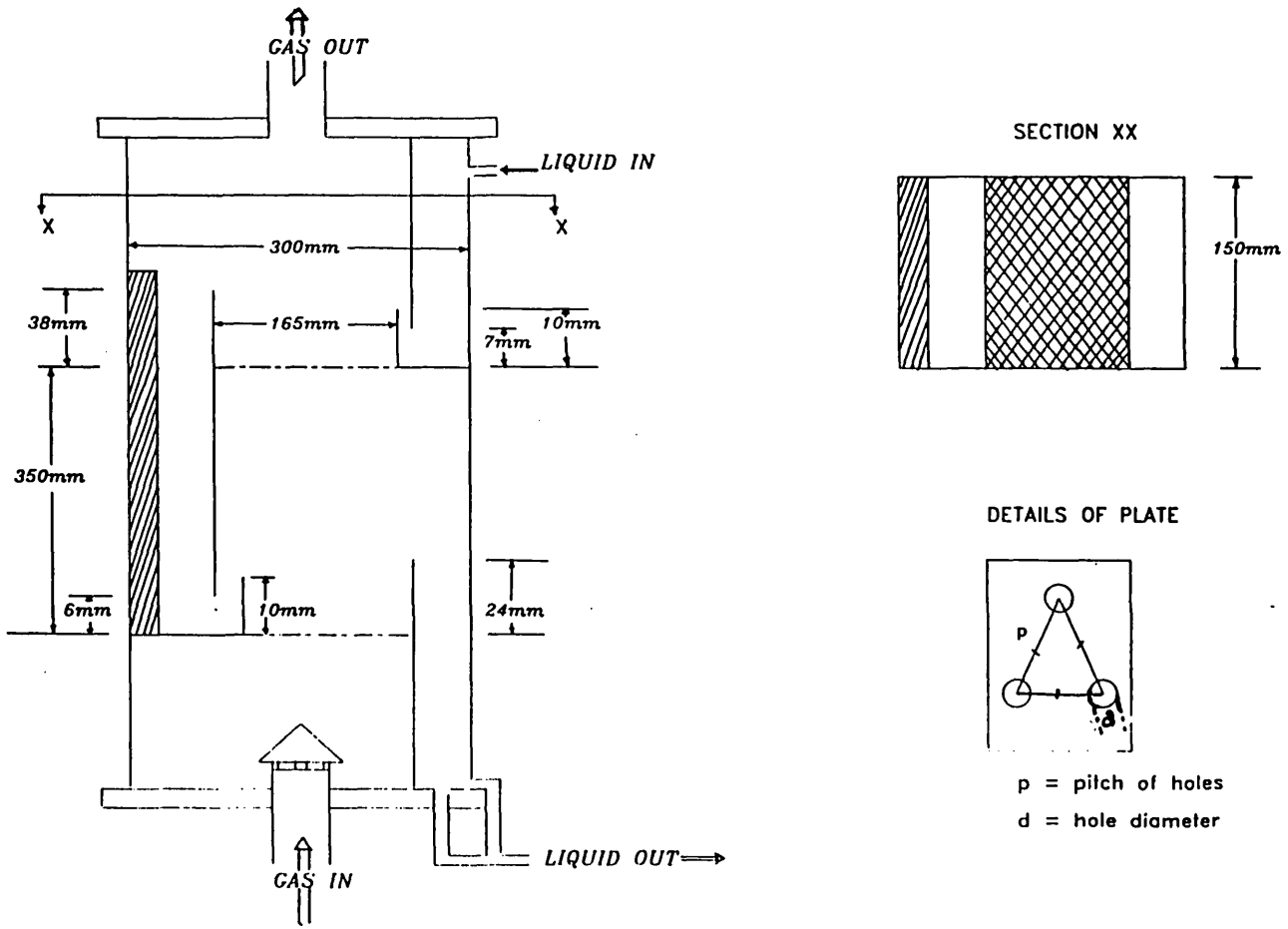

Figure 4.4 :- Details of column and Plate

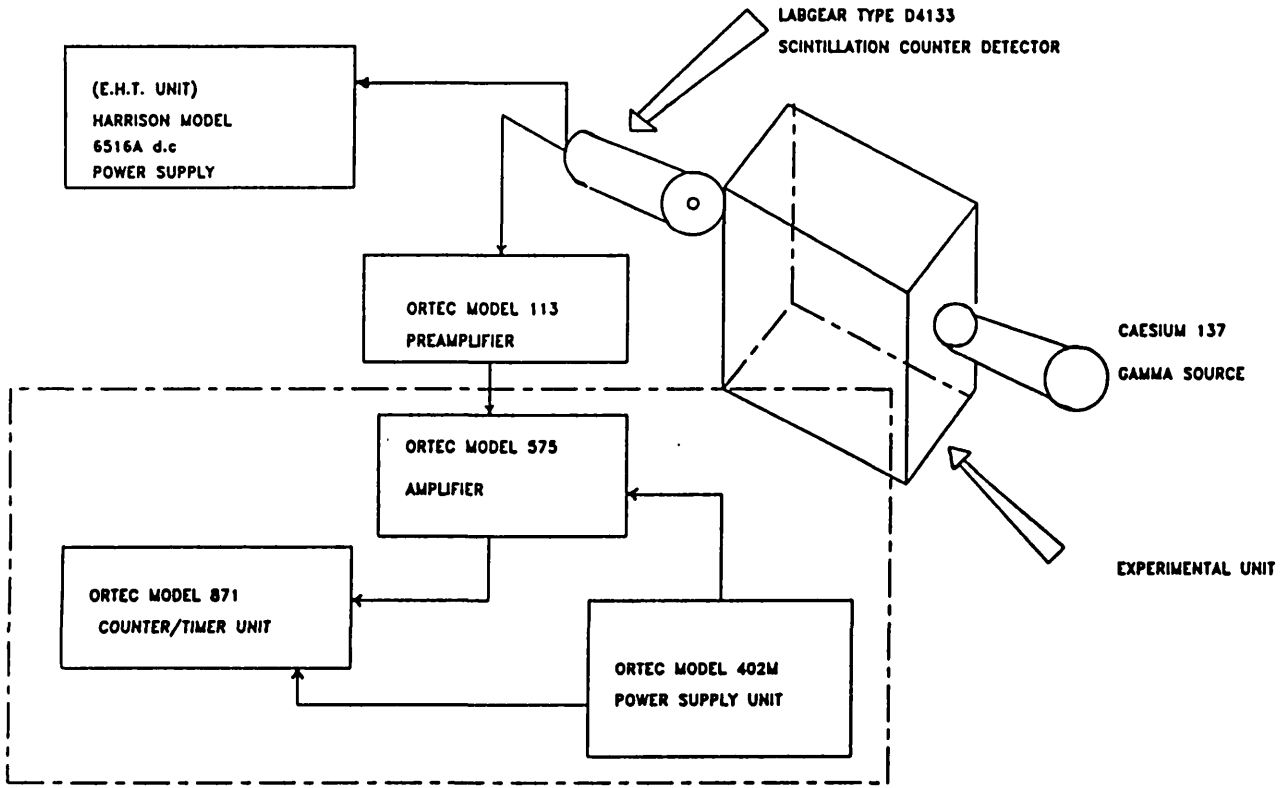

Figure 4.5 :- Gamma Ray Traverse System and Monitoring Unit

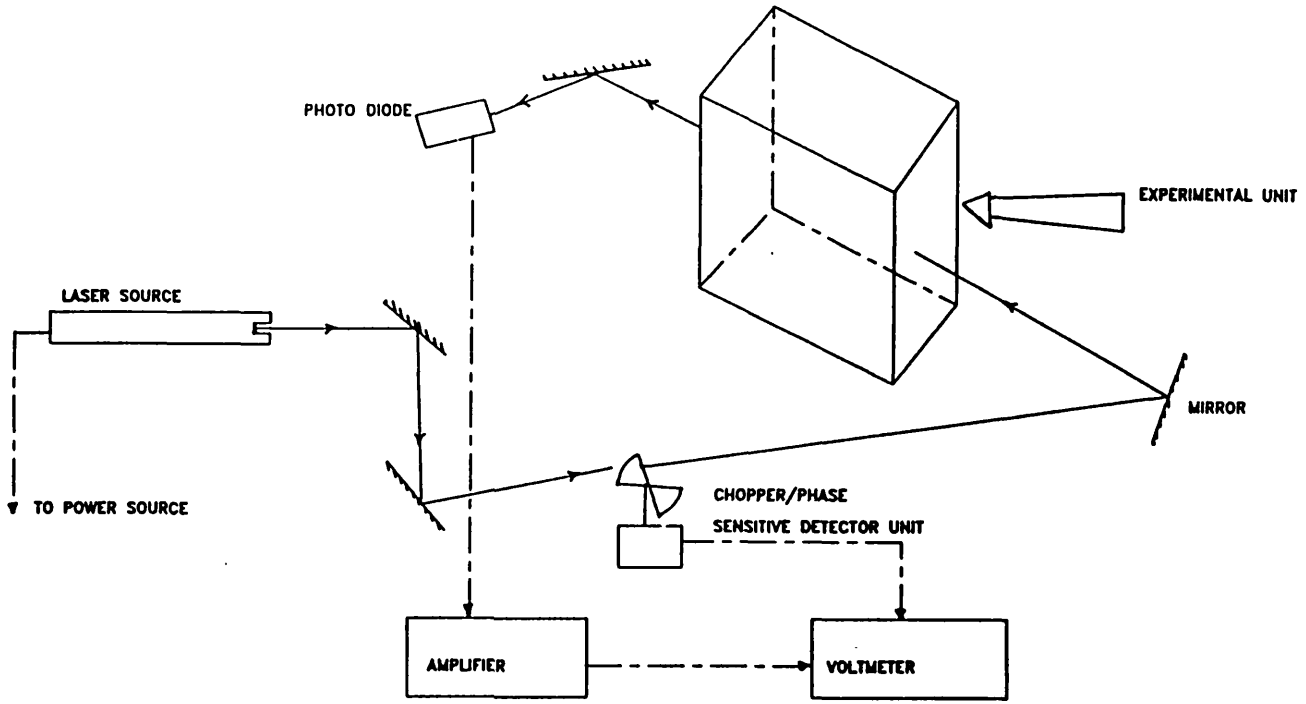

Figure 4.6 :- Light Transmittance Traverse System and Monitoring Unit

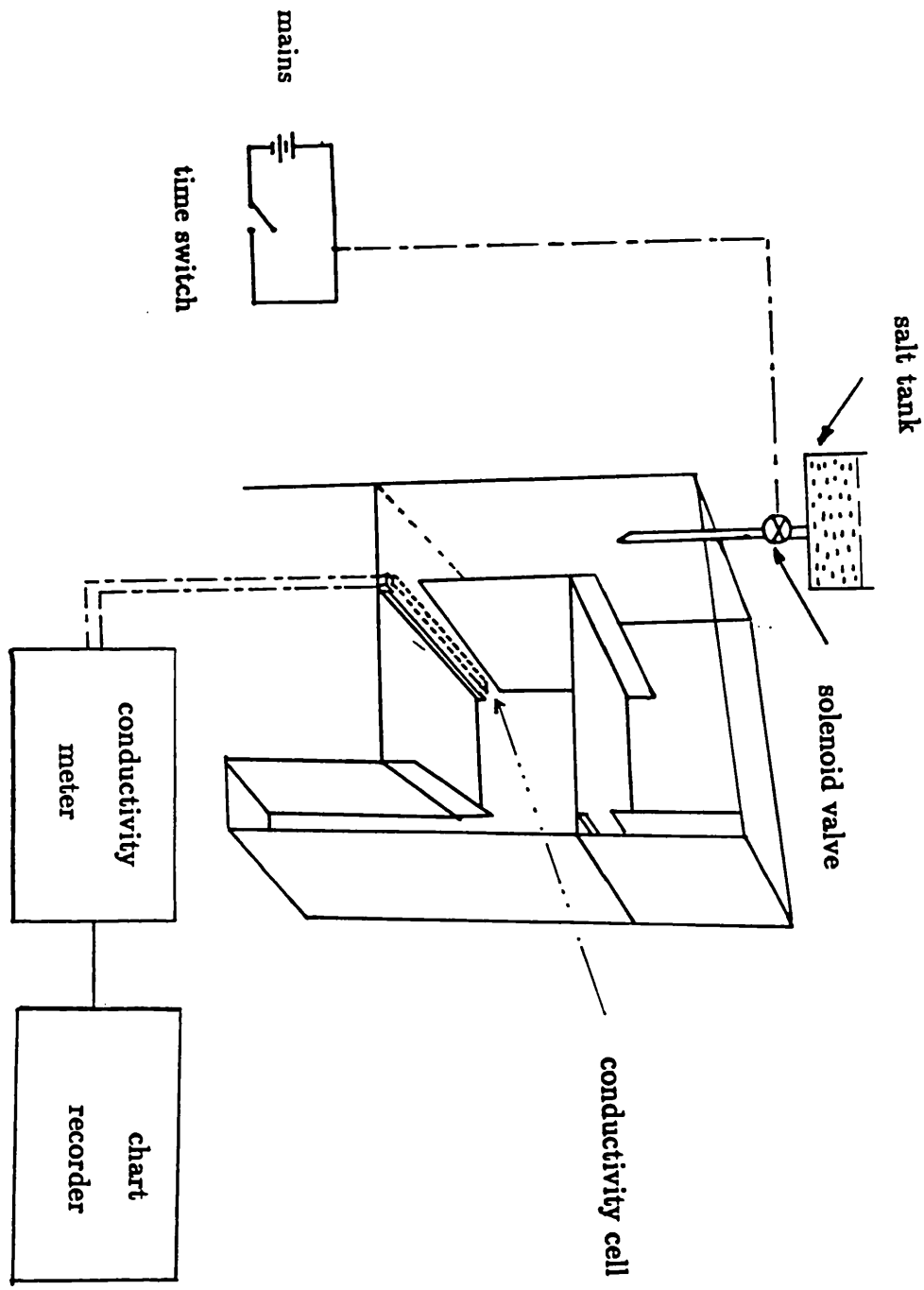

Figure 4.7 :- Experimental Set-up for Residence Time Studies

CHAPTER 5

RESULTS AND DISCUSSIONS

5.1 Introduction

The major factors determining downcomer performance are

(a) Gas and liquid loadings on the plate

(b) Physical properties of the system used (they determine the foamability of the system)

(c) Operating conditions with respect to temperature and pressure

(d) Size of holes and hole pitch (They are important in elucidating the flow regime of plate operation

(e) Weir height

(f) Downcomer size

(g) Free area of the plate

In this chapter, results of the studies described in previous chapters will be presented and discussed. For the sake of clarity, it will be broken down into the following subsections

(1) Downcomer Studies

(a) Dispersion density profiles

(b) Sauter mean diameter profiles

(c) Downcomer backup

(2) Plate Studies

(a) Dispersion density profiles

(b) Sauter mean diameter profiles

(c) Plate liquid holdup

(d) Plate pressure drop

(3) Residence Time Studies

(4) Prediction of Froth/Foam Heights in Downcomers

(5) Prediction of Froth/Foam Profiles on Plates

5.2 Calculation of Data

Since the gas, air, was passesd through a saturator, it was necessary to calculate its density, based on the degree of saturation achieved. For the purposes of this work, and based on the premise of little or no heat/mass transfer between liquid and gas in the experimental column, gas density was calculated assuming perfect saturation at 20^oC to be 1.2252 Kg/m^3. The density of a 1.3 $vol.\%$ n-Pentanol/Water solution

was measured at $20°C$ to be 999.4 Kg/m^3. The liquid holdup in the downcomer and on the plate, expressed as clear liquid heights, were determined by graphical integration of the dispersion density profiles. From these results, average values of dispersion density for the plate and downcomer respectively were calculated.

5.3 Downcomer Studies

5.3.1 Dispersion Density Profiles

Dispersion density profiles of the two phase mixture in the downcomer for the 6 cm and 8 cm downcomers are shown in figures 5.1 - 5.12 and figures 5.13 - 5.16 respectively. Figures 5.1 - 5.12 show dispersion density profiles of n-Pentanol, n-Butanol and Water plotted compositely for plates A, B and C respectively. Figures 5.13 - 5.16 show dispersion density profiles for the n-Pentanol/Water only plotted compositely for plates A, B and C respectively for the 8 cm downcomer. It was only necessary to carry out downcomer studies with the 8 cm downcomer for the n-Pentanol/Water system only. This is principally because it was necessary to test the behavior of the downcomer at high downcomer area for the high foaming system. For the low foaming to non-foaming systems futher necessary information would not have been revealed since 6 cm downcomer was able to contain these systems adequately. Generally, the dispersion density profiles can be seen to vary in shape for the foaming systems for different gas and liquid loadings on the plate. This variation is, however, non-existent for the non-foaming system (air/water). The

only significant variation for the system air/water is with respect to the height of froth in the downcomer. The results obtained for the 6 cm and 8 cm downcomers show that the foam/froth height obtained in the 8 cm downcomer is lower than that obtained in the 6 cm downcomer, under the same conditions of liquid and gas loadings on the plate. This is an expected result and its consequences will be discussed in subsequent sections. The dispersion density profiles for the foaming and non-foaming systems are similar only in the sense that they are high in liquid content at the bottom of the downcomer and high in gas content at the top of the foam/froth in the downcomer. This is also an expected result from hydrodynamic considerations. Thus, those bubbles with free rise velocities greater than the liquid velocity in the downcomer tend to rise due to buoyancy, thereby leaving localised areas with high liquid content as the aerated mass flows in the downcomer. For a foaming system, these bubbles are stabilized by the surfactant present in solution, thus producing a large amount of froth/foam which is directly responsible for the dispersion heights obtained for the foaming systems. Generally, there exists a marked transition from conditions where there is foaming to that where there is no foaming for the foaming systems in the downcomer. This transition can be seen in the change of shape of the dispersion density profiles from the sigmoidal shape to that characteristic of the non-foaming system. A plausible explanation of this behaviour can be provided by considering the flow regime of plate operation. Thus, foaming is not generally expected to occur when operating in the bubbly or spray regimes of plate operation. The bubbling regime is of no industrial

and practical consequence, and hence, results in this direction will not be discussed futher. In the spray regime of plate operation, there normally exist liquid droplets entrained in the gas stream. It is generally believed that under this regime of plate operation, the liquid phase is dispersed in the gas stream as opposed to the gas in liquid dispersions observed in other regimes of flow. Therefore, there is no problem of gas disengagement since the gas jets through the dispersion formed on the plate. Also, and of significant importance is the fact that in this regime of flow, there is significant gas disengagement on the plate before the dispersion flows into the downcomer. The shape of the dispersion density profile characteristic of the foaming systems, when there is high foaming in the downcomer, suggests high degree of aeration. Futhermore, it suggests that bubbles in the downcomer are stable under conditions of dynamic equilibruim between coalescence and breakup. This is evidenced by the almost constant average bubble sizes that are represented in the Sauter mean diameter profiles of figures 5.18 - 5.33 for the foaming systems. These results point out the strong influence of the surface active agent, and consequently the effect of surface tension, in downcomer hydrodynamics.

5.3.1.1 Effect of Gas and Liquid Rates

The effect of gas and liquid rates on the dispersion in the downcomer can be adequately described in terms of the regimes of plate operation. This approach is considered appropriate since, what happens directly on

the plate above, affects the behaviour of the dispersion in the downcomer below. It can also provide a simple guide towards an understanding of the trends of dispersion density profiles observed in the downcomer. In describing the effect of liquid and gas rates, tables 5.1 - 5.3 may be used as a guide in the delineation exercise. From figures 5.1 to 5.16, it can be seen that for a constant liquid rate, the froth/foam height in the downcomer increases with gas superficial velocity to a maximum value and then decreases for all the plates studied. This trend can be explained in terms of data on flow regimes presented in tables 5.1 to 5.3. In normal tray operations, at low liquid and high gas rates, the plate operates in the spray regime. At high liquid and low gas rates, the plate operates in the bubbling regime. The intermediate regime is what is normally refered to as the frothing regime or what Hofhuis and Zuiderweg[16] refer to as the mixed froth regime. Data obtained from this work, therefore show that downcomer limitations due to the effect of foaming are important only in the mixed froth regime. The patterns described so far, indicate that it should be possible to predict what happens in the downcomer from a knowledge of

(a) Type of system used (Foaming or non-foaming)

(b) Regime of plate operation

(c) Downcomer size

In subsequent sections, attempts will be made to incorporate these conclusions in the formulation of an appropriate concept for downcomer behaviour.

Table 5.1 :- Flow Regimes of Plate Operation for Plate A

U_g (m/s)	Liquid Rate (lit/min)			
	3.0	4.0	5.0	6.0
0.492	B	B	B	B
0.821	M	M	M	M
0.985	M	M	M	M
1.313	M	M	M	M
1.642	M	M	M	M
1.970	S^1 M^2 M^3	S^1 M^2 M^3	M	M
2.298	S^1 S^2 M^3	S^1 M^2 M^3	S^1 M^2 M^3	S^1 M^2 M^3

Table 5.2 :- Flow Regimes of Plate Operation for Plate B

U_g (m/s)	Liquid Rate (lit/min)			
	3.0	4.0	5.0	6.0
0.492	B	B	B	B
0.821	M	M	M	M
0.985	M	M	M	M
1.313	M	M	M	M
1.642	S^1 M^2 M^3	S^1 M^2 M^3	M	M
1.970	S^1 S^2 S^3	S^1 M^2 M^3	S^1 M^2 M^3	S^1M^2 M^3
2.298	S^1 S^2 S^3	S^1 S^2 S^3	S^1 S^2 S^3	S^1 S^2 M^3

Table 5.3 :- Flow Regimes of Plate Operation for Plate C

U_g (m/s)	Liquid Rate (lit/min)			
	3.0	4.0	5.0	6.0
0.492	B	B	B	B
0.821	M	M	M	M
0.985	M	M	M	M
1.313	S^1 M^2 M^3	M	M	M
1.642	S^1 M^2 M^3	S^1 M^2 M^3	S^1 M^2 M^3	S^1 M^2 M^3
1.970	S^1 S^2 S^3	S^1 S^2 S^3	S^1 S^2 S^3	S^1S^2 M^3
2.298	S^1 S^2 S^3	S^1 S^2 S^3	S^1 S^2 S^3	S^1 S^2 S^3

Nomenclature for Tables 5.1 - 5.3

B = Bubbling Regime

M = Mixed Froth Regime

S = Spray Regime

E = Emulsion Flow Regime

Superscripts

1 = Spray Regime located using equation due to Hofhuis and Zuiderweg[16]

2 = Spray Regime located using equation of Barber and Wijn[9]

3 = Spray Regime located using equation due to Lockett[106]

5.3.1.2 Effect of Downcomer Size

In this study, 6 cm and 8 cm downcomer representing 23.1% and 28.6% of total column cross-sectional area were used. The 2 cm and 4 cm downcomers representing 9.1% and 16.7% of the total column cross-sectional area, respectively, could not be studied principally due to the effect of impact of overflow from the plate, on the opposite wall as demonstrated by Porter and Jenkins[56]. Also since the n-Pentanol/Water solution was very high foaming, it was envisaged that downcomer flooding in smaller downcomers would be limiting even in regimes of plate operation where foaming would not have been envisaged. Hence, data obtained for such

downcomers with high foaming systems may be misleading and therefore not useful in characterisation of froth/foam behaviour in downcomers.

The capacity of any downcomer is usually defined in terms of its ability to handle the load of the dispersion from the plate above and be able to deliver clear to the next tray. Hence, a downcomer must be able to accomodate the flow of liquid from the plate above, without it becoming completely filled by froth/foam. This capacity, is usually measured in terms of the height of froth in the downcomer which in turn, is closely related to the cross-sectional area of the downcomer for a given tray spacing. A comparison of data for the n-Pentanol/Water system in figures 5.1 - 5.12 for the 6 cm downcomer, with figures 5.13 - 5.16 for the 8 cm downcomer for same liquid/gas rates and plate type demonstrates the effect of downcomer size vividly. It can be seen that an increase in downcomer area leads to a decrease in foam/froth height in the downcomer - an expected result. The effect of the change in the downcomer area can be directly attributed to the change in liquid velocity in the downcomer. This particular parameter affects

(a) Liquid and Gas residence time in the downcomer

(b) Available area for vapour/gas disengagement

(c) Time available for bubble coalescence

A high downcomer liquid velocity decreases the residence time of liquid and gas, and hence leads either to a situation whereby the downcomer chokes and is flooded, or to a situation in which the gas hardly disengages in the downcomer. This condition of limited disengagement of gas

leads to gas carry under, which in turn might give rise to maldistribution of fluid on the next tray and subsequently, to general instability of flow within the column. The effect of high downcomer liquid velocity on conditions (b) and (c) above can be similarly explained along the same lines. A low downcomer liquid velocity, on the other hand, favours increased residence time of gas and liquid in the downcomer, increased area available for vapour/gas disengagement and increased time available for bubble coalescence and breakup. These factors are directly responsible for adequate separation of gas and liquid in the downcomer. A close examination of the dispersion density data for the 8 cm and 6 cm downcomers indicate that froth height is directly proportional to the downcomer area. Hence, extrapolation, to, say, a 4 cm downcomer indicates that for most of the liquid and gas gas rates studied here, limitations would have arisen due to increased froth height in the downcomer. For the non-foaming system, this limitation should not arise since the dispersion from the plate is already high in liquid content. A simple deduction from these results is that downcomer area is a crucial factor in the design of columns, especially for systems that foam. Moreover, the normally recommended downcomer size of 5 - 14 % of total column cross-sectional area is grossly inadequate for handling medium to high foaming systems.

5.3.1.3 Effect of Hole Size and Pitch

Three plates with the same hole area of 11% were studied. The basic difference between the plates is with respect to hole area and hole pitch. The plate characteristics are

Plate	*Hole Diameter (mm)*	*Hole Pitch (mm)*
A	3.5	10.0
B	4.75	12.5
C	6.0	16.0

A comparison of the effect of hole size and pitch on the froth height and behaviour in the downcomer can be deduced from figures 5.1 - 5.16. The basic feature of the profiles is that there is little or no effect of these parameters on the behaviour of the froth in the downcomer for the non-foaming system. This is expected because for the non-foaming system, the bubbles formed are unstable thereby leading to quick disengagement of gas on the plate and also to almost instantaneous disengagement in the downcomer. This particular concept will be explained futher in Section 5.3.1.4. The effect of hole size and pitch is significant with respect to the foaming systems. At low to medium gas velocities, for a given liquid flowrate, froth heights increases with decrease in the pitch to diameter ratio (p/d). With respect to figures 5.1 - 5.16, these show that at these moderate gas flowrates, plate C foams more than plate B and

in turn more than plate A. As the gas rate is increased for a given liquid flowrate, generally, froth/foam heights in the downcomer decrease faster in the pattern plate C, plate B and plate A, the reverse of the former, from the maximum value. These trends can be explained on the basis of

(1) Regime of operation of the plate

(2) Size of bubbles generated on the plate

The second condition (bubble size on plate) shall be explained in depth in Section 5.4 when plate results are presented and discussed. Tables 5.1 - 5.3 give some indication of the regime of plate operation for all the liquid and gas rate combinations studied. Generally, plates with large holes tend to traverse the regimes - bubbly, mixed and spray more quickly than those with smaller holes. This then explains the trends observed as regards hole diameter and pitch. Hence, it should appear to be more advantageous to use plates with sizable holes and operate them near the spray regime to be able to minimize the degree of foaming on the plate and in the downcomer.

5.3.1.4 Effect of Surface Tension

Theoretically, the more surface active a material is, the lower the surface tension of the resulting solution formed from it. This simply implies a greater tendency of the solution to foam under appropriate conditions. Another important parameter which helps to explain the effect of surface tension is the amount of surfactant adsorbed at the interface. This

is usually measured and characterised in terms of the surface excess of the solution considered. A system which is strongly adsorbed at the interface has a greater tendency to foam. For the systems n-Pentanol and n-Butanol, it is seen that Pentanol adsorbs much more strongly at the interface than Butanol, hence a higher propensity to produce foam than Butanol†. From the dispersion density profiles presented in figures 5.1 - 5.12, these effects can be seen clearly. For the non-foaming system, (water), there are no surfactant molecules present in solution, hence, there is no foaming. This is responsible for the low froth heights characteristic of this system and also the characteristic shape of the dispersion density profiles. For the foaming systems, air/n-Butanol-Water, air/n-Pentanol-Water, there is foaming which is a consequence of the adsorption at the interface of the n-Butanol and n-Pentanol molecules and which leads to high dispersion heights in the downcomer, depending on the regime of plate operation. Note that because n-Pentanol is more strongly adsorbed at the interface than n-Butanol, the foam heights obtained for the n-pentanol system are higher than those obtained for the n-Butanol system. A plausible conclusion from this is that one of the major parameters responsible for foaming in any system is the surface tension of the solution.

† *See Appendix B*

5.3.2 Horizontal Variation of Dispersion Density in the Downcomer

It was necessary to investigate the variations of dispersion density across the downcomer at different froth heights and gas/liquid loads. The result of this investigation is shown in figure 5.17 for a liquid rate of 5.0 lit/min and gas rate of 0.985 m/s with plate B. This figure indicates that there is no significant variation of dispersion density in the horizontal direction at any level in the downcomer. This then justifies the measurement of downcomer parameters at the center of the downcomer. Another significant point worth noting is that modelling of the downcomer can be done effectively in the vertical direction only.

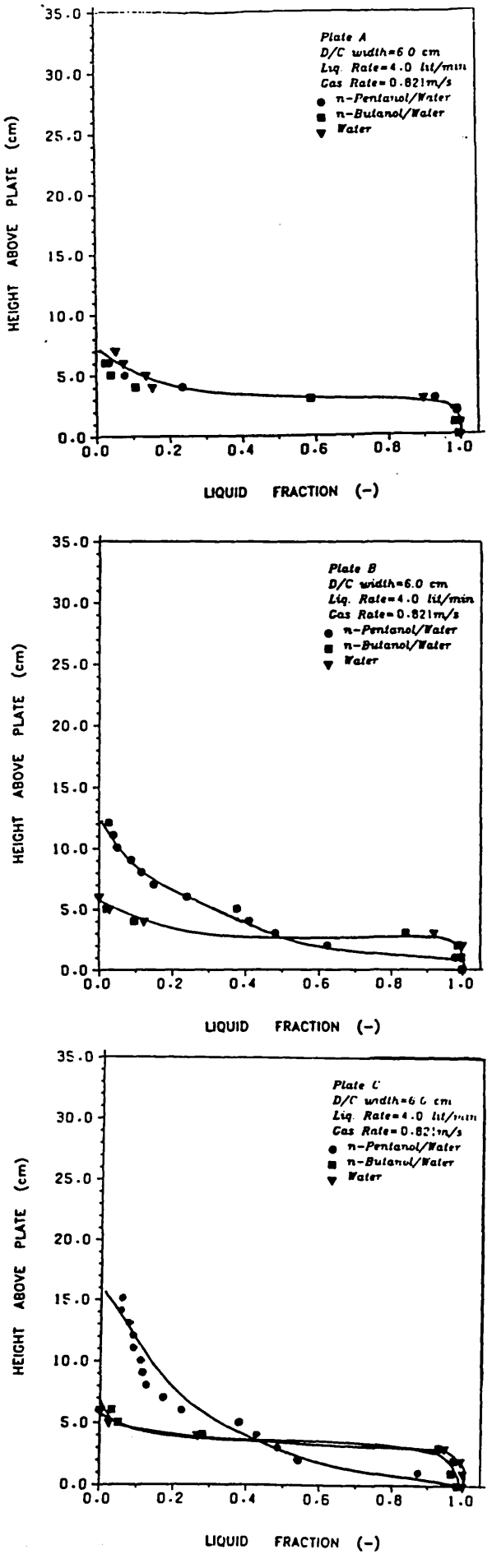

Figure 5.1 :- Variation of Liquid Fraction with Height of Dispersion in the Downcomer (Liquid Rate = 4.0 lit/min; Gas Rate = 0.821 m/s; Downcomer size =6.0cm)

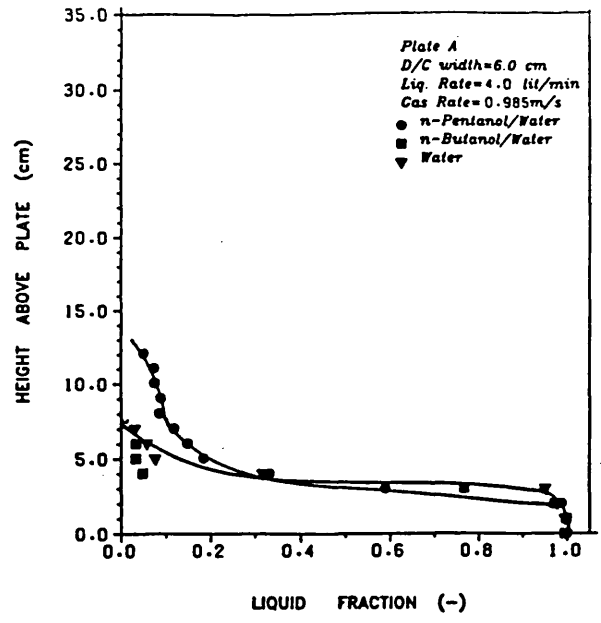

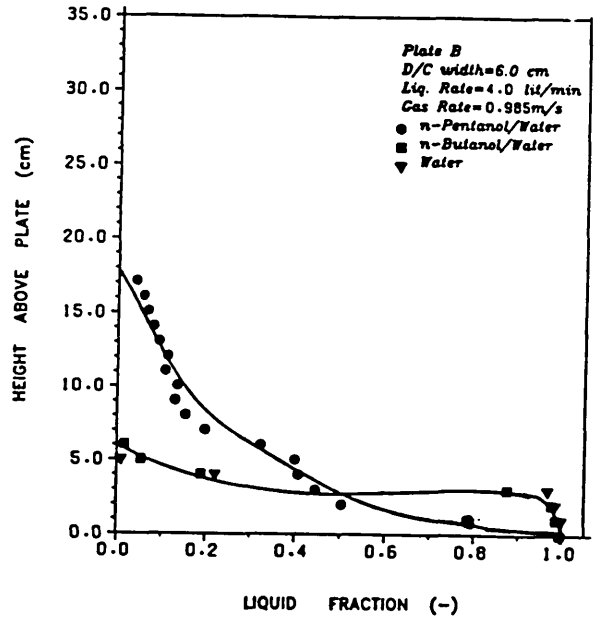

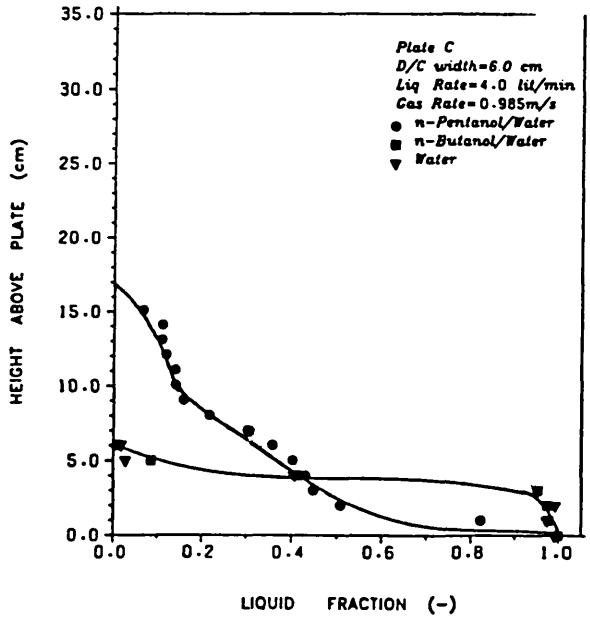

Figure 5.2 :- Variation of Liquid Fraction with Height of Dispersion in the Downcomer (Liquid Rate = 4.0 lit/min; Gas Rate = 0.985 m/s; Downcomer size = 6.0cm)

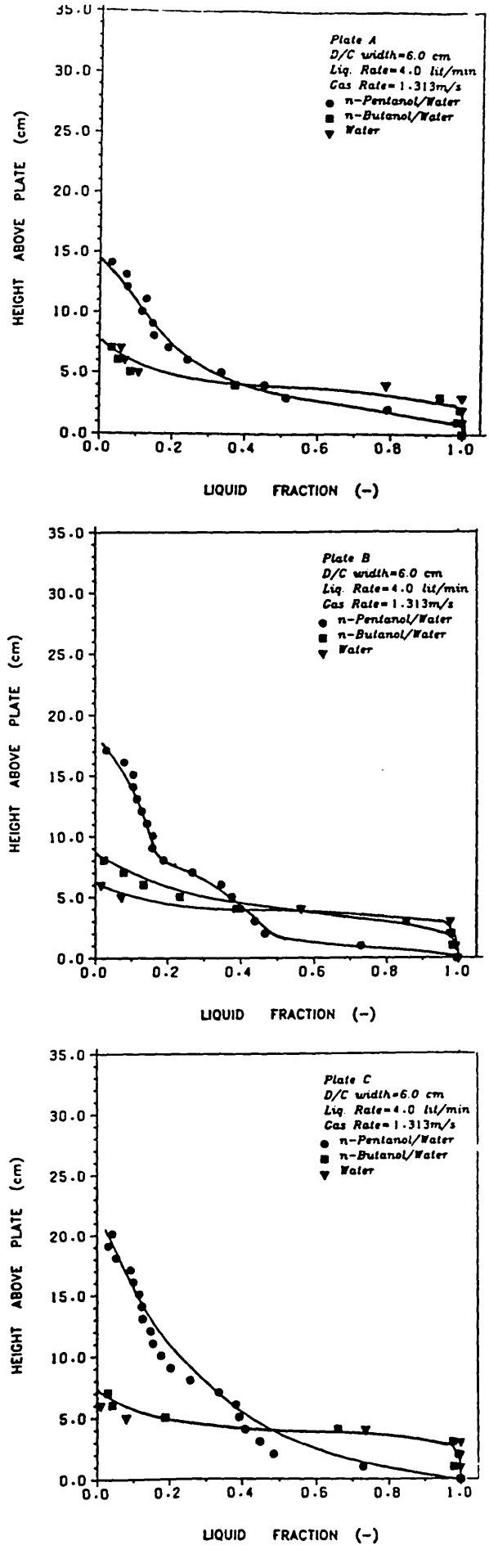

Figure 5.3 :- Variation of Liquid Fraction with Height of Dispersion in the Downcomer (Liquid Rate = 4.0 lit/min; Gas Rate = 1.313 m/s; Downcomer size = 6.0cm)

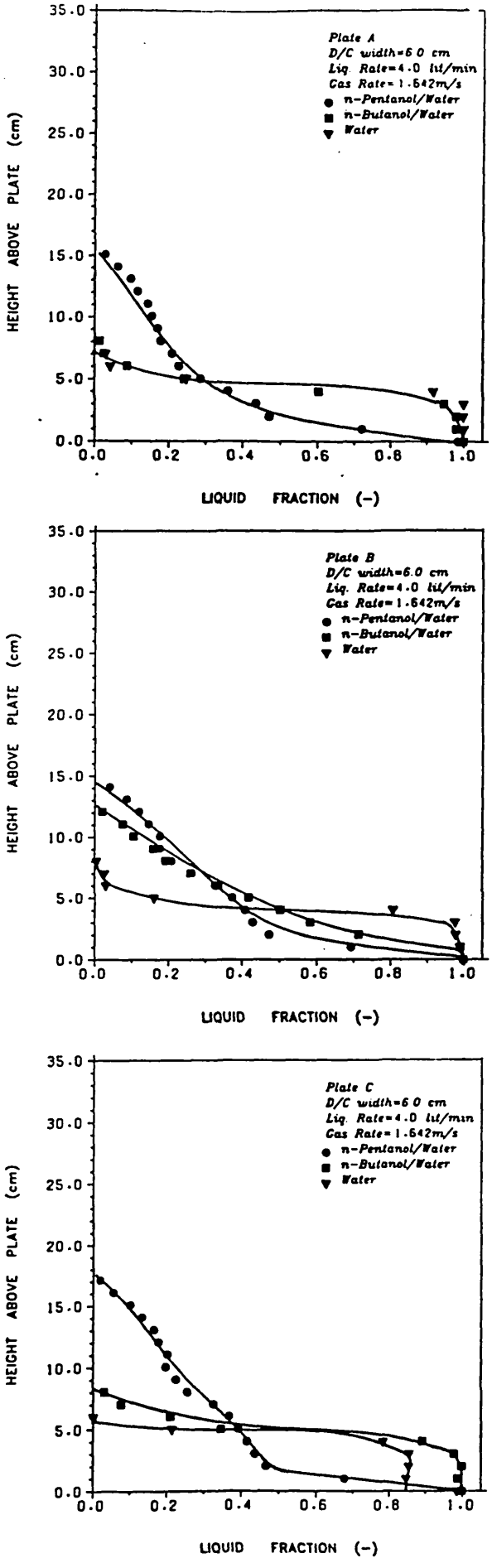

Figure 5.4 :- Variation of Liquid Fraction with Height of Dispersion in the Downcomer (Liquid Rate = 4.0 lit/min; Gas Rate = 1.642 m/s; Downcomer size = 6.0cm)

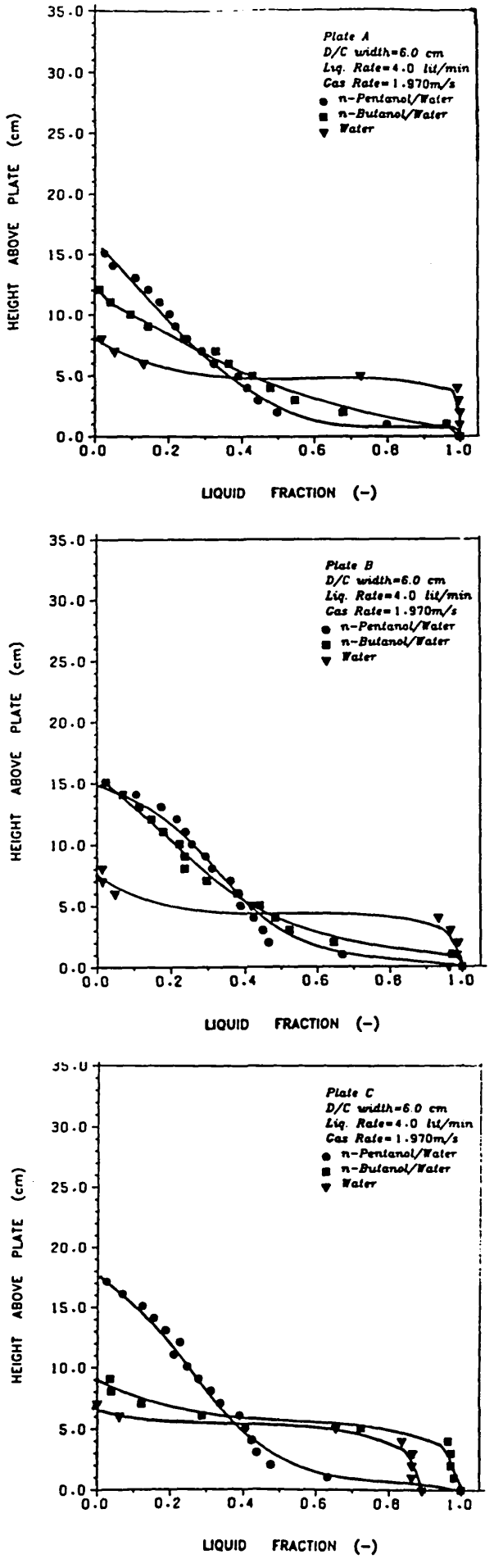

Figure 5.5 :- Variation of Liquid Fraction with Height of Dispersion in the Downcomer (Liquid Rate = 4.0 lit/min; Gas Rate = 1.970 m/s; Downcomer size = 6.0cm)

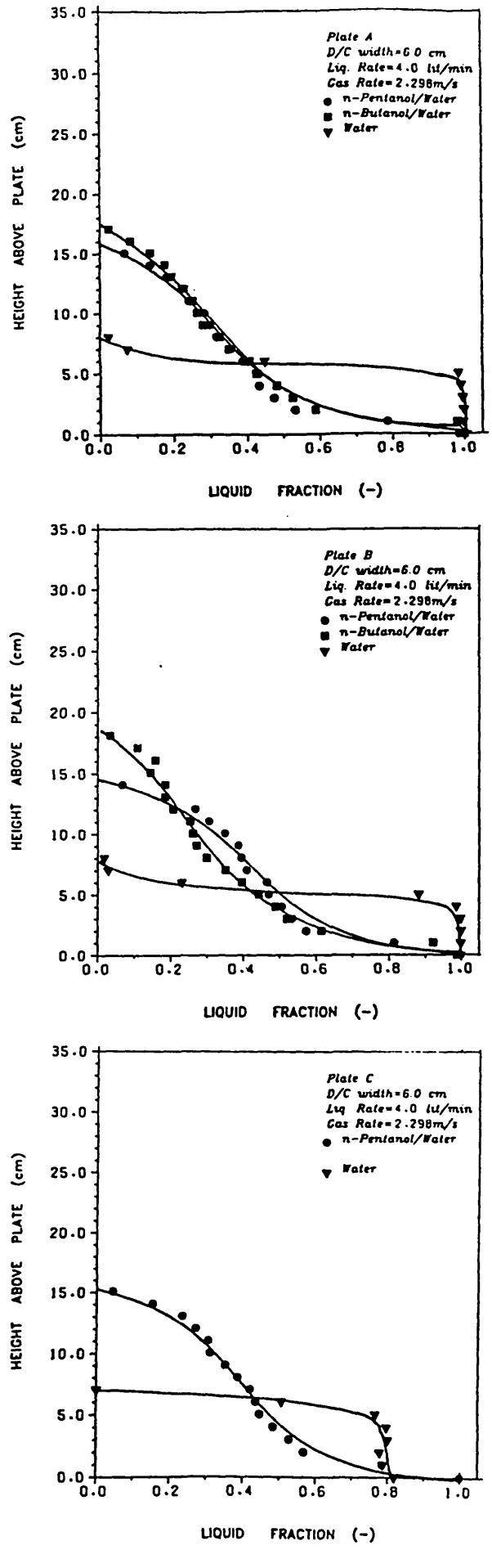

Figure 5.6 :- Variation of Liquid Fraction with Height of Dispersion in the Downcomer (Liquid Rate = 4.0 lit/min; Gas Rate = 2.298 m/s; Downcomer size = 6.0cm)

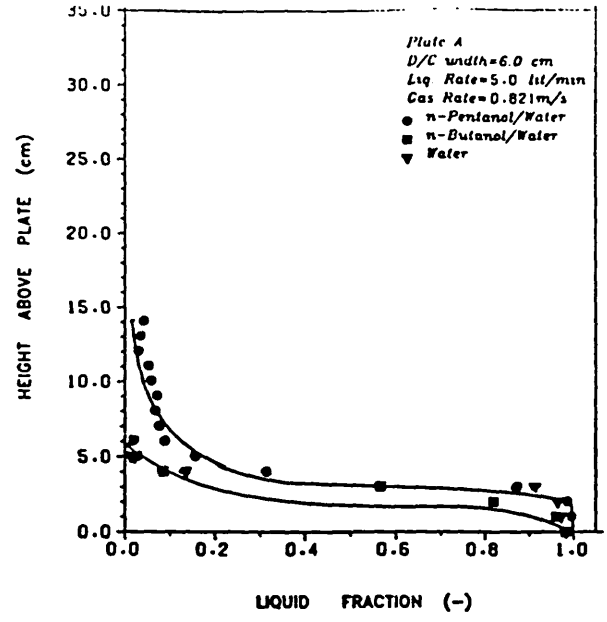

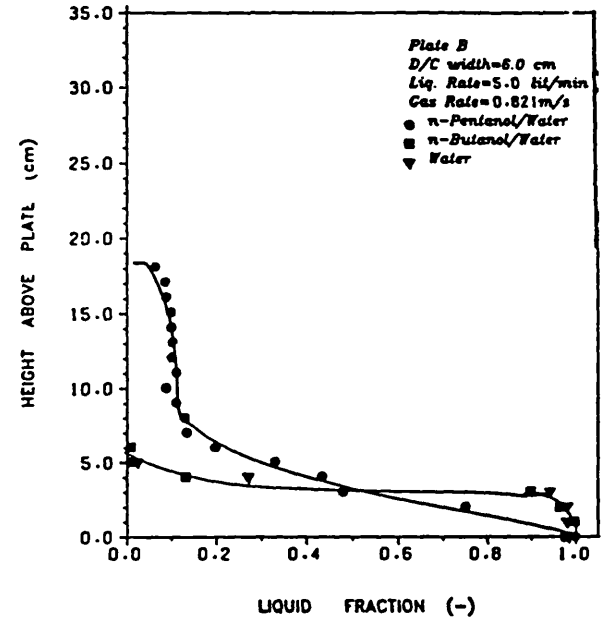

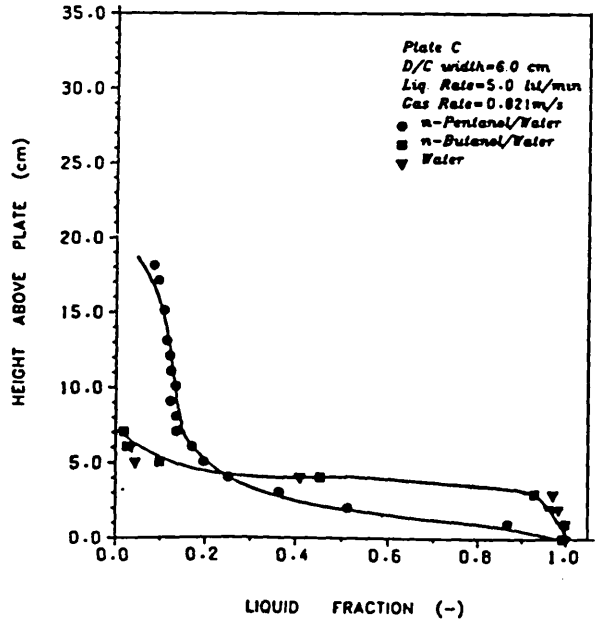

Figure 5.7 :- Variation of Liquid Fraction with Height of Dispersion in the Downcomer (Liquid Rate = 5.0 lit/min; Gas Rate = 0.821 m/s; Downcomer size = 6.0cm)

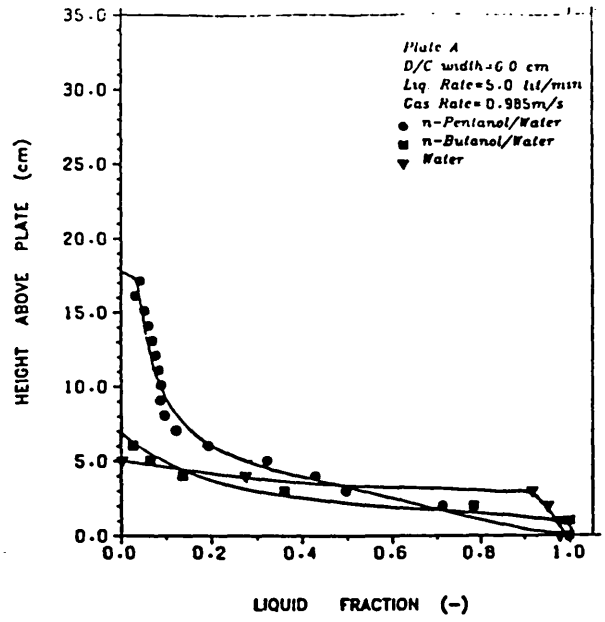

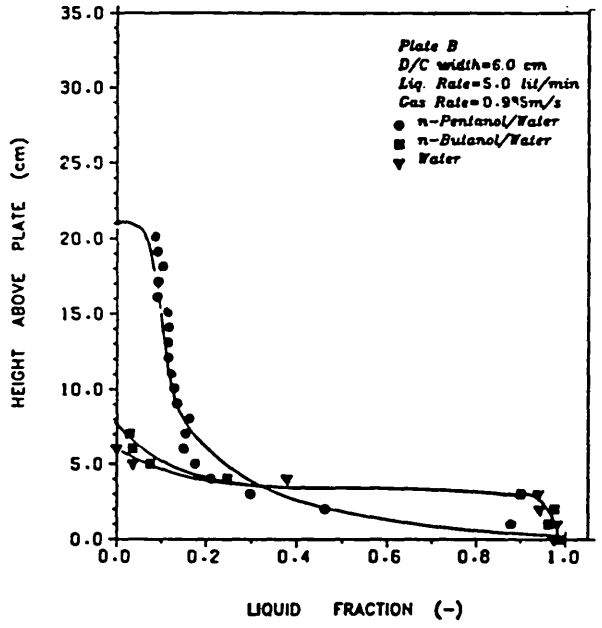

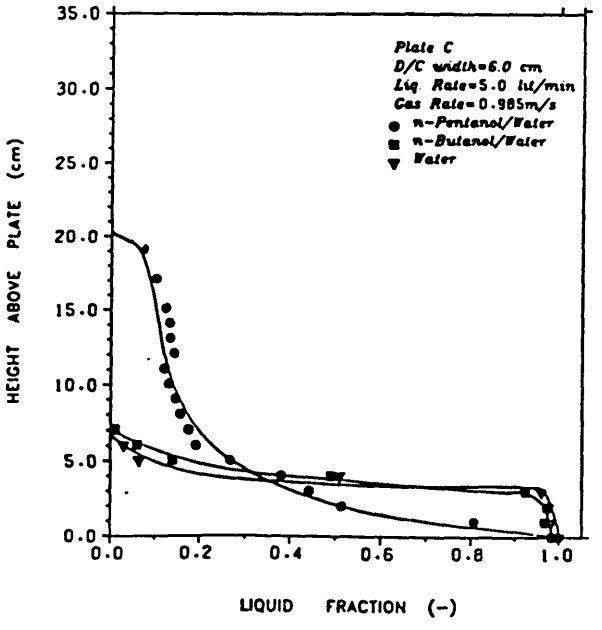

Figure 5.8 :- Variation of Liquid Fraction with Height of Dispersion in the Downcomer (Liquid Rate = 5.0 lit/min; Gas Rate = 0.985 m/s; Downcomer size = 6.0cm)

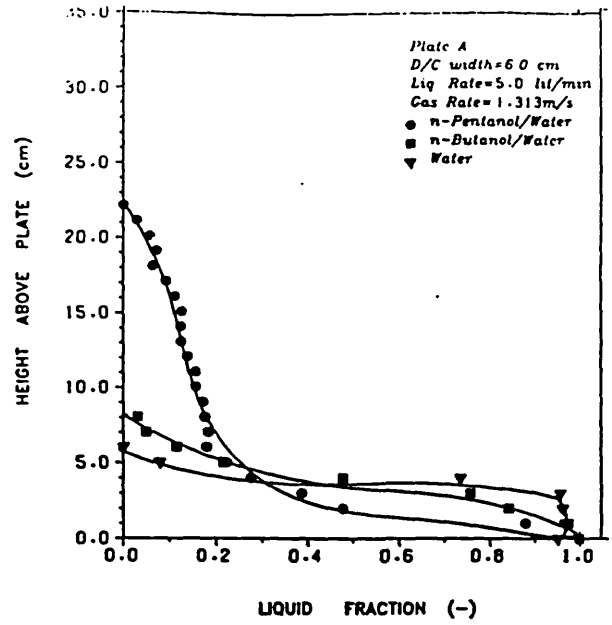

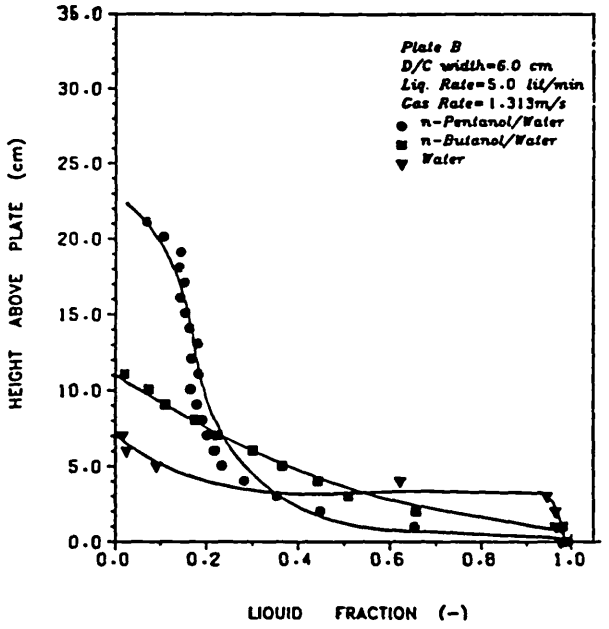

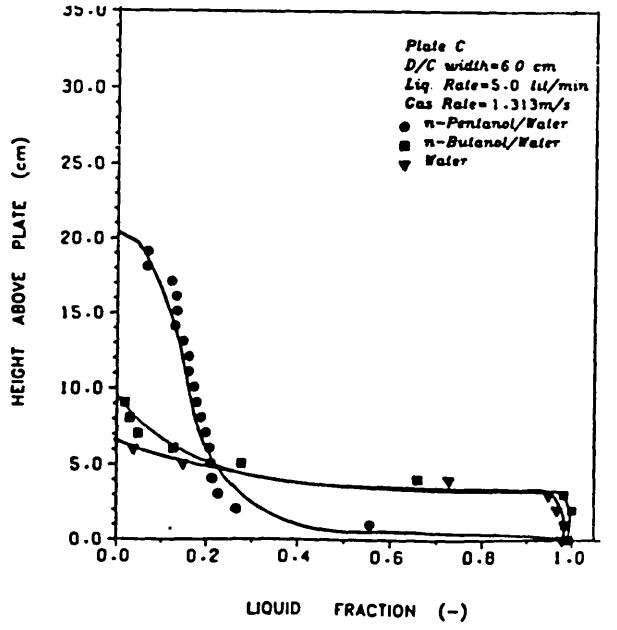

Figure 5.9 :- Variation of Liquid Fraction with Height of Dispersion in the Downcomer (Liquid Rate = 5.0 lit/min; Gas Rate = 1.313 m/s; Downcomer size = 6.0cm)

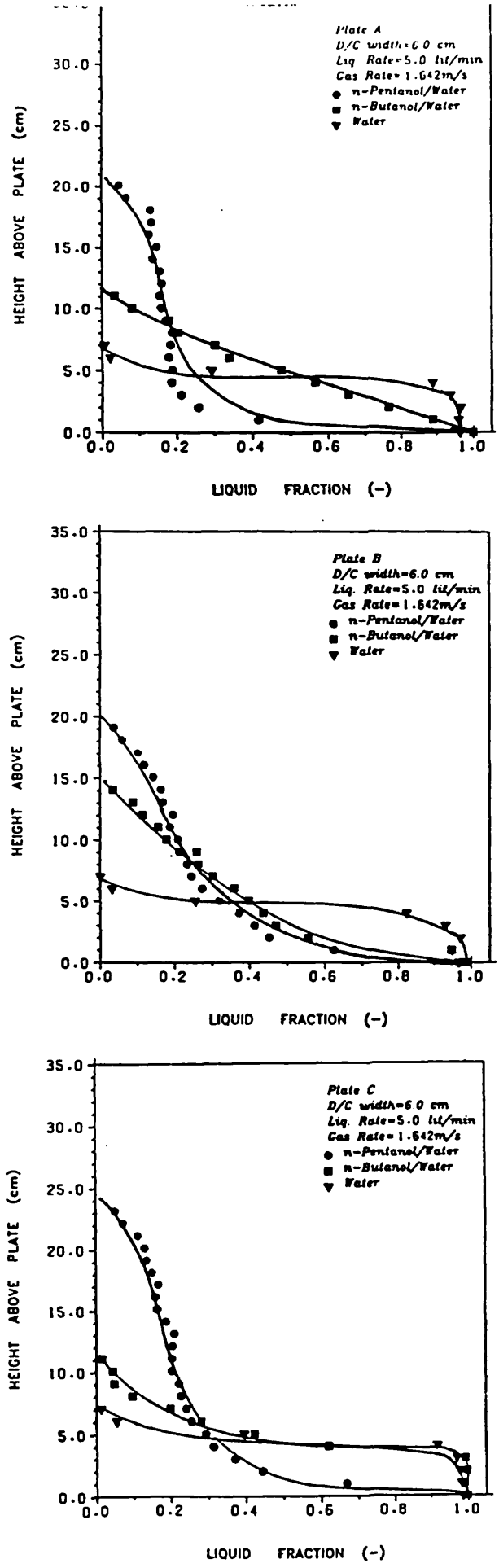

Figure 5.10 :- Variation of Liquid Fraction with Height of Dispersion in the Downcomer (Liquid Rate = 5.0 lit/min; Gas Rate = 1.642 m/s; Downcomer size = 6.0cm)

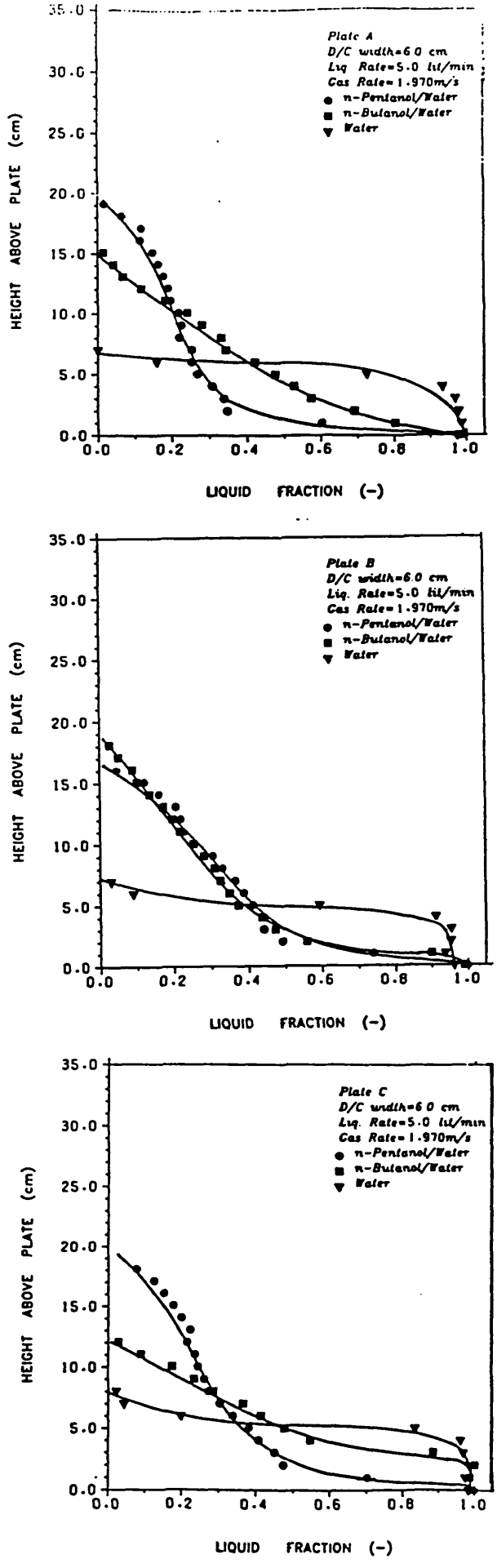

Figure 5.11 :- Variation of Liquid Fraction with Height of Dispersion in the Downcomer (Liquid Rate = 5.0 lit/min; Gas Rate = 1.970 m/s; Downcomer size = 6.0cm)

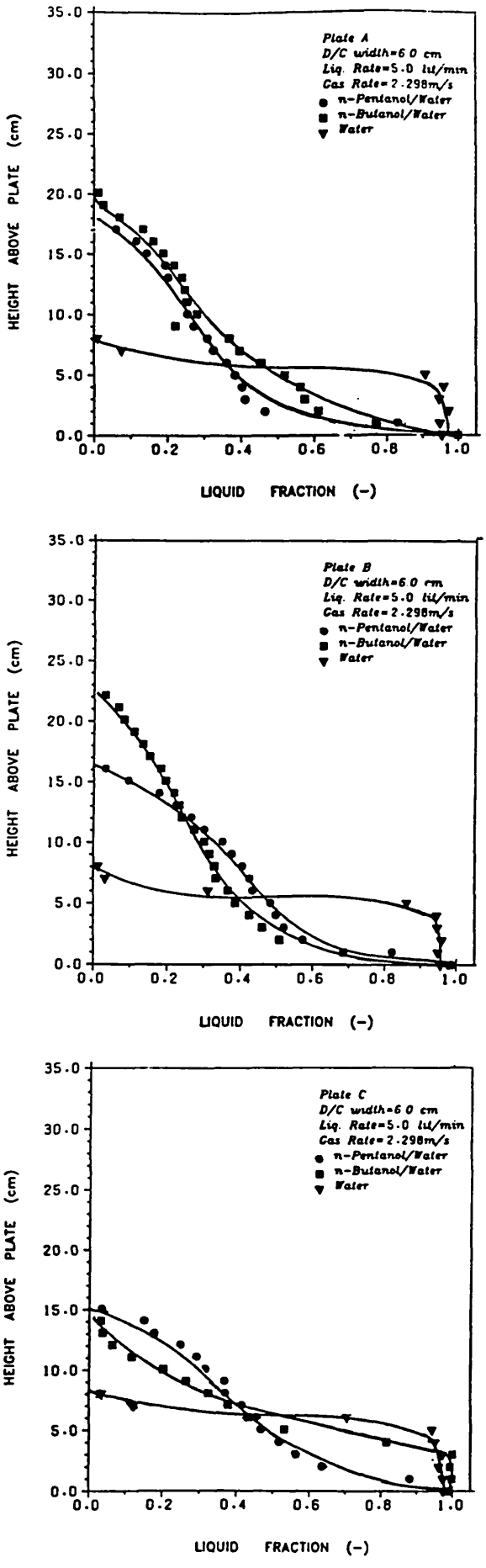

Figure 5.12 :- Variation of Liquid Fraction with Height of Dispersion in the Downcomer (Liquid Rate = 5.0 lit/min; Gas Rate = 2.298 m/s; Downcomer size = 6.0cm)

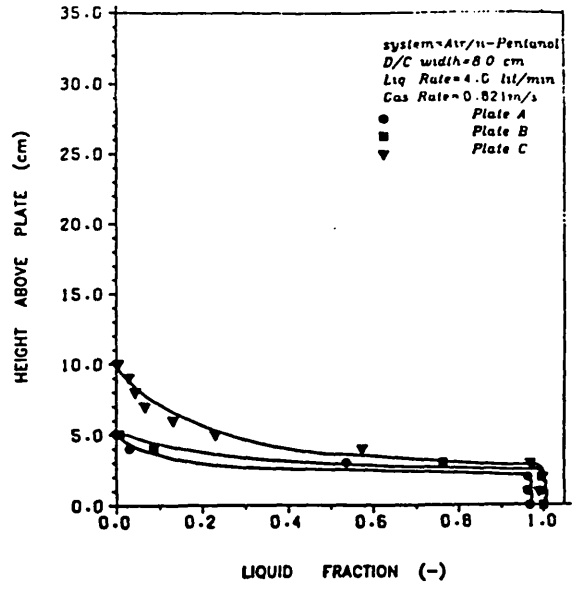

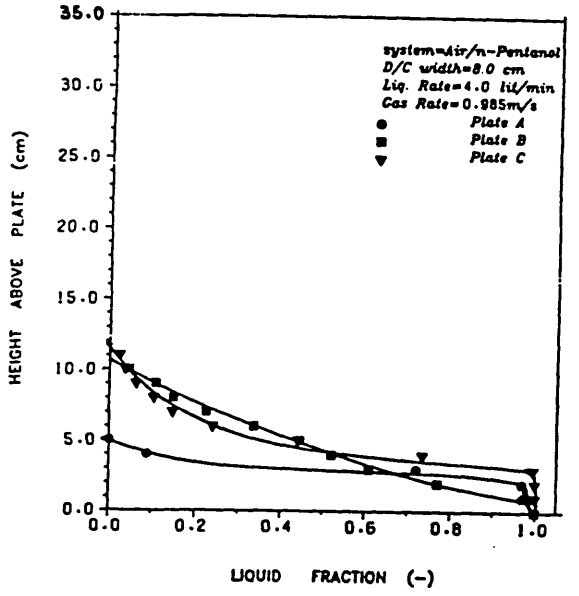

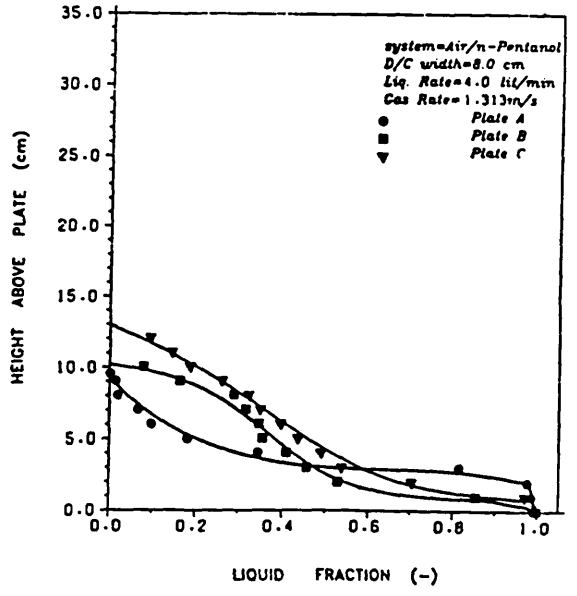

Figure 5.13 :- Variation of Liquid Fraction with Height of Dispersion in the Downcomer (Liquid Rate = 4.0 lit/min; Gas Rates = 0.8 21, 0.985, 1.313 m/s; Downcomer size = 8.0 cm)

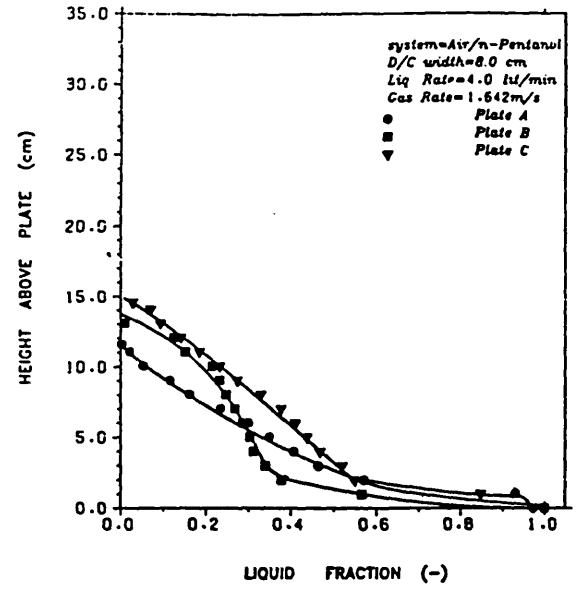

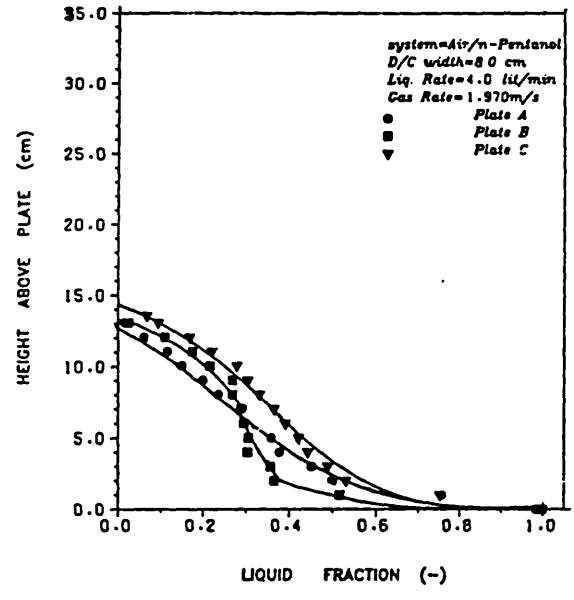

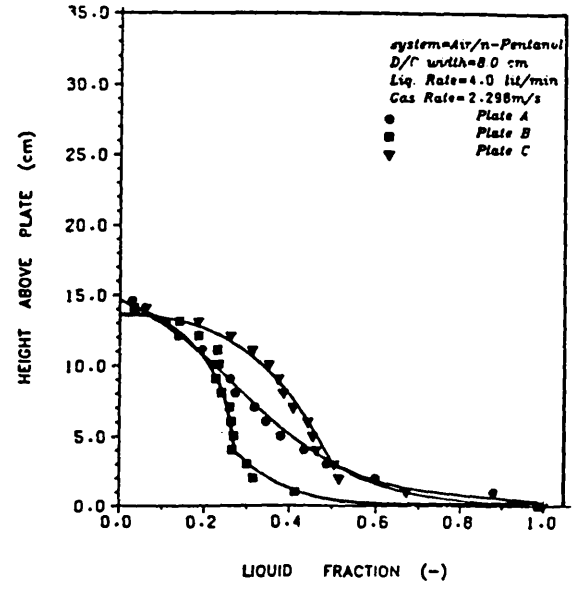

Figure 5.14 :- Variation of Liquid Fraction with Height of Dispersion in the Downcomer (Liquid Rate = 4.0 lit/min; Gas Rates = 1.642, 1.970, 2.298 m/s; Downcomer size = 8.0 cm)

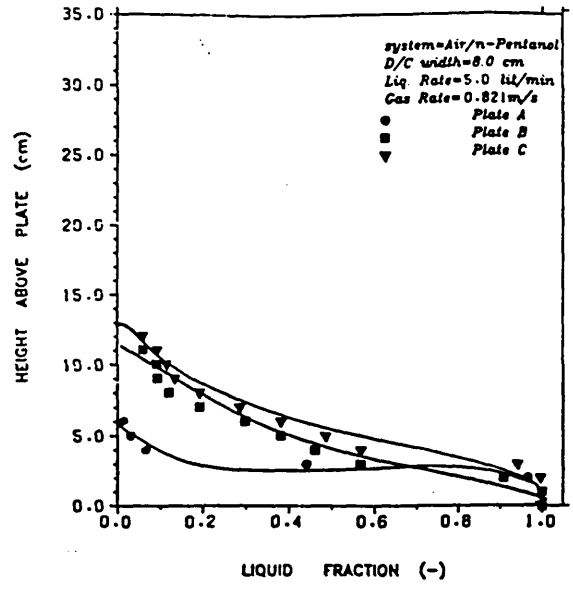

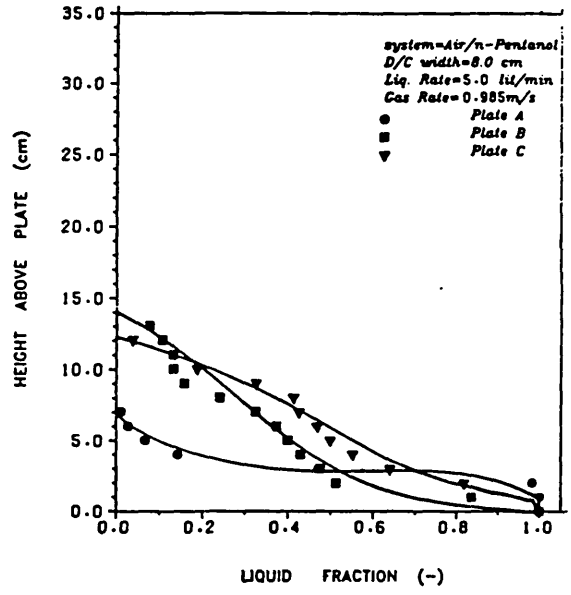

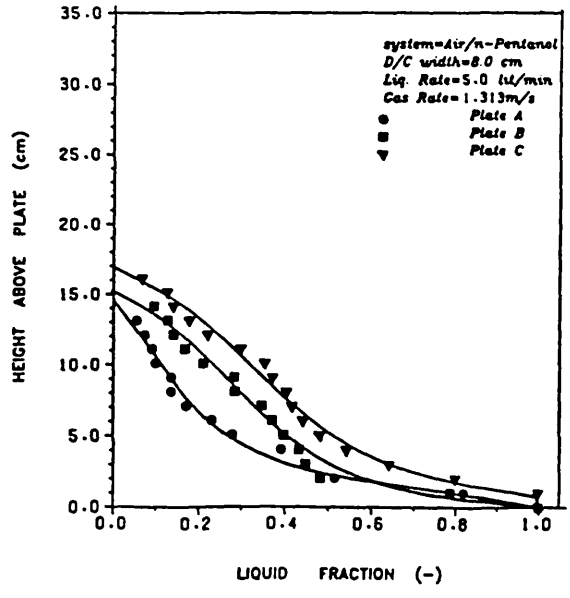

Figure 5.15 :- Variation of Liquid Fraction with Height of Dispersion in the Downcomer (Liquid Rate = 5.0 lit/min; Gas Rates = 0.821, 0.985, 1.313 m/s; Downcomer size = 8.0 cm)

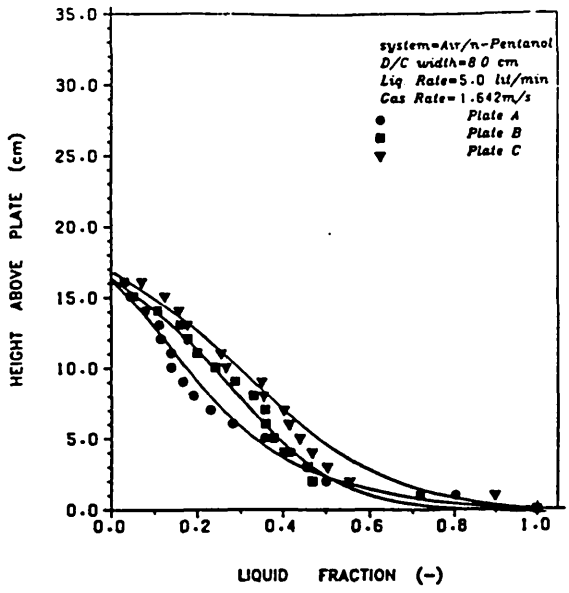

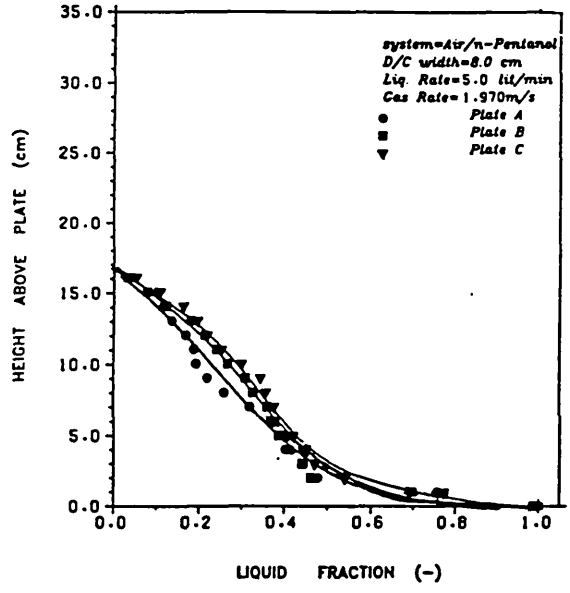

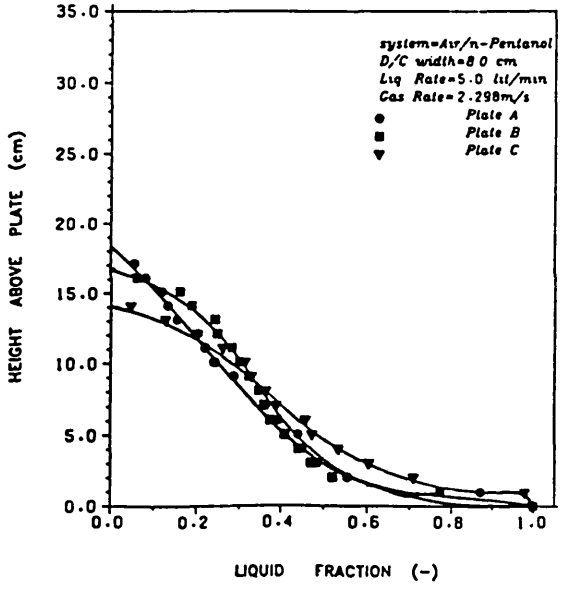

Figure 5.16 :- Variation of Liquid Fraction with Height of Dispersion in the Downcomer (Liquid Rate = 5.0 lit/min; Gas Rates = 1.642, 1.970, 2.298 m/s; Downcomer size = 8.0 cm)

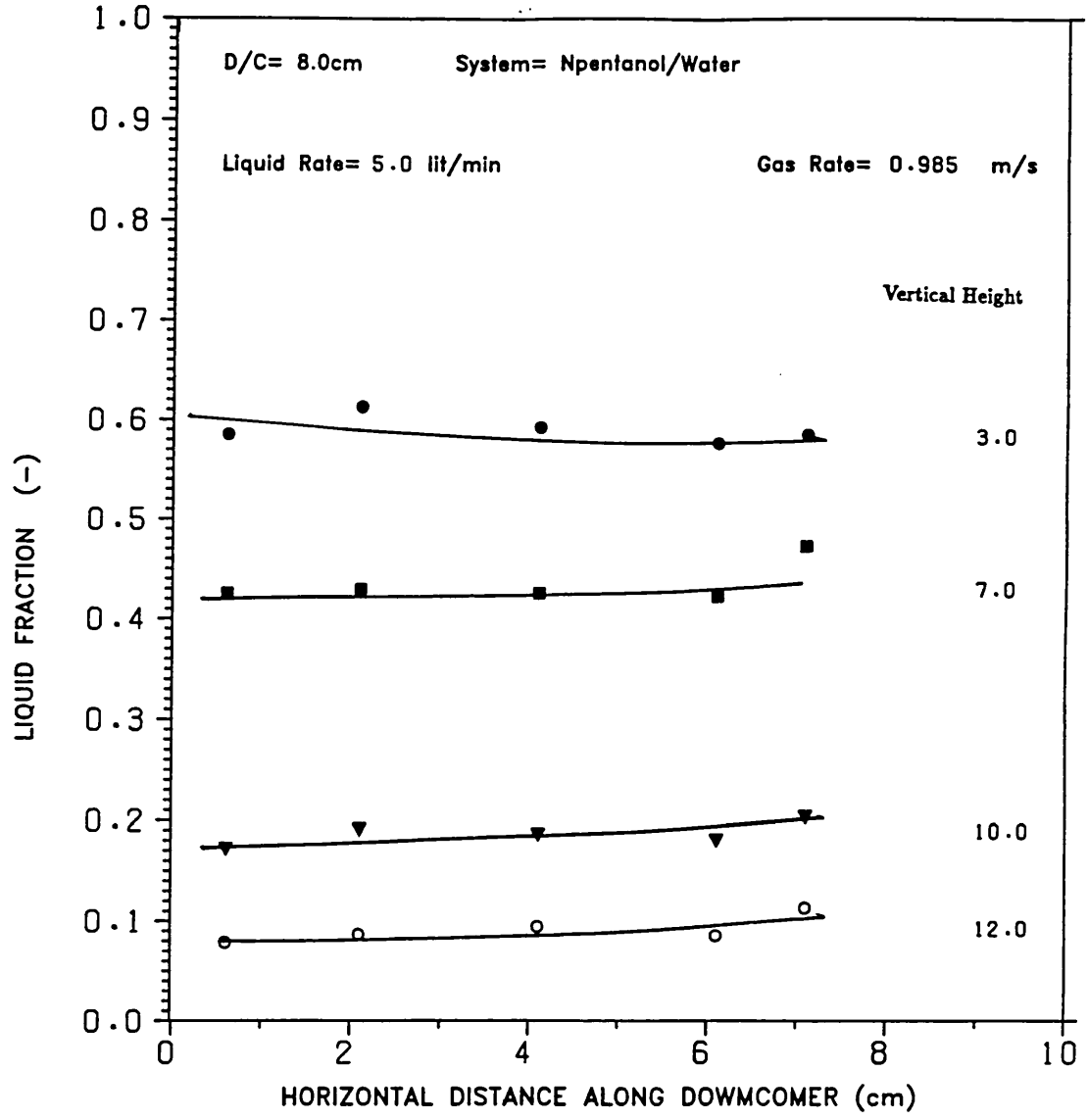

Figure 5.17a :- Horizontal Variation of Liquid Fraction in the Downcomer

5.3.3 Sauter Mean Diameter Profiles

Sauter mean diameter profiles are shown in figures 5.18 - 5.33 for the different gas/liquid loadings and downcomer size considered. The profiles for the foaming systems show an almost constant bubble diameter between 6 - 8 mm in regions where there is foaming. In regions where there is no foaming and generally for the non-foaming system, the profiles are characterised by small bubbles at the bottom of the dispersion and fairly large bubbles at the top. The tails of these profiles should however, be disregarded. This is mainly due to constant oscillations of the dispersion level at the top, brought about by the impact of fluid from the plate above, that lead to uncertainty in the data obtained in that region. Similarly, the seemingly large bubble near the bottom of the downcomer for the foaming systems should also be disregarded. This is due the effect of the separating line between the foam and clear liquid. In this situation the laser light sees a large surface and hence, the transmission of data corresponding to a large bubble. Profiles characteristic of the non-foaming system, and also in the regions where there is no foaming in the case of the foaming systems, suggest there is quick gas disengagement from the dispersion. For proper interpretation of these results, the mechanism of gas disengagement must be understood. In the case of the non-foaming system, two modes of gas disengagement may be considered, namely;

1) Bubbles coalesce and disengage easily

2) There is little or no bubble coalescence

A closer look at the two modes shows that mode 2 is highly favoured for the non-foaming system and in regions where there is no foaming in the case of foaming systems. This due to the fact that in these cases, bubble density in the dispersion is very low. Hence the probability of bubble coalescence is also low. Therefore, the only mode of gas disengagement is through breakup of the bubbles at the top gas-liquid interface. In regions of foaming, in the case of foaming systems, the surfactant adsorbed at the interface prsents a barrier to bubble coalescence and breakup. Therefore, the rate of gas disengagement is reduced and the froth/foam grows, leading to high dispersion heights and an almost uniform bubble sizes in the downcomer. The effect of gas and liquid rates on the Sauter mean diameter is not significant. This indicates that bubble diameters obtained in the downcomer are not a significant parameter in determining the flow of froth/foam in downcomers. From the results obtained, it appears that one of the dominating parameters leading to foaming/frothing in downcomers is the surface activity of the solution employed.

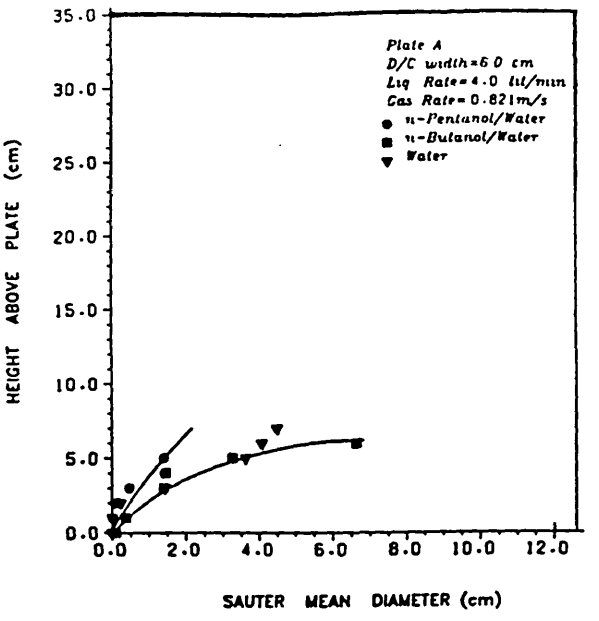

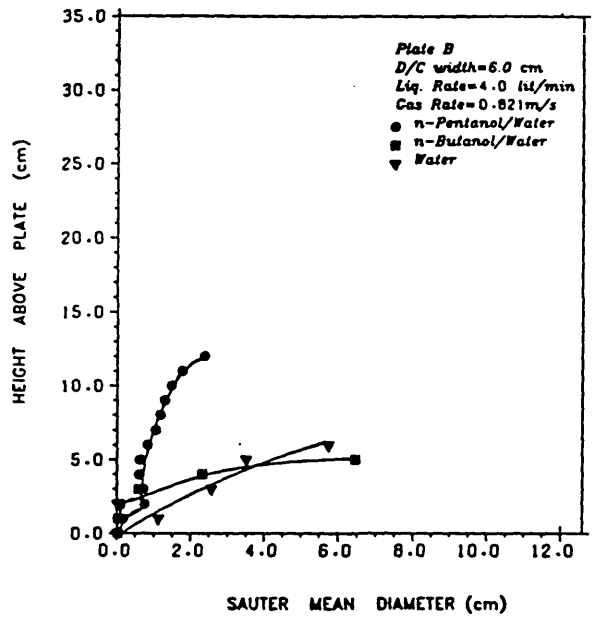

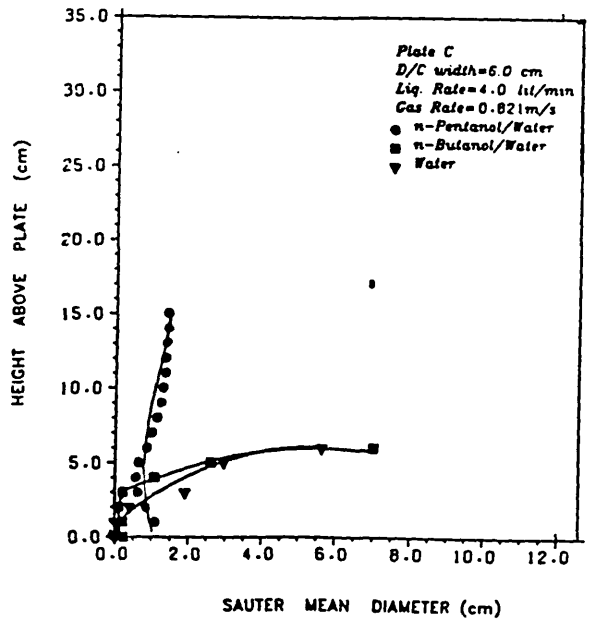

Figure 5.18 :- Variation of Sauter Mean Diameter with Height of Dispersion in Downcomer (Liquid Rate = 4.0 lit/min; Gas Rate = 0.821 m/s Downcomer size = 6.0cm)

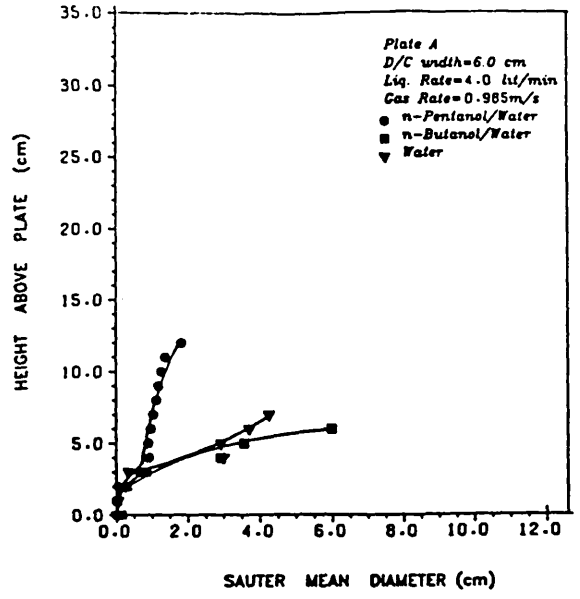

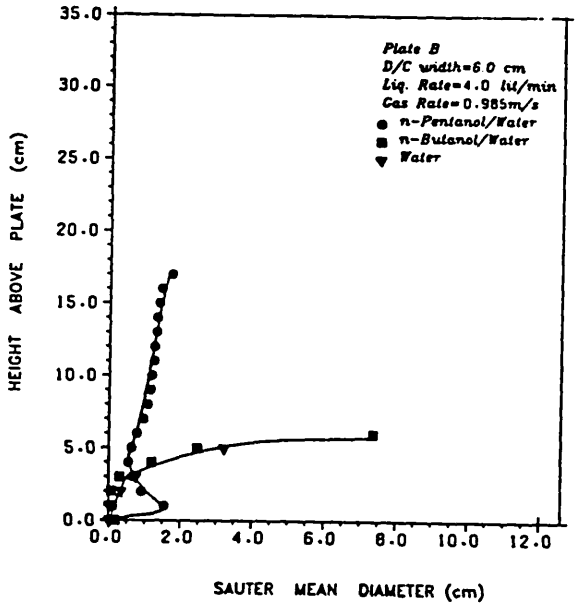

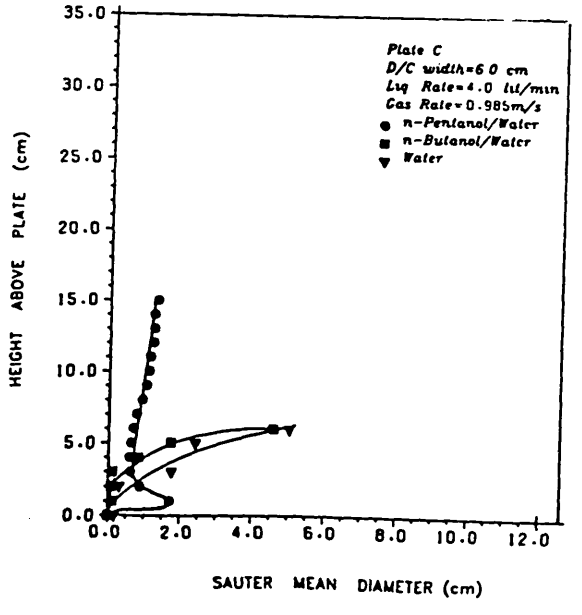

Figure 5.19 :- Variation of Sauter Mean Diameter with Height of Dispersion in Downcomer (Liquid Rate = 4.0 lit/min; Gas Rate = 0.985 m/s; Downcomer size = 6.0cm)

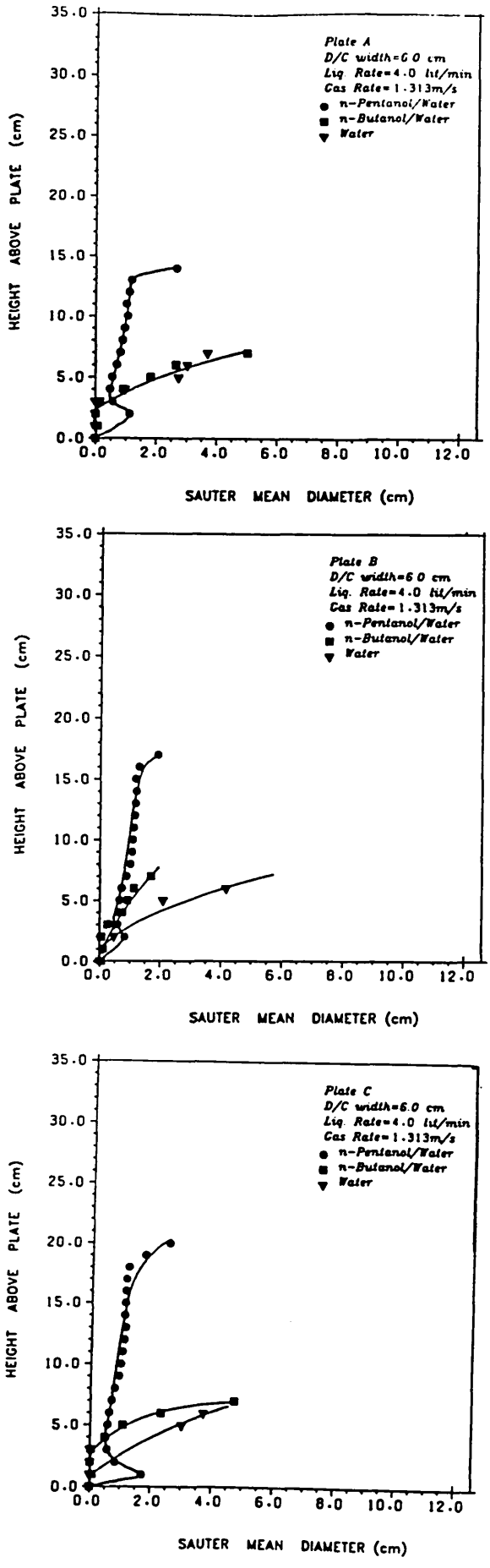

Figure 5.20 :- Variation of Sauter Mean Diameter with Height of Dispersion in Downcomer (Liquid Rate = 4.0 lit/min; Gas Rate = 1.313 m/s; Downcomer size = 6.0cm)

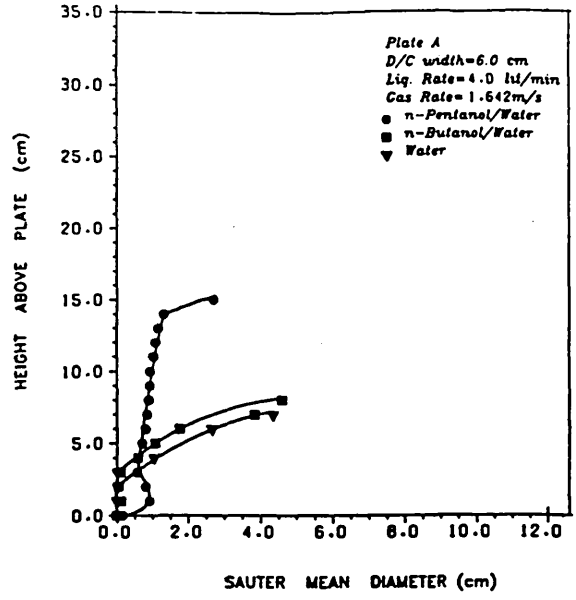

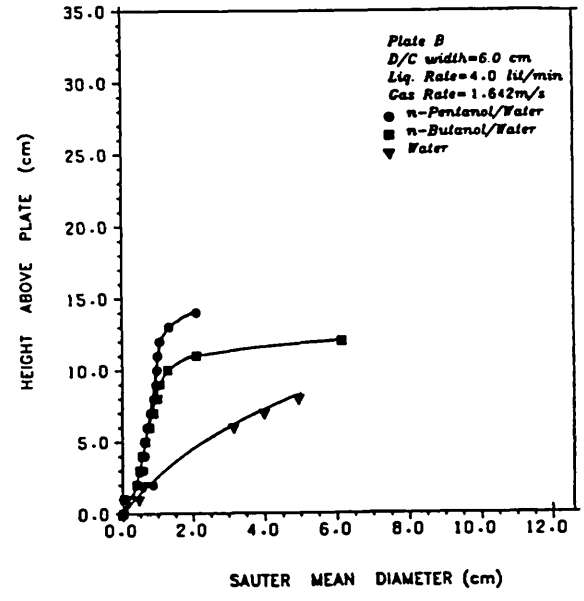

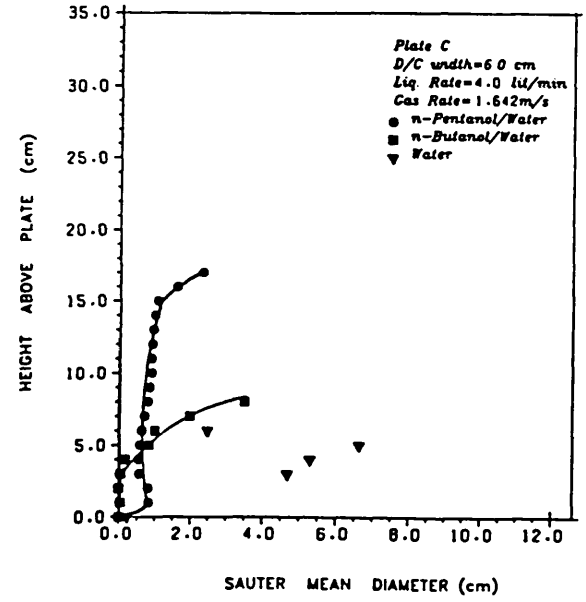

Figure 5.21 :- Variation of Sauter Mean Diameter with Height of Dispersion in Downcomer (Liquid Rate = 4.0 lit/min; Gas Rate = 1.642 m/s; Downcomer size = 6.0cm)

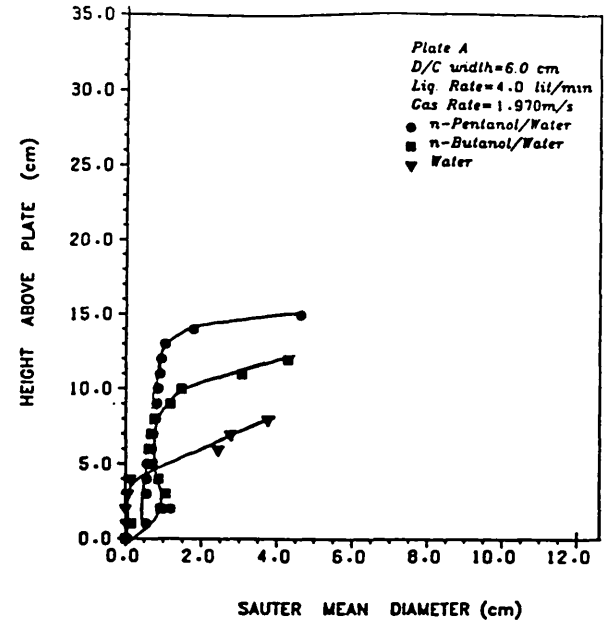

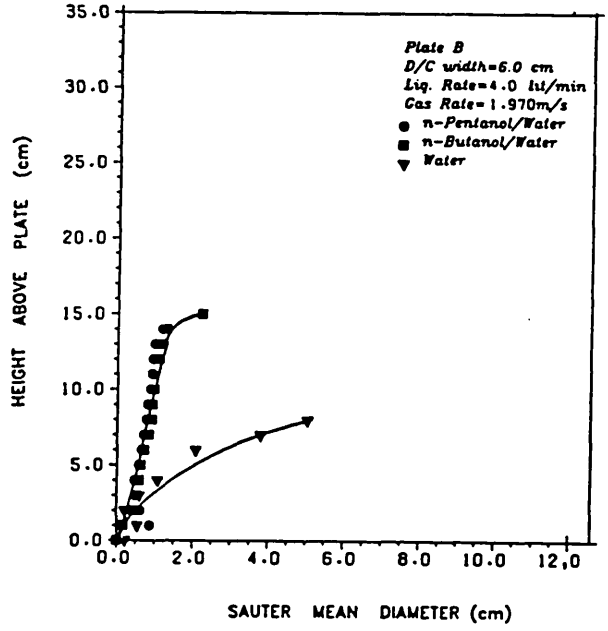

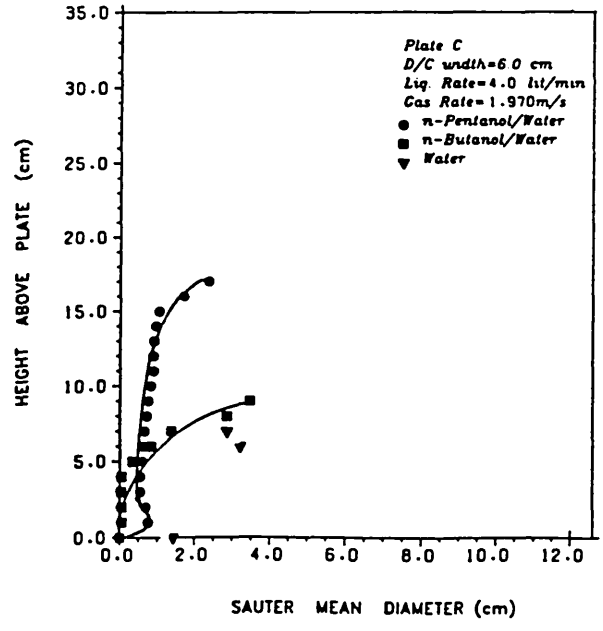

Figure 5.22 :- Variation of Sauter Mean Diameter with Height of Dispersion in Downcomer (Liquid Rate = 4.0 lit/min; Gas Rate = 1.970 m/s; Downcomer size = 6.0cm)

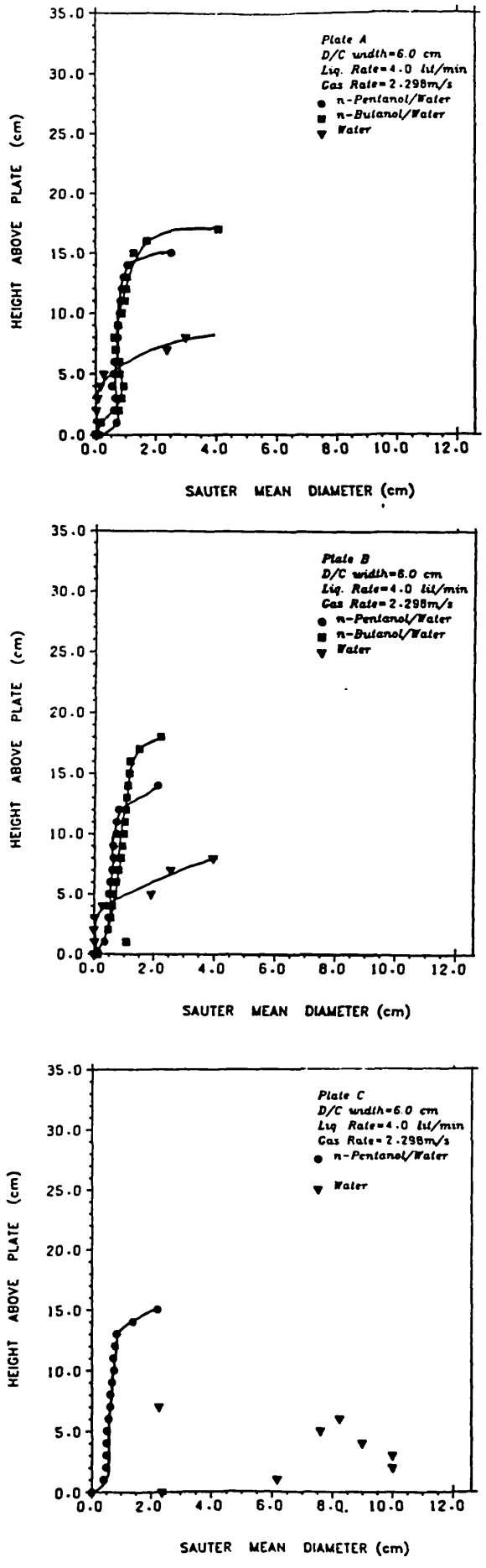

Figure 5.23 :- Variation of Sauter Mean Diameter with Height of Dispersion in Downcomer (Liquid Rate = 4.0 lit/min; Gas Rate = 2.298 m/s; Downcomer size = 6.0cm)

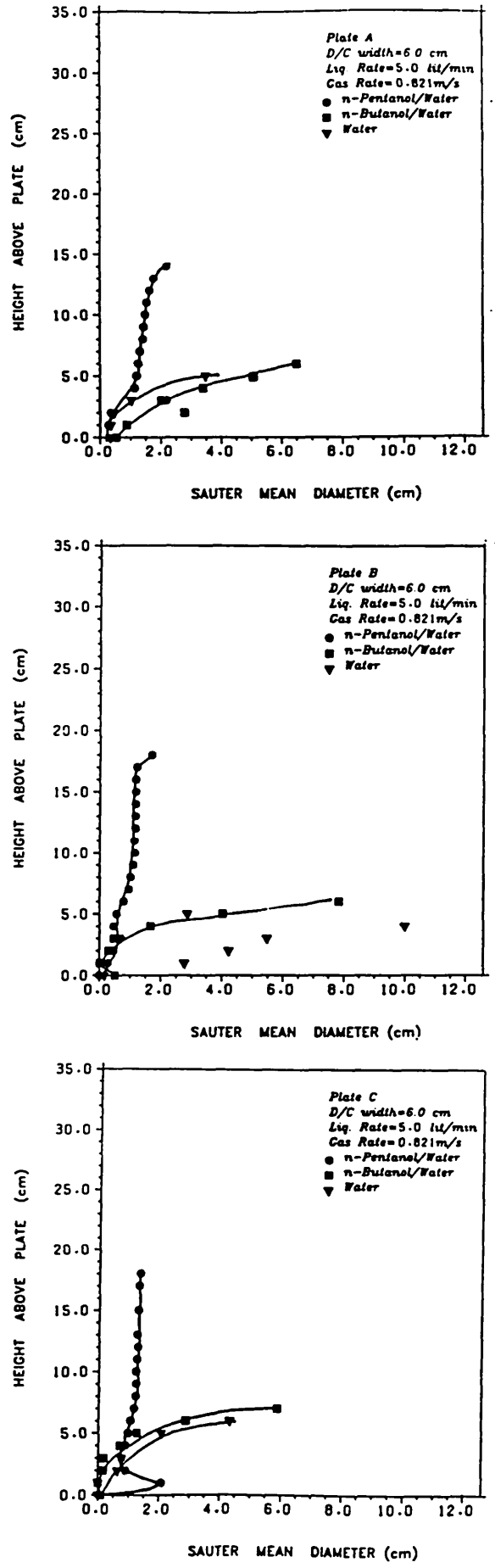

Figure 5.24 :- Variation of Sauter Mean Diameter with Height of Dispersion in Downcomer (Liquid Rate = 5.0 lit/min; Gas Rate = 0.821 m/s; Downcomer size = 6.0cm)

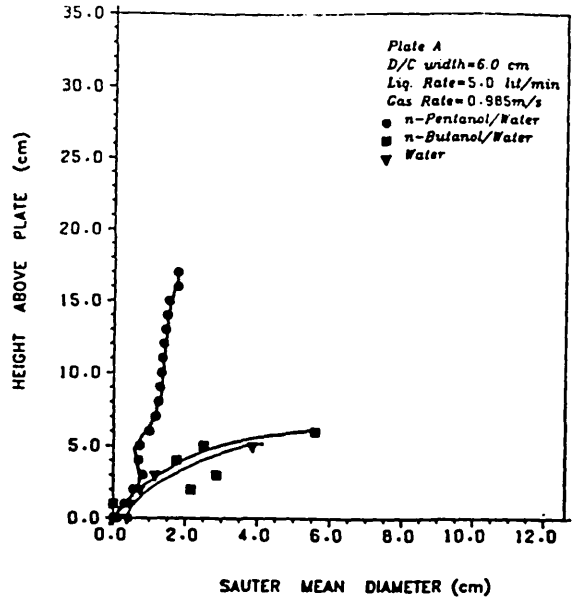

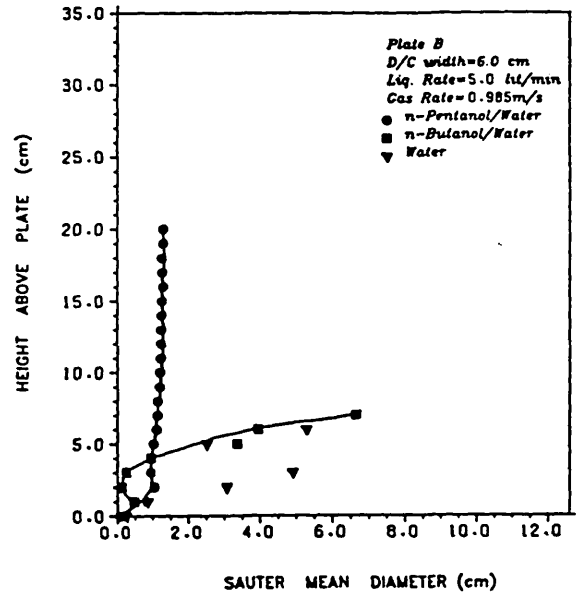

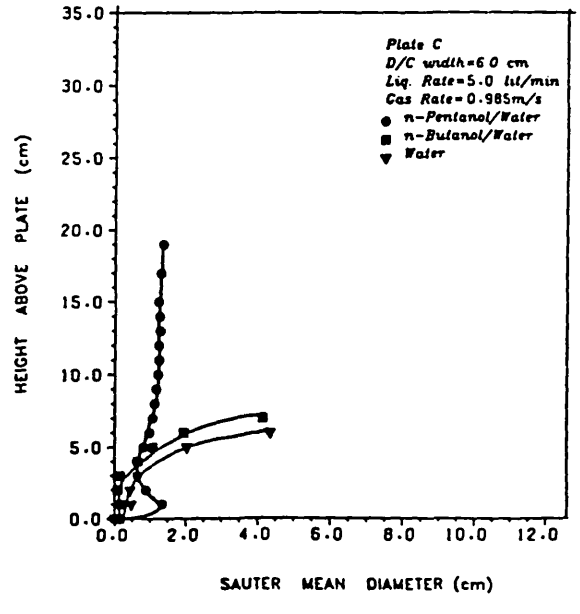

Figure 5.25 :- Variation of Sauter Mean Diameter with Height of Dispersion in Downcomer (Liquid Rate = 5.0 lit/min; Gas Rate = 0.985 m/s; Downcomer size = 6.0cm)

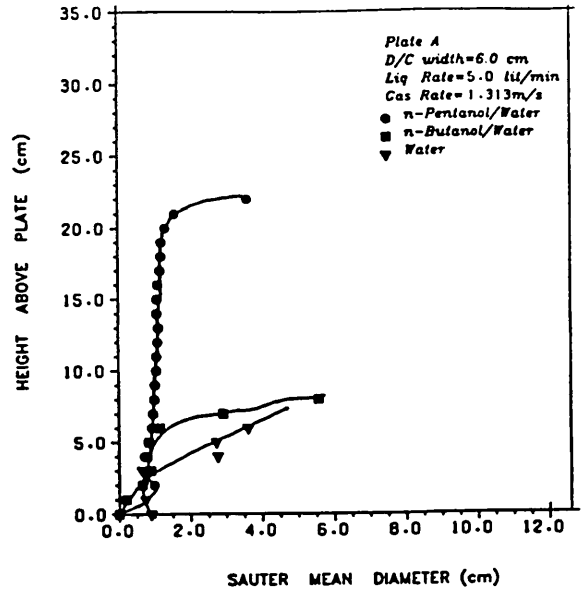

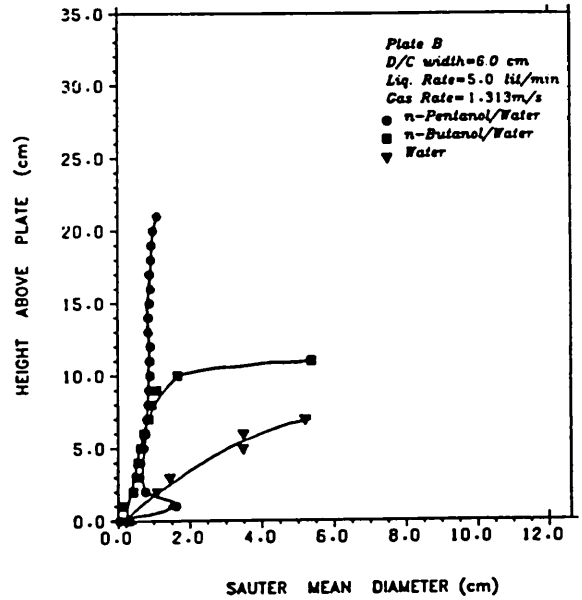

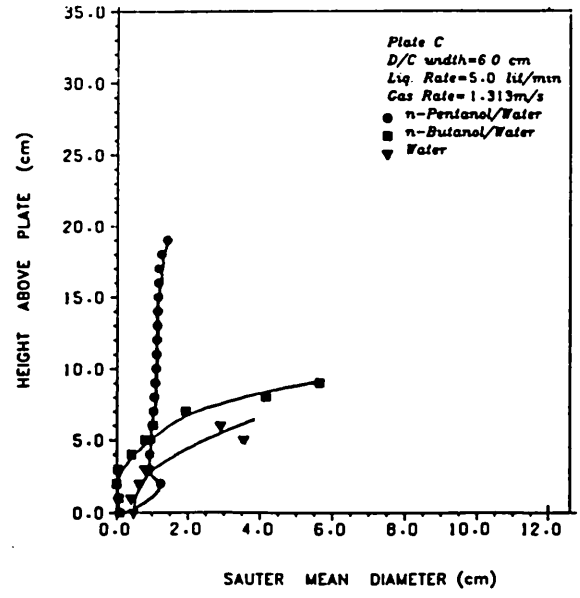

Figure 5.26 :- Variation of Sauter Mean Diameter with Height of Dispersion in Downcomer (Liquid Rate = 5.0 lit/min; Gas Rate = 1.313 m/s; Downcomer size = 6.0cm)

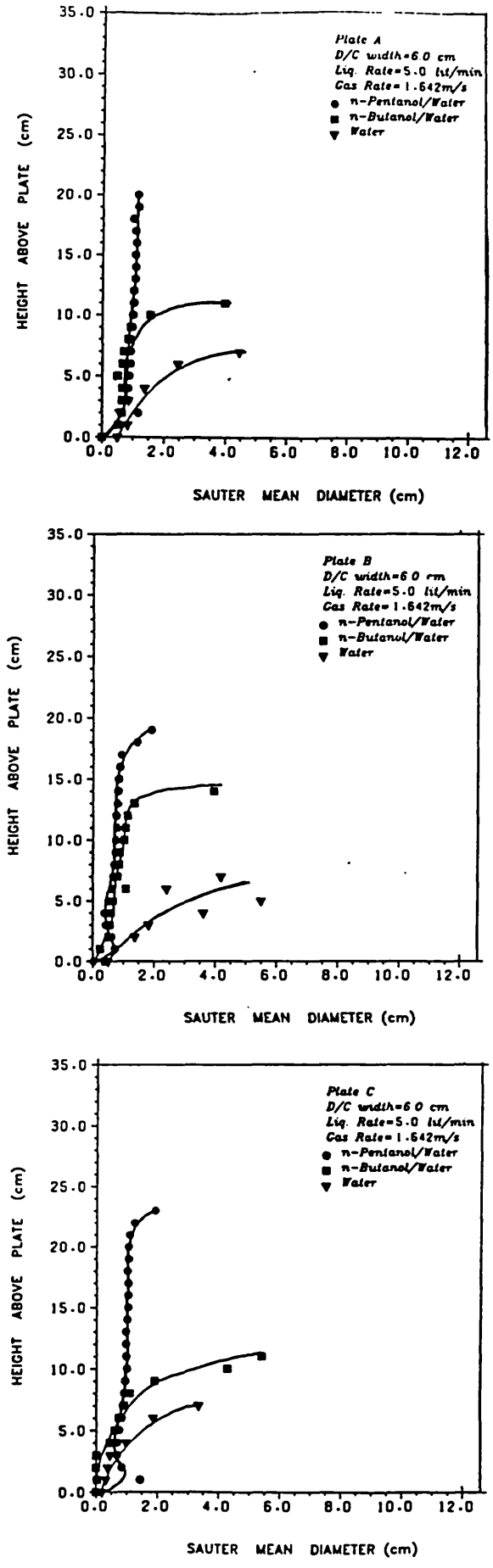

Figure 5.27 :- Variation of Sauter Mean Diameter with Height of Dispersion in Downcomer (Liquid Rate = 5.0 lit/min; Gas Rate = 1.642 m/s; Downcomer size = 6.0cm)

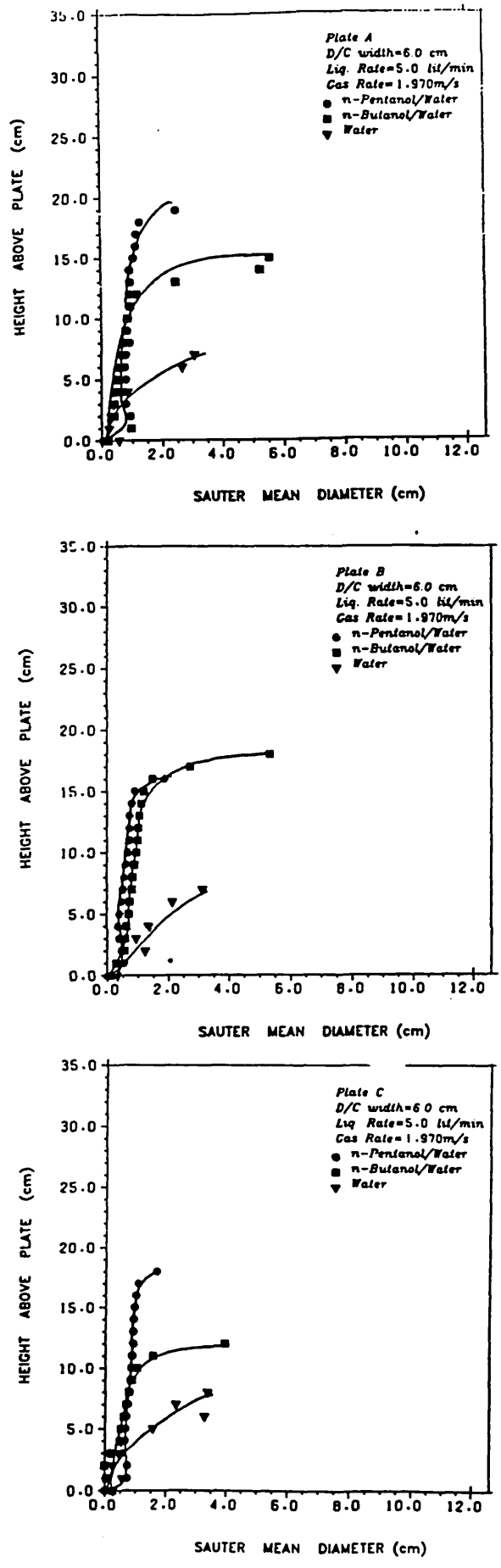

Figure 5.28 :- Variation of Sauter Mean Diameter with Height of Dispersion in Downcomer (Liquid Rate = 5.0 lit/min; Gas Rate = 1.970 m/s; Downcomer size = 6.0cm)

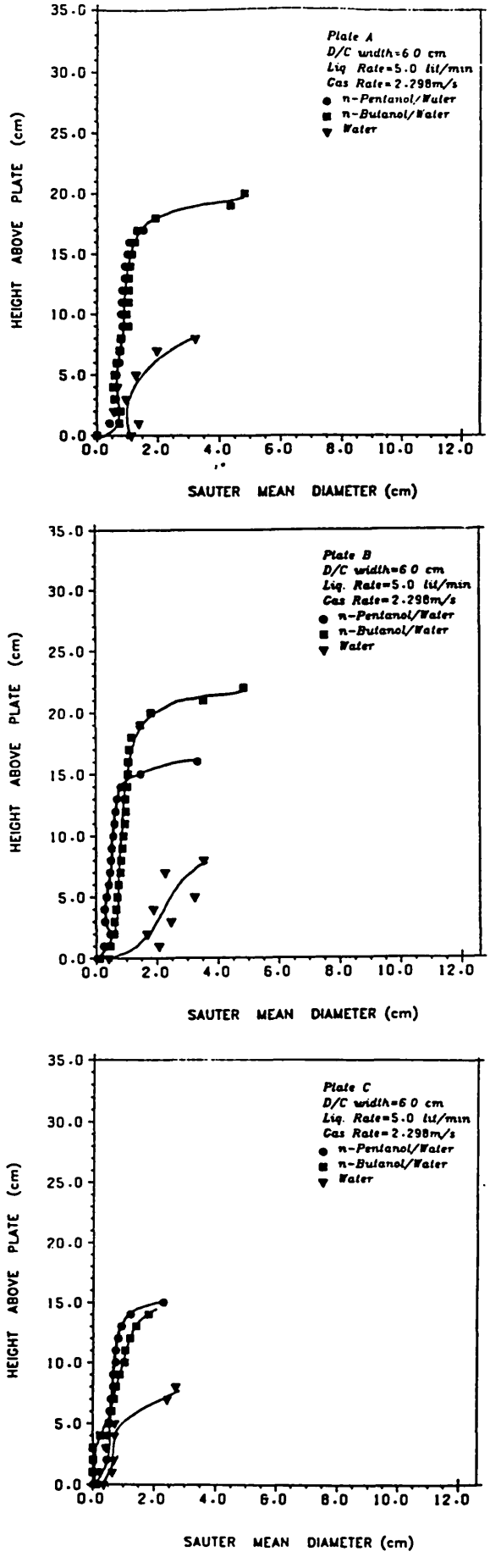

Figure 5.29 :- Variation of Sauter Mean Diameter with Height of Dispersion in Downcomer (Liquid Rate = 5.0 lit/min; Gas Rate = 2.298 m/s; Downcomer size = 6.0cm)

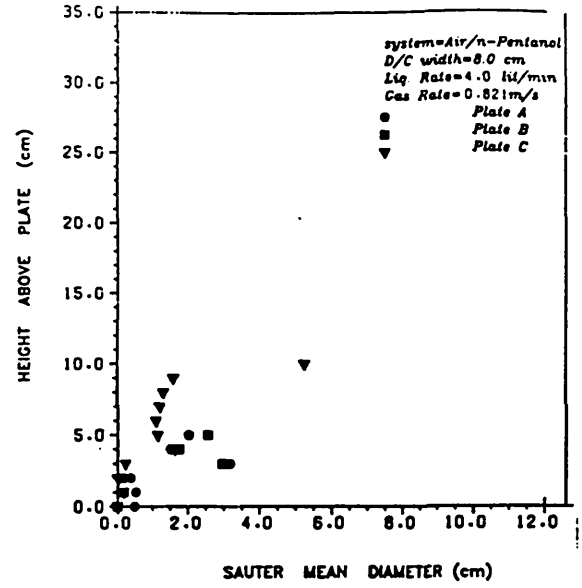

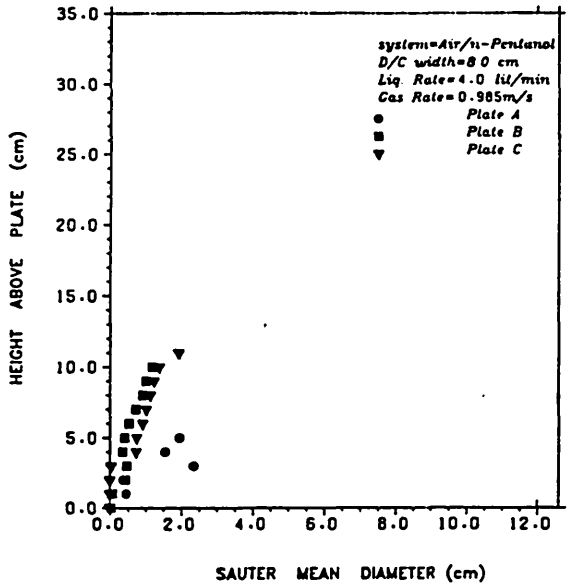

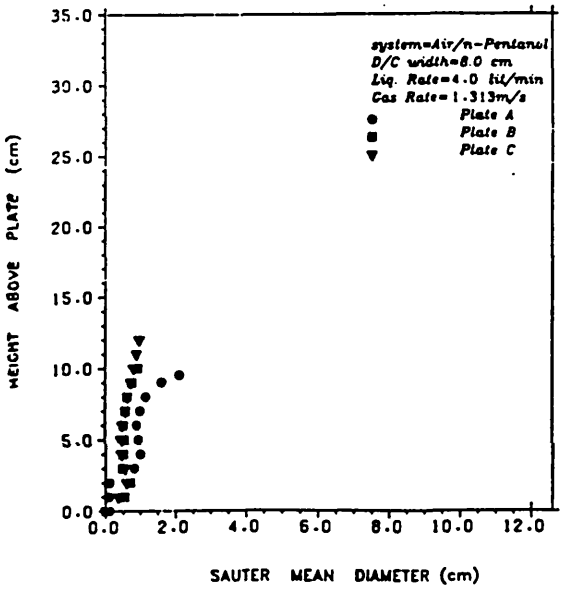

Figure 5.30 :- Variation of Sauter Mean Diameter with Height of Dispersion in Downcomer (Liquid Rate = 4.0 lit/min; Gas Rates = 0.821, 0.985, 1.313 m/s; Downcomer size = 8.0 cm)

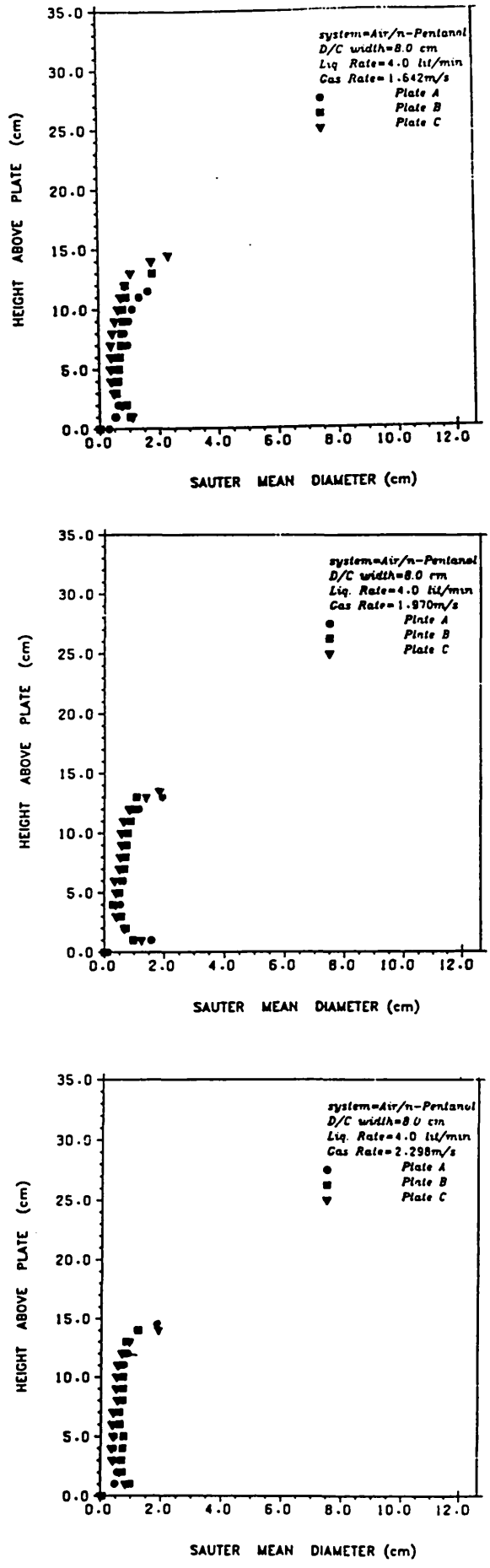

Figure 5.31 :- Variation of Sauter Mean Diameter with Height of Dispersion in Downcomer (Liquid Rate = 4.0 lit/min; Gas Rates = 1.642, 1.970, 2.298 m/s; Downcomer size = 8.0 cm)

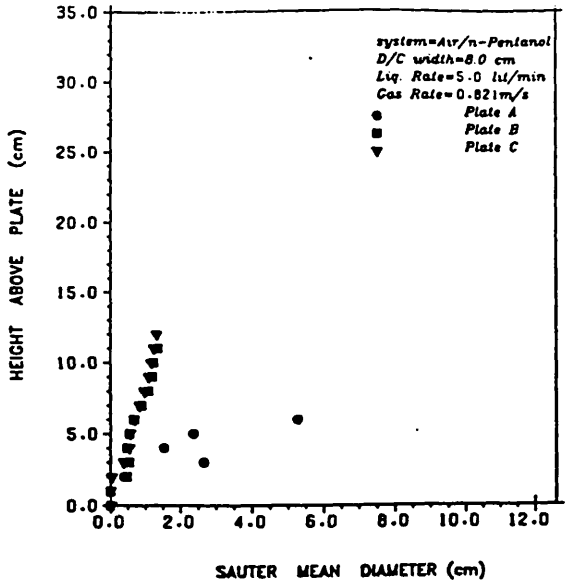

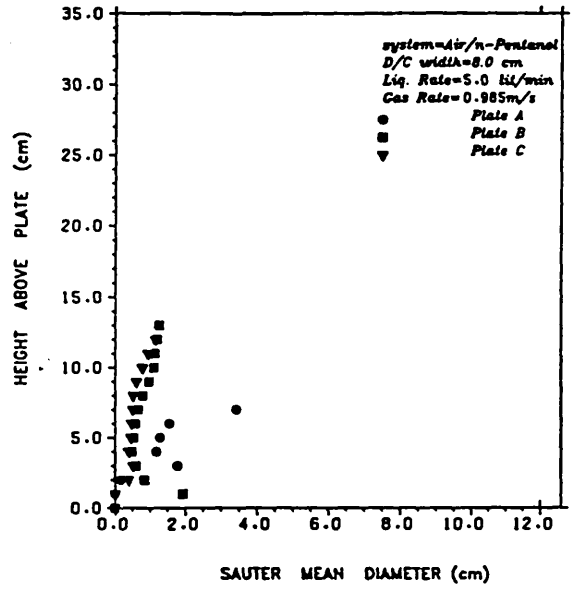

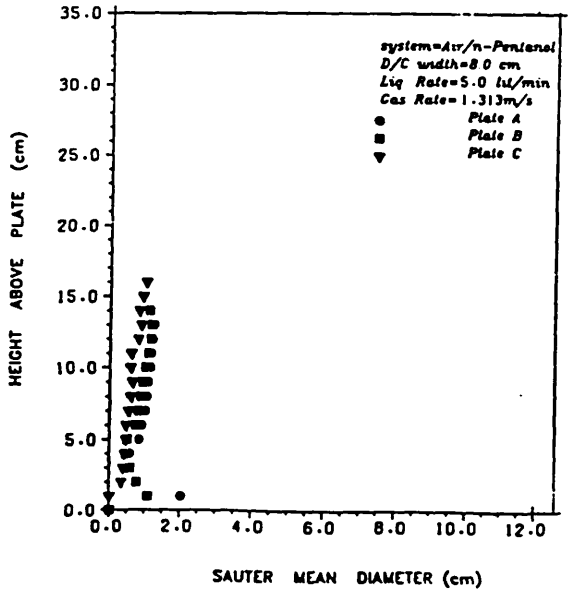

Figure 5.32 :- Variation of Sauter Mean Diameter with Height of Dispersion in Downcomer (Liquid Rate = 5.0 lit/min; Gas Rates = 0.821, 0.985, 1.313 m/s; Downcomer size = 8.0 cm)

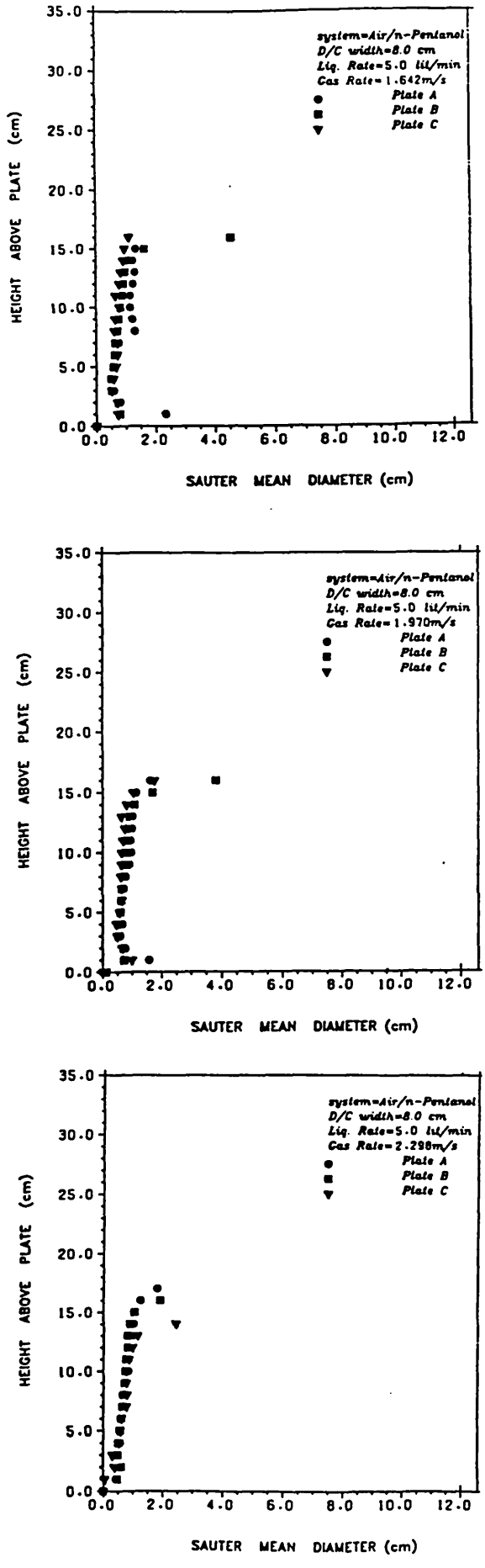

Figure 5.33 :- Variation of Sauter Mean Diameter with Height of Dispersion in Downcomer (Liquid Rate = 5.0 lit/min; Gas Rates = 1.642, 1.970, 2.298 m/s; Downcomer size = 8.0 cm)

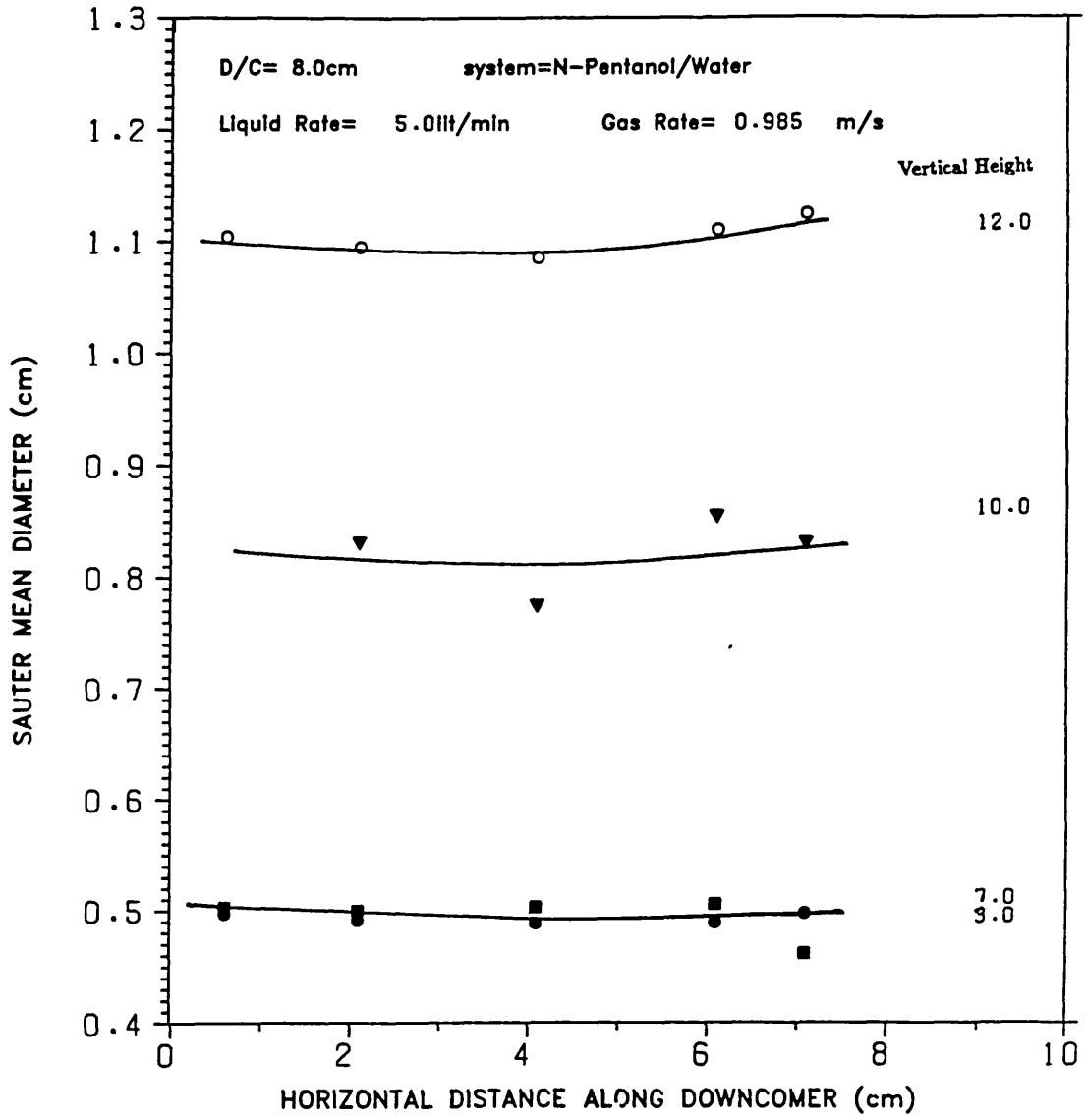

Figure 5.33a :- Horizontal variation of Sauter mean diameter in the downcomer

5.3.4 Liquid Holdup in Downcomers (Downcomer Backup)

Liquid holdup data were obtained by graphical integration of the dispersion density profiles obtained in this study. Theoretically, the liquid holdup in the downcomer can be translated into pressure drop data. In Section 2.4.3, a review of analytical ways of establishing the liquid holdup in the downcomer was given leading to the presentation of equation 27. Results obtained using equation (27) are compared to experimental results obtained using equation (153) and presented in figures 5.34 - 5.41.

$$h_B = \int_0^{H_f} (1 - \epsilon)\, dx \tag{153}$$

The results in these figures are divided into two basic groups, namely,

1) That in which the liquid holdup on the plate is calculated using equation (30)

2 That in which the liquid holdup on the plate is calculated using equation (32)

From these figures and allowing for experimental errors, it can be seen that the height of clear liquid in the downcomer can be calculated using equation (27) with plate liquid holdup calculated using equation (32). However, for some of the results of plate C the use of equation (30) for the calculation of plate liquid holdup fits better.

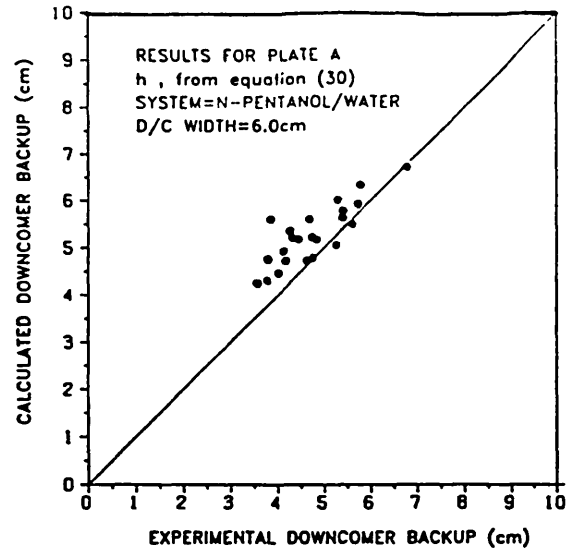

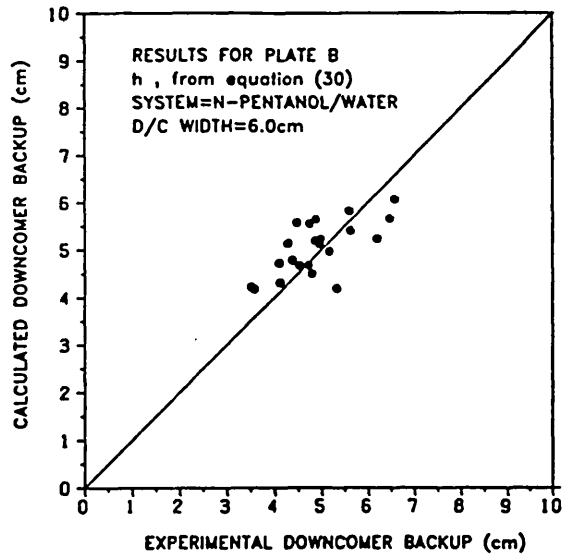

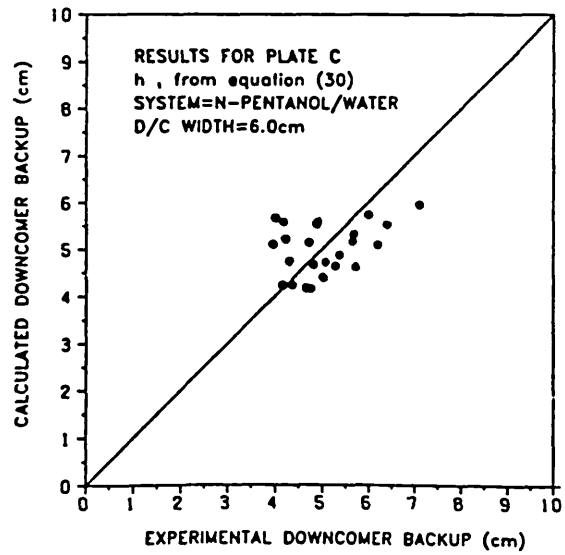

Figure 5.34 :- Comparison between experimental and Calculated Liquid Holdup in the Downcomer for n-Pentanol/Water system (Downcomer Size = 6.0 cm; Plate Liquid Holdup from equation 30)

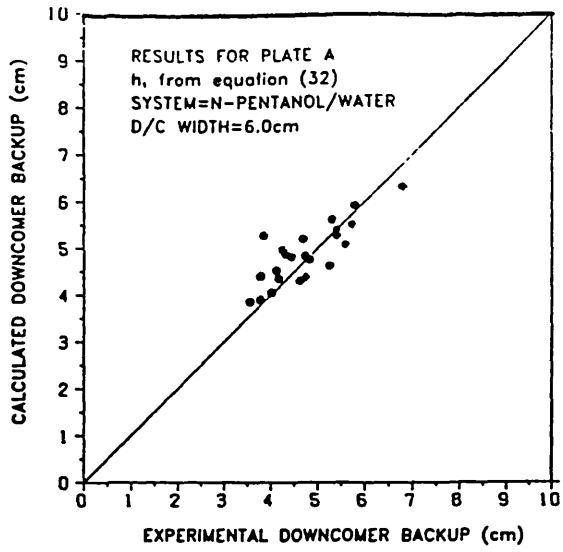

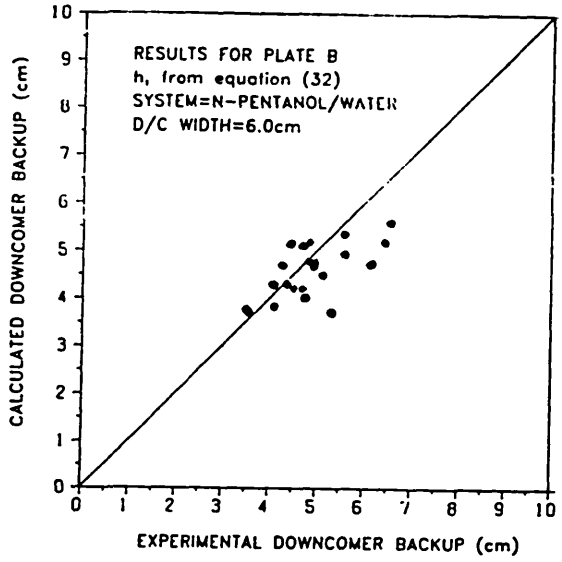

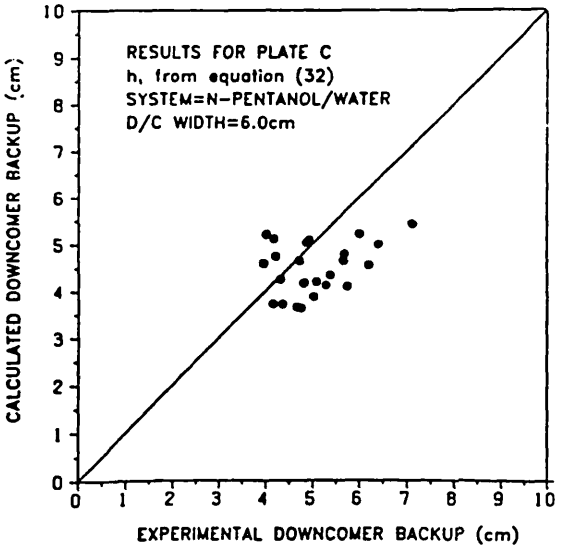

Figure 5.35 :- Comparison between experimental and Calculated Liquid Holdup in the Downcomer for n-Pentanol/Water system (Downcomer Size = 6.0 cm; Plate Liquid Holdup from equation 32)

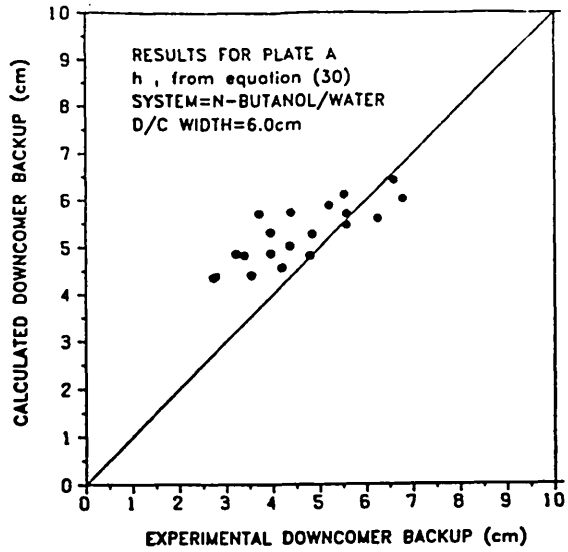

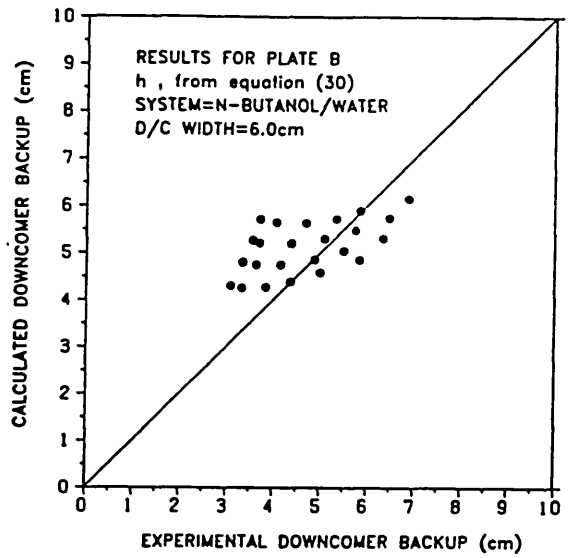

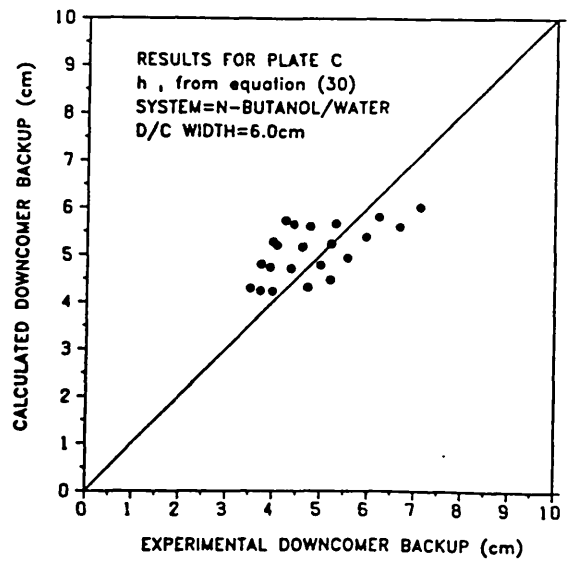

Figure 5.36 :- Comparison between experimental and Calculated Liquid Holdup in the Downcomer for n-Pentanol/Water system (Downcomer Size = 8.0 cm; Plate Liquid Holdup from equation 30)

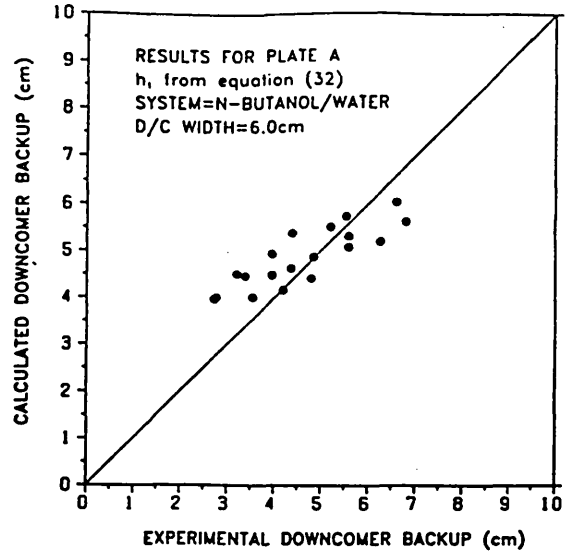

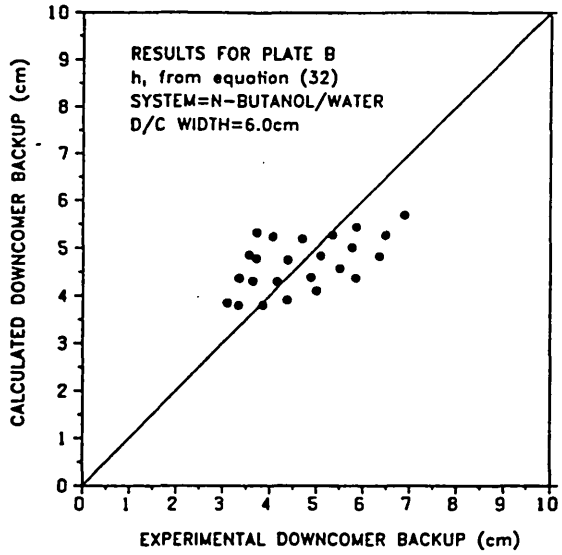

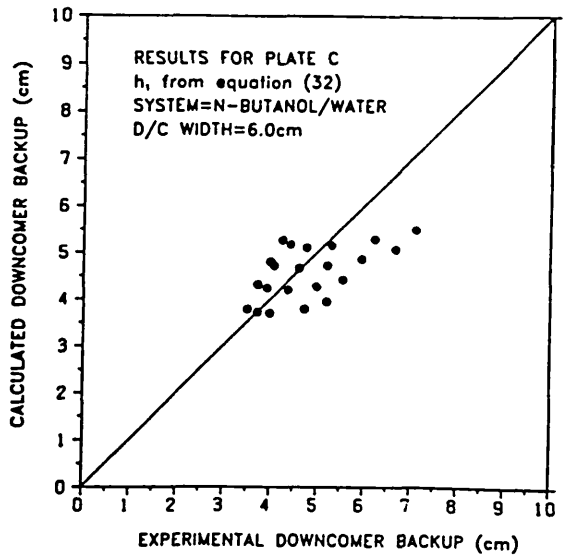

Figure 5.37 :- Comparison between experimental and Calculated Liquid Holdup in the Downcomer for n-Pentanol/Water system (Downcomer Size = 8.0 cm; Plate Liquid Holdup from equation 32)

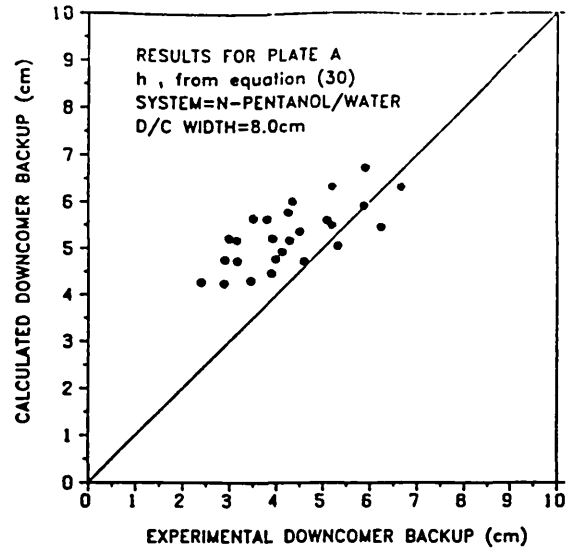

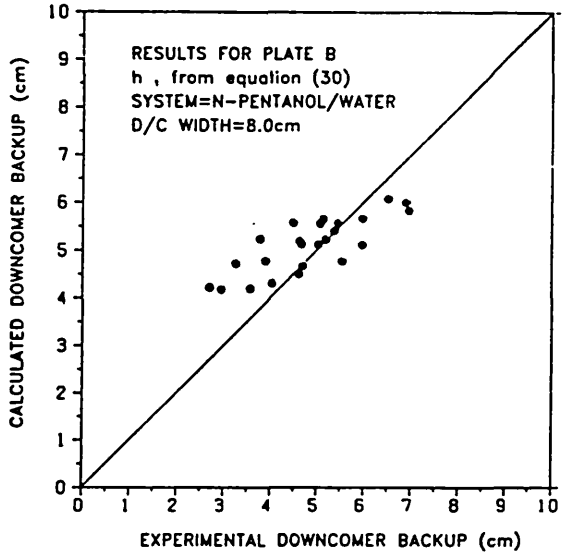

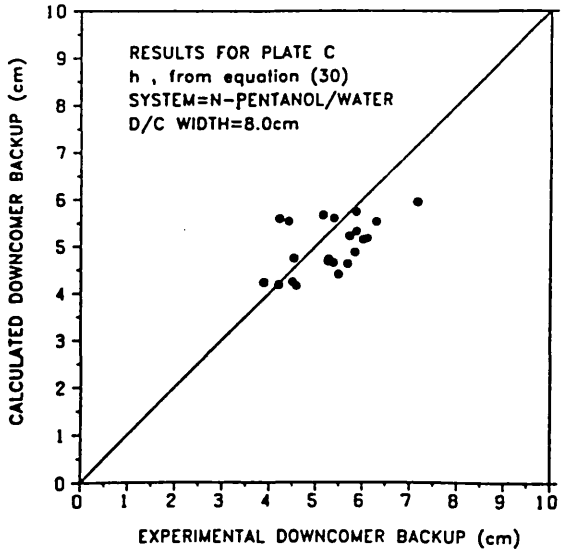

Figure 5.38 :- Comparison between experimental and Calculated Liquid Holdup in the Downcomer for n-Butanol/Water system (Downcomer Size = 6.0 cm; Plate Liquid Holdup from equation 30)

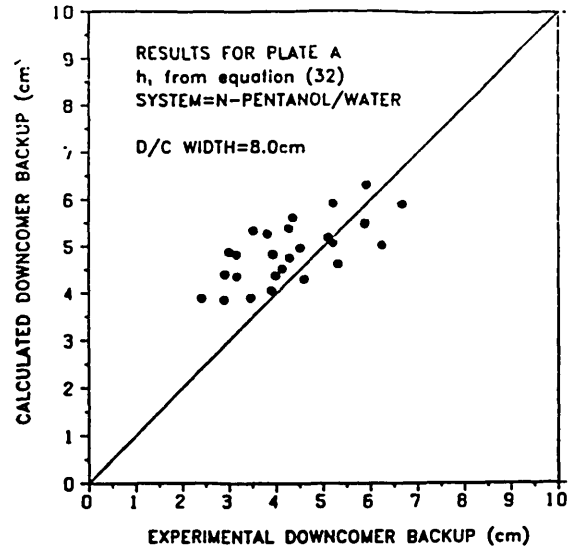

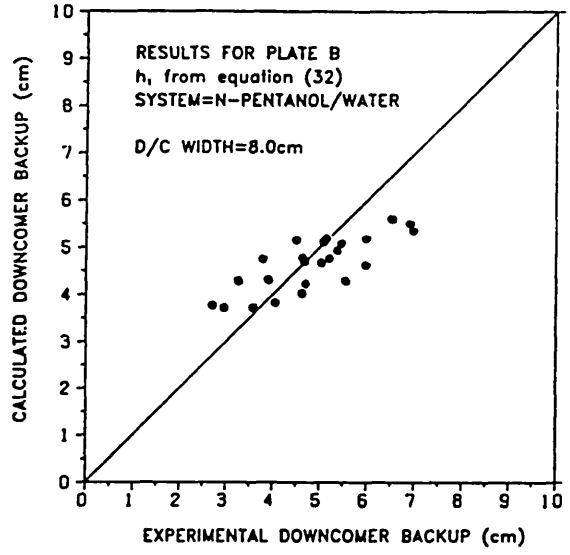

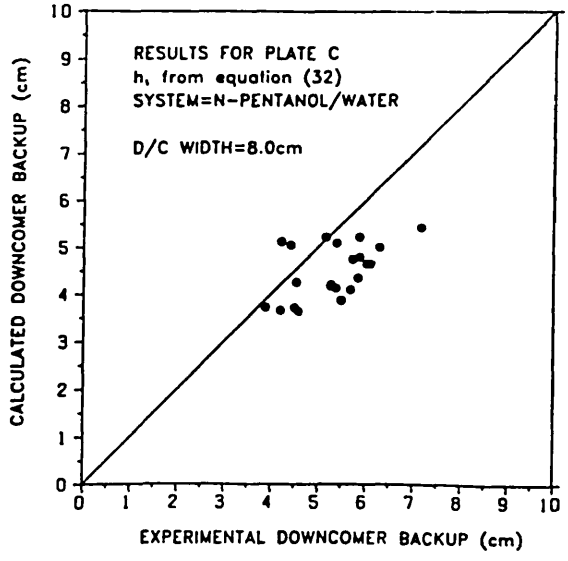

Figure 5.39 :- Comparison between experimental and Calculated Liquid Holdup in the Downcomer for n-Butanol/Water system (Downcomer Size = 6.0 cm; Plate Liquid Holdup from equation 32)

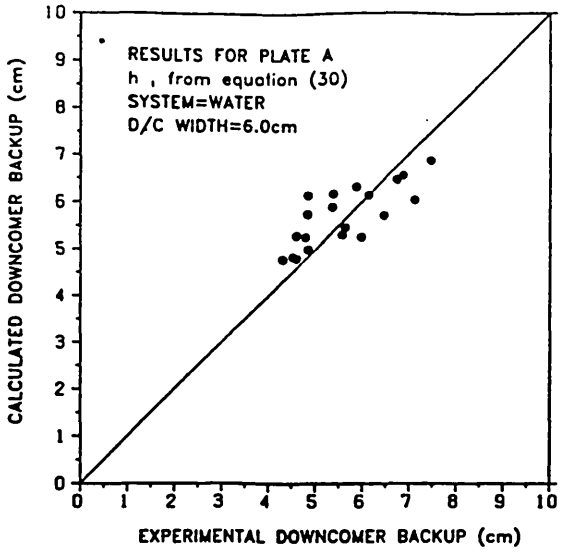

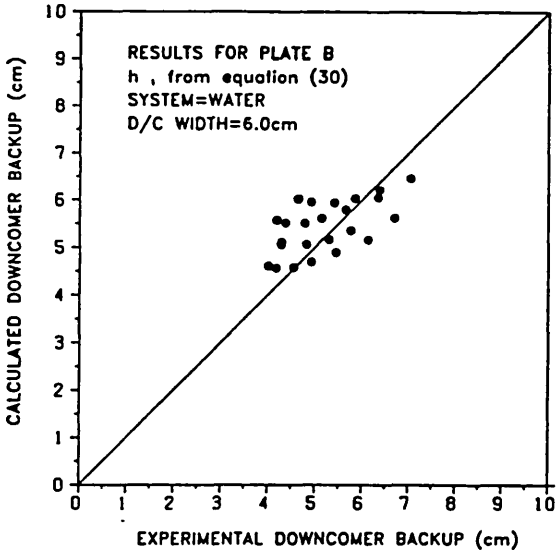

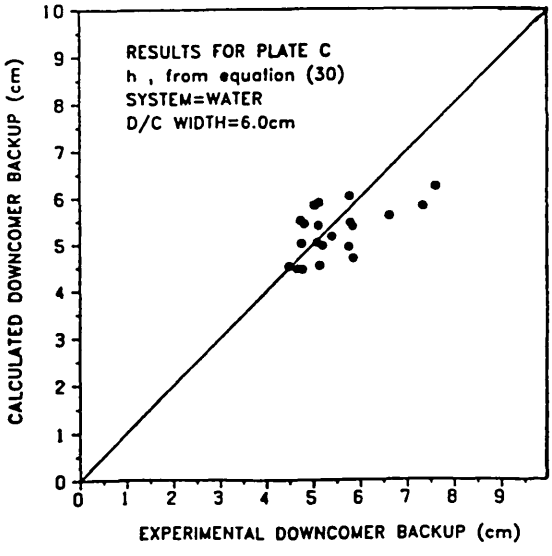

Figure 5.40 :- Comparison between experimental and Calculated Liquid Holdup in the Downcomer for Water (Downcomer Size = 6.0 cm; Plate Liquid Holdup from equation 30)

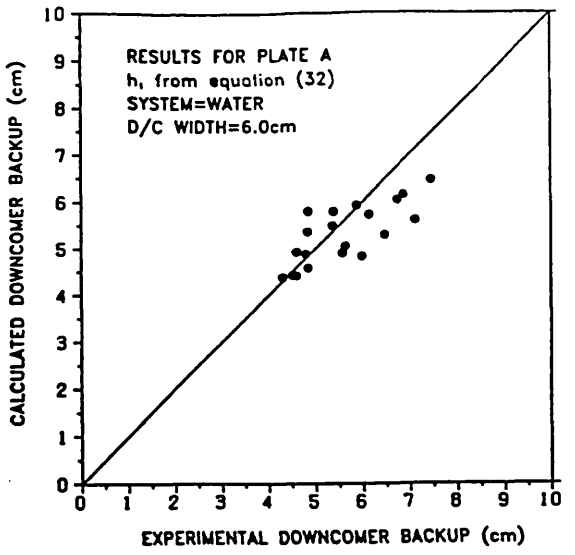

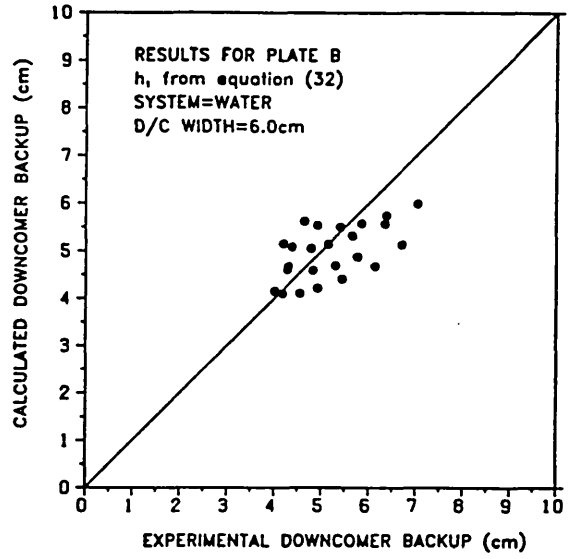

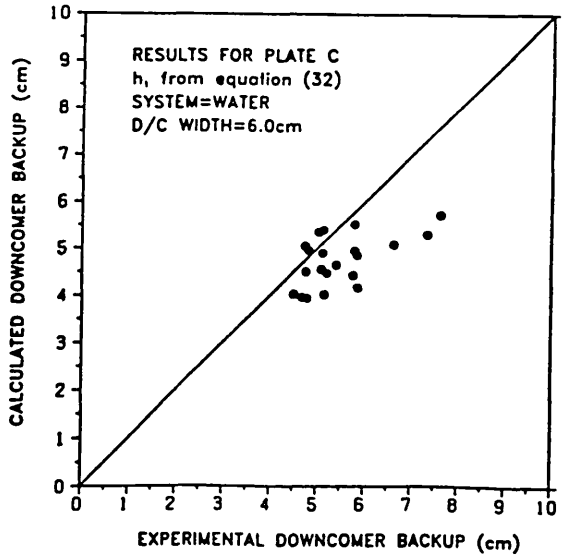

Figure 5.41 :- Comparison between experimental and Calculated Liquid Holdup in the Downcomer for Water (Downcomer Size = 6.0 cm; Plate Liquid Holdup from equation 32)

5.3.5 Froth Heights in Downcomers

Diagrams showing the variation of froth/foam heights in downcomers with plate superficial gas velocities, for different liquid flowrates, downcomer area and systems studied, are shown in figures 5.42 - 5.45. The basic feature here as described in Section 5.3.1 is that the froth heights in the downcomer vary with regime of plate operation. The general trend for foaming systems is a gradual increase of froth height from near the bubbling regime through the intermediate regime to a maximum value in the mixed froth regime. Further increases in plate gas superficial velocity leads to a decrease in froth height from the maximum attainable value as the spray regime is approached. For the non-foaming system, there is no significant change in froth height in the downcomer throughout all the regimes of plate operation. The reasons for this behaviour were put forward in Section 5.3.1. Results for the n-Butanol system do not follow the set pattern strictly. However, if the gas rate is increased further, it is envisaged that the trends observed generally for the foaming systems will be obtained in this case. In this study, gas rates could not be increased further due to limitations of the design capacity of the column.

5.3.6 Average Downcomer Froth Density

The mean liquid fraction or froth density in the downcomer was calculated according to the relation

$$\epsilon_L = \frac{\int_0^{H_f} \epsilon_L \, dx}{\int_0^{H_f} dx} = \frac{h_L}{H_f} \tag{156}$$

Where

ϵ_L = Mean liquid fraction

h_L = Liquid holdup in the downcomer (m)

H_f = Foam/froth height in downcomer (m)

Generally,for the foaming systems in regions or regimes where foaming is significant, it was found that the average froth density lies in the range 0.2 - 0.4. In regions where foaming is not significant for the foaming systems, the average froth density was found to lie in the range 0.4 - 0.6. For the non-foaming system, generally, the average froth density was found to lie in the range 0.68 - 0.9.

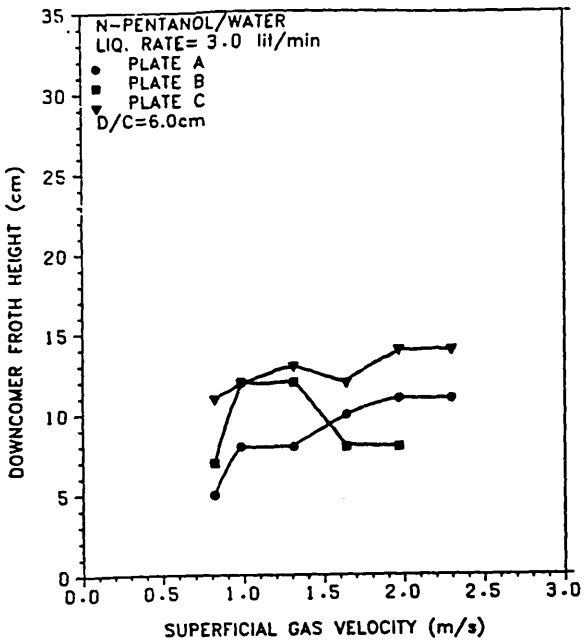

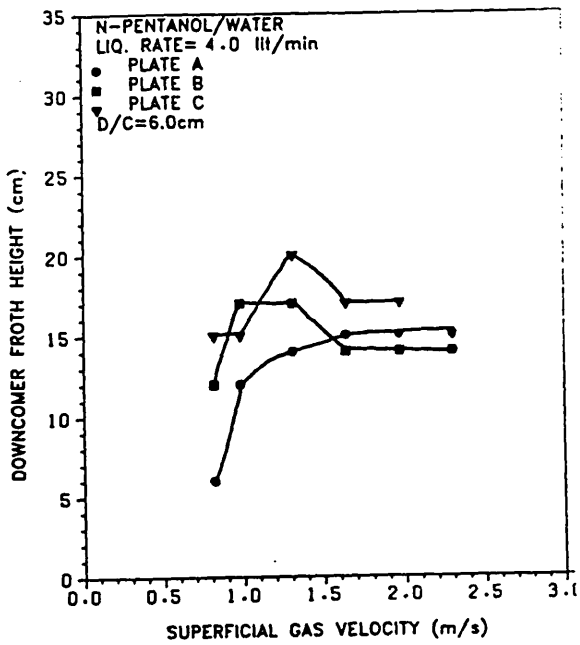

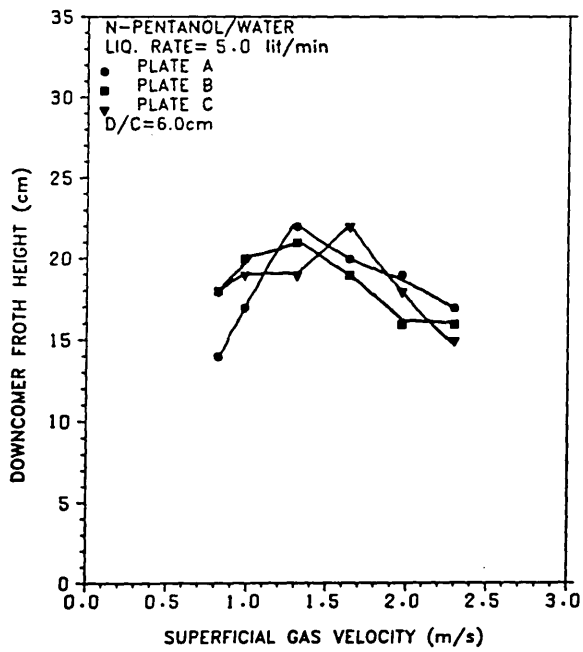

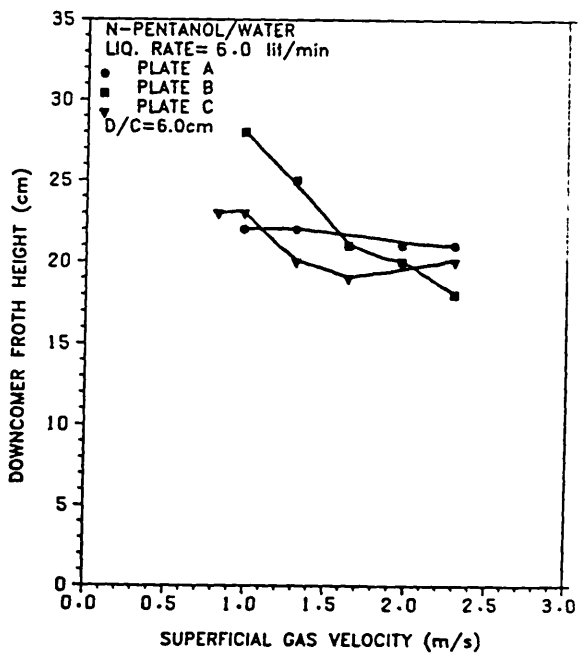

Figure 5.42 :- Variation of Downcomer Froth Height with Plate Superficial Gas Velocity for n-Pentanol/Water System (Downcomer size = 6.0 cm)

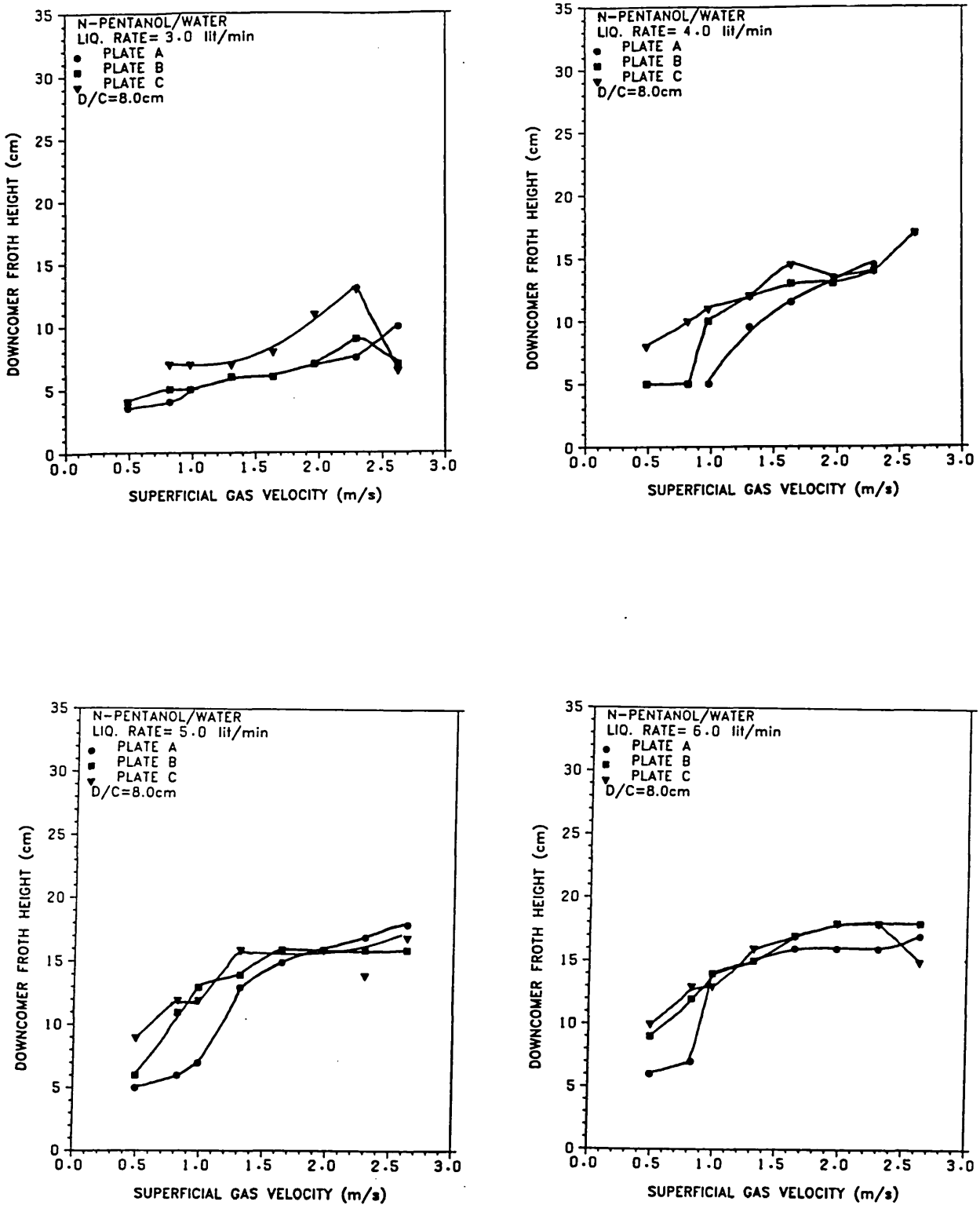

Figure 5.43 :- Variation of Downcomer Froth Height with Plate Superficial Gas Velocity for n-Pentanol/Water System (Downcomer size = 8.0 cm)

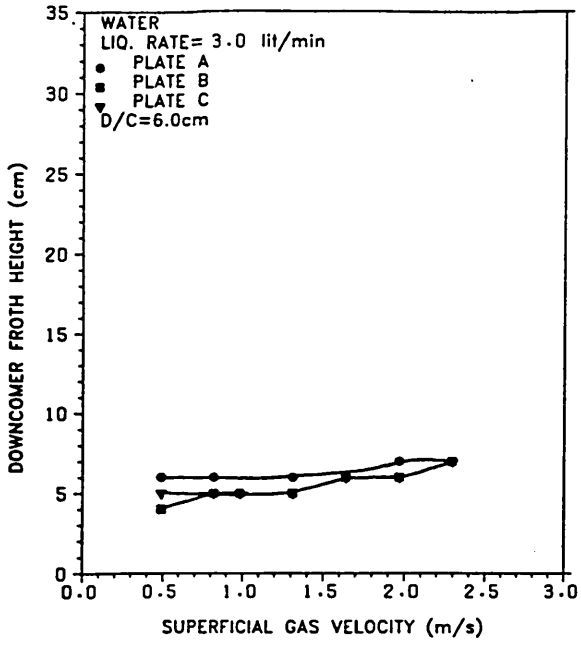

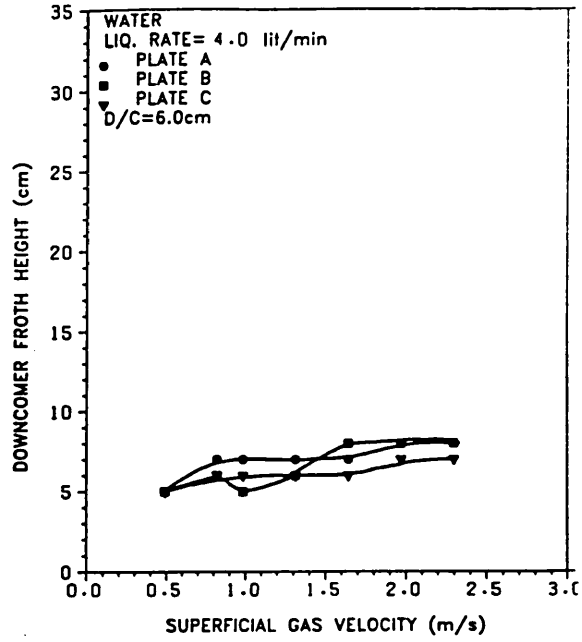

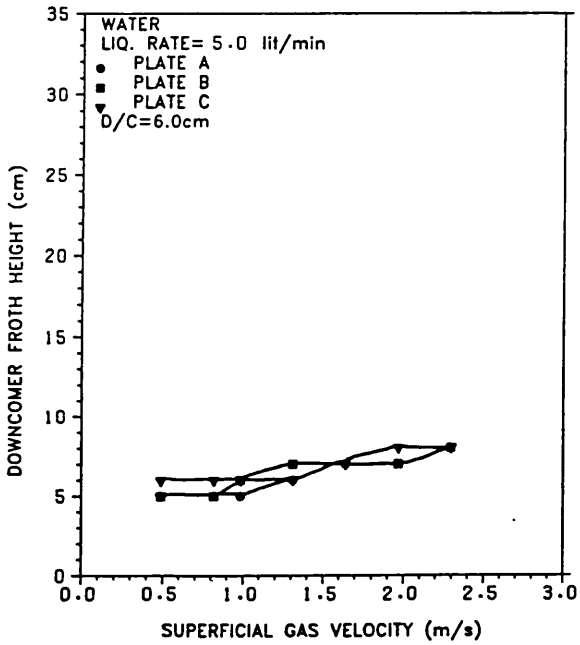

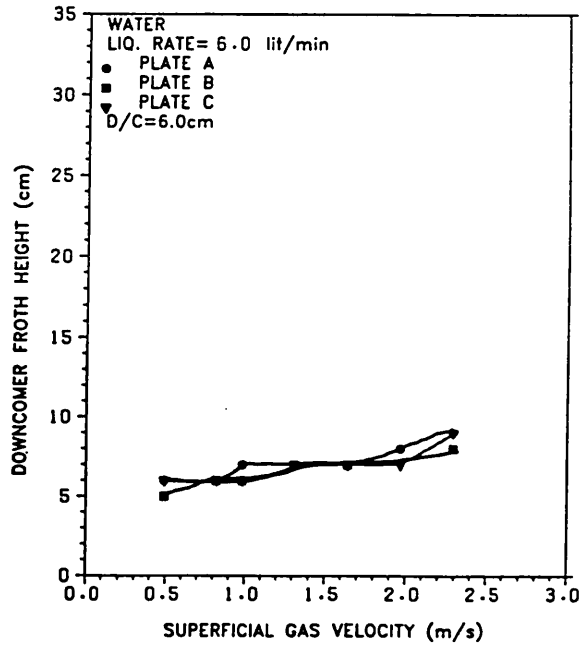

Figure 5.44 :- Variation of Downcomer Froth Height with Plate Superficial Gas Velocity for Water (Downcomer size = 6.0 cm)

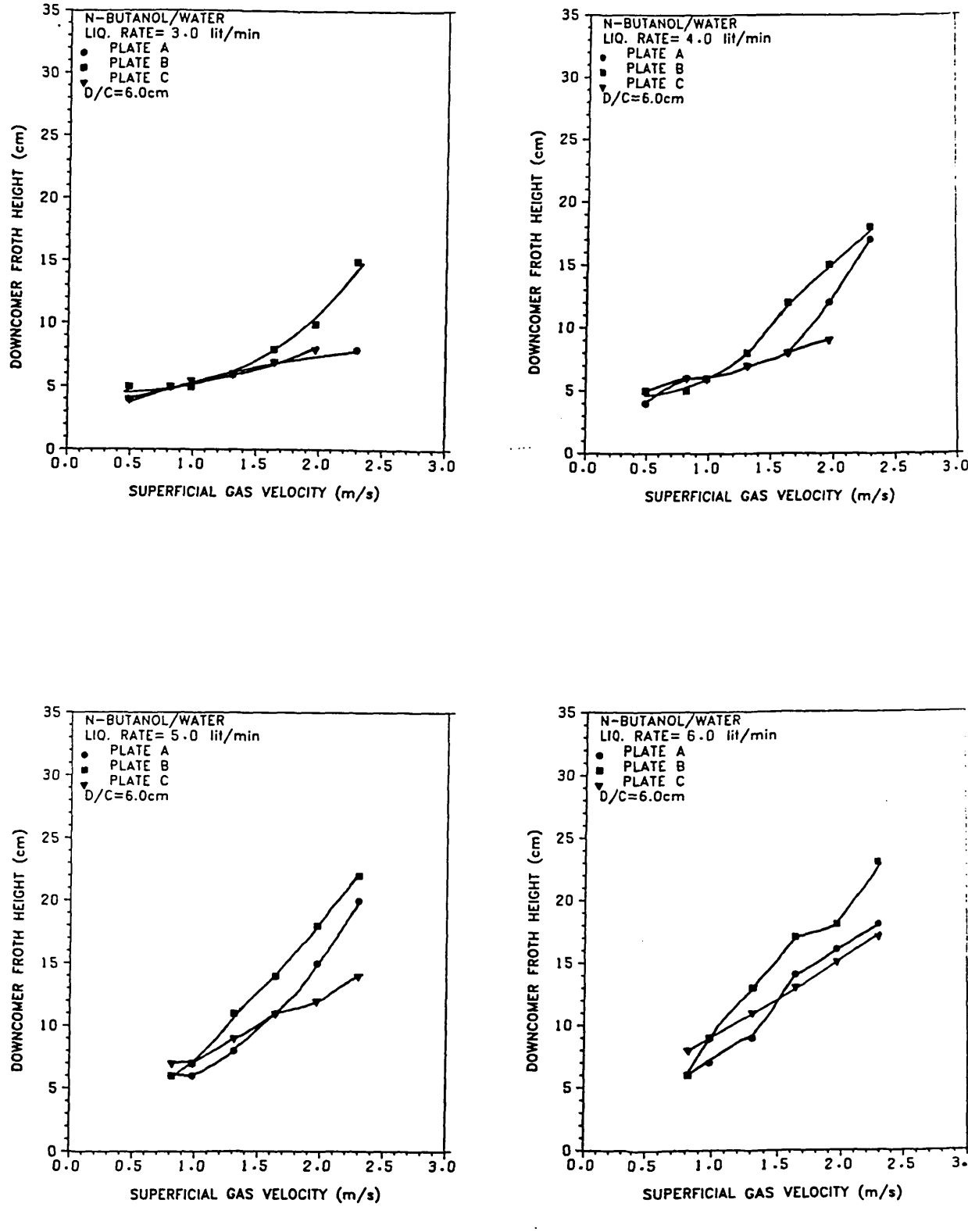

Figure 5.45 :- Variation of Downcomer Froth Height with Plate Superficial Gas Velocity for n-Butanol/Water System (Downcomer size = 6.0 cm)

5.4 Plate Studies

Introduction

Studies of plate behaviour were carried out for the systems Water and n-Butanol. Due to hardware difficulties, it was not possible to carry out plate studies for the n-Pentanol system. Results of these studies is presented and discussed in this section.

5.4.1 Dispersion Density Profiles

Dispersion density profiles on the plate for the systems Water and n-Butanol are presented in figures 5.46 - 5.47 and 5.48 - 5.49, respectively, plotted compositely for plates A, B and C. It can be observed that the basic difference between the two systems studied is in the height of froth/foam obtained in each case. Froth heights in the case of n-Butanol are generally higher than those obtained for Water. This may be explained in terms of the degree of aeration, thus, it is much easier to aerate a solution of n-Butanol than Water in view of its lower surface tension. This comparison is justified on the basis that both systems have almost the same density and viscosity.

As the gas rate is increased, there is a gradual change in the shape of the dispersion density profile from an averagely uniform dispersion to a condition in which there is high liquid holdup just above the plate than at the bottom of the plate. This corresponds to a situation in

which the liquid appears to be lifted up from the plate. This behaviour can be attributed to the formation of jets as the gas passes through the dispersion and, therefore, corresponds to the jetting or spray regime of plate operation. At low gas rates, the profiles show a significant holdup of liquid equally distributed throughout the dispersion. Such profiles correspond to the operation of the plate near to the bubbling regime. Between this regime and the previous one, the profiles combine the effects of jetting and bubbling and corresponds to what is usually described as the mixed froth regime. The major differences between profiles for plates A, B and C can be discussed on two major counts.

(1) The profiles generally show higher holdup of liquid in the order plate C > plate B > plate A. This general behaviour has been pointed out by Macmillan[127], Bernard[128], Dhulesia[85] and Hofhuis and Zuiderweg[16]. It can be explained in terms of the rate of dispersion of gas in the gas-liquid mixture on the plate. For this particular studies, this effect can be attributed to the difference in hole pitch as the hole area of the plates was maintained constant at approximately 11%.

(2) Another marked difference between the profiles obtained for plates A, B, C, respectively is in the transition from the uniformly dispersed profile to that characteristic of the jetting or spray regime. It can be seen that for all the systems considered, plate C goes faster into the spray regime than plate B and, in turn, than plate A. This then confirms established knowledge as regards the influence of hole area on

performance of sieve plates (i.e:- Plates with larger holes are more likely to operate in the spray regime than plates with smaller holes.)

5.4.1.1 Horizontal Variation of Dispersion Density

Horizontal variations of dispersion density on the plate were investigated to add credibility to measurements undertaken in this work. The results of these studies are shown in figure 5.50. From these figures, it can be seen that there is little or no variations of dispersion density across the plate in the horizontal direction, at any height above the plate. This then justifies measurements of dispersion density at the midpoint of the plate for most of the studies undertaken.

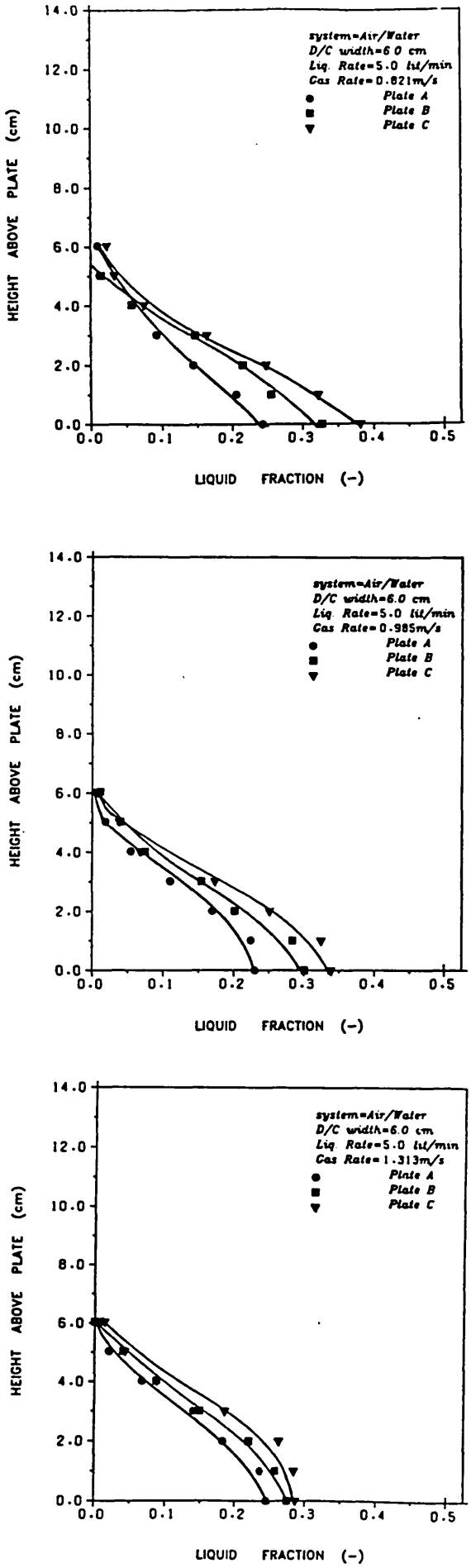

Figure 5.46 :- Variation of Liquid Fraction with Froth Height on the Plate for Water (Liquid Rate = 5.0 lit/min; Gas Rates = 0.821, 0.985, 1.313 m/s)

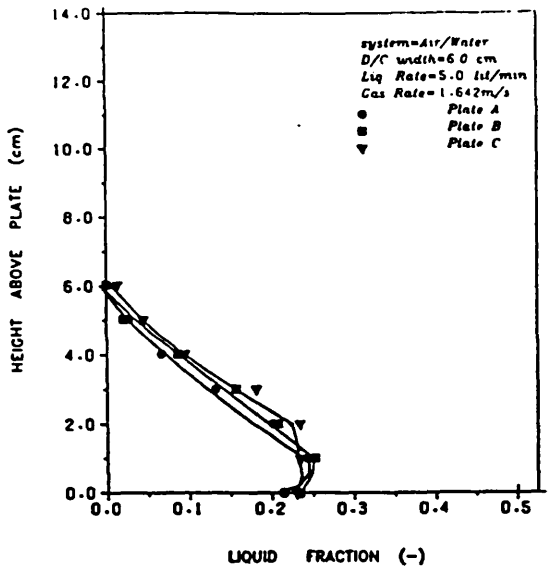

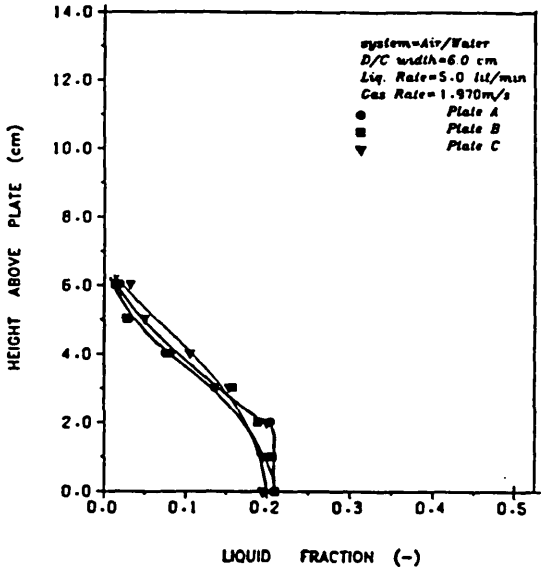

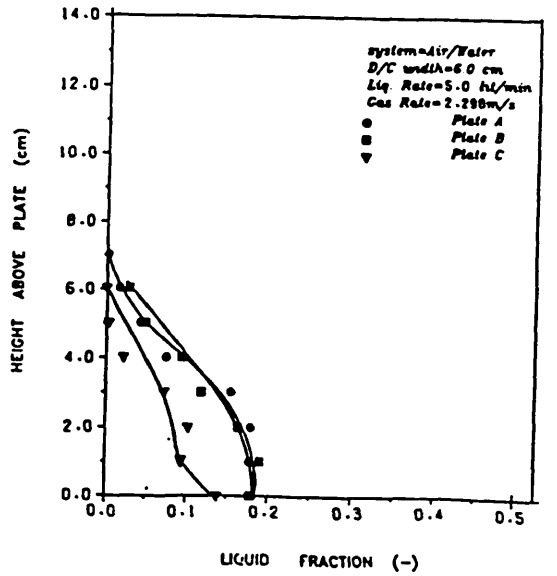

Figure 5.47 :- Variation of Liquid Fraction with Froth Height on the Plate for Water (Liquid Rate = 5.0 lit/min; Gas Rates = 1.642, 1.970, 2.298 m/s)

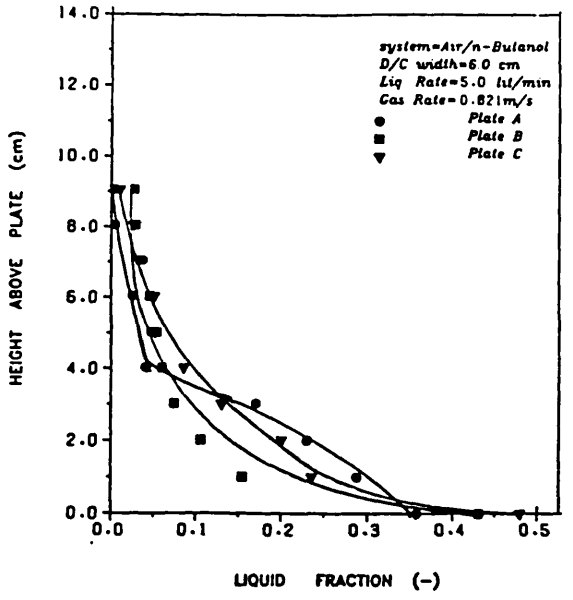

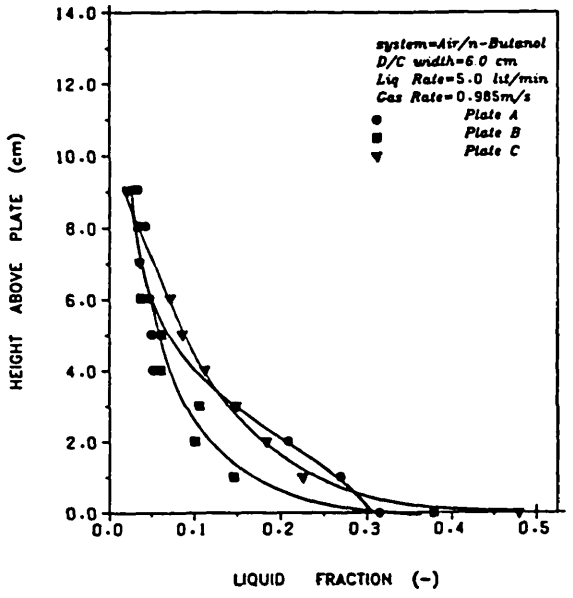

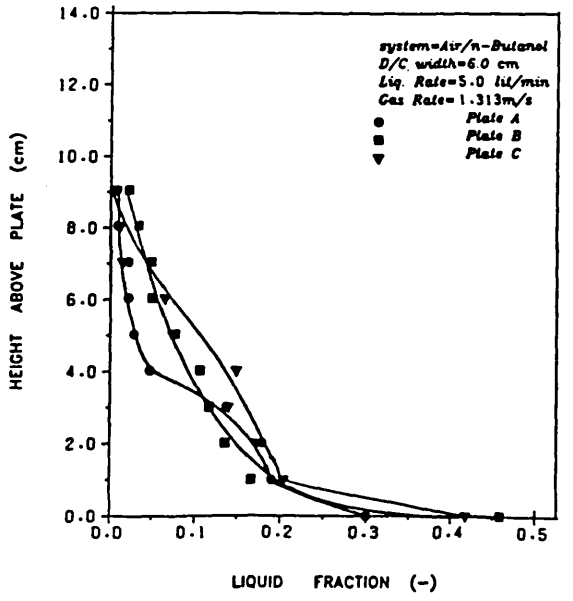

Figure 5.48 :- Variation of Liquid Fraction with Froth Height on the Plate for Butanol (Liquid Rate = 5.0 lit/min; Gas Rates = 0.821, 0.985, 1.313 m/s)

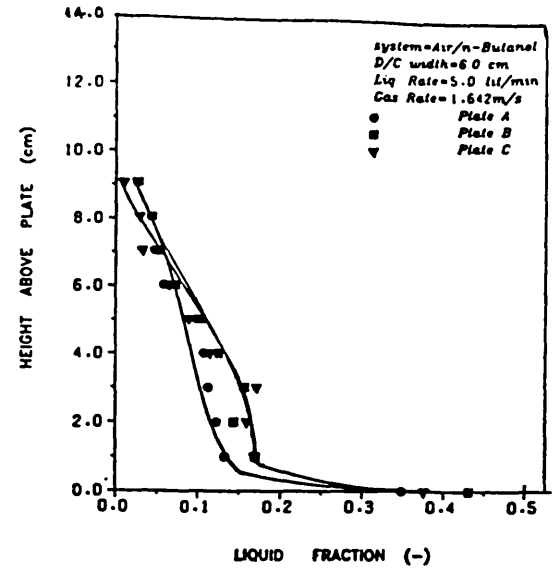

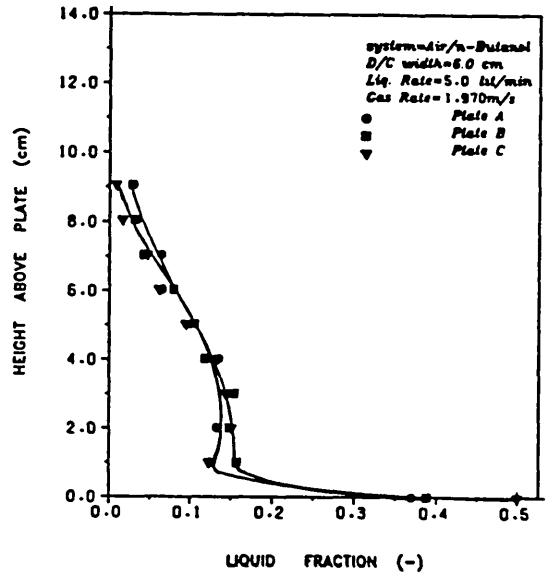

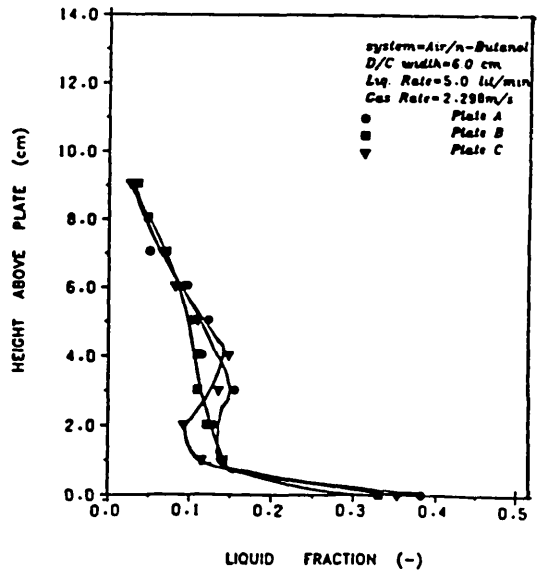

Figure 5.49 :- Variation of Liquid Fraction with Froth Height on the Plate for Butanol (Liquid Rate = 5.0 lit/min; Gas Rates = 0.821, 0.985, 1.313 m/s)

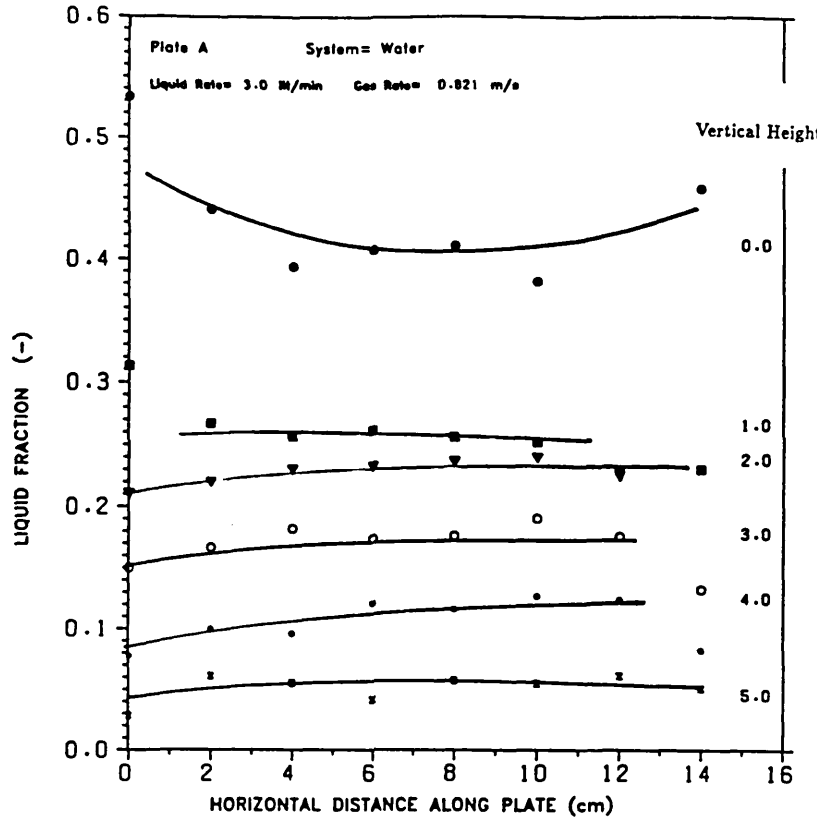

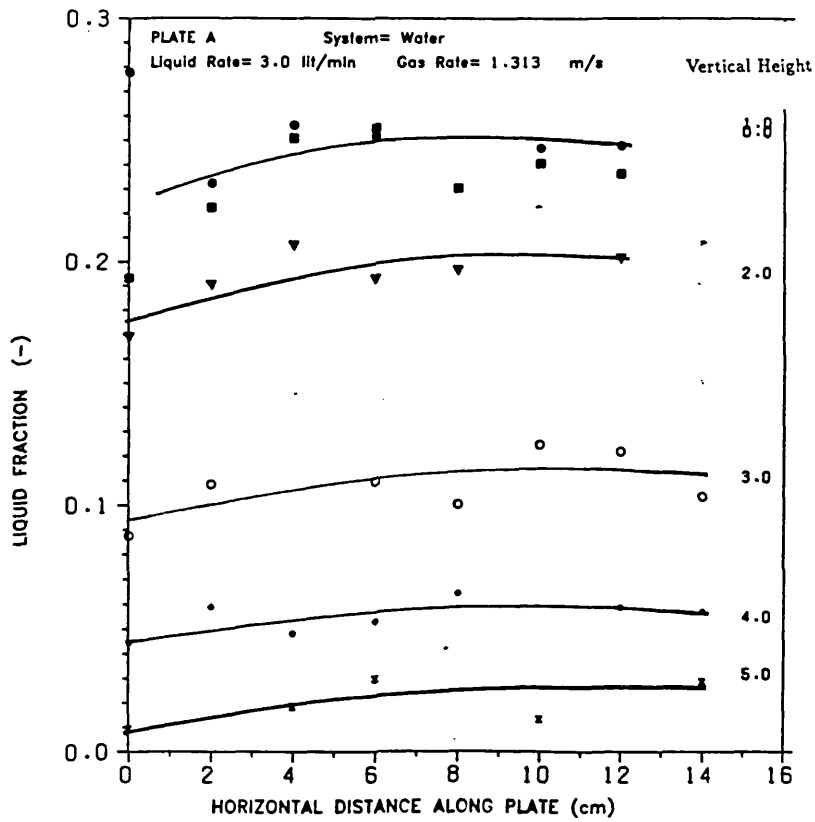

Figure 5.50 :- Horizontal Variation of Liquid Fraction on the Plate

5.4.1.2 Plate Liquid Holdup

Plate liquid holdup was calculated by graphical integration of the dispersion density profiles according to equation (153) of Section 5.3.4. In chapter 2, empirical relations proposed for the calculation of plate liquid holdups by Zuiderweg et al[84] and Dhulesia[85] were given in the form of equations (30) and (32) respectively. In this section, data obtained in these studies are compared to those predicted by these equations. The results are presented in figures 5.51 - 5.52 for the system Water and figures 5.53 - 5.54 for the system n-Butanol. From these figures,it can be seen that predictions made from equation (32) fit the experimental data much more closely than those made from equation (30). Hence for all practical purposes, plate liquid holdup can be calculated using the equation

$$h_L = 0.5 H_w^{0.5} p^{0.33} \Psi^{0.33} \qquad (equation\ 32)$$

$$(Where\ h_L\ is\ measured\ in\ meters)$$

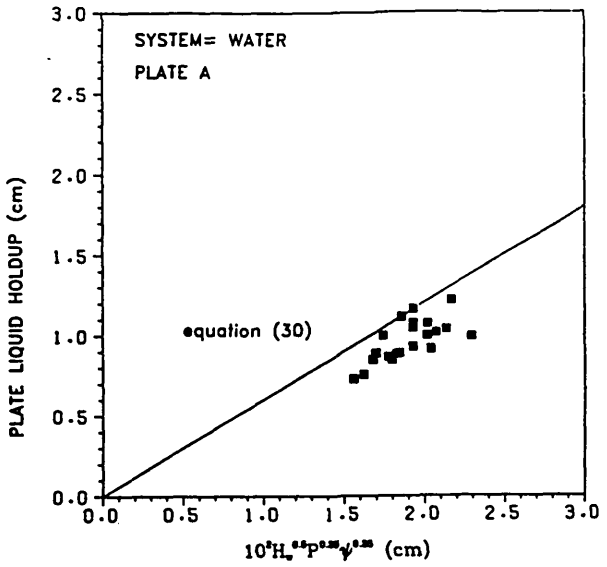

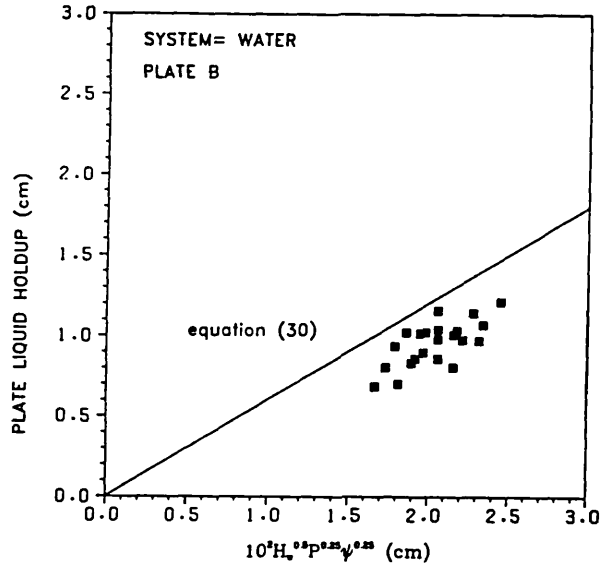

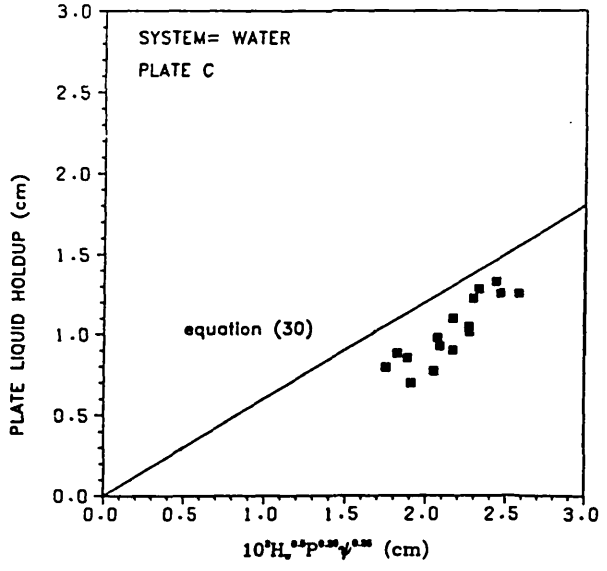

Figure 5.51 :- Comparison between Experimental and Calculated Plate Liquid Holdup using Equation (30) for Water

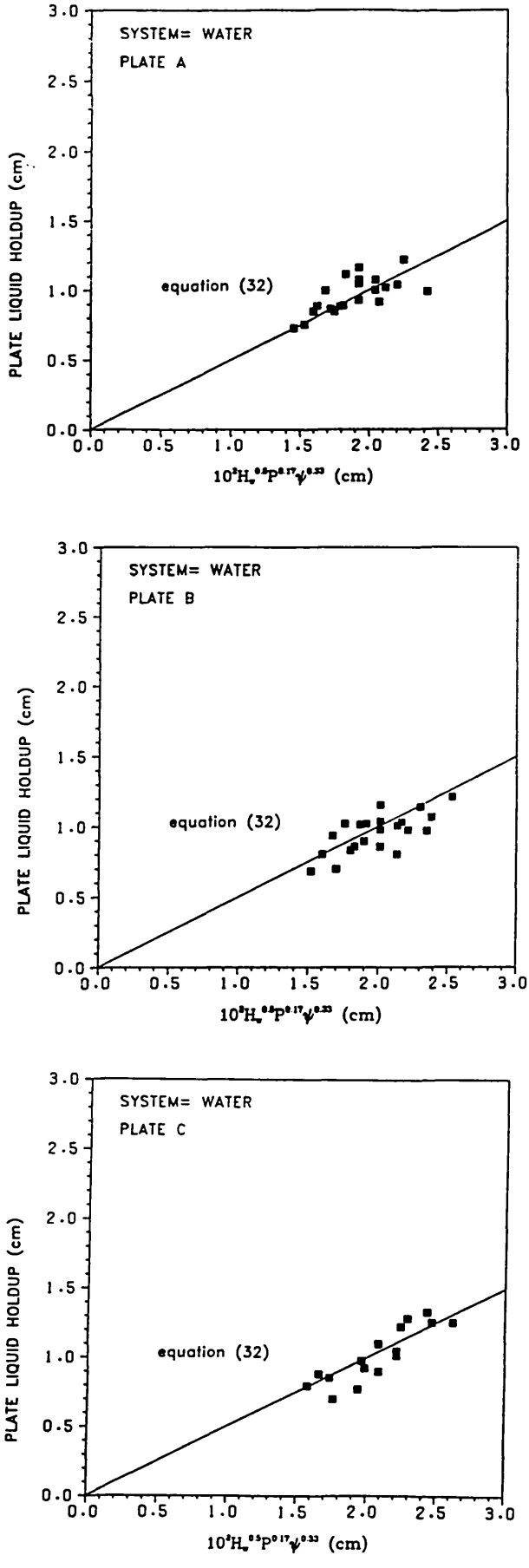

Figure 5.52 :- Comparison between Experimental and Calculated Plate Liquid Holdup using Equation (32) for Water

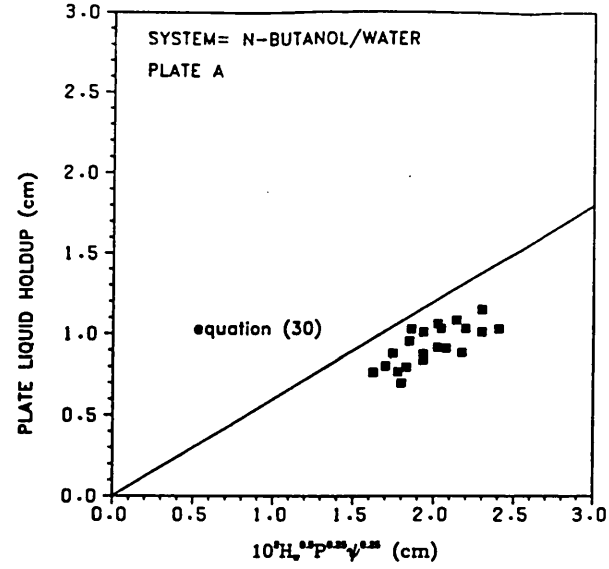

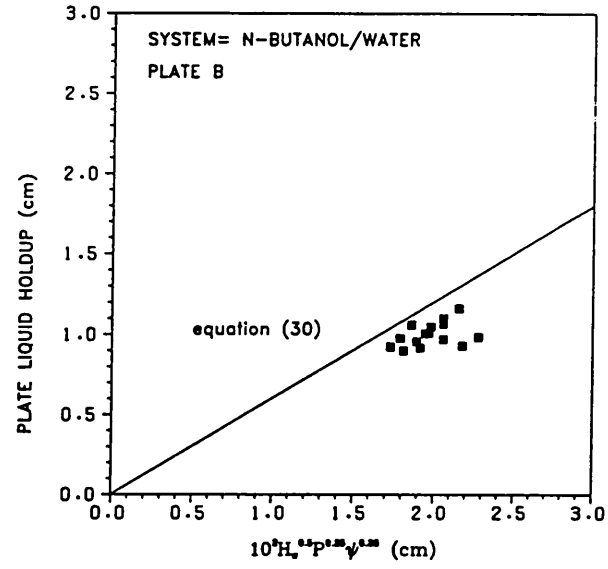

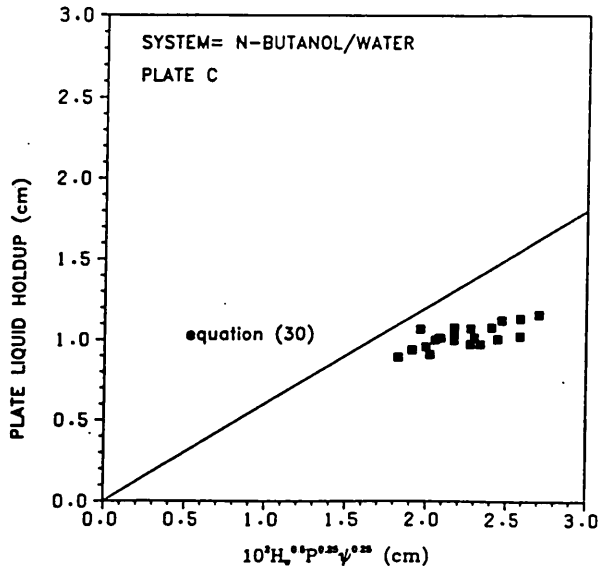

Figure 5.53 :- Comparison between Experimental and Calculated Plate Liquid Holdup using Equation (30) for n-Butanol/Water System

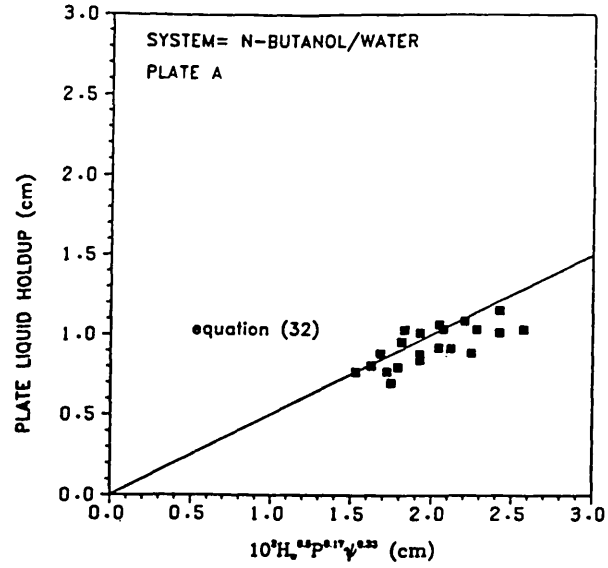

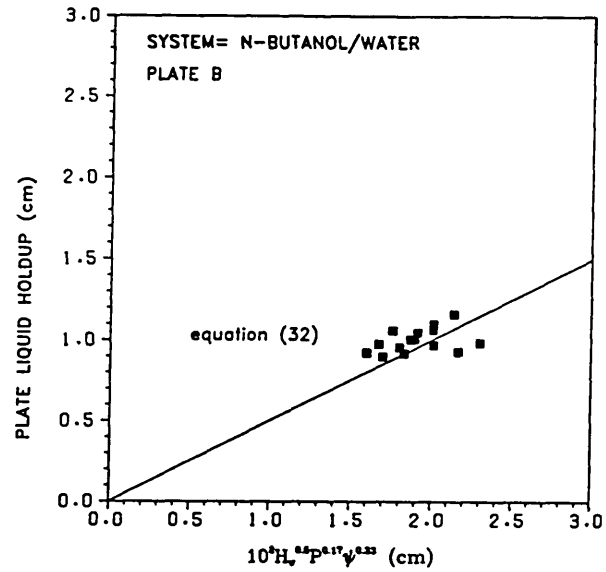

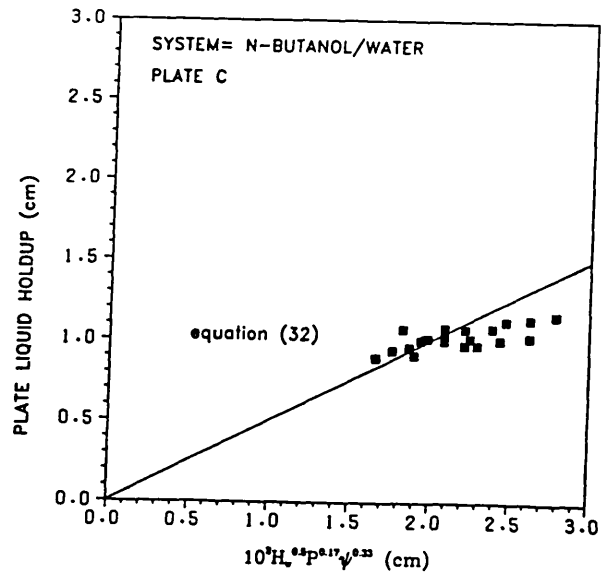

Figure 5.54 :- Comparison between Experimental and Calculated Plate Liquid Holdup using Equation (32) for n-Butanol/Water System

5.4.2 Sauter Mean Diameter Profiles

The results of the measured dispersion Sauter mean diameters on the plate are shown in figures 5.55 - 5.56 and figures 5.57 - 5.58 for the systems Water and n-Butanol respectively. The basic feature of all these profiles is that there generally exist bubbles of about 1 cm in diameter near the plate and relatively larger bubbles at the top of the dispersion. This is an expected result since bubbles can undergo coalescence as they rise through a dispersion. Generally, the effects of gas and liquid loadings on the plate do not appear to have a significant effect on the size and distribution of the bubbles. The differences in bubble sizes obtained for the different plates can be attributed to the pitch to hole diameter ratio. Thus bubbles obtained for plate C are generally smaller than those obtained for plate B which in turn is smaller than those obtained for plate A in all the experiments carried out. This behaviour was also pointed out by Klug and Vogelpohl[80] in their study of bubble formation at single holed and sieve plates with superimposed liquid motion. In their work, the hole diameter was maintained constant and the pitch was varied. The explanation for these trends, according to Klug and Vogelpohl[80], is attributed to the dispersive action of the generated shear field. Basically, since the ascending bubbles are much nearer to each other, larger shear stresses result and hence, also smaller limiting values of stable bubble diameters. In the present work, the pitch to hole diameter ratio of plates A, B and C are 2.857, 2.736 and 2.666, respectively. This therefore implies that bubbles generated with these

plates, according to the theory of Klug and Vogelpohl[80], will decrease in diameters in the order plate A, plate B, plate C. This definitely fits observed trends of bubble diameter profiles found in this work.

5.4.2.1 Horizontal Variation of Sauter Mean Diameter

Horizontal variations of Sauter mean diameter of bubbles on the plate are shown in figure 5.59. From these figure, it is evident that there is no significant variations of bubble diameters in the horizontal direction on the plate at any vertical position in the dispersion. It therefore justifies measurements of plate parameters taken at the midpoint of the plate.

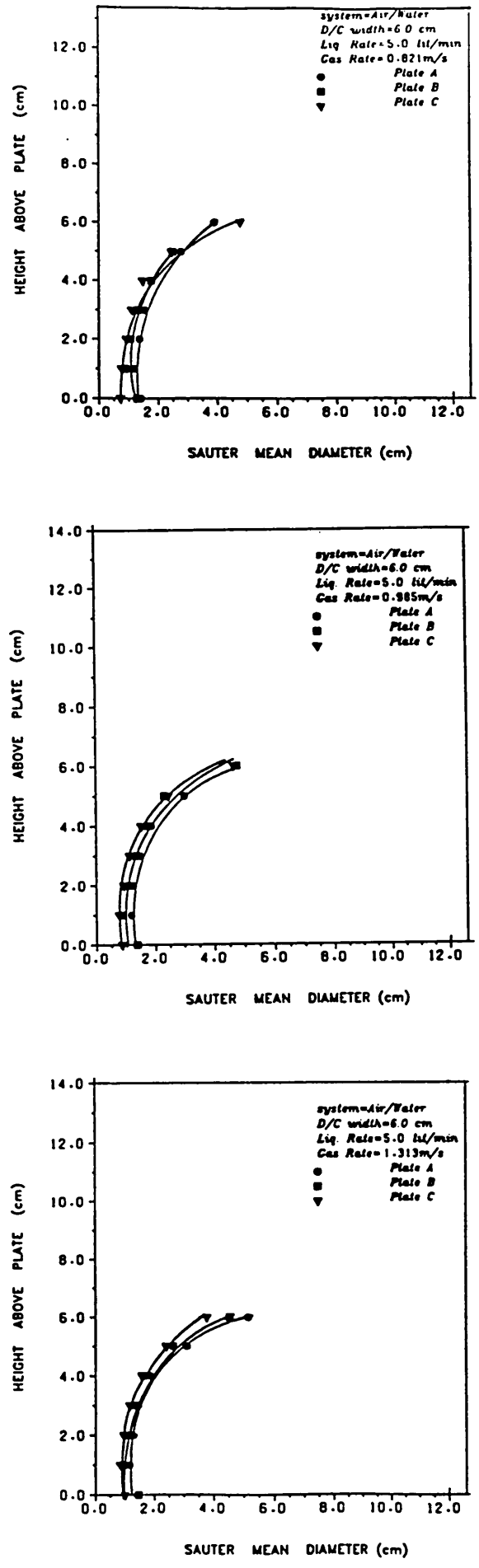

Figure 5.55 Variation of Sauter Mean Diameter with Height of Dispersion on the Plate for Water (Liquid Rate = 5.0 lit/min; Gas Rates = 0.821, 0.985, 1.313m/s)

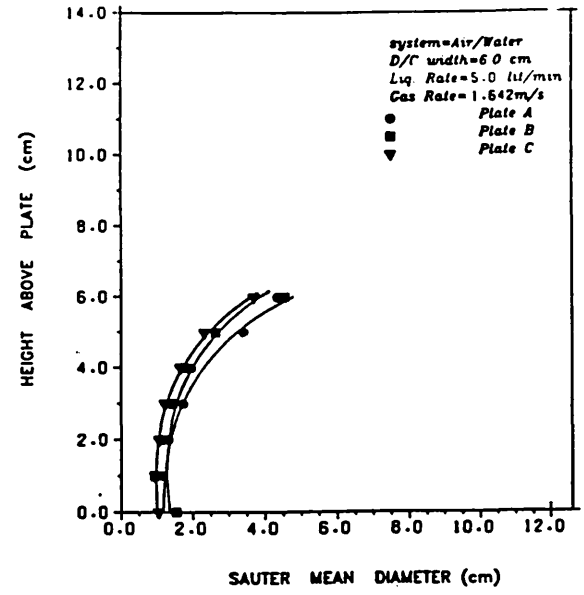

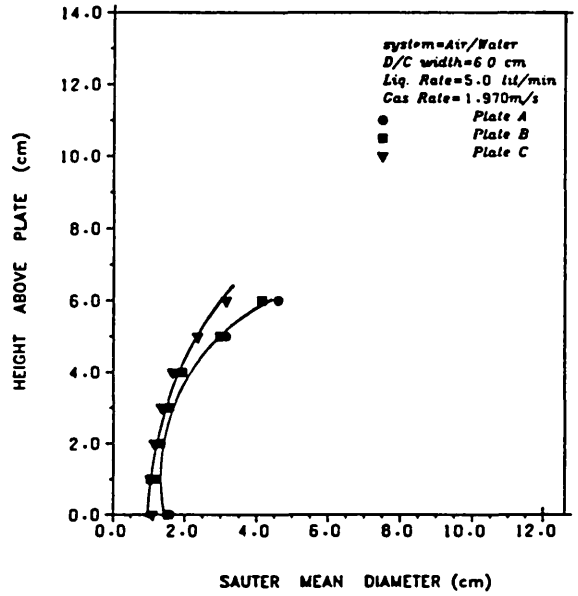

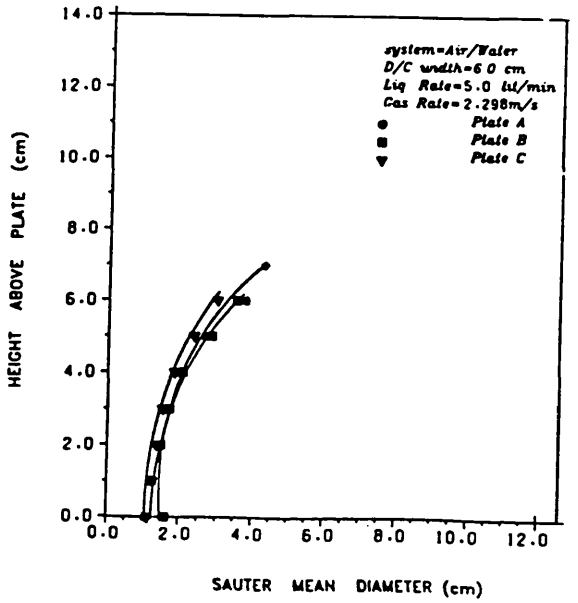

Figure 5.56 Variation of Sauter Mean Diameter with Height of Dispersion on the Plate for Water (Liquid Rate = 5.0 lit/min; Gas Rates = 1.642, 1.970, 2.298m/s)

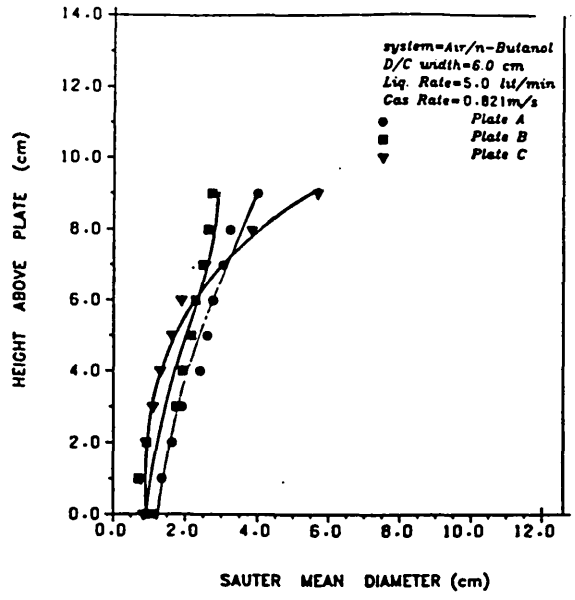

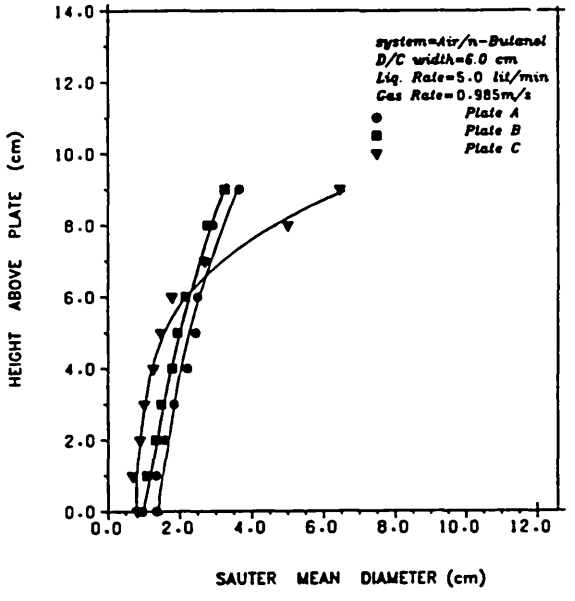

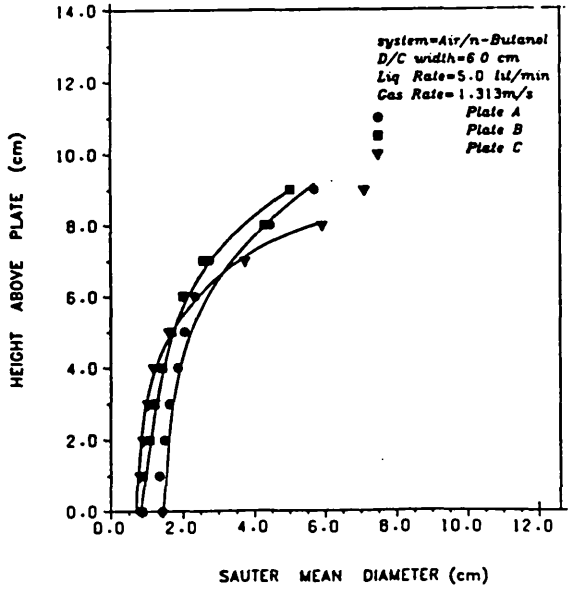

Figure 5.57 Variation of Sauter Mean Diameter with Height of Dispersion on the Plate for n-Butanol (Liquid Rate = 5.0 lit/min; Gas Rates = 0.821, 0.985, 1.313m/s)

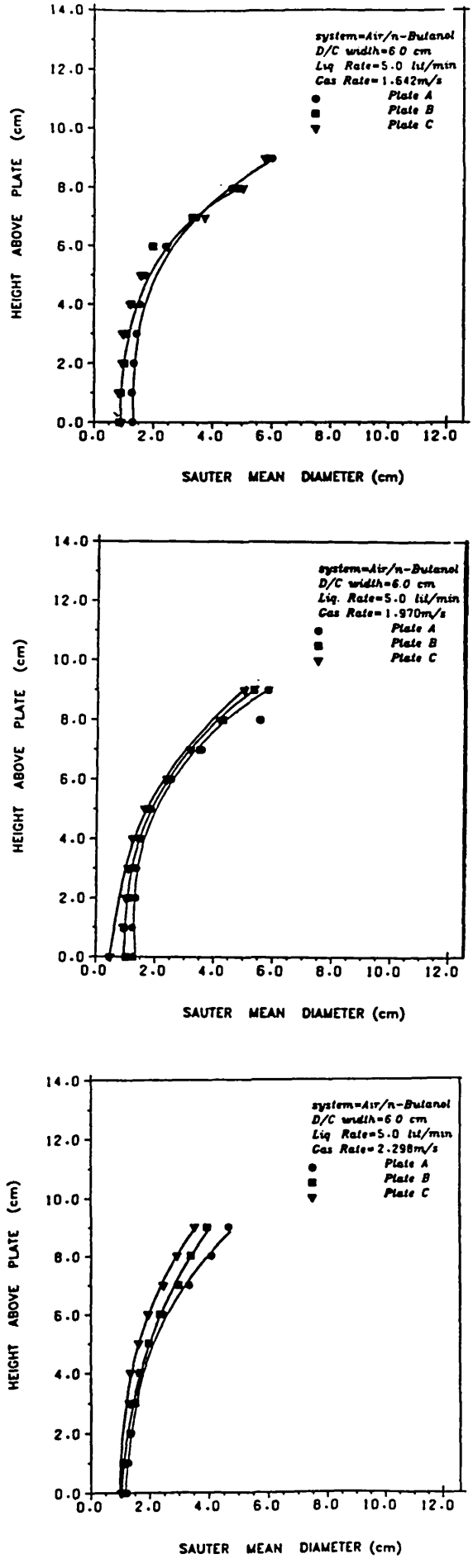

Figure 5.58 Variation of Sauter Mean Diameter with Height of Dispersion on the Plate for n-Butanol (Liquid Rate = 5.0 lit/min; Gas Rates = 1.642, 1.970, 2.298m/s)

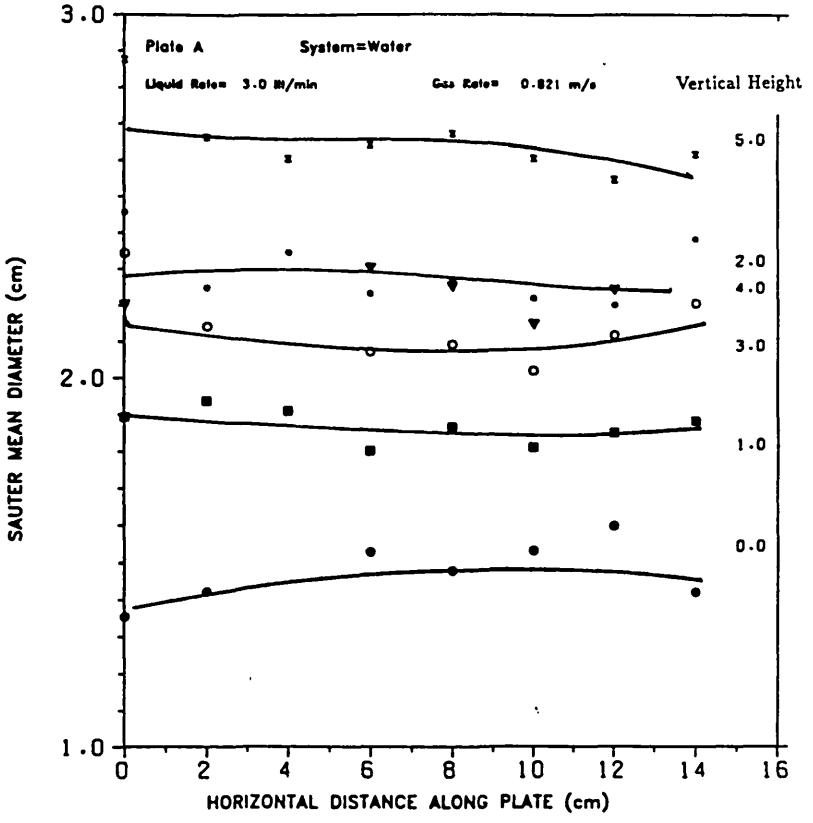

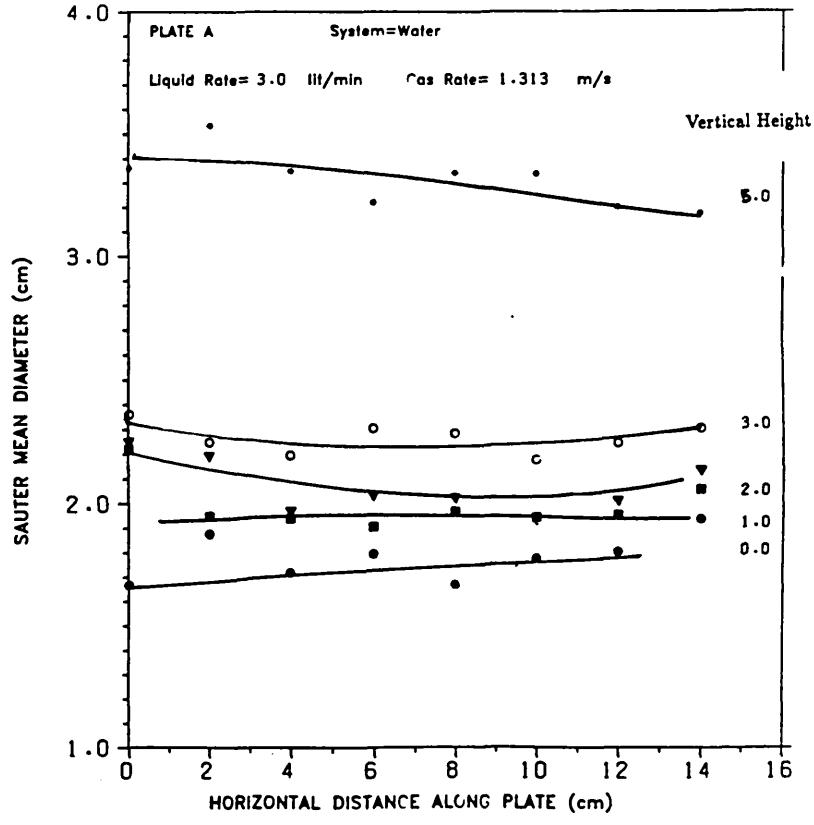

Figure 5.59 Horizontal Variation of Sauter Mean Diameter on the Plate

5.4.3 Plate Pressure Drops

Dry and wet pressure drops were measured on the plate by means of pressure tappings. These measurements were regarded necessary so as to enable the monitoring of the effect of plate pressure drop on the behaviour of the froth/foam for all systems considered. Results from these measurements are compared to those obtained from standard equations.

5.4.3.1 Dry Pressure Drop

For all gas rates used, dry pressure drops were measured for all the plates studied. Also, dry pressure drops for plates A, B and C, respectively, were calculated by means of equation (34). The measured values of dry pressure drop were then compared to those calculated. The results are shown in figure 5.60 which clearly indicates that dry pressure drops can be calculated effectively using equation (34).

5.4.3.2 Wet Pressure Drop

Wet pressure drops were measured on the plate for all gas-liquid loadings and plates studied. In chapter 2, the standard way of calculating wet pressure drop on the plate was given in the form of equation (36). Pressure drop results are shown in figures 5.61, 5.62, 5.63 for the n-Pentanol, n-Butanol and Water systems, respectively. For these figures, data are reported separately for plates A, B and C respectively. The figures indicate experimentally measured values and those calculated using

equation (36). For most of the cases considered, measured values of wet pressure drop are generally higher than those calculated from equation (36) for moderate to high gas flowrates. However, the difference between experimental and calculated values of wet pressure drop are generally small and in most cases within 10% error margin. Therefore, it can be concluded that for all practical purposes, equation (36) can be adequately used to predict wet pressure drops on the plate.

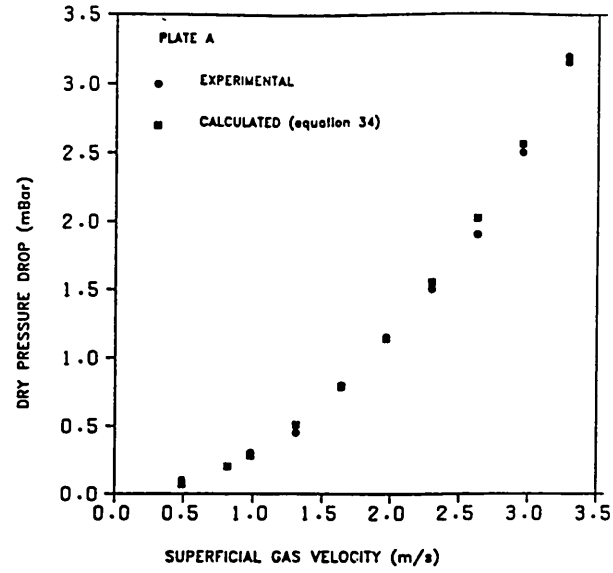

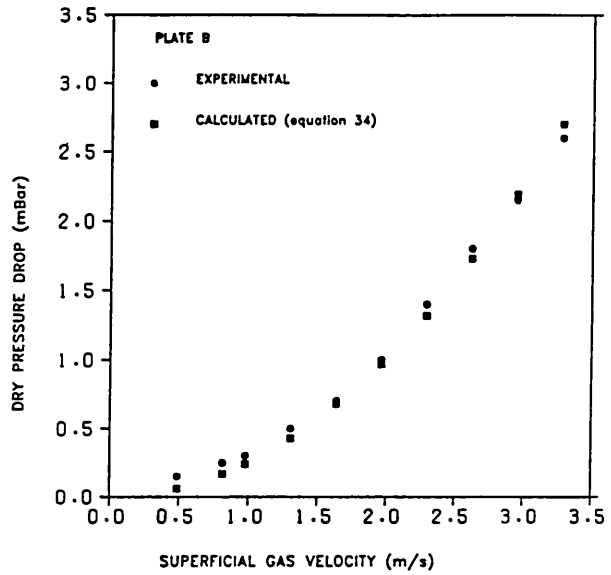

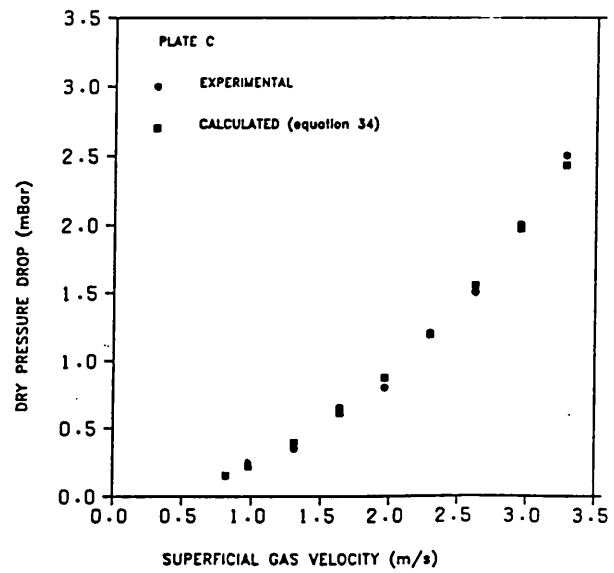

Figure 5.60 Experimental and Calculated Dry Tray Pressure Drops

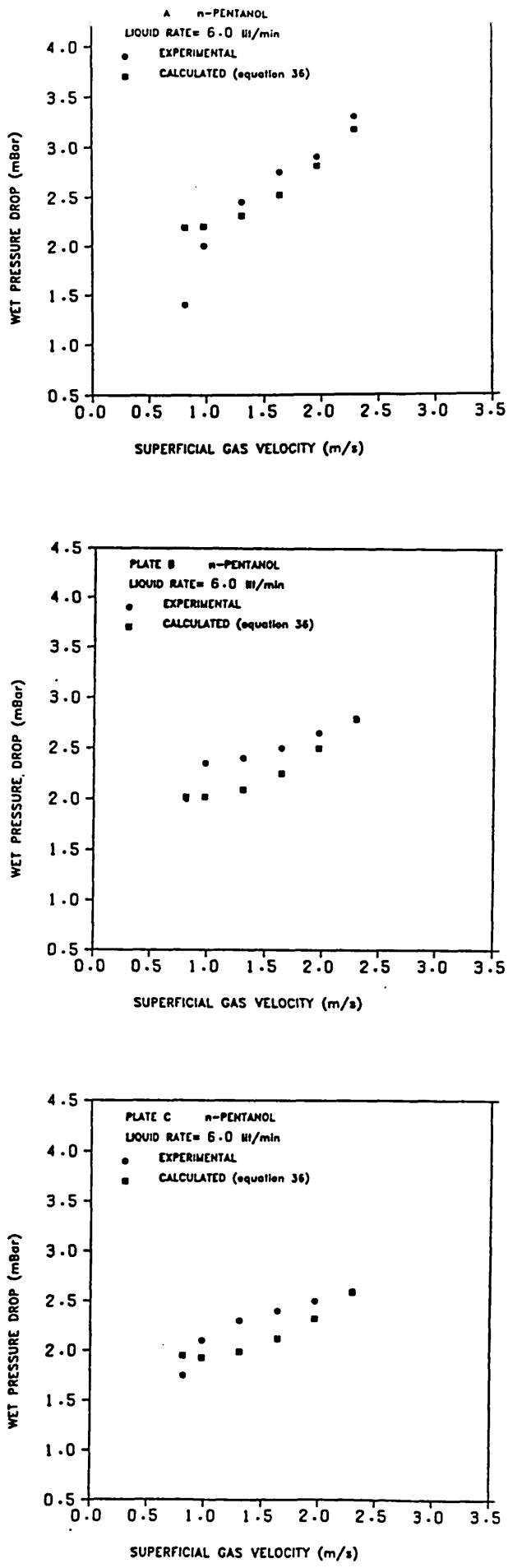

Figure 5.61 Experimental and Calculated Wet Tray Pressure Drops for n-Pentanol/Water System

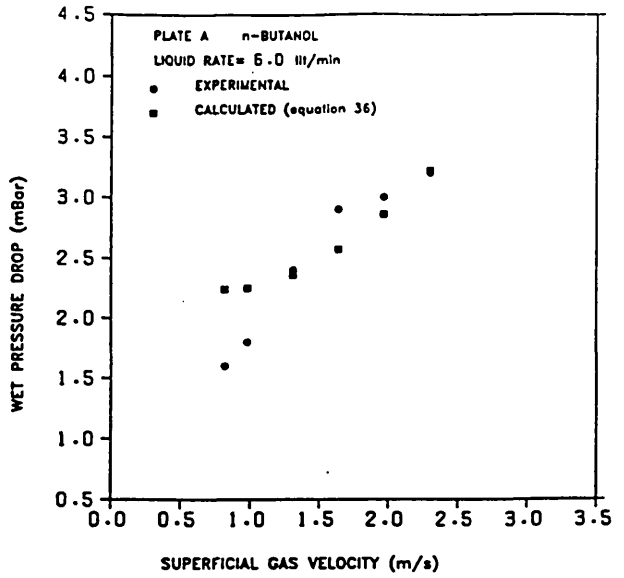

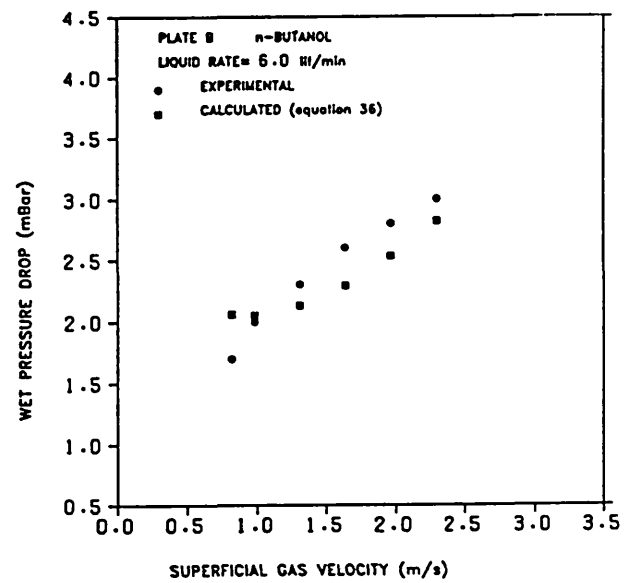

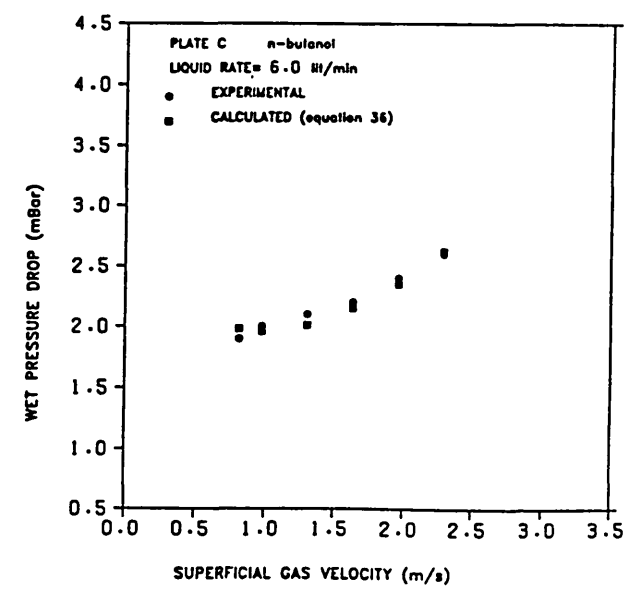

Figure 5.62 - Experimental and Calculated Wet Tray Pressure Drops for n-Butanol/Water System

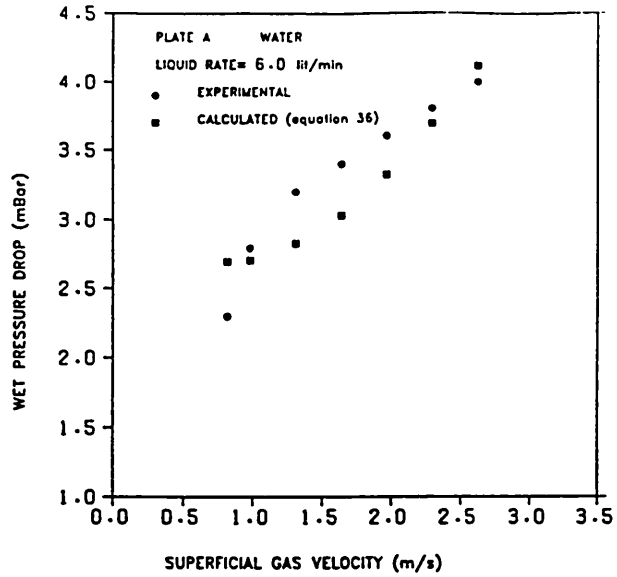

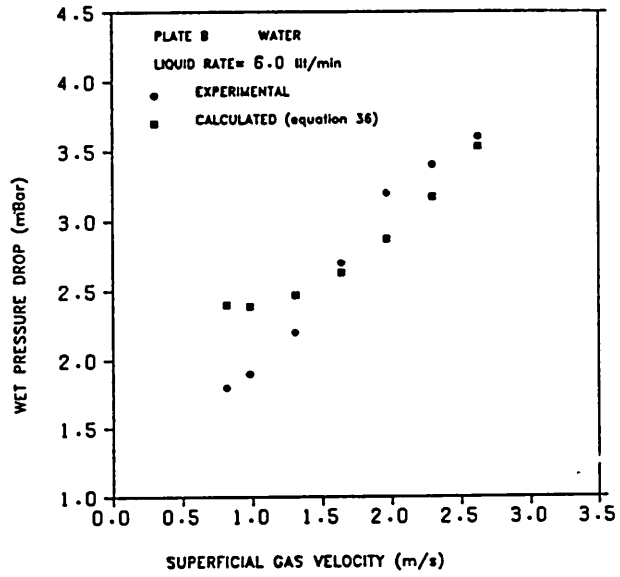

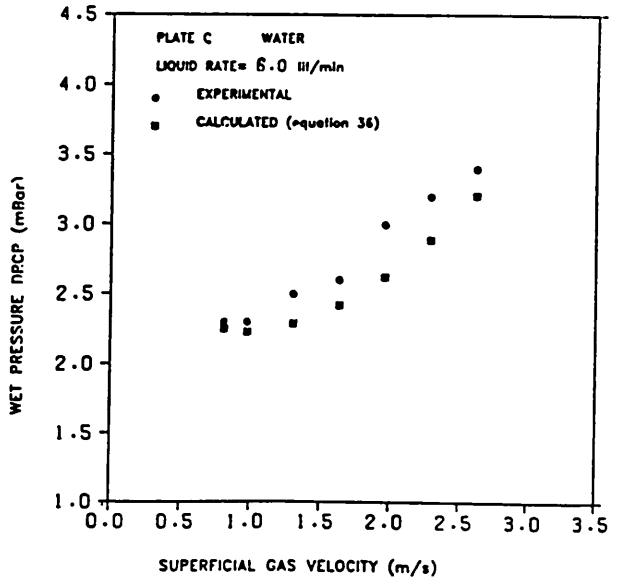

Figure 5.63 - Experimental and Calculated Wet Tray Pressure Drops for Water

5.5 Liquid Residence Time in the Downcomer

Introduction

Results of the investigation of liquid residence times in the downcomer are presented in this section. In chapter 2, a brief review of the traditional method of calculating liquid residence time in the downcomer was presented. In chapter 3, a detailed analysis of models of residence time distribution was presented. This section examines the results of these chapters in the light of experimental data obtained in this work.

5.5.1 Distribution of Residence Time in the Downcomer

Downcomer liquid residence times were measured by means of the tracer technique discussed in chapter 4. A typical chart, showing the distribution of residence times from an experiment carried out here is shown in figure 5.64. From this figure, it can be seen that the flow of liquid in the downcomer is far from conforming to the plug flow model traditionally assumed to model downcomer behaviour. The distribution of residence times shown in figure 5.65 suggests that there is some degree of mixing, especially for the foaming systems, in all cases considered. To be able to determine the degree of liquid mixing in the downcomer, it is necessary to examine theoretical models which may fit the patterns described in figure 5.64 adequately. These models were discussed in chapter 3. For all cases studied here, the dispersion model was found to fit the experimental distribution data better. Representative examples of the degree

of fit of theoretical distribution functions with experimental data are shown in figure 5.65 for plates A, B and C, respectively. This implies that the degree of mixing of liquid in the downcomer can be adequately defined in terms of the Péclet number, Pe,. However, since the liquid holdup, h_{Ld}, and the froth height, H_f, are different for each experiment, the use of the Péclet number for data interpretation becomes limited. A parameter that best describes mixing is the axial dispersion coefficient, D_E, which is obtained from the Péclet number. Section 5.5.3 analyses the degree of mixedness of liquid in the downcomer in terms of the axial dispersion coefficient, D_E.

5.5.2 Measured and Calculated Residence Times

The treatment of the experimental residence time distribution curve, according to the method outlined in chapter 2, Section 2.7, gives measured mean residence times. Calculated mean residence times or what is refered to in this text as the characteristic time is estimated from equation (40).

$$t_R = \frac{h_{Ld} A_d}{Q} \qquad (equation\ (40))$$

A comparison between calculated and measured residence times is shown in figures 5.66 for the foaming and non-foaming systems, respectively. Figure 5.66 indicates that residence time calculated from equation (40) give good approximation to the measured mean residence times for the non-foaming system. Another important deduction that can be

made from this figure is that the minimum design residence time in the downcomer for the non-foaming system is 5 seconds. This is in accordance with standard practice and therefore confirms one of the criteria of downcomer design strictly applicable to systems that do not foam. For the foaming system, mean residence times calculated from equation (40) are lower than the real mean residence time by a factor of 1.2 as shown in figure 5.57 (*top*). This is to be expected since for a foaming system, a high level of froth/foam exists in the downcomer. Hence, the time it takes for the liquid to flow through the dispersion increases with froth height for a given liquid flowrate. The residence times of figure 5.57 (*bottom*) does not imply no axial dispersion in the downcomer. There exists some degree of axial dispersion for all the systems considered but the degree of axial dispersion of liquid in the downcomer decreases with increasing liquid content of the dispersion (see Section 5.5.3).

5.5.3 Axial Dispersion Coefficient, D_E

The axial dispersion coefficient, D_E, in the downcomer was calculated from a knowledge of the Péclet number, liquid holdup, and average liquid fraction according to the relation

$$D_E = \frac{u_L\, h_{Ld}}{Pe\, \epsilon_L} \tag{154}$$

Generally, downcomer liquid holdup is a function of the downcomer liquid velocity. Hence, the axial dispersion coefficient can be represented solely as a function of the interstitial liquid velocity, u_L/ϵ_L, .

This dependence is shown in figure 5.67 which indicates that a simple correlation can be obtained between the axial dispersion coefficient and the interstitial liquid velocity according to the relation

$$D_E = 0.0177 \left(\frac{u_L}{\epsilon_L} \right)^{1.08} \tag{155}$$

A graphical representation of the degree of fit of the correlated axial dispersion coefficient, D_E, with the measured values is shown in figure 5.68. The axial dispersion coefficient obtained in this work varied between $9.0 \times 10^{-5} - 1.5 \times 10^{-3}\ m^2/s$. These values are at variance with those of Thomas et al[55]. This can be attributed to the fact that Thomas et al[55] studied mixing in a plate/downcomer system. Hence, the degree of mixing in their case is expected to be higher and consequently their dispersion coefficients. The correlation of equation (155) shows the effect of gas fraction and hence, gas velocity on mixing in the downcomer. This is also at variance with the findings of Thomas et al[55] and also of Welch et al[105]. The raeson for this is also due to the fact that Thomas et al[55] and Welch et al[105] investigated mixing in a combined plate/downcomer system.

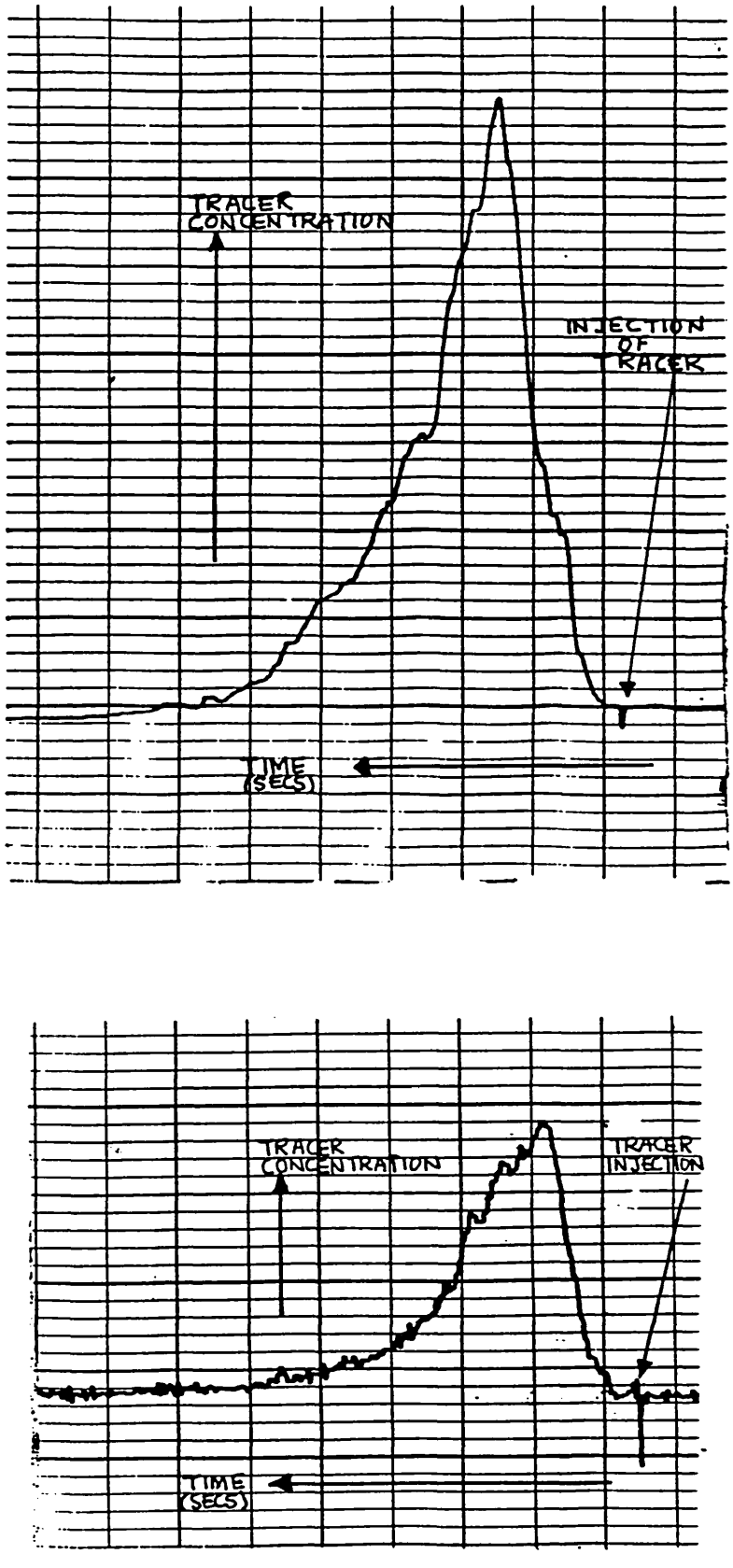

Figure 5.64 Typical Chart showing Distribution of Residence Times in the Downcomer

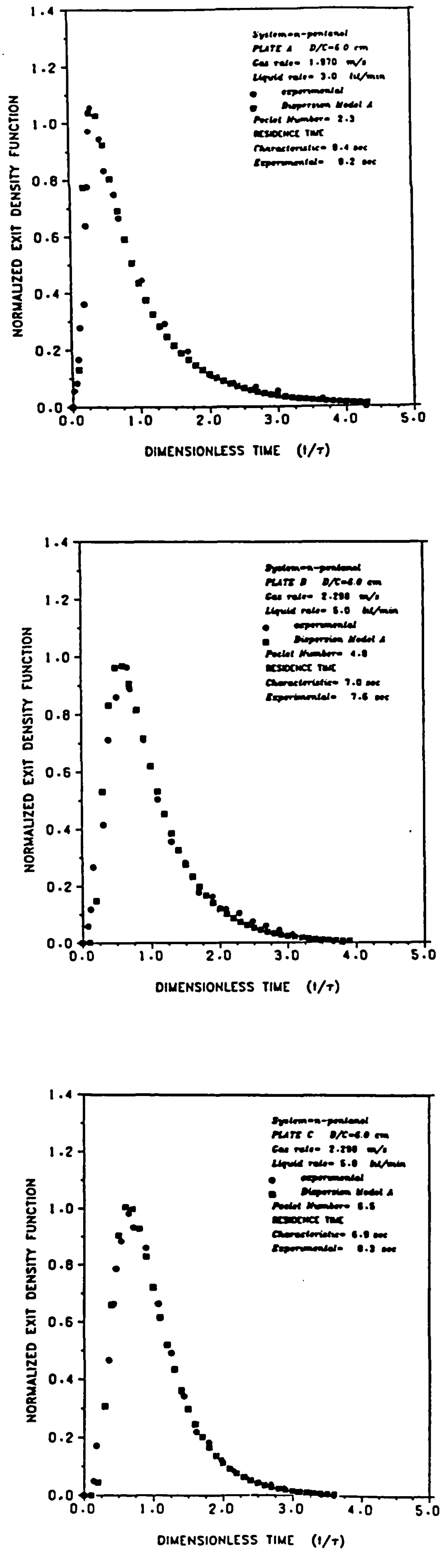

Figure 5.65 - Degree of fit of Dispersion Model with Experimental Data

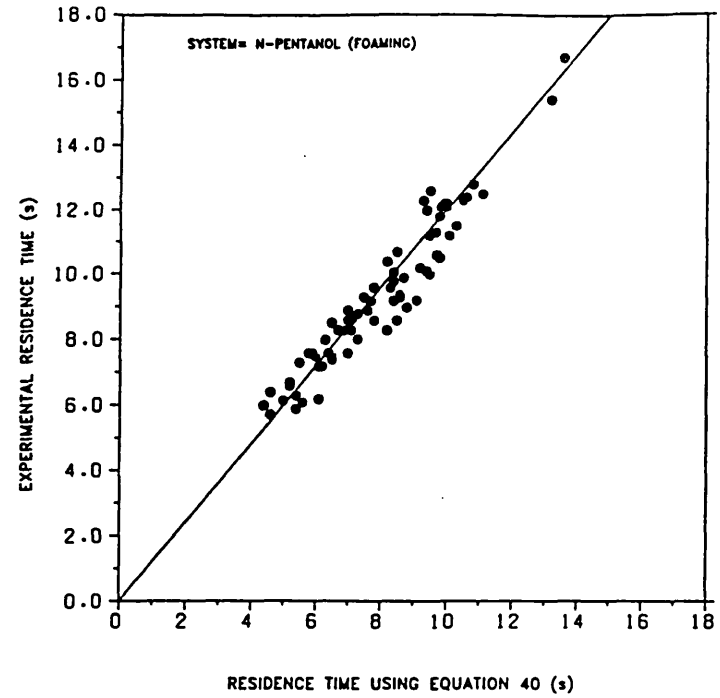

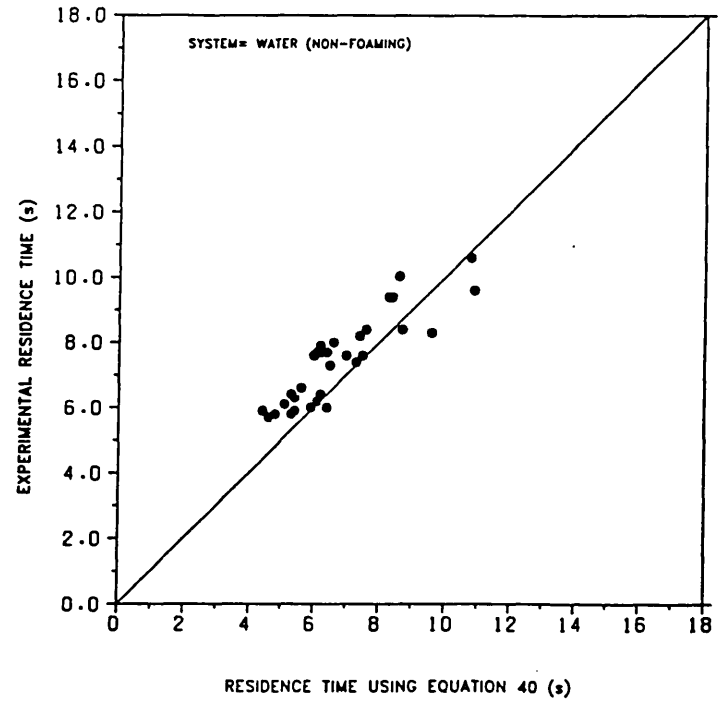

Figure 5.66 · Comparison Between Experimental and Calculated Liquid Residence Time in Downcomer (Foaming and Non-Foaming Systems)

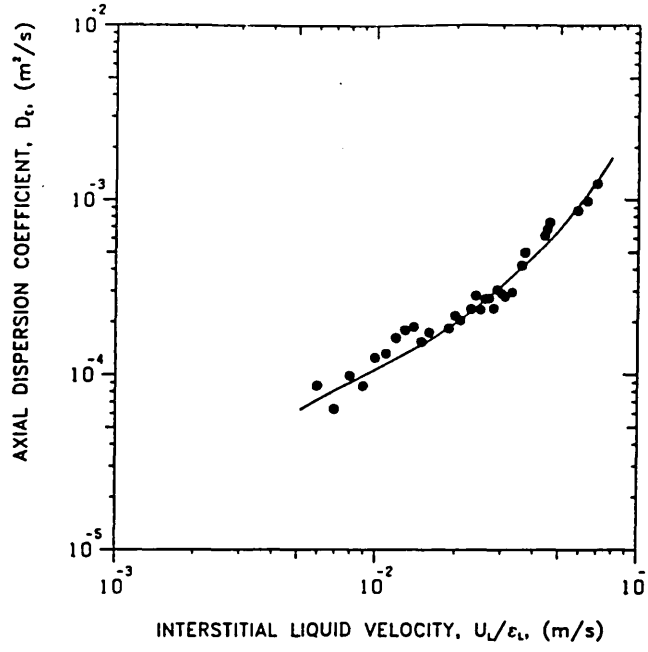

Figure 5.67 Graph of D_E versus U_L/ϵ_L

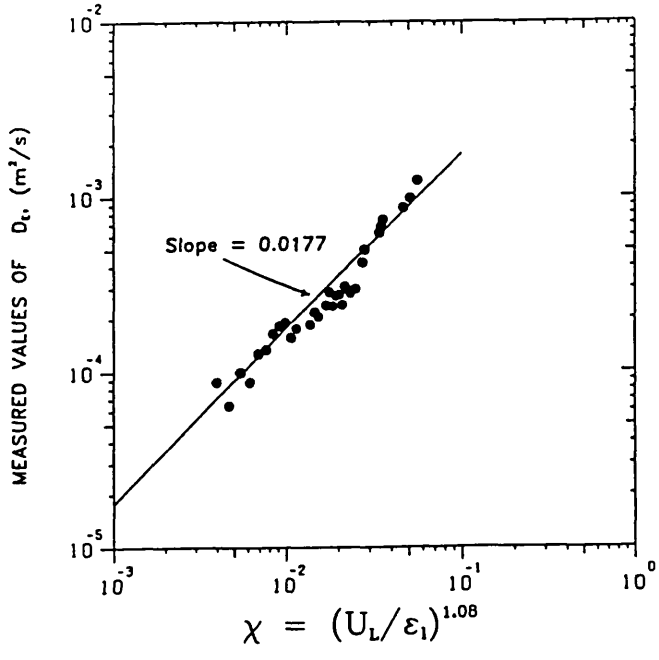

Figure 5.68 Graph of D_E versus $(U_L/\epsilon_L)^{1.08}$

5.6 Prediction of Froth/Foam Heights in Downcomers

In chapter 3, Section 3.2, a theoretical analysis was carried out which resulted in a predictive equation for the estimation of froth/foam heights in downcomers useful for design. In this section, results obtained from the application of this equation (equation (129)) are compared to expermental froth/foam heights. This is shown in figures 5.69 - 5.72. Figures 5.69 and 5.70 show a comparison between experimental froth/foam heights and calculated values for the system n-Pentanol for the 6 cm and 8 cm downcomers, respectively. Similarly figures 5.71 and 5.72 show a comparison between experimental froth/foam heights and calculated values for the systems n-Butanol and Water respectively, for the 6 cm downcomer.

From these figures, it can be seen that the calculated froth/foam heights are in agreement to within 10% of experimental data for most of the cases considered. This implies that equation (129) gives a strong predictive tool for the estimation of froth/foam heights in any downcomer system. The little scatter in the results for Water is due to the fact that a large span of heights could not be traversed and largely due to measurements.

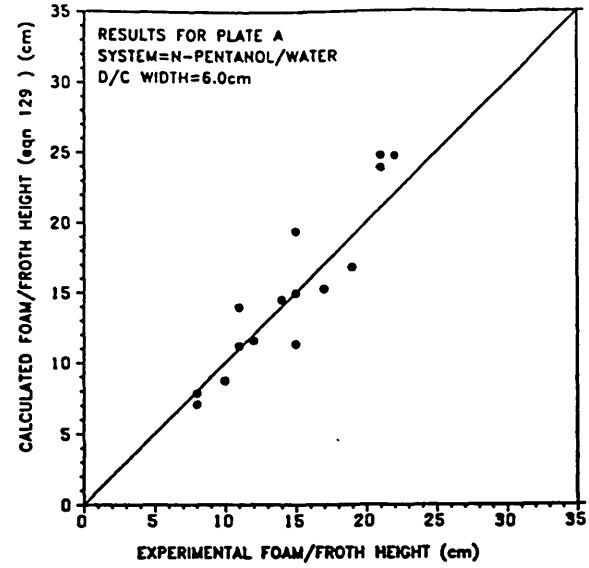

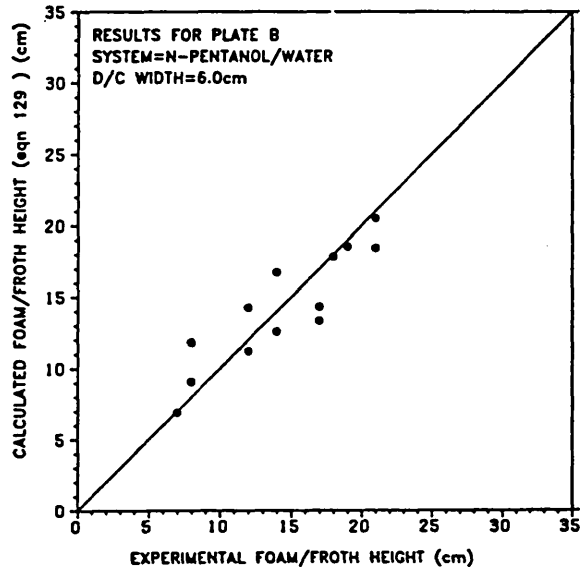

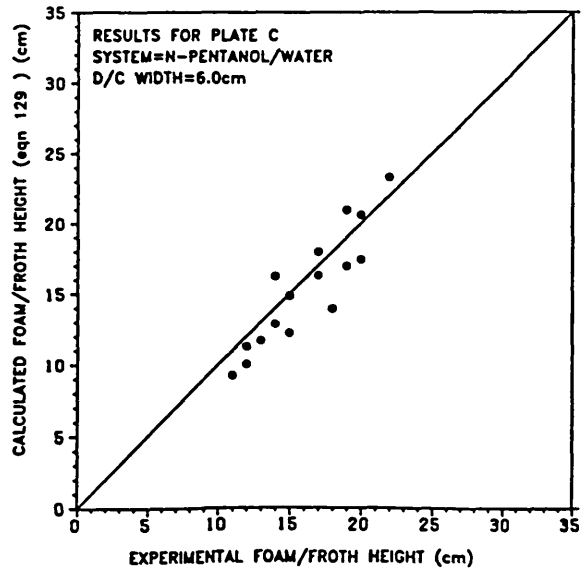

Figure 5.69 :-Comparison between Experimental and Calculated Froth/Foam height in the downcomer for n-Pentanol (6cm Downcomer)

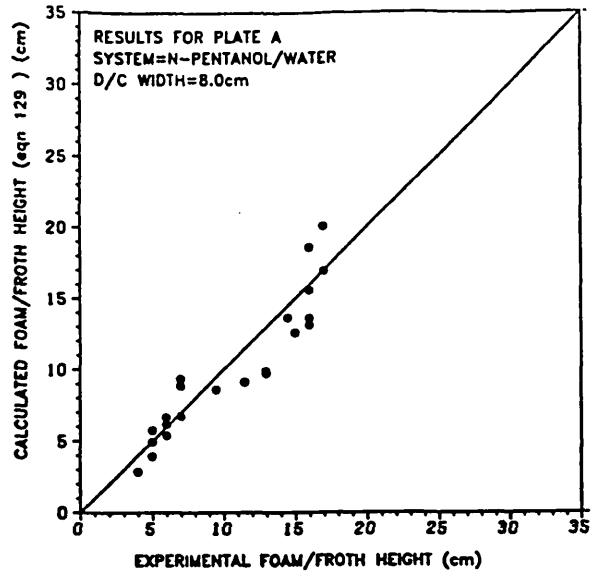

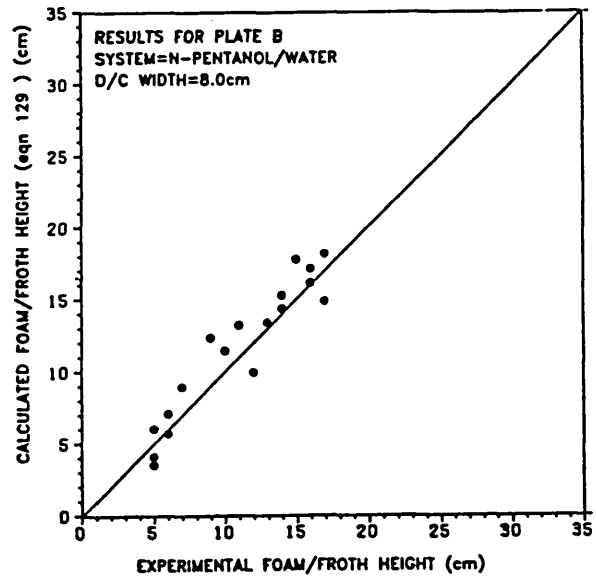

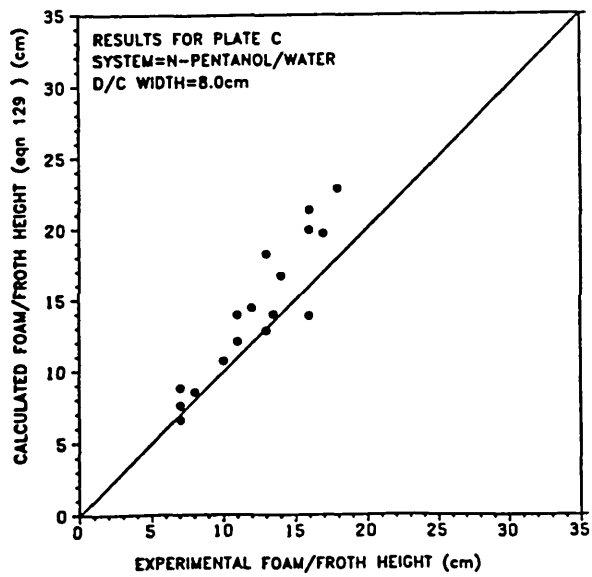

Figure 5.70 :- Comparison between Experimental and Calculated Froth/Foam height in the downcomer for n-Pentanol (8cm Downcomer)

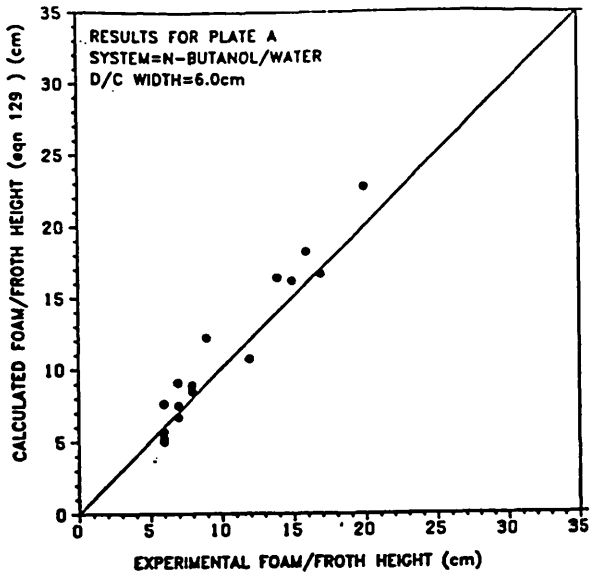

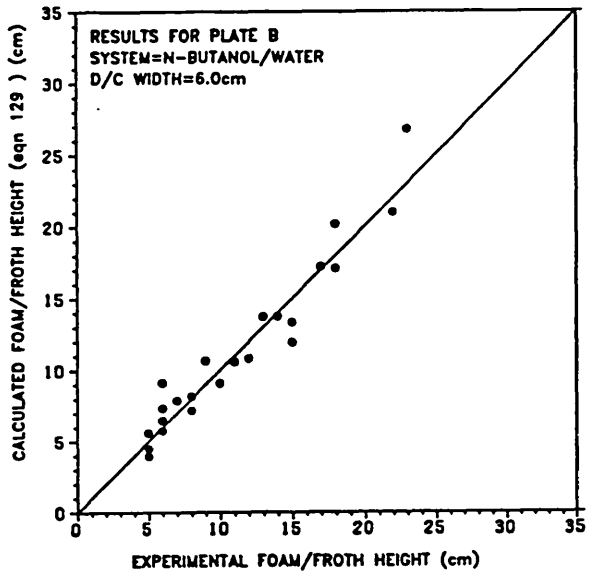

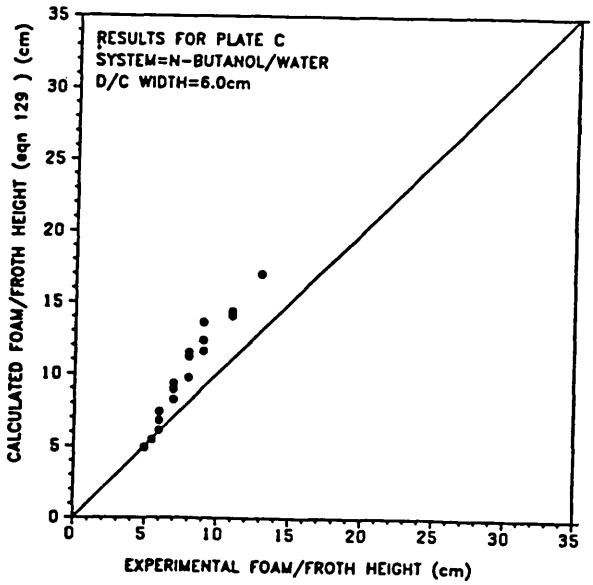

Figure 5.71 :- Comparison between Experimental and Calculated Froth/Foam height in the downcomer for n-Butanol (6cm Downcomer)

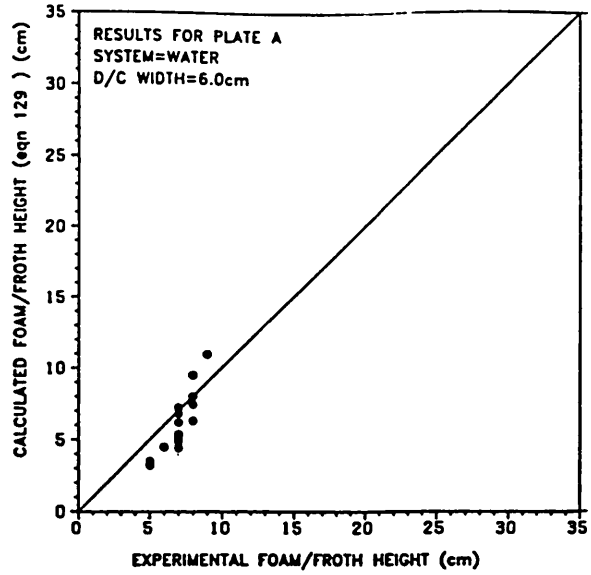

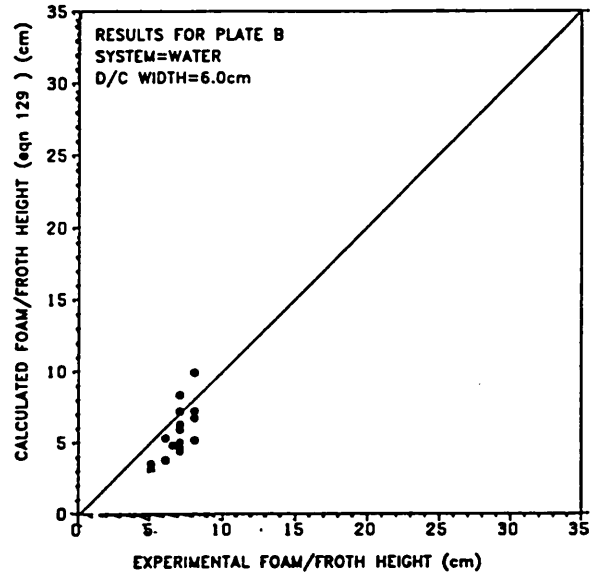

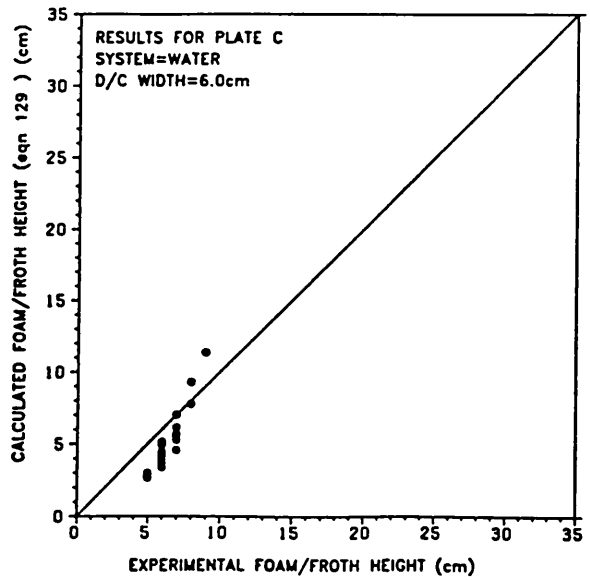

Figure 5.72 :- Comparison between Experimental and Calculated Froth/Foam height in the downcomer for Water (6cm Downcomer)

5.7 Hydrodynamic Study of Froth Flow on Plates

A theoretical analysis of the froth hydrodynamics on sieve plates was made in chapter 3, Section 3.3. Plate studies were carried out only for the n-Butanol and Water systems . The aim of this section is to consider and discuss results obtained from the use of the equations resulting from Section 3.3 for the prediction of froth profile on sieve plates for the systems studied. The equations resulting from the theoretical analysis were also applied to the data of Macmillan[127], which are therefore included here.

5.7.1 Simulation Results

Equations (151) and (152) for the estimation and characterization of froth profiles on the plate can be solved only by simulation. These equations were applied to the systems n-Butanol and Water and the results are shown in figures 5.73 - 5.84 and 5.85 - 5.94 for the systems Water and n-Butanol, respectively. A careful study of the graphs shown in these figures indicates that this method of characterising froth profiles on sieve plates is quite appropriate, especially when using equation (151). For all the cases shown, it can be seen that simulation results obtained using equation (151) fits the experimental data much more closely than those obtained using equation (152). Generally, it can be seen that theoretical froth profiles determined by means of equation (151) fit experimental profiles well only in the frothing or mixed froth† regimes of plate op-

† *See Tables 5.1 - 5.3 for flow Regimes*

eration. As the gas rate is increased futher, there exist the peculiar plateau shapes of dispersion density profiles which cannot be approximated by the theory. Basically, in this regime of plate operation, there is usually a large degree of oscillation and hence, more than one energy level by which the froth can be stabilized may exist. The theoretical approach used does not apply to the spray regime or very close to it. This regime of plate operation can be effectively described by using the drop trajectory model[14,15]. In the frothing or mixed froth regime of plate operation, there usually exists a well defined froth on the plate. The froth can be said to be stabilised at a finite and characteristic energy level necessary for all the forces acting on the dispersion to equilibrate. Any disturbance introduced, by either changing the liquid or the gas loading on the plate, shifts stability of the system to a new energy level, different from the initial level. This simple picture appears to apply to those conditions leading to the plate profiles of dispersion density shown and discussed in Section 5.4. If the plate operation is carried out very near or in the bubbling regime, the minimum energy required to stabilise the froth is not, and cannot be reached. This is another unstable point in plate operation and behaviour, and it corresponds to conditions usually described as weeping.

In conclusion, based on the theoretical analysis of Chapter 3, Section 3.3, it should now be possible to map the froth profile on the plate, prior to operation, by using equation (151). However, the use of equation (151) is based on a prior knowledge of liquid holdup on the plate

as well as of the gas fraction just above the plate. In Section 5.4.1.2, it was shown that the total liquid holdup on the plate can be confidently approximated by the use of equation (32). However, no explicit and universal relation is available yet for the evaluation of initial gas fraction on the plate. Hence, this parameter must still be determined experimentally to be able to map froth profiles in the frothing regime of plate operation on the plate

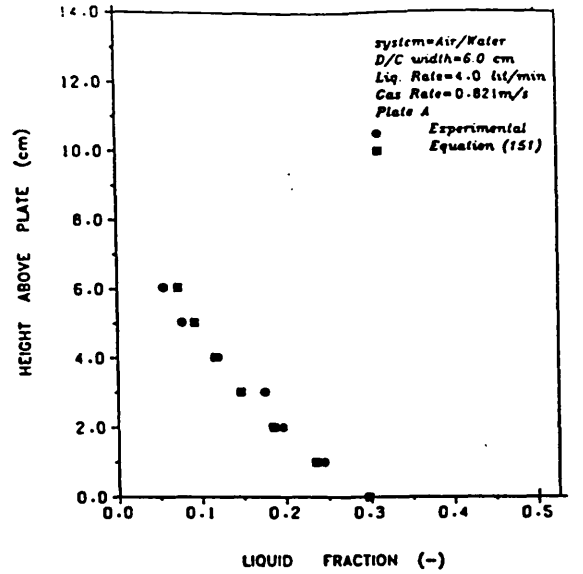

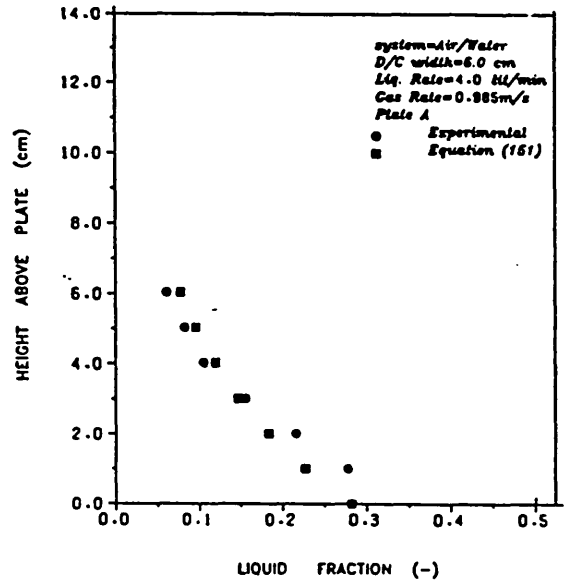

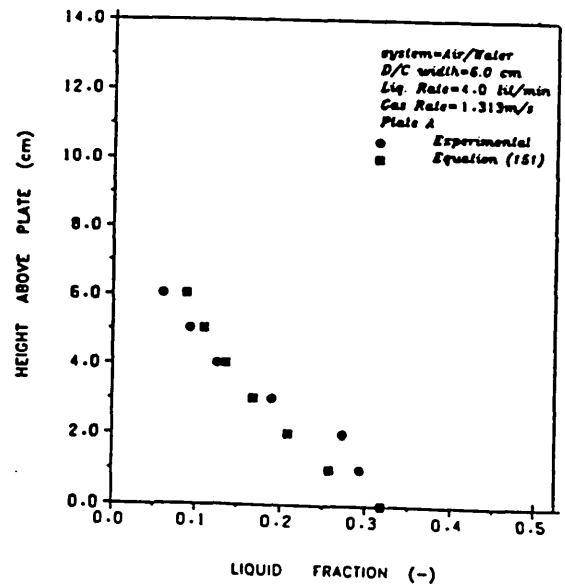

Figure 5.73 :- Experimental and Simulated Froth Profiles on the plate using equation (151) for Plate A (Water, Liquid Rate = 4.0 lit/min, Gas Rates = 0.821, 0.985, 1.313 m/s)

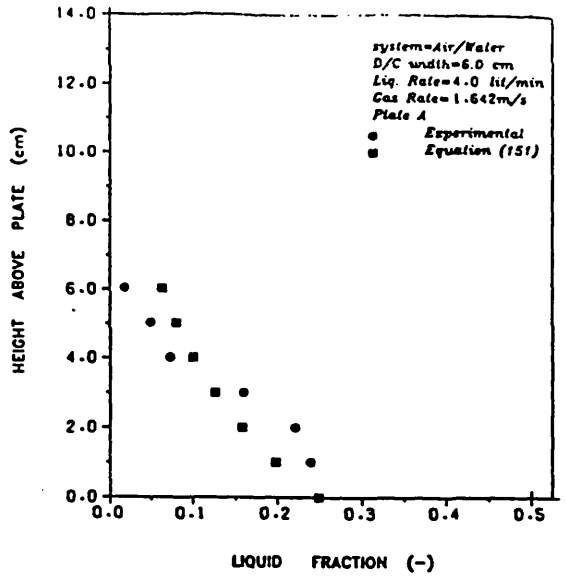

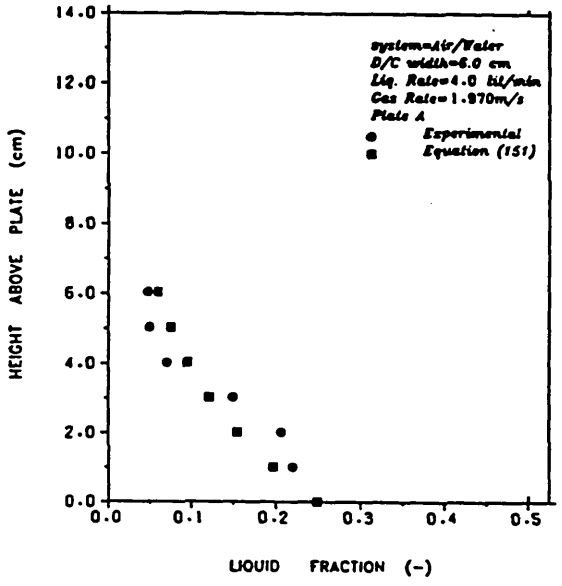

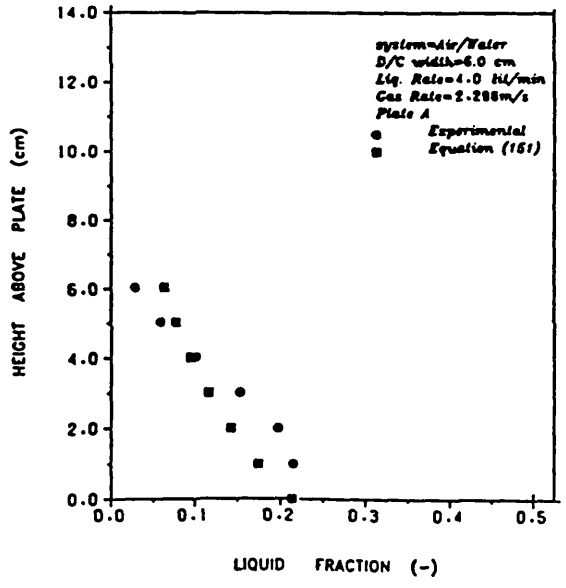

Figure 5.74 :- Experimental and Simulated Froth Profiles on the plate using equation (151) for Plate A (Water, Liquid Rate = 4.0 lit/min, Gas Rates = 1.642, 1.970, 2.298 m/s)

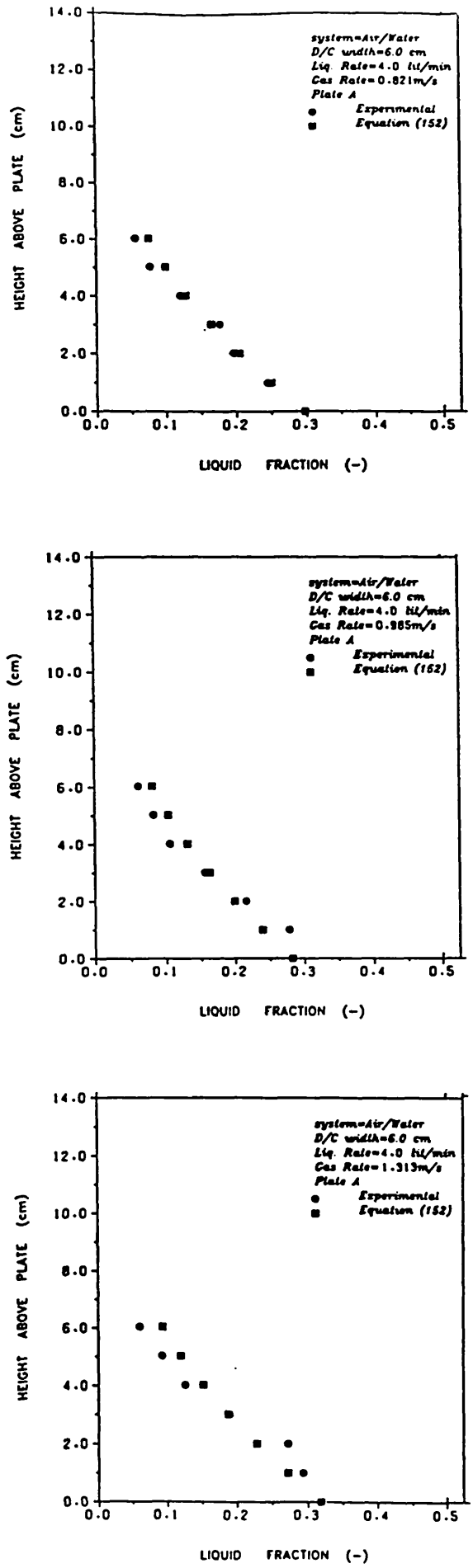

Figure 5.75 :- Experimental and Simulated Froth Profiles on the plate using equation (152) for Plate A (Water, Liquid Rate = 4.0 lit/min, Gas Rates = 0.821, 0.985, 1.313 m/s)

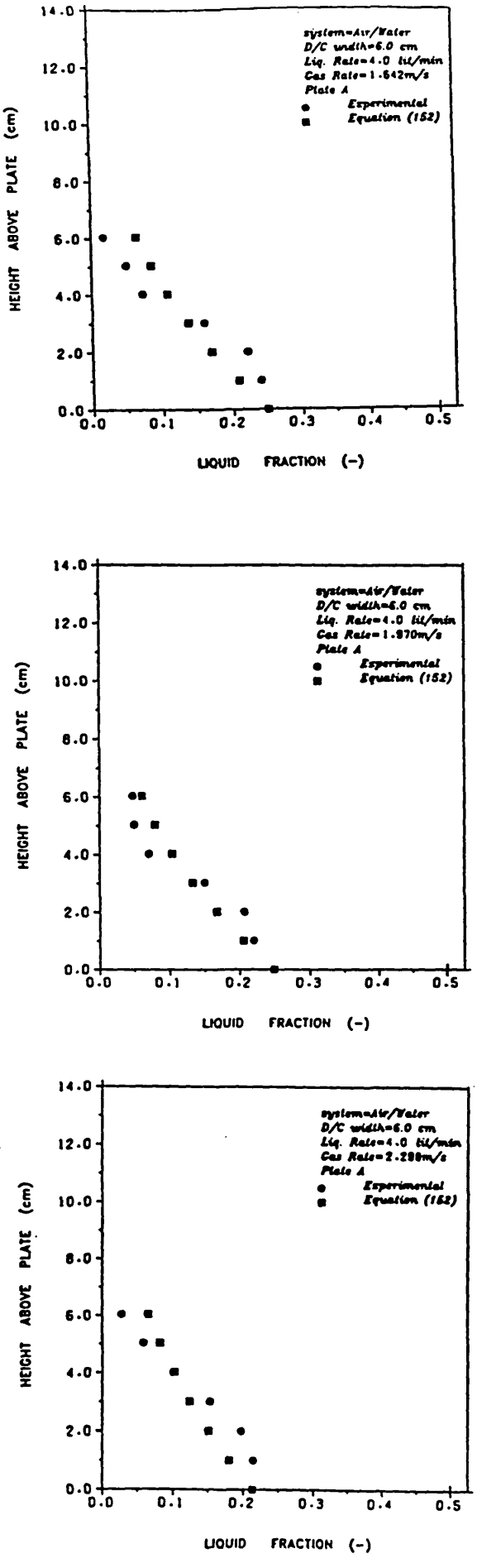

Figure 5.76 :- Experimental and Simulated Froth Profiles on the plate using equation (152) for Plate A (Water, Liquid Rate = 4.0 lit/min, Gas Rates = 1.642, 1.970, 2.298 m/s)

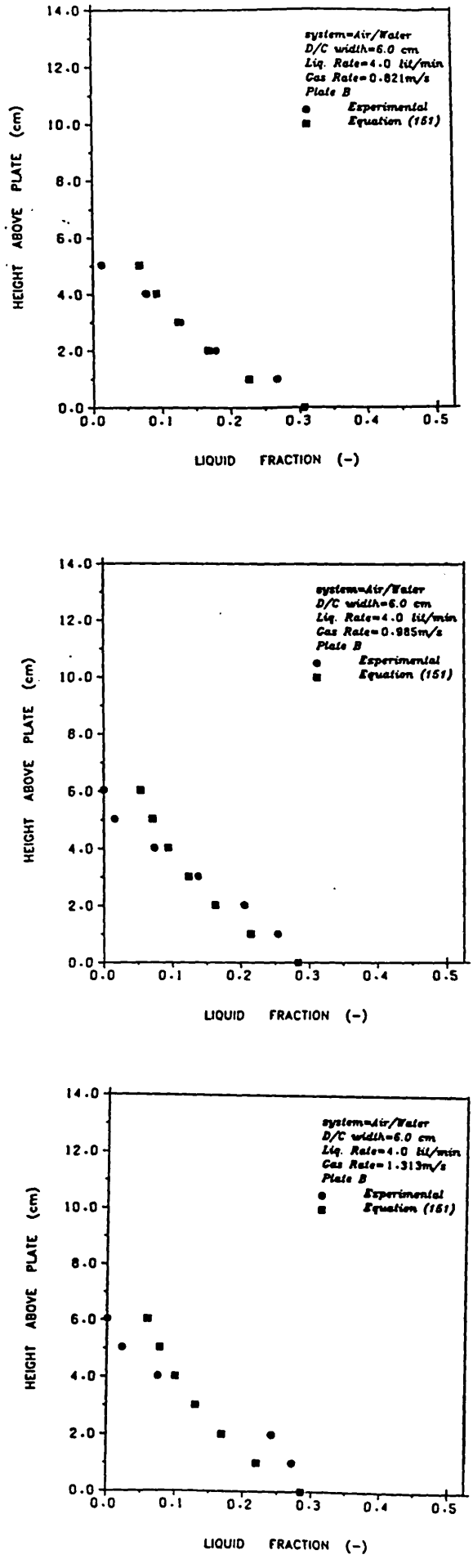

Figure 5.77 :- Experimental and Simulated Froth Profiles on the plate using equation (151) for Plate B (Water, Liquid Rate = 4.0 lit/min, Gas Rates = 0.821, 0.985, 1.313 m/s)

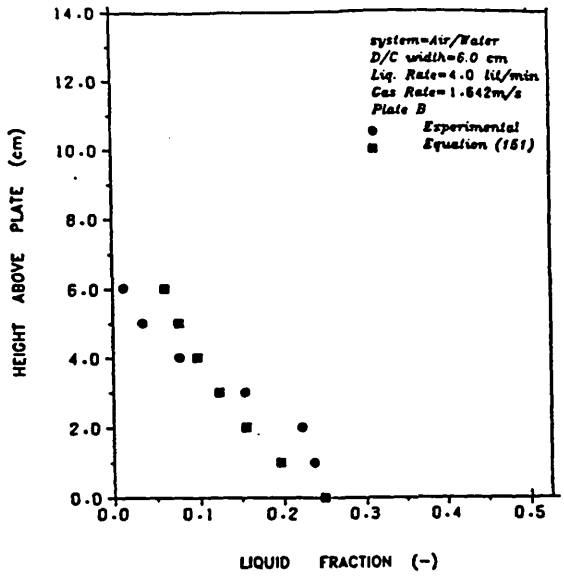

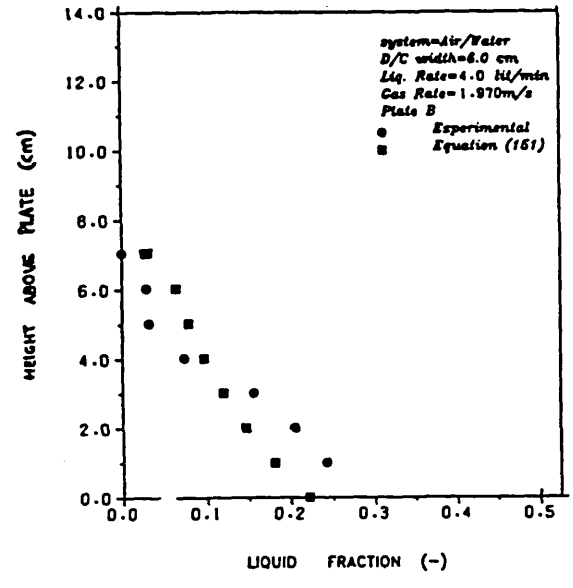

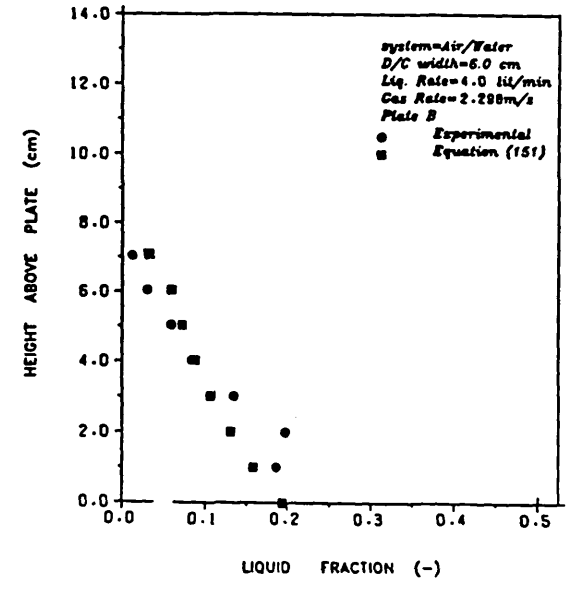

Figure 5.78 :- Experimental and Simulated Froth Profiles on the plate using equation (151) for Plate B (Water, Liquid Rate = 4.0 lit/min, Gas Rates = 1.642, 1.970, 2.298 m/s)

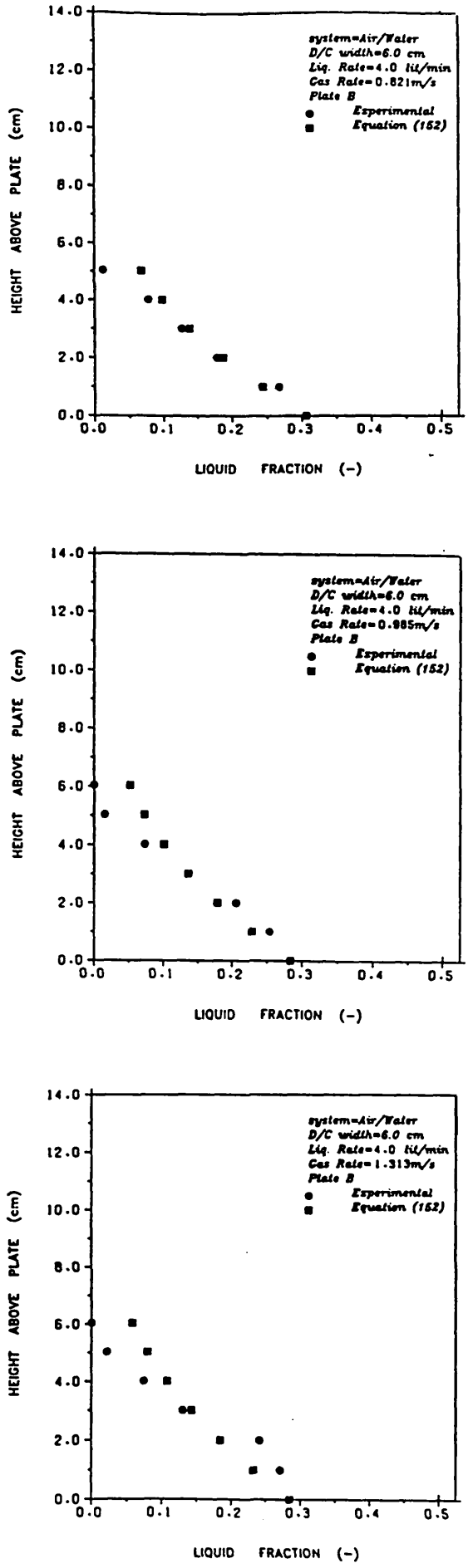

Figure 5.79 :- Experimental and Simulated Froth Profiles on the plate using equation (152) for Plate B (Water, Liquid Rate = 4.0 lit/min, Gas Rates = 0.821, 0.985, 1.313 m/s)

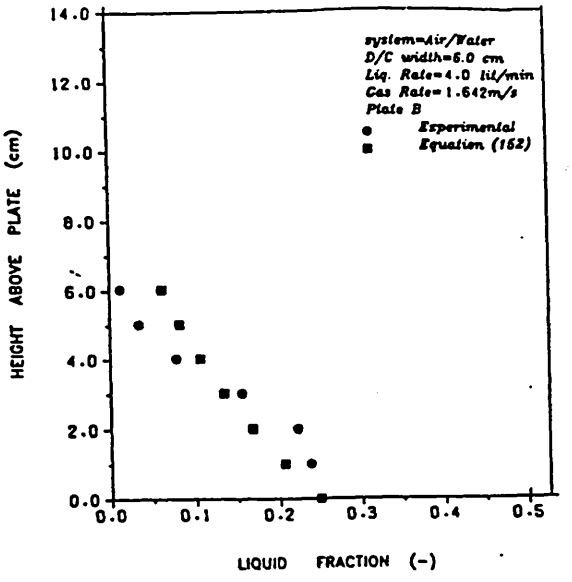

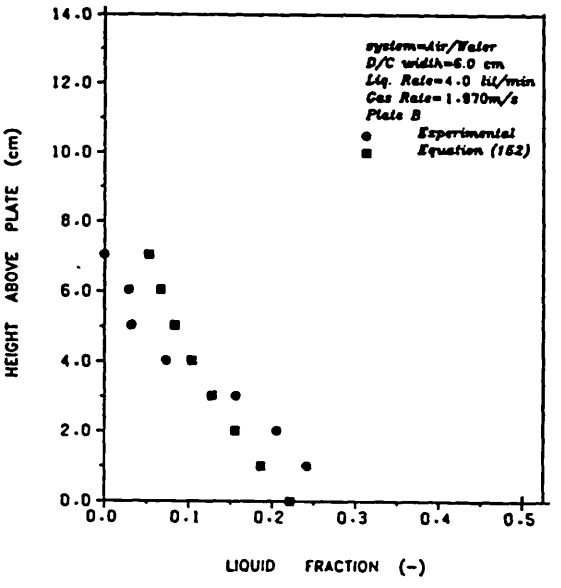

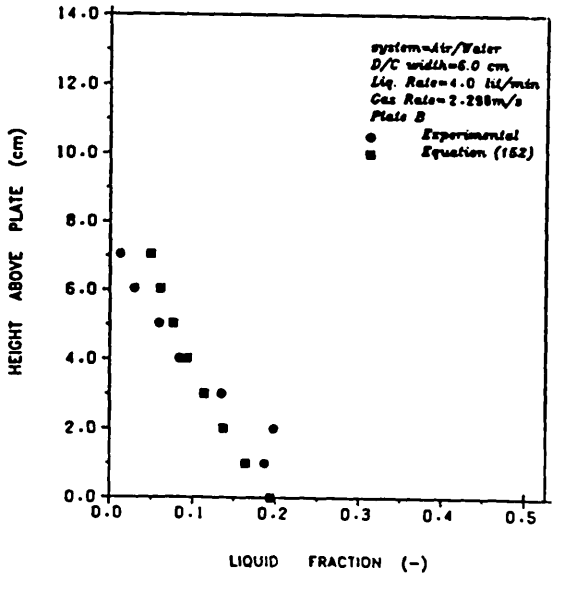

Figure 5.80 :- Experimental and Simulated Froth Profiles on the plate using equation (152) for Plate B (Water, Liquid Rate = 4.0 lit/min, Gas Rates = 1.642. 1.970, 2.298 m/s)

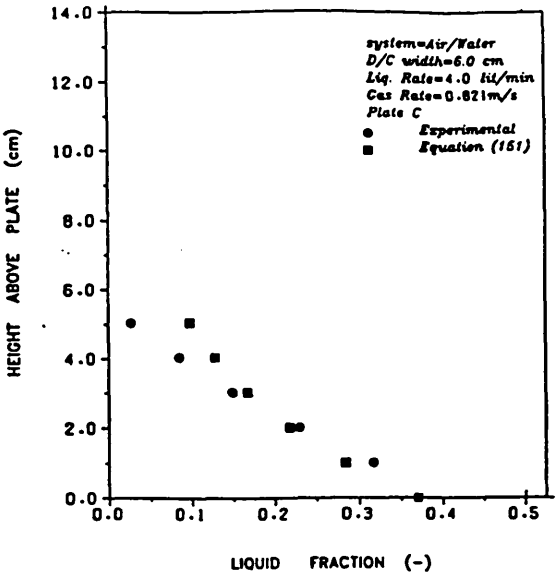

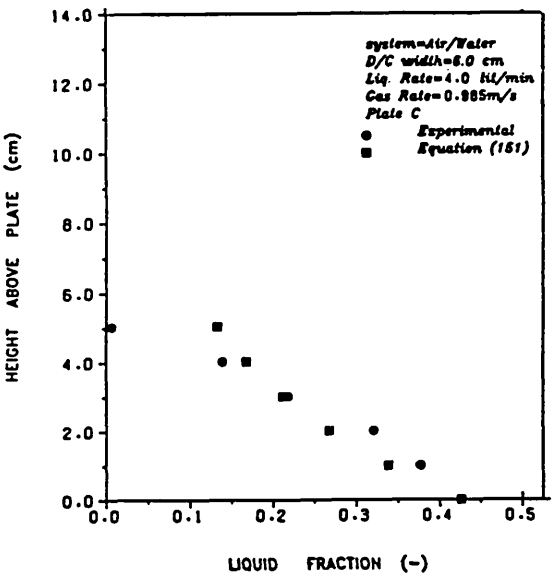

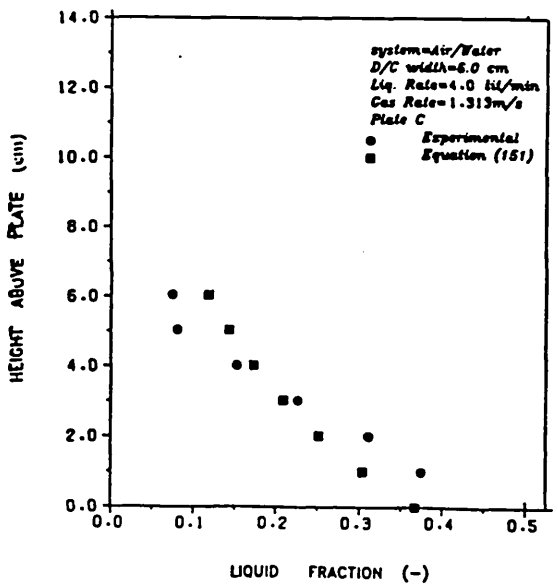

Figure 5.81 :- Experimental and Simulated Froth Profiles on the plate using equation (151) for Plate C (Water, Liquid Rate = 4.0 lit/min, Gas Rates = 0.821, 0.985, 1.313 m/s)

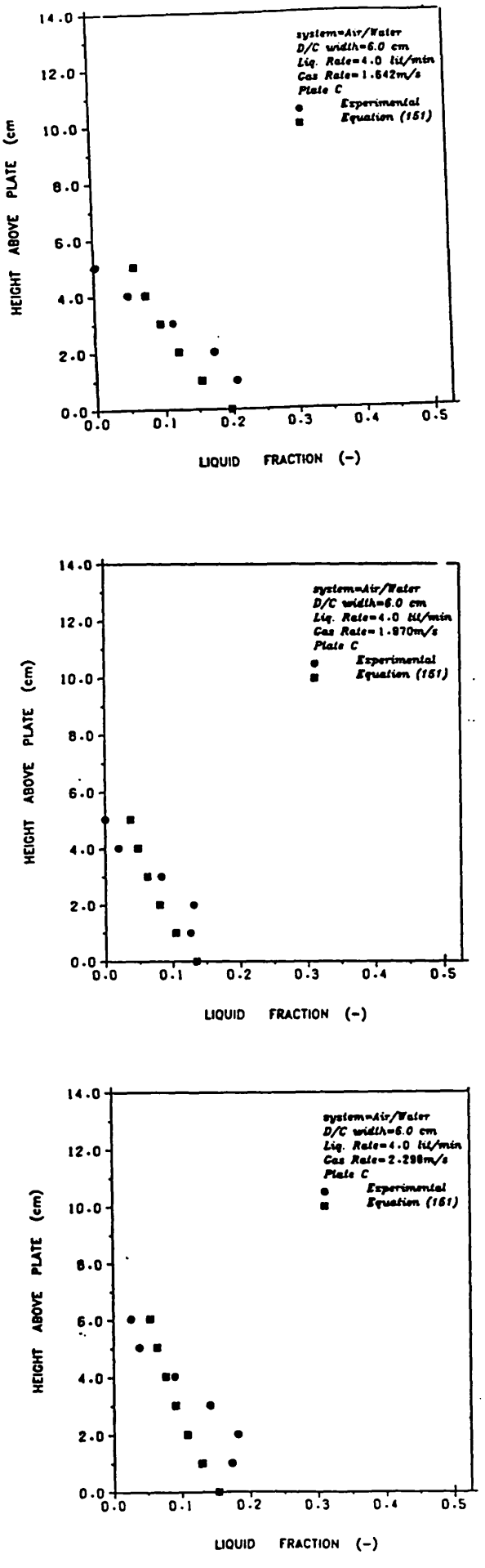

Figure 5.82 :- Experimental and Simulated Froth Profiles on the plate using equation (151) for Plate C (Water, Liquid Rate = 4.0 lit/min, Gas Rates = 1.642, 1.970, 2.298 m/s)

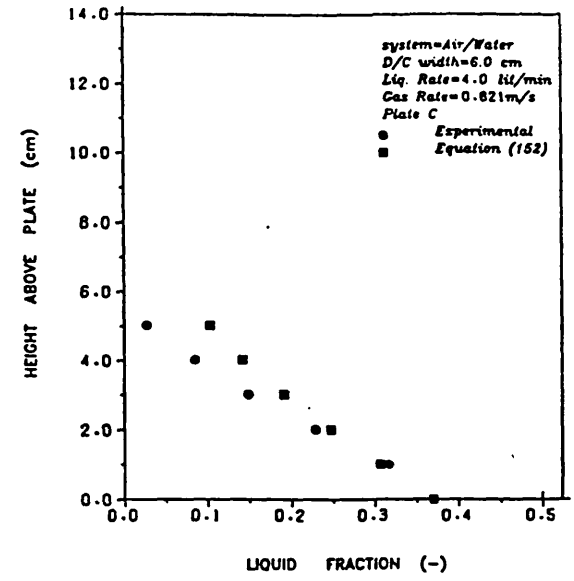

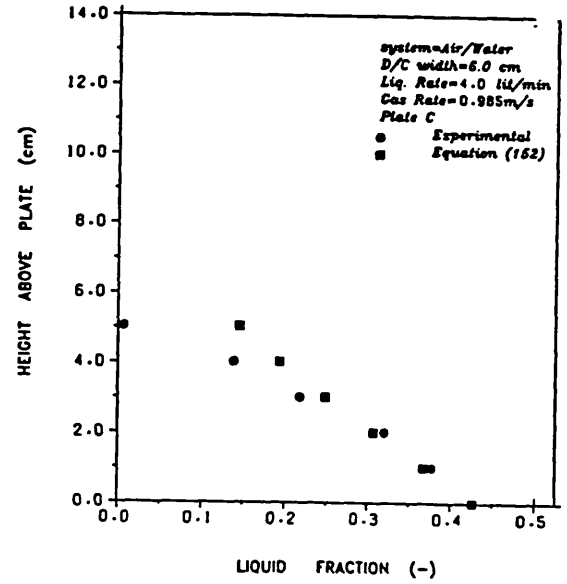

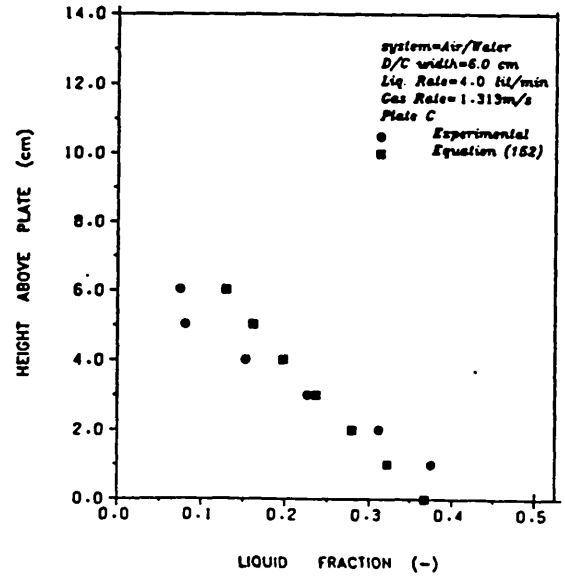

Figure 5.83 :- Experimental and Simulated Froth Profiles on the plate using equation (152) for Plate C (Water, Liquid Rate = 4.0 lit/min, Gas Rates = 0.821, 0.985, 1.313 m/s)

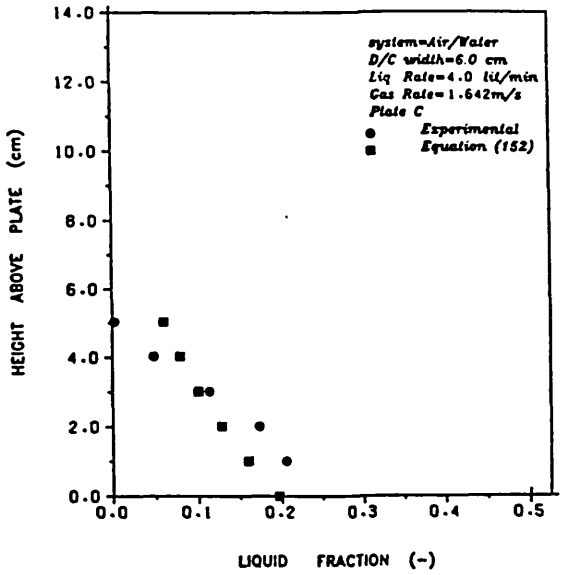

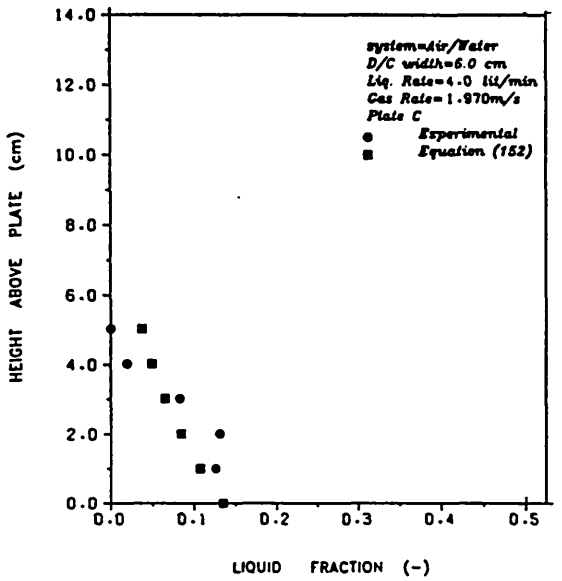

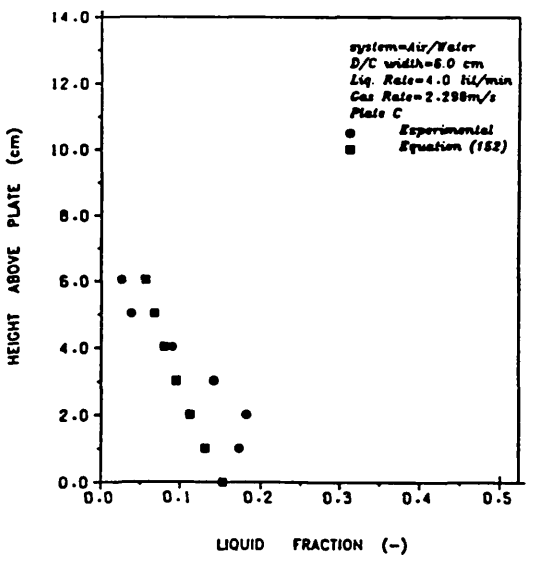

Figure 5.84 :- Experimental and Simulated Froth Profiles on the plate using equation (152) for Plate C (Water, Liquid Rate = 4.0 lit/min, Gas Rates = 1.642, 1.970, 2.298 m/s)

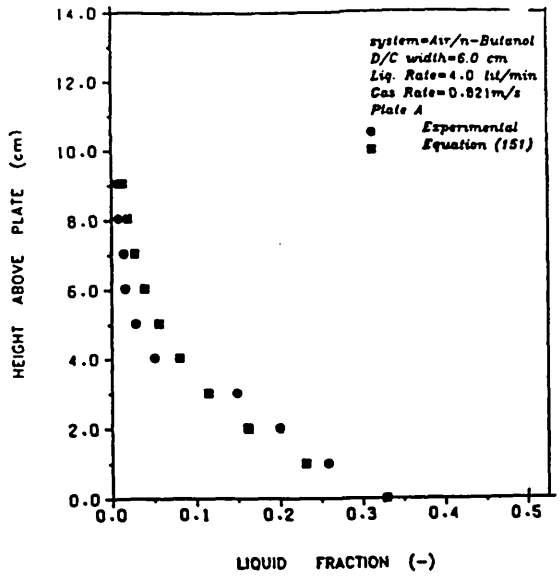

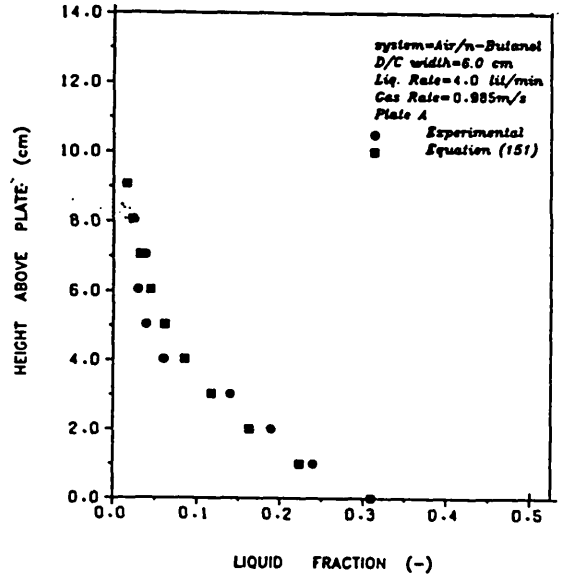

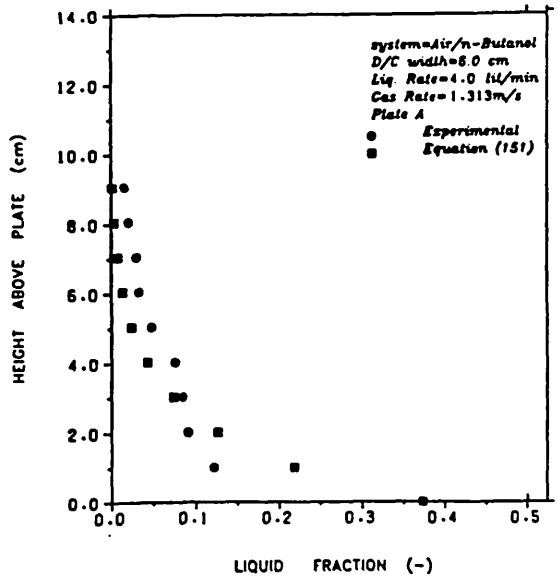

Figure 5.85 :- Experimental and Simulated Froth Profiles on the plate using equation (151) for Plate A (n-Butanol, Liquid Rate = 4.0 lit/min, Gas Rates = 0.821, 0.985, 1.313 m/s)

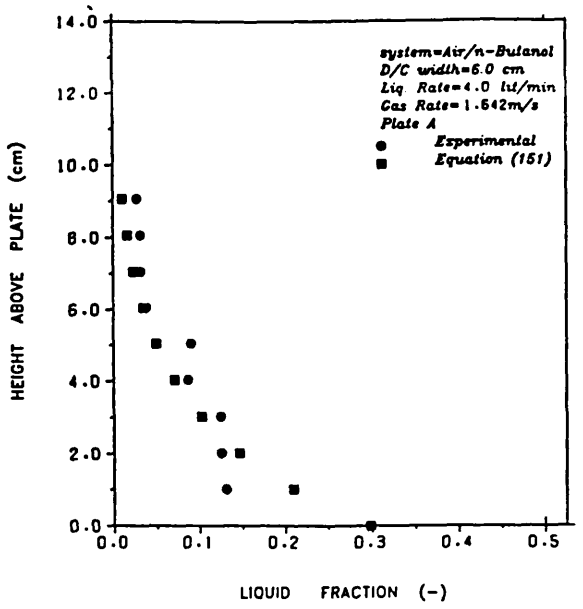

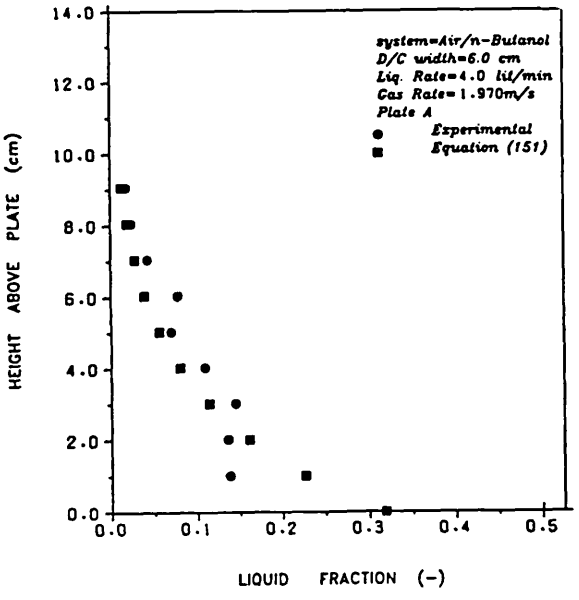

Figure 5.86 :- Experimental and Simulated Froth Profiles on the plate using equation (151) for Plate A (n-Butanol, Liquid Rate = 4.0 lit/min, Gas Rates = 1.642, 1.970 m/s)

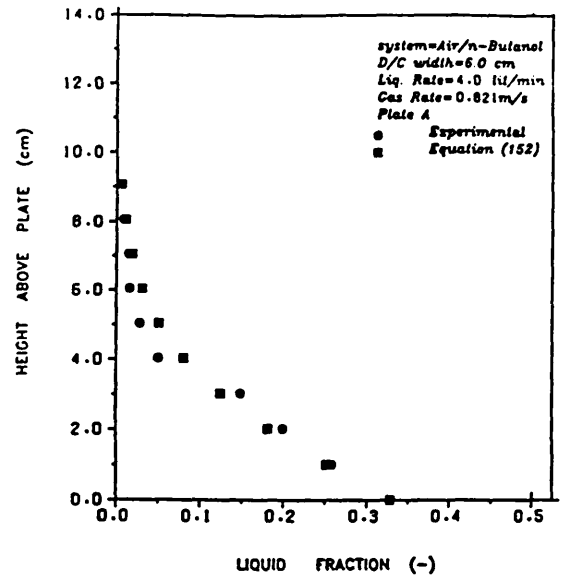

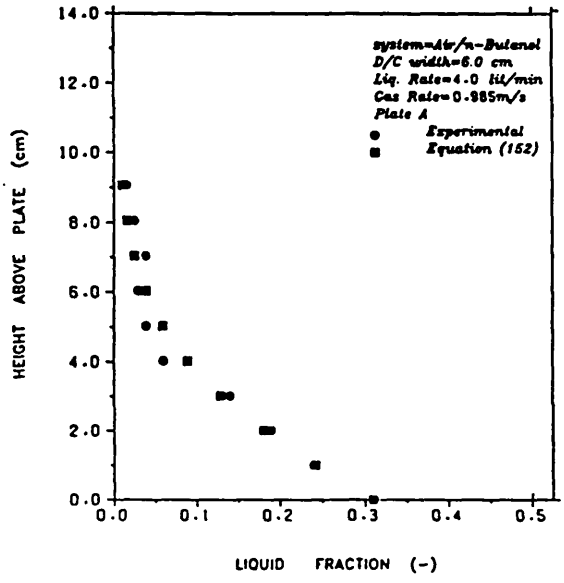

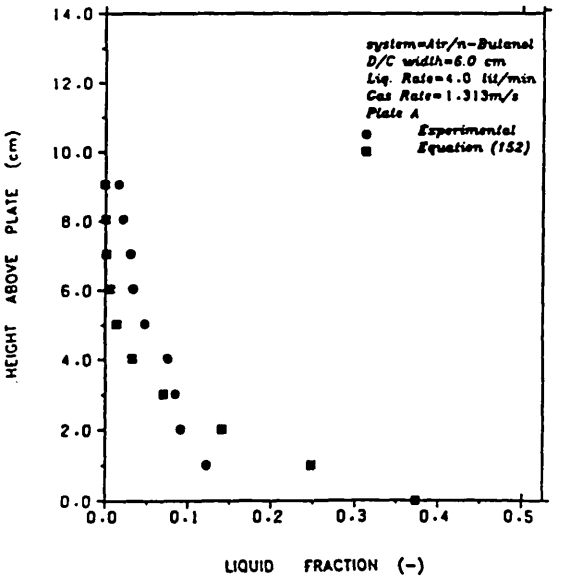

Figure 5.87 :- Experimental and Simulated Froth Profiles on the plate using equation (152) for Plate A (n-Butanol, Liquid Rate = 4.0 lit/min, Gas Rates = 0.821, 0.985, 1.313 m/s)

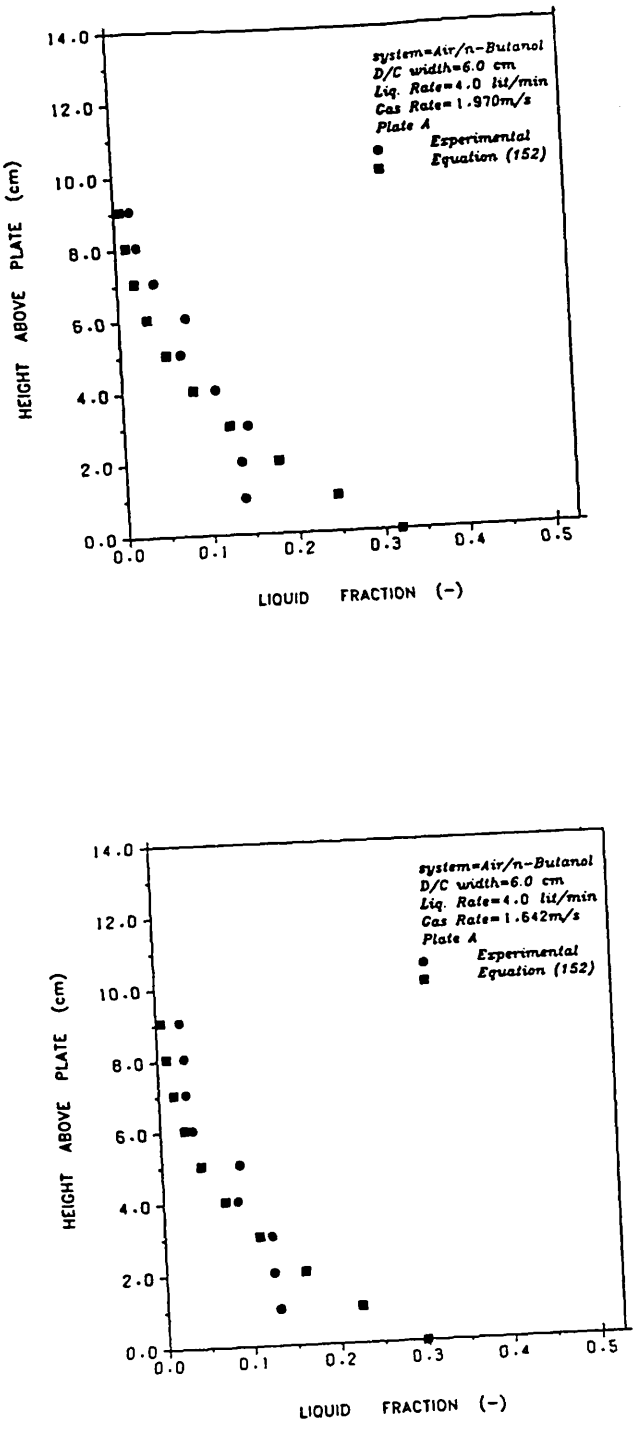

Figure 5.88 :- Experimental and Simulated Froth Profiles on the plate using equation (152) for Plate A (n-Butanol, Liquid Rate = 4.0 lit/min, Gas Rates = 1.642, 1.970 m/s)

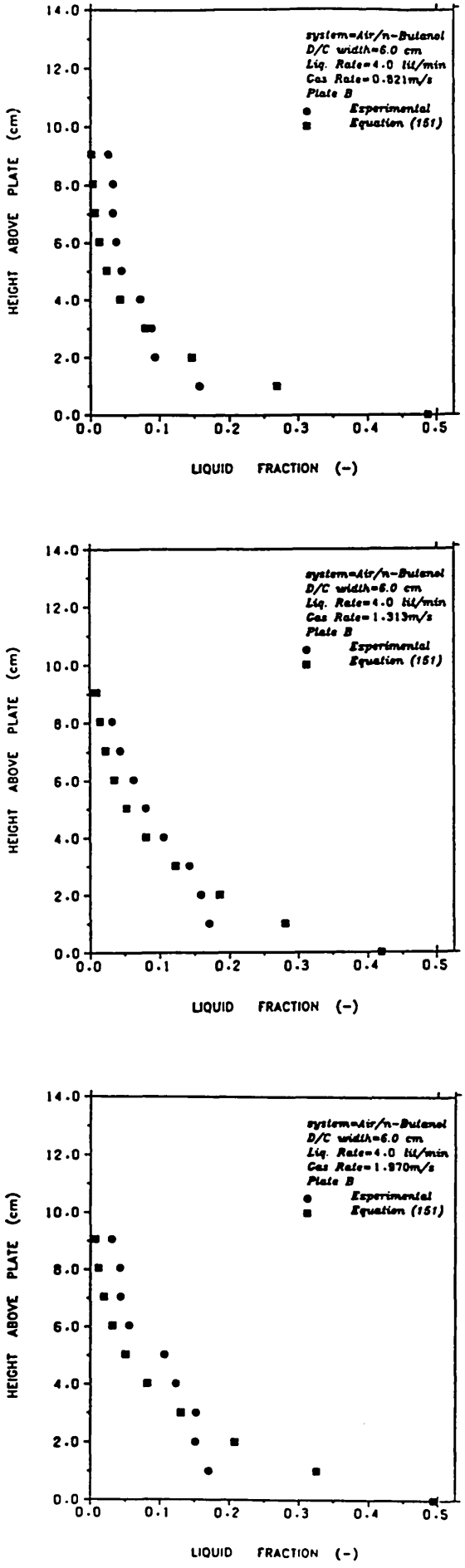

Figure 5.89 :- Experimental and Simulated Froth Profiles on the plate using equation (151) for Plate B (n-Butanol, Liquid Rate = 4.0 lit/min, Gas Rates = 0.821, 1.313, 1.970 m/s)

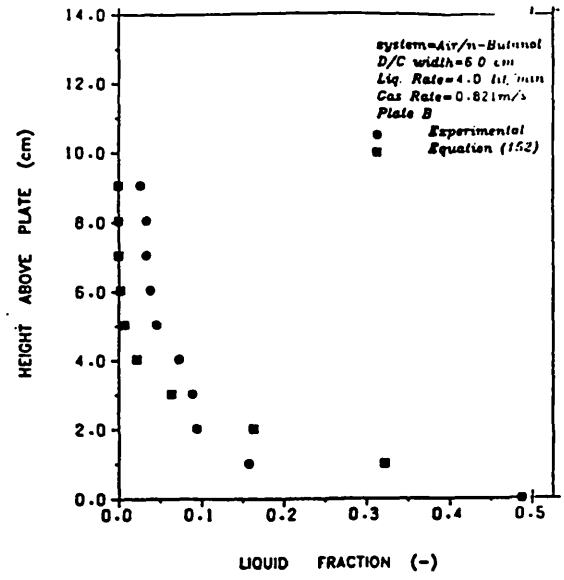

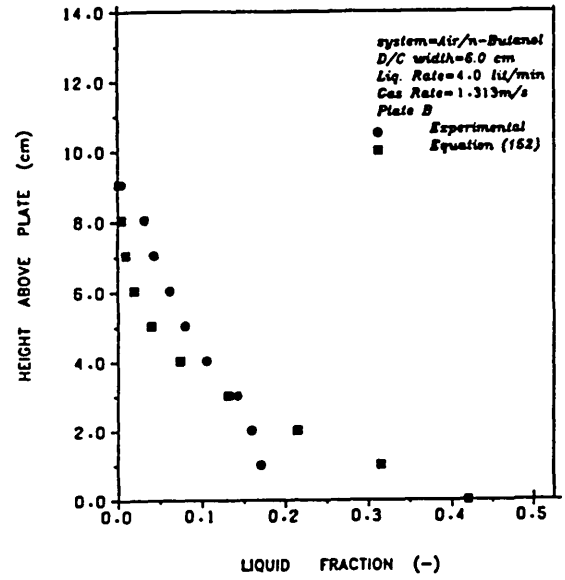

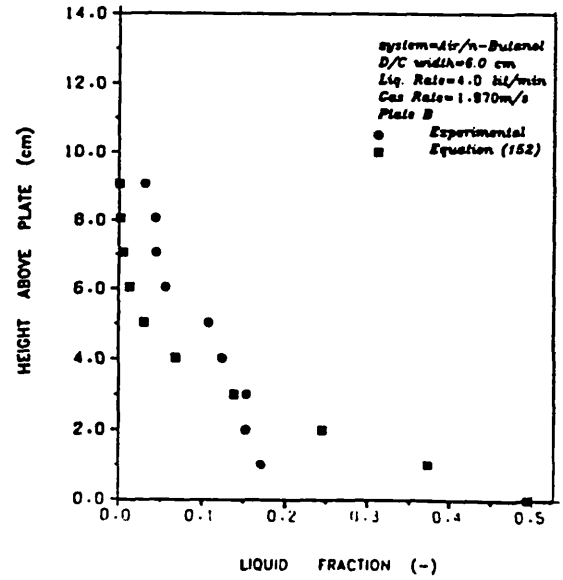

Figure 5.90 :- Experimental and Simulated Froth Profiles on the plate using equation (152) for Plate B (n-Butanol, Liquid Rate = 4.0 lit/min, Gas Rates = 0.821, 1.313, 1.970 m/s)

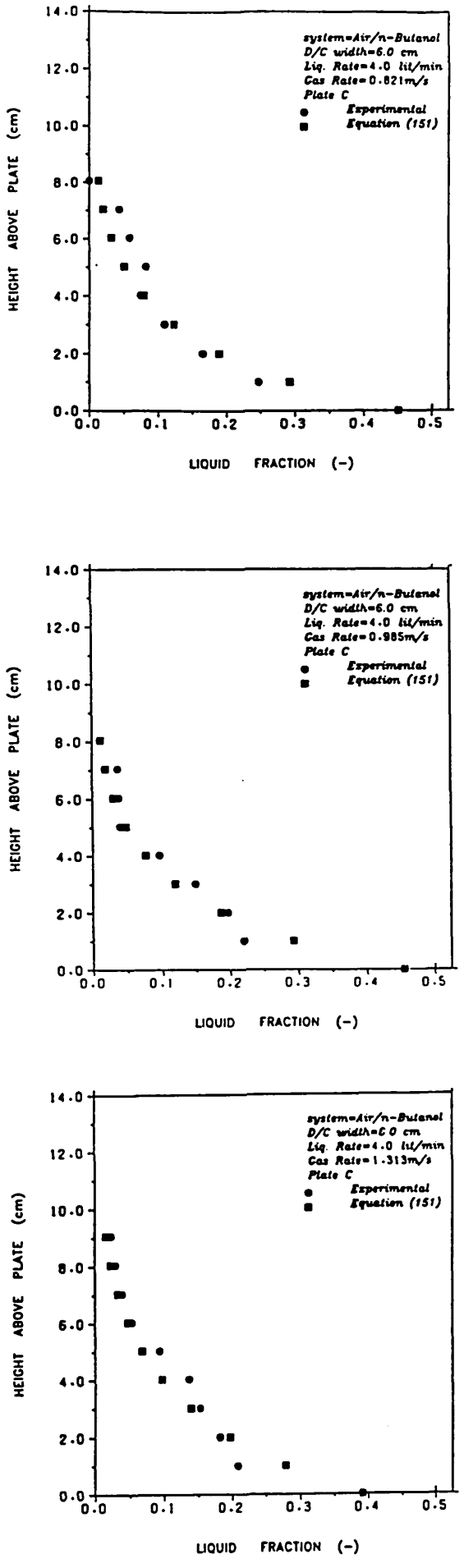

Figure 5.91 :- Experimental and Simulated Froth Profiles on the plate using equation (151) for Plate C (n-Butanol, Liquid Rate = 4.0 lit/min, Gas Rates = 0.821, 0.985, 1.313 m/s)

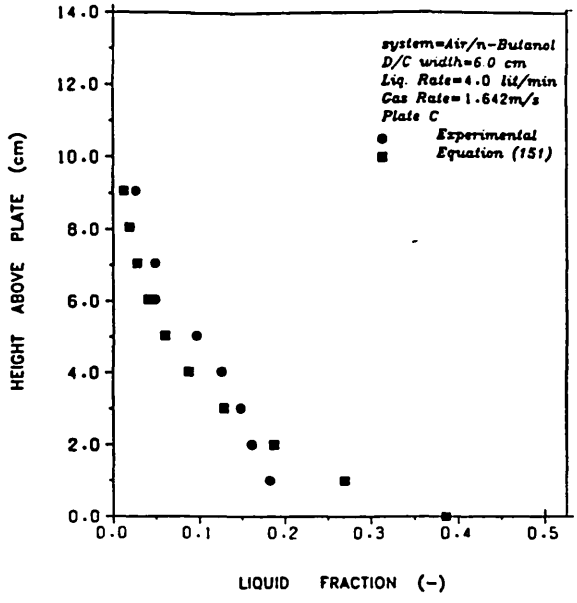

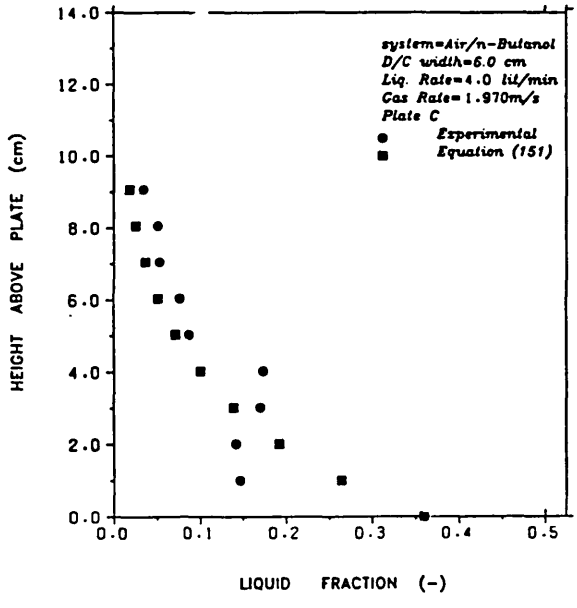

Figure 5.92 :- Experimental and Simulated Froth Profiles on the plate using equation (151) for Plate C (n-Butanol, Liquid Rate = 4.0 lit/min, Gas Rates = 1.642, 1.970 m/s)

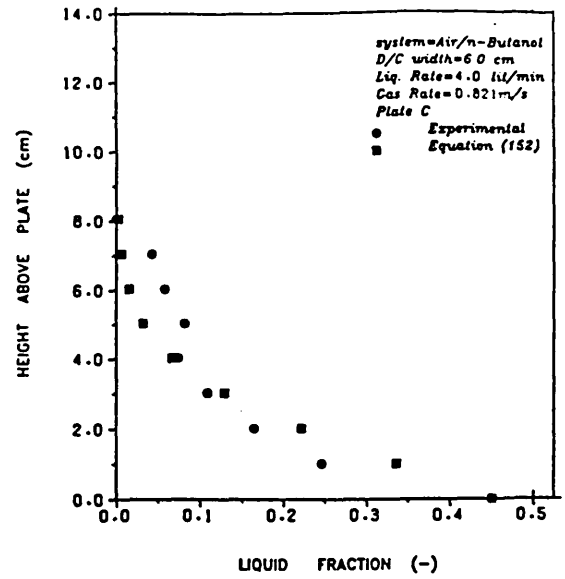

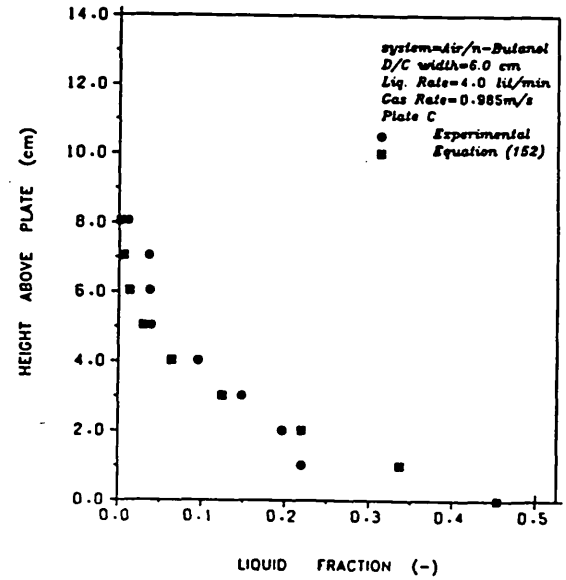

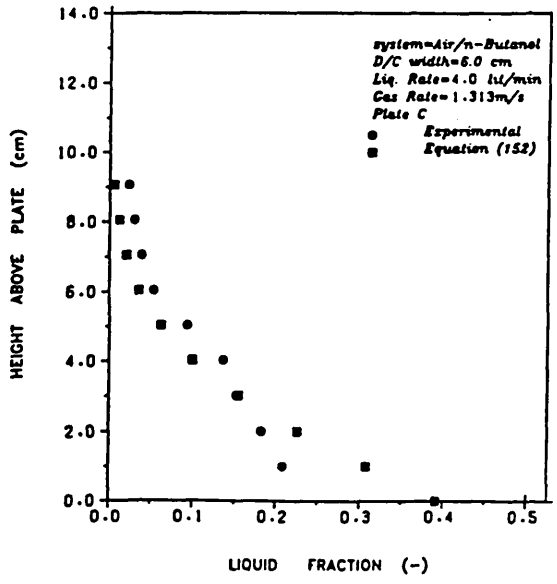

Figure 5.93 :- Experimental and Simulated Froth Profiles on the plate using equation (152) for Plate C (n-Butanol, Liquid Rate = 4.0 lit/min, Gas Rates = 0.821, 0.985, 1.313 m/s)

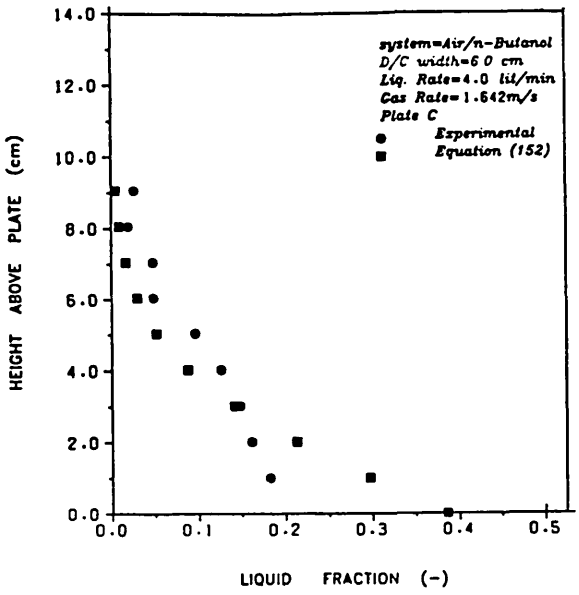

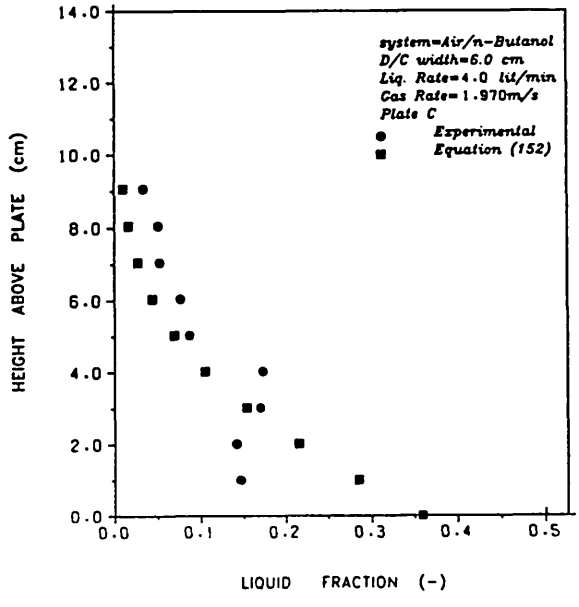

Figure 5.94 :- Experimental and Simulated Froth Profiles on the plate using equation (152) for Plate C (n-Butanol, Liquid Rate = 4.0 lit/min, Gas Rates = 1.642, 1.970 m/s)

5.7.2 Simulation Results of Macmillans[127] Data

It was necessary to apply the theory and therefore equation (151) to the data of Macmillan[127] obtained for pure distillation of n-Pentane/iso-Pentane solutions. The general applicability of the theory depends on the extent of fit of data of other workers with other systems.

Nomenclature for Macmillans[127] Results

Plate	Hole Diameter	Hole Pitch	% Free Area
Mac A	1.6mm	4.8mm	10
Mac B	1.6mm	3.2mm	23
Mac C	3.2mm	6.4mm	23

The results of the simulation based on the data of Macmillan[127] are shown in figures 5.95 - 5.99. It can be seen from these figures that the simulated results fits experimental data very well for all gas and liquid loadings and plate type considered. From this, it is evident that generally, the behaviour of froth on the plate in the frothing regime of plate operation can be adequately described in terms of the minimum energy concept and generalised in the form of equation (151).

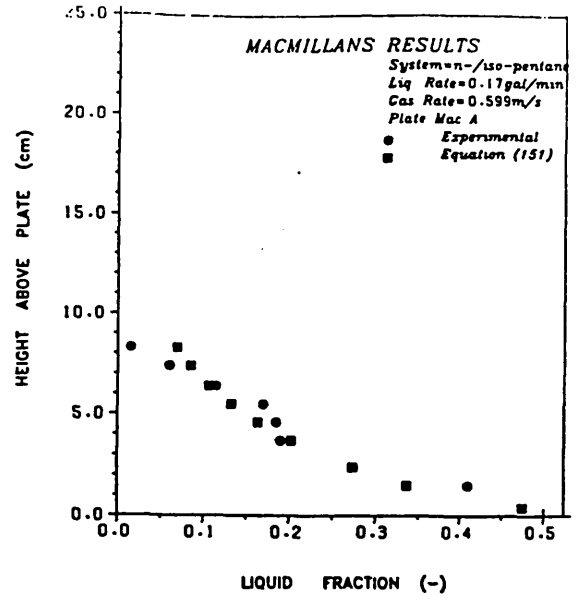

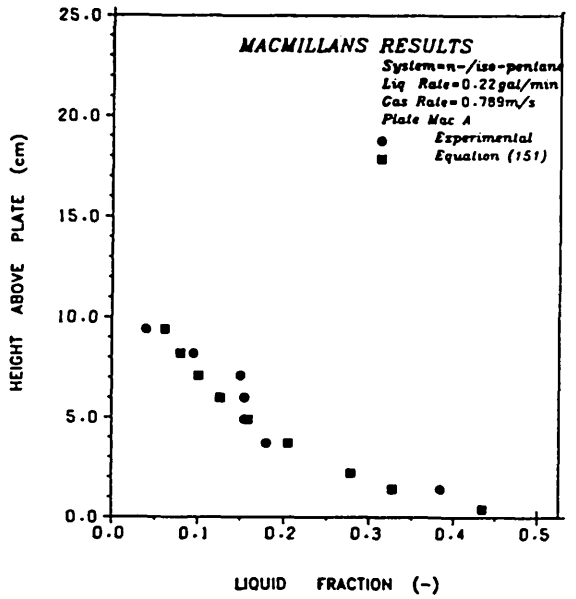

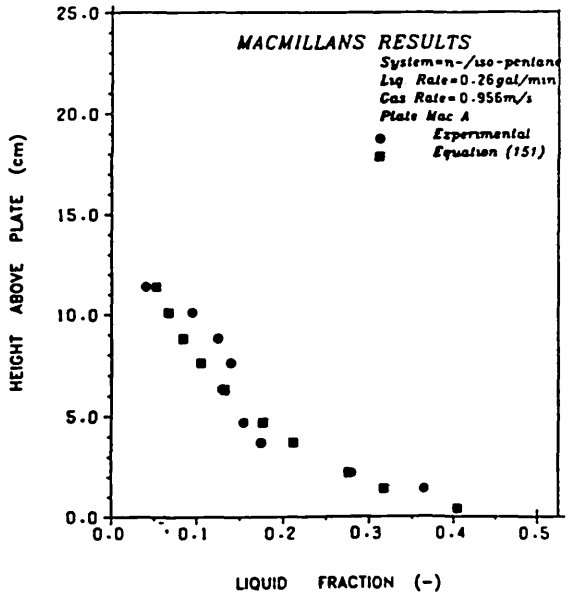

Figure 5.95 :- Experimental and Simulated Froth Profiles on the plate using Macmillans[127] Results, Plate A (L = 0.17, 0.22, 0.26 gal/min, Gas Rates = 0.599, 0.789, 0.956 m/s respectively)

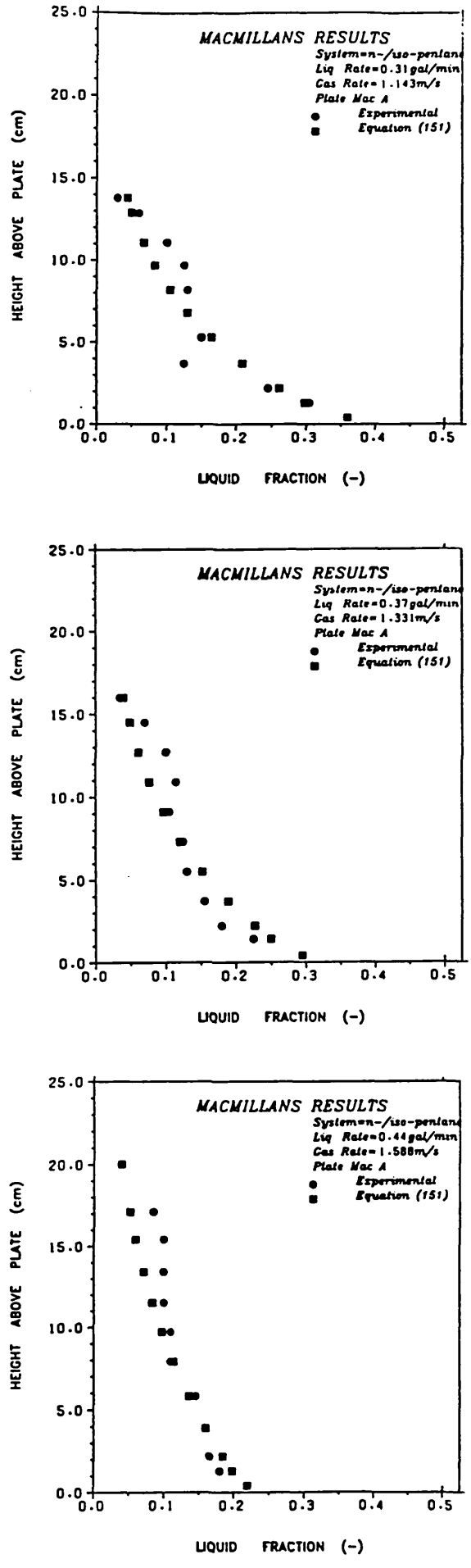

Figure 5.96 :- Experimental and Simulated Froth Profiles on the plate using Macmillans[127] Results, Plate A (L = 0.31, 0.37, 0.44 gal/min, Gas Rates = 1.143, 1.331, 1.588 m/s respectively)

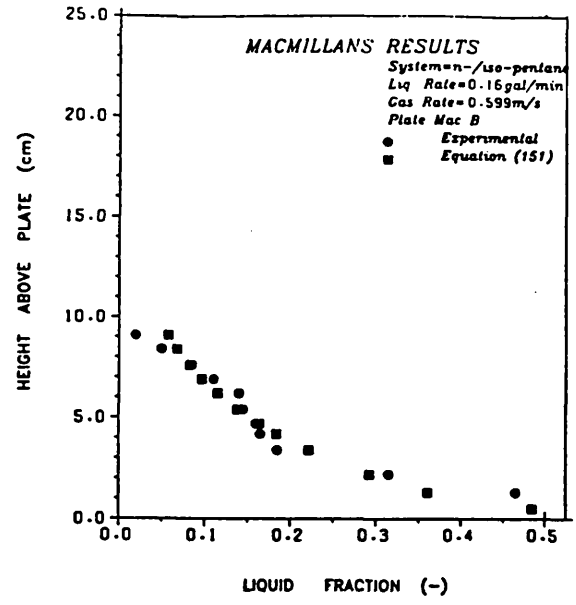

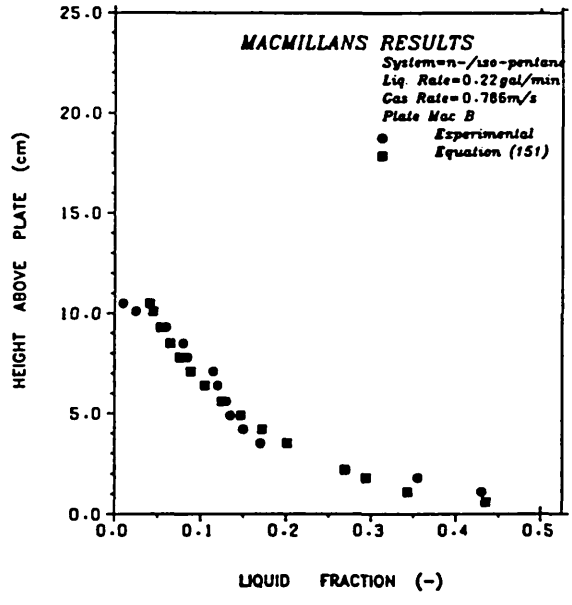

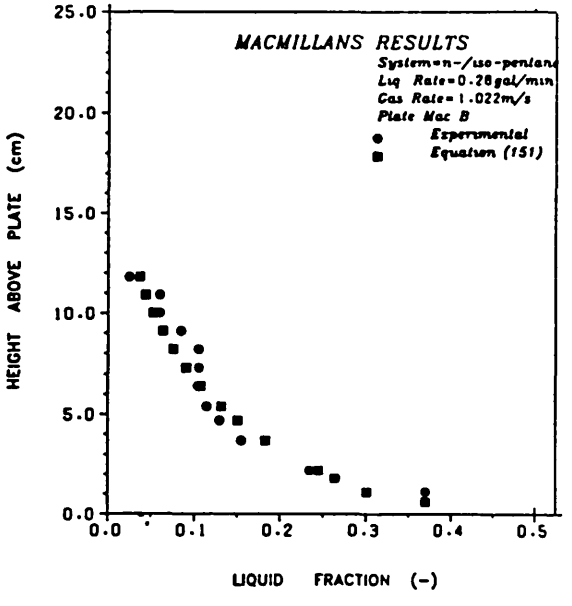

Figure 5.97 :- Experimental and Simulated Froth Profiles on the plate using Macmillans[127] Results, Plate B (L = 0.16, 0.22, 0.28 gal/min, Gas Rates = 0.599, 0.786, 1.022 m/s respectively)

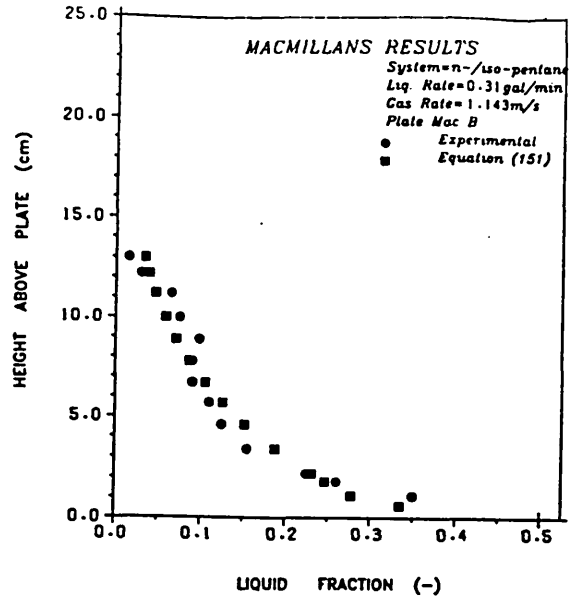

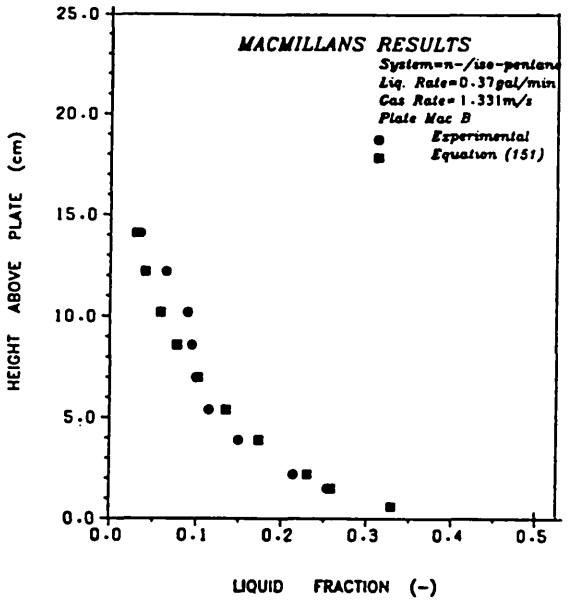

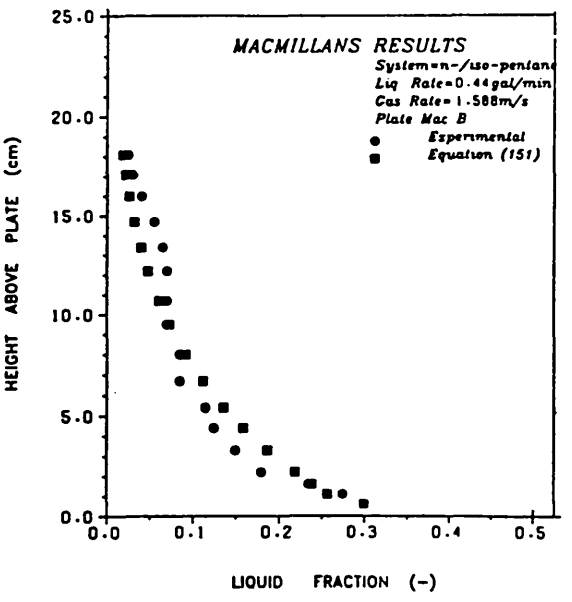

Figure 5.98 :- Experimental and Simulated Froth Profiles on the plate using Macmillans[127] Results, Plate B (L = 0.31, 0.37, 0.44 gal/min, Gas Rates = 1.143, 1.331, 1.588 m/s respectively)

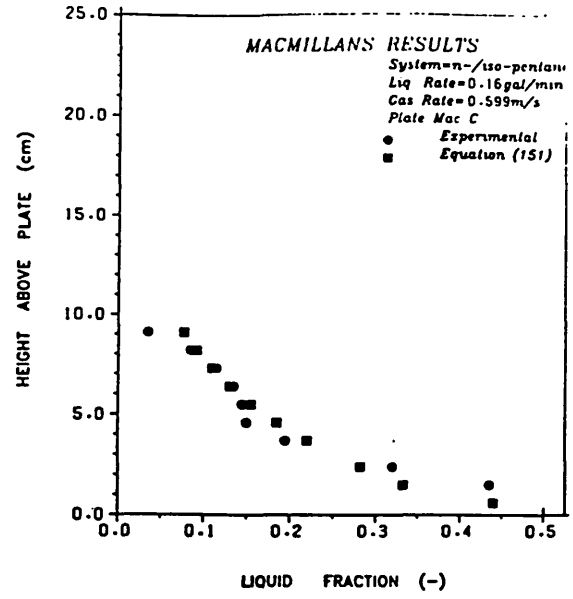

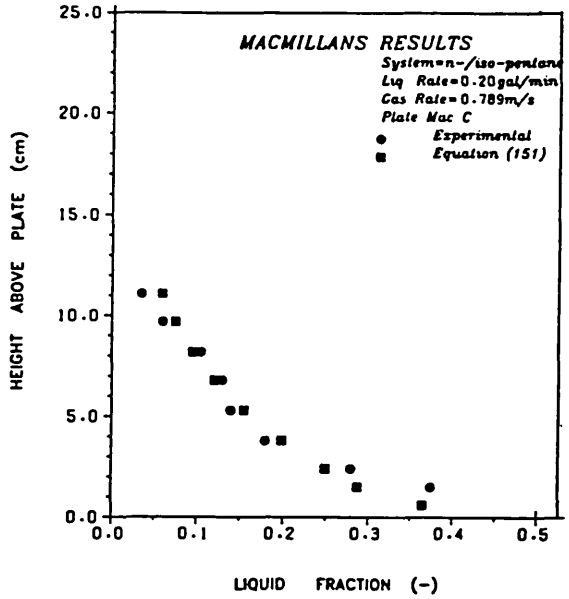

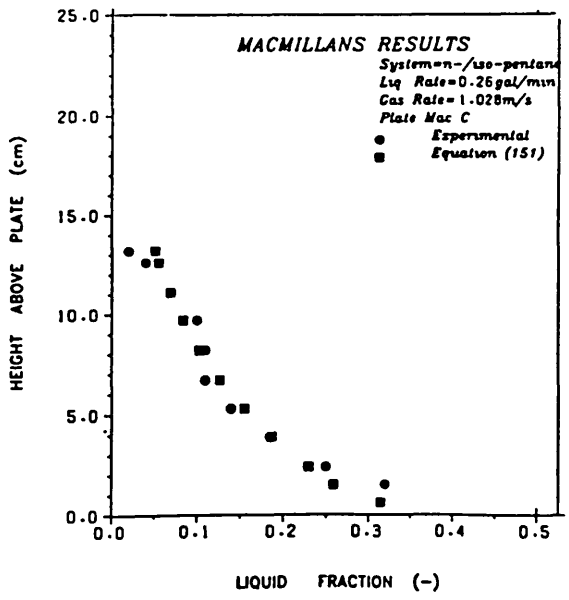

Figure 5.99 :- Experimental and Simulated Froth Profiles on the plate using Macmillans[127] Results, Plate C (L = 0.16, 0.20, 0.26 gal/min, Gas Rates = 0.599, 0.789, 1.028 m/s respectively)

CHAPTER 6

CONCLUSIONS AND RECOMMENDATIONS

6.1 CONCLUSIONS

From the results of this work, the following conclusions can be drawn

Downcomer limitations due to flooding only arise when using systems that tend to foam.

Foaming in downcomers is a function of the regime of plate operation. Downcomer flooding is more likely to occur when operating in the frothing or mixed froth regimes of plate operation.

An average froth density in the downcomer of 0.5, normally recommended for non-foaming systems, is rather conservative. A value of between 0.68 - 0.90 with an average of 0.79 was obtained from this study. An average value of 0.2 - 0.3 normally recommended for foaming systems is in line with results obtained from this study.

For good downcomer design, the downcomer area should be chosen so as to minimize the level of foam/froth in it. A fixed value of 5 - 14% of total column cross-sectional area is grossly inadequate, especially for high liquid loadings and for foaming systems.

From the results of this work, it is believed that a good criterion for downcomer design should be based on the interstitial liquid velocity as against the superficial liquid velocity in the downcomer.

For non-foaming systems, a minimum liquid residence time of 3 seconds usually recommended for design purposes is in line with what was obtained in this study. However, for systems that foam, this time is clearly inadequate for complete vapour/gas disengagement. A minimum liquid residence time of 6 seconds is found to be required for the foaming systems studied in this work.

Pressure drops on the plate and in the downcomer were found to follow the traditional equations used for design purposes for both the foaming and non-foaming systems.

Based on the results of this work, it is now possible to trace the characteristics of the froth on the plate, prior to column operation by means of equation (151). This equation is expected to strictly apply to the frothing or mixed froth regime of plate operation.

A predictive equation has also been proposed for the calculation of froth heights in the downcomer. This equation provides a rational design basis for the choice of downcomer area and characteristics.

6.2 RECOMMENDATIONS

The equation proposed for the calculation of froth/foam height in downcomers should be rigourously tested using foaming systems other than those studied in this work.

Systems with varying viscosities and densities should also be studied to allow complete characterisation of the mechanisms of foaming in downcomers.

The effect of varying plate free area and weir height on the behaviour of froth on the plate and in the downcomer should be fully investigated.

Bigger capacity columns should be used in futher studies so as to give a complete picture of the effect of foams in downcomers over a wide range of liquid velocities.

NOMENCLATURE

A = Interfacial area per unit volume (m^2/m^3)

AL = A× L (-)

A^* = Mass of tracer injected (Kg)

A^{**} = Initial concentration of tracer (Kg/m^3)

A_a = Active area of plate (m^2)

A_d = Downcomer area (m^2)

A_n = Net area of plate (m^2)

A_o = Hole area of plate (m^2)

B = Constant derived from Szyskowski's equation

B^* = Constant defined by equation (113)

c = concentration ($Kmol/m^3$)

$\overline{c}$ = Laplace transform of c(x,t)

c_1 = Constant

c(x,t) = Tracer concentration at any point and time (Kg/m^3)

C_D, C_W = Drag coefficient (-)

C_F = Capacity factor (m/s)

$C'_F = F_{ST}F_{HA}F_FC_F$ (m/s)

C_{Fc} = Critical capacity factor (m/s)

D = Bubble diameter (m)

D_E, D_S = Effective diffusion coefficient (m^2/s)

d_B = Bubble diameter (m)

d_{32} = Sauter mean diameter (m)

d_h = Hole or Orifice diameter (m)

E, e_d = Rate of energy dissipation per unit mass (J/Kgs)

E(t) = Exit density function

E_k = Rate of energy generation to phase, k, at the interphase

E_m = Surface energy source due to surface tension

F = Force pressing two bubbles together (N)

FP = Flow parameter = $u_L/u_g \sqrt{\rho_L/\rho_g}$ (-)

F_F = Foaming correction factor (-)

F_G = F-factor for gas = $u_g \sqrt{\rho_g}$ $(Kg^{\frac{1}{2}} m^{-\frac{1}{2}} s^{-1})$

F_{Gc}, F_{Gmax} = Critical F-factor

F_{Gd} = Design f-factor

F_{HA} = Hole area correction factor (-)

F_{ST} = Surface tension correction factor (-)

g = Acceleration due to gravity (m/s^2)

G' = Mass flowrate of gas (Kg/s)

h_B = Downcomer backup (mm)

$h'_B = h_B/\phi(dc)$ (mm)

h_d = Dry plate pressure drop (mm)

h_{dc} = Head loss under downcomer apron (mm)

H_f, h_f, H_F = Foam/Froth height (m)

h_{fd} = Froth height in downcomer (m)

H_{Fo} = Initial foam height (m)

H_{12} = Average curvature of the interface

h_L = Liquid holdup on the plate (m)

h_{Ld} = Clear liquid height in the downcomer (m)

h_{ow} = Height of clear liquid over the weir (mm)

h_r = Residual pressure drop (mm)

h_t = Total plate pressure drop (mm)

h_w, H_w, H_W = Weir height in (m),(m) and (ft)

h_Δ = Liquid gradient on the plate (mm)

k, K_1, K_2, K_3 = Constants (-)

L = Path length or thickness of medium (m)

L_A = Liquid flowrate (gal/min-ft)

L' = Mass flowrate of liquid (Kg/s)

L'_d = Liquid mass flowrate in downcomer (Kg/s)

l_w = Length of overflow weir (m)

M_k = Momentum generation rate of phase, k, at the interphase

M_m = Mixture volumtric mommentum source

M_m^H = Forces arising due to changes in curvature of interphase

n = constant

N = Pe/4 equation 98 (-)

N = Number of coalescence (eqn. 107)

N_A = Mass Flux = $-D\delta c/\delta x \quad (Kg/m^2 s)$

p = Hole pitch (m)

P = Pressure (N/m^2)

P_k = Pressure due to phase, k

Pe = Peclet number (-)

Q, Q_L = Volumetric flowrate of liquid (m^3/s)

q_k = Conductive heat flux in phase, k

q_k^T = Turbulent heat flux in phase, k

R = Gas constant $(J/Kmol\,K)$

r = Film radius (m)

S = Liquid seal on plate (mm)

S_F = System derating factor (-)

t = Time (secs)

T = Total coalescence time defined by eqn. (118) (secs)

T = Temperature (K)

T_P = Tray/Plate spacing (m)

t_p = Characteristic time (secs)

t_R = Liquid residence time (secs)

t^* = Characteristic time defined by eqn.(122)

u_g = Gas superficial velocity (m/s)

u_H = Hole gas velocity (m/s)

u_L = Liquid superficial velocity (m/s)

u_{Ld} = Superficial liquid velocity in downcomer (m/s)

u_o = Bubble free rise velocity (m/s)

u_s = Relative rise velocity of a bubble (m/s)

$\dot{V}_B$ = Bubble volume (m^3)

V_B = Velocity of bubble base (m/s)

V_{Bo} = Velocity of bubble base in stagnant fluid (m/s)

V_E = Expansion velocity of bubble (m/s)

V_d = Design flooding velocity (m/s)

V_F = Flooding velocity (m/s)

$\dot{V}_g$ = Volumetric flowrate of gas (m^3/s)

V_R = Relative velocity of bubble (m/s)

v_i = Inlet velocity (m/s)

v_k = Average velocity of phase, k (m/s)

x = distance (m)

W = Width of downcomer (m)

We = Weber number (-)

We_c = Critical Weber number (-)

Greek Characters

α = Void fraction

α_k = Volume fraction of phase, k

α_1 = Constnat defined by equation (12)

$\alpha' = d\alpha/dx$

α_h = Gas fraction at $x = H_f$

α_o = Fraction of gas at x= 0

β = Aeration factor (-)

β_1 = Constant defined by equation (13)

δ = Film thicness (m)

ϵ = Gas fraction (-)

ϵ_L = Liquid fraction (-)

ϕ_{dc} = Downcomer froth density (-)

ϕ_f = Froth density (-)

ϕ_1 = Fractional free area of plate (-)

ρ_g = Gas density (Kg/m^3)

ρ_L = Liquid density (Kg/m^3)

ρ_k = Density of phase, k (Kg/m^3)

$\Delta\rho = \rho_L - \rho_g$ (Kg/m^3)

σ = Surface tension (N/m)

σ_o = Surface tension at zero surfactant concentration (N/m)

η = Viscosity (Ns/m^2)

ψ = Percentage approach to flooding

$\Psi = (Q/u_g l_w)\sqrt{\rho_L/\rho_g}$ (-)

τ = Dimensionless time (-)

τ_k = Viscous stress tensor

τ_k^T = Turbulent stree tensor

ξ = Resistance coefficient (-)

λ = Lagrange multiplier

Γ = Surface concentration of surfactant ($Kmol/m^2$)

Γ_k = Rate of mass generation at interphase (eqn. 129a)

Γ_∞ = Equilibruim surface concentration of surfactant ($Kmol/m^2$)

REFERENCES

1 Davy, C. A. and G. G. Haselden :- 'Prediction of the Pressure Drop Across Sieve Trays', A. I. Che J., 21, 1218 (1975)

2 Rietema, K. :- 'Science and Technology of Dispersed Two Phase Systems 1 and 2' Chem. Eng. Sci., 37, 1125 (1982)

3 Bikerman, J. J :- 'Foams', (Springer - Verlag, New York, (1973)

4 Valentin, F. H. H :- 'Absorption in Gas - Liquid Dispersions (E. and F. N. Spon. Ltd., London, 1967)

5 Schoen, H. M. :- 'New Chem. Eng. Separation Techniques', (Interscience Publishers, John Wiley, New York, (1974)

6 Bile, K; O. Chekhoz and N. Kochergin :- 'The Hydrodynamics of a Bubbling Layer on a Tray with Two-Phase Contact Zones' Theo. Found. Chem. Eng., 9, 432 (1976)

7 Hartland, S and A. Barber :- 'A Model of Cellular Foams' Trans. Inst. Chem. Engrs., 52, 43 (1974)

8 Hartland, S and A. Barber :- 'The Collapse of Cellular Foams' Trans. Inst. Chem. Engrs., 53, 106 (1975)

9 Baber, A. and E. Wijn :- 'Foaming in Crude Distillation Units', (3rd Int. Symp. on Distillation, London, 1979, pg 3.1/15)

10 Barber, A. D :- 'Effects of Surface Properties on the prediction of Hydrocarbon Foam Heights in Industrial Equipment' (Sym. on Non-Aqueous Foams, Glasgow, 1974)

11 Sawistowski, H and G. Bainbridge :- Chem. Eng. Sci., 19, 992 (1964)

12 Zuiderweg, F. J. and A. Harmens :- Chem. Eng. Sci., 9, 89 (1958)

13 Kitchener, J. A and C. F. Cooper :- Quarterly Reviews, 13, 71 (1959)

14 Prince, R. G; A. P. Jones; R. J. Panic :- 'The Froth Spray Transition': (3rd Int. Symp. on Distillation London, 1979, pp 2.2/27)

15 Jeronimo, M and H. Sawistowski :- Characterisation of Dispersion in the Spray Regime of a Sieve Plate Operation', (3rd Int. Symp. on Distillation, London, 1979, pp 2.2/41)

16 Hofhuis, P. A. M and F. J. Zuiderweg :- 'Sieve Plates - Dispersion Density and Flow Regimes', (I. Chem. E., 3rd Int. Symp. on Distillation, London, 1979, pp 2.2/1)

17 Lockett, M. J and A. A. W. Gharani :- 'Downcomer Hydraulics at High Liquid Rates', (I. Chem. E., 3rd Int. Symp. on Distillation, London, 1979, pp 2.3/43)

18 Jeronimo, M. A and H. Sawistowski :- Trans. Inst. Chem. Engrs., 51, 265 (1973)

19 Steiner, L; R. Hunkeller and S. Hartland :- Trans. Inst. Chem. Engrs., 55, 153 (1977)

20 Rennie, J. and F. Evans :- B. Chem. Eng., 7, 498 (1962)

21 Thomas, W. J. and M. Campbell :- Trans. Inst. Chem. Engrs., 45, T53 (1967)

22 Calderbank, P. H. and J. Rennie :- Trans. Inst. Chem. Engrs., 40, 3 (1962)

23 Thomas, W. J and A. N. Shah :- Trans. Inst. Chem. Engrs., 42, T71 (1964)

24 Berkman and Egloff :- 'Emulsion and Foams' , (Reinhold Publishing Company, New York, 1941)

25 Adamson, A. W. :- 'Physical Chemistry of Surfaces, (John Wiley, New York, 1982)

26 Danielli, Pankhurst and Riddiford :- ' Recent Progress in Surface Science':- (Academic Press, New York, 1964)

27 Huang, C. J. and J. R. Hodson :- Pet. Ref., 37, 104 (1958)

28 Bolles, W. L :- Pet. Ref., 11, 64 (1956)

29 Kirkbridge, C. G. :- Pet. Ref., 23, 321 (1944)

30 Davis, J. A. :- Pet. Ref., 29, 93 (1950)

31 Leibsum, I; R. E. Kelly and L. A. Bullington :- Pet. Ref., 36, 127 (1957)

32 Hughmark, G. A and H. E. O'Connell :- Chem. Eng. Prog., 53, 127 (1957)

33 Ross, S. :- Ind. Eng. Chem., 61, N° 10, 48 (1969)

34 Ross, S. and G. Nishioka :- J. Phys. Chem., 79, 1561 (1975)

35 Ross, S. and G. Nishioka :- Chemistry and Industry, Jan. 1987, pp 47

36 Ross, S. :- J. Phys. Chem., 17, 266 (1943)

37 Ross, S. :- Ind. Eng. Chem., (Annal Ed.) 15, 329 (1943)

38 Ross, S. and M. J. Cutillas :- J. Phys. Chem., 59, 863 (1955)

39 Danckwerts, P. V., W. Smith and H. Sawistowski :- Int. Symp. on Distillation, Rottenburg, 1960

40 Manickampillai :- Ph.D Thesis, Imperial College, London, 1980

41 Ho, G. E; R. L. Muller and R. G. H. Prince :- 'Characterisation of Two - Phase Flow Patterns in Plate Columns', (Distillation, 1969, Inst. of Chemical Engrs., London)

42 Rennie, J. and W. Smith :- 'A Photographic Study of the Formation and Properties of Large Bubbles and Their Breakdown into Froth' (Proc. Symp. on Transport Phenomena, 1965 ; Inst. Chem. Engrs., London)

43 Gardner, R. G. and A. Y. Maclean :- 'Effect of System Properties on Sieve Plate Froths', in Pirie, J. M. (Ed.) Distillation, 1969 (Inst. of Chemical Engrs., London)

44 Economopolous, A. P. :- 'Computer Design of Sieve Trays and Tray Columns':- Chem. Engng., 85, 4 (1978)

45 De Goederen, C. W. J. :- Chem. Eng. Sci., 20, 1115 (1965)

46 Andrew, S. P. S. in Pirie, J. M. (Ed.), Distillation, 1969 (Institution of Chemical Engrs., London)

47 Foss, A. S. and J. A. Gerstner :- Chem. Eng. Prog., 52, 28 (1956)

48 Porter, K. E. and P. F. Y. Wong :- 'Transition from Spray to Bubbling on Sieve Plates':- Distillation, 1969, London

49 Brambilla, A., G. Nardini; G. F. Necentti and S. Zanelli :- 'Hydrodynamic Behaviour of Distillation Columns' (Proc. Int. Symp. on Distillation, London, 1969)

50 Yoshida, F; T. Nishibe and S. Nagai :- 'Performance of high Capacity Perforated Plate Columns' (ABCM/BCPMA Final Report of Distillation Panel, 1964)

51 Prince, R. G. H. :- 'Characteristics and Design of Perforated plate Columns':- (Int. Symp. on Distillation, Brighton, 1960)

52 Thomas, W. J. :- 'Sieve Plate and Downcomer Studies in a frothing System':- (ABCM/BCPMA Final Report of Dist. Panel, 1964)

53 Backhurst, J. R. and J. H. Harker :- 'Process Plant Design' (Heinemann Educational Books, London, 1979)

54 Sargent, R. W. H, J. D. T. Bernard., W. P. Macmillan and R. Schroter :- 'The Performance of Sieve Plates in Distillation' (ABCM/BCPMA Final Report of Dist. Panel, 1964)

55 Thomas, W. J and M. Campbell :- 'Mixing Efficiency and Mass Transfer Studies in a Sieve Plate Downcomer System' Trans. Inst. Chem. Engrs., 45, T64 (1967)

56 Proter, K. E. and J. D. Jenkins :- ' The Interrelationship between Industrial Practice and Academic Research in Distillation and Absorption' (Int. Symp. on Distillation, London, April 1979)

57 Rao, A. A., D. T. Wasan and E. D. Manev :- 'Foam Stability - Effect of Surfactant Composition on Drainage of Microscopic Aqueous Films': Chem. Eng. Communications, 15, 63 (1982)

58 Jones, A. R. :- 'Scattering of Electromagnetic Radiation in Particulate Laden Fluids': Prog. Energy Combustion Sci., 5, 73 (1979)

59 Calderbank, P. H. :- Physical Rate Processes in Industrial Fermentation Part 1': Trans. Inst. Chem. Engrs., 36, 443 (1958)

60 McLaughlin, C. M. and J. H. Rushton :- 'Interfacial Areas of Liquid - Liquid Dispersion from Liqht Transmission Measurements A. I. ChE J., 19, 817 (1977)

61 Landau, J., J. Boyle ; H. G. Gomma and A. M. Al Taweel :- Can. J. Chem. Eng., 55, 13 (1977)

62 Lockett, M. J. and A. A. Safekourdi :- 'Light Transmission Through Bubble Swarms' : A. I. ChE. J., 23, 395 (1977)

63 Landau, J., H. G. Gomma and A. M. Al Taweel :- 'Measurement of Large Interfacial Areas by Light Attenuation' Trans. Inst. Chem. Engrs., 55, 212 (1977)

64 Al Taweel, A. M., R. Divakarla and H. G. Gomma :- 'Measurement of Large Gas - Liquid Interfacial Areas' Can. J. Chem. Eng., 62, 73 (1984)

65 Perry, R. and Chilton :- 'Chemical Engineers Handbook' (McGraw Hill Book Company, New York, 1973)

66 Treybal, R. E. :- 'Mass Transfer Operations' (McGraw Hill Book Company, New York, 1980)

67 Henley, E. J. and J. D. Seader :- 'Equilibrium Stage Separation Operations in Chem. Eng.' (John Wiley, New York, 1981)

68 Coulson, J. M. and J. F. Richardson :- 'Chemical Engineering Vol.6' (Pergamon Press, Oxford, 1983)

69 Kler, S. C. :- Ph.D Thesis, Imperial College, London, 1986

70 Van Vinkle, M :- 'Distillation': (McGraw Hill, New York, 1967)

71 Smith, B. D. :- 'Design of Equilibrium Stage Processes' (McGraw Hill Book Co., New York, 1963)

72 Ludwig, E :- Applied Process Design for Chem. and Petrochemical Plants, Vol.2' (Gulf Publishing Company, Houston, Texas, 1979)

73 King, C. J. :- 'Separation Processes' (McGraw Hill Book Company, New York, 1980)

74 Sawistowski, H. and W. Smith :- 'Mass Transfer Process Calculations': Interscience Publishers, New York, 1963

76 Azbel, D. S :- 'The Hydrodynamics of Bubbler Processes', Int. Chem. Eng., 3, Number 3, 319 (1963)

77 Klug, P and A. Vogelpohl :- 'Bubble Formation at Sieve Plates - Effects of Gas Holdup in Bubble Columns': Ger. Chem. Eng., 9, 93 (1986)

78 Räbiger, N and A. Vogelpohl :- 'Calculation of Bubble Size in the Bubble and Jet Regimes for Stagnant and Flowing Newtonian Liquids': Ger. Chem. Eng., 6, 173 (1983)

79 Räbiger, N and A. Vogelpohl :- 'Bubble Formation in Stagnant and Flowing Liquids': Ger. Chem. Eng. 5, 314 (1982)

80 Klug, P and A. Vogelpohl :- 'Bubble Formation with Super-imposed Liquid motion at Single - holed and Sieve Plates' Ger. Chem. Eng., 6, 311 (1983)

81 Miyahara, T; Y. Matsuba and T. Takahashi :- 'The Size of Bubbles Generated from Perforated Plates': Int. Chem. Eng., 23, 517 (1983)

82 Davidson, J. F. and B. O. G. Schüler :- 'Bubble Formation at an Orifice in a Vicous Fluid': Trans. Inst. Chem. Engrs., 38, 144 (1960)

83 Mahiout, S and A. Vogelpohl :- 'Fluid Dynamics and Mass Transfer of Highly Viscous Media on a Sieve Tray', Ger. Chem. Eng., 8, 152 (1985)

84 Zuiderweg, F. G; P. A. M. Hofhuis and J. Kuzniar :- 'Flow Regimes on Sieve Trays; The Significance of the Emulsion Flow Regime': Chem. Eng. Res. Des., 62, 39 (1984)

85 Dhulesia, H :- 'Clear Liquid Heights on Sieve and Valve Trays' Chem. Eng. Res. Des., 62, 321 (1984)

86 Zuiderweg, F. J. :- 'Sieve Trays - A View on the State of the Art': Chem. Eng. Sci., 37, 1441 (1982)

87 Azbel, D. S. :- 'Two Phase Flows in Chemical Engineering' Cambridge University Press (1981)

88 Takahashi, T; R. Matsuno and T. Miyahara :- 'Theoretical Consideration of Gas Void Fraction and Froth Height on Perforated Plates': J. Chem. Eng. of Japan, 6, 38 (1973)

89 Clark, N and R. Flemmer :- 'Gas Liquid Contacting in Vertical Two Phase Flow' : Ind. Eng. Chem., 24, 231 (1985)

90 Gaddis, E. S. and A. Vogelpohl :- 'Bubble Formation in Quiescent Liquids under Constant Flow': Chem. Eng. Sci., 41, 97 (1986)

91 Clint, J. H; J. M. Corkhill; J. F. Goodman and J. R. Tate 'Adsroption of n-Alkanols at the Air/Aqueous Solution Interface': J. Colloid and Interface Science, 28, 522 (1968)

92 Posner, A. M; J. R. Anderson and A. E. Alexander :- 'The Surface Tension and Surface Potential of Aqueous Solutions of Aliphatic Alchohols': - J. Colloid Sci., 7, 623 (1952)

93 Solomakha, G. P; G. G. Shaubert and V. I. Vashchuk :- 'Calculattion of Height of a Static Liquid Layer in Plate Devices equipped with Overflow': Theor. Found. of Chem. Eng., 17, 516 (1983)

94 Kim, S. K. :- 'Theoretical Study of Vapour-Liquid Hold-up on a Perforated Plate': Int. Chem. Eng., 6, 634 (1966)

95 Urua, I. J. and M. C. G. del Cerro :- 'Measurment of Large Gas-Liquid Interfacial Areas by the Light Transmission Technique': Can. J. Chem. Eng., 65, 565 (1987)

96 Urua, I. J. :- 'Studies of Downcomer Behaviuor for Foaming and Non -Foaming Systems' ; M.Sc Thesis, Imperial College, London (1984)

97 Kolář, V :- 'The Structure of Gas - Liquid Mixtures on Sieve Plates of Separation Columns': Chem. Eng. Sci., 24, 1285 (1969)

98 Steiner, L and V. Kolář :- Hydrodynamics of Plate Columns 1' Coll. Czech. Chem. Comm., 33, 2207 (1968)

99 Unno, H and I. Inoue :- 'Froth Density Profiles and Froth Height on Perforated Plates': J. Chem. Eng. of Japan, 9, 92 (1976)

100 Danckwerts, P. V :- Chem. Eng. Sci., 2, 1 (1953)

101 Gilbert, T. J :- Chem. Eng. Sci., 10, 243 (1959)

102 Taylor, G. I :- Proc. Roy. Soc., A219, 189 (1953); A225, 473 (1954)

103 Tichacek, L. J :- A. I. Che J., 3, 439 (1957)

104 Johnson, A and J. Marangozis :- Can. J. Chem. Engrs., 36, 161 (1958

105 Welch, N. E; L. D. Durbin and C. D. Holland :- 'Mixing on Valve Trays and in Downcomers of a distillation Column' A. I. Che J., 10, N^o 3, 373 (1964)

106 Lockett, M. J :- Trans. Inst. Chem. Engrs., 59, 26 (1981)

107 Davidson, J. F and B. O. G. Schüler :- Trans. Inst. Chem. Engrs., 38, 335 (1960)

108 Hofhuis, P. A. M :- 'Flow Regimes on Sieve Trays for Gas-Liquid Contacting' :- Thesis, Delft University, Netherlands, (1980)

109 Levenspiel, O :- 'Chemical Reaction Engineering' (John Wiley, New York, 1976)

110 Bell, R. L :- A.I. Che J., 18, N° 3, 491 (1972)

111 Baker, P. E and M. F. Self :- Chem. Eng. Sci., 17, 541 (1962)

112 Oliver, E. D and C. C. Watson :- A. I. Che J., 2, 18 (1956)

113 Nauman, E. B and B. A. Buffam :- 'Mixing in Continuous Flow Systems': (John Wiley, New York, 1983)

114 Luyben, W. L :- 'Process Modelling, Simulation and Control for Chemical Engineers': (McGraw Hill New York, 1974)

115 Levenspiel, O and W. K. Smith :- Chem. Eng. Sci., 6, 227 (1957)

116 Taitel, Y. and D. Barnea :- 'Counter Current Gas - Liquid Vertical Flow Model for Flow Pattern and Pressure Drop' Int. J. Multiphase Flow, 19, 637 (1983)

117 Thomas, R. M :- 'Bubble Coalescence in Turbulent Flows' Int. J. Multiphase Flow, 7, 709 (1981)

118 Marrucci, G :- 'A Theory of Coalescence', Chem. Eng. sci., 24, 975 (1969)

119 Lee, J. C and T. D. Hodgson :- Chem. Eng. Sci., 23, 1375 (1968)

120 Rosen, M. J :- 'Surfactant and Interfacial Phenomena' (John Wiley, New York, 1978)

121 Wallis, G. B :- 'One Dimensional Two Phase Flow' (McGraw Hill Book Company, New York, 1969)

122 Radoëv :- Colloid and Polymer Sci., 252, 50 (1974)

123 Ishii, M :- 'Thermo - Fluid Dynamic Theory of Two Phase Flow' : Eyrolles, France, 1975

124 Drew, D. A. and R. T. Lahey (Jr.) :- J. of Multiphase Flows, 5, 243 (1979)

125 Eversole, W. G; G. H. Wagner and E. Stackhouse Ind. Eng. Chem., 33, 1459 (1941)

126 Utkin, V. A; A. M. Stepanov and O. S. Checkhov :- 'Study of the Gas Content in the Two - Phase Downflow in a Sieve Plate Column': J. Appld. Chem. (USSR), 58, 2205 (1985)

127 Macmillan, W. P :- Ph.D Thesis, University of London, 1962

128 Bernard, J. D. T :- Ph.D Thesis, University of London, 1968

129 Hinze, J. O :- 'Turbulence - An Introduction to its Mechanism and Theory': (McGraw Hill, New York, 1959)

130 Spiegel, M. R :- 'Laplace Transforms', Schaums Outline Series McGraw Hill ,New York, 1965

131 Stephenson, G :- 'Mathematical Methods for Science Students' Longman, London, 1982

132 Gallant, R. W :- 'Physical Properties of Hydrocarbons, Vol. 1' Gulf Publishing Company, Houston, Texas, 1968

133 del Cerro, M. C. G :- Private Communications, 1987

134 Hewitt, G. F :- Private Communications, 1987

135 Sawistowski, H :- Private Communications, 1984

APPENDIX *A*

EXPERIMENTAL DATA

APPENDIX *B*

B* and Film Thickness, δ

B.1 Determination of Value of B*

Recall that the value of B* was defined by equation (113) of Chapter 3, that is

$$B^* = \left[\frac{RT\Gamma_\infty^2 B^2 c}{RT\Gamma_\infty^2 B^2 c + 3D_s\mu(1+Bc)^2}\right] \qquad (B.1)$$

To evaluate B*, for surfactant solutions, the values of Γ_∞, B and D_s must be found first. The following sections show how Γ_∞, B and D_s are determined for the systems n-Pentanol and n-Butanol respectively.

B.1.1 Determination of Γ_∞ and B :-

By definition, surface excess, Γ, denotes the excess surface concentration of surfactant or adsorbed species at the interface. The basic equation relating Surface excess, Γ, to solution concentration is

$$\Gamma = -\frac{1}{RT}\frac{\delta\sigma}{\delta ln a_B} \qquad (b.2)$$

Where

σ = Surface Tension of solution (N/m)

R = Gas constant = 8.314 J/mol K

T = Temperature (K)

a_B = Activity of Surfactant in solution

For dilute solutions, the activity of the surfactant in solution can be approximated by its concentration. Hence, equation (B.2) becomes

$$\Gamma = -\frac{c_B}{RT}\frac{d\sigma}{dc_B} \qquad (B.3)$$

Equation (B.3) shows that the surface excess of the surfactant solution can be found at different solution concentrations. A graphical representation of the dependence of Γ on c_B is as shown in figure B1 for the systems n-Butanol and n-Pentanol respectively.

Since most surfactant adsorption obey the Langmuir isotherm, then

$$\Gamma = \frac{\Gamma_\infty Bc}{1 + Bc} \qquad (B.4)$$

$$\Rightarrow \frac{1}{\Gamma} = \frac{1}{\Gamma_\infty Bc} + \frac{1}{\Gamma_\infty} \qquad (B.5)$$

Equation (B.5) indicates that, if $1/\Gamma$ is plotted against 1/c, a straight line is obtained with slope equal to $1/\Gamma_\infty B$ and intercept $1/\Gamma_\infty$. From the slope and intercept of the graph, the values of Γ_∞ and B can be determined. A graphical representation of equation (B.5) for the systems n-Butanol and n-Pentanol are shown in figure B2. From this figure, the values of Γ_∞ and B for the systems n-Butanol and n-Pentanol are 6.25×10^{-9} $kmols/m^2$, 22.54 and 8.33×10^{-9} $kmols/m^2$, 30.77 respectively.

B.1.2 Determination of Diffusivity, D_s

The diffusivity of a solute (liquid), A, in a slovent (liquid), B, at infinite dilution can be calculated using the relation of Wilke and Chang[66,127].

$$D_{AB} = \frac{(117.3 \times 10^{-8})(\varphi M_B)^{0.5} T}{\eta \nu_A^{0.6}} \qquad (B.6)$$

Where

D_{AB} = Diffusivity of A in Solvent B (m^2/s)

M_B = Molecular weight of solvent, (Kg/kmol)

T = Temperature (^oK)

η = Solvent viscosity (Kg/ms)

ν_A = Solute molal volume at normal boiling point $(m^3/kmol)$

φ = Association factor for solvent

Using equation (B.6) and estimating the related parameters from tables[66], the diffusivities of n-Pentanol and n-Butanol solutions were found to be $7.734 \times 10^{-10} m^2/s$ *and* $8.8694 \times 10^{-10}\ m^2/s$, respectively.

B.2 Determination of Film Thickness, δ

In Chapter 3, Section 3.2.6, the film thickness of the gas liquid dispersion in the downcomer was shown to follow the expression

$$\delta^2 = A\left(\frac{u_L}{\epsilon_L}\right)^{B1} \qquad equation(126)$$

To be able to evaluate the constants A and B1, experimental data were used for one set of experiments. The results for Plate A and downcomer size of 6cm were used to calculate these values. It was found out that the constant, A, followed the relation

$$A = A1\left(\frac{\sigma}{\sigma_w^+}\right)^{A2} \qquad equation127$$

Figures B3 and B4 show how the constants A1, A2, and B1 were determined. These constants were found to be 2.249×10^{-4}, -3.0 *and* 4.0 respectively.

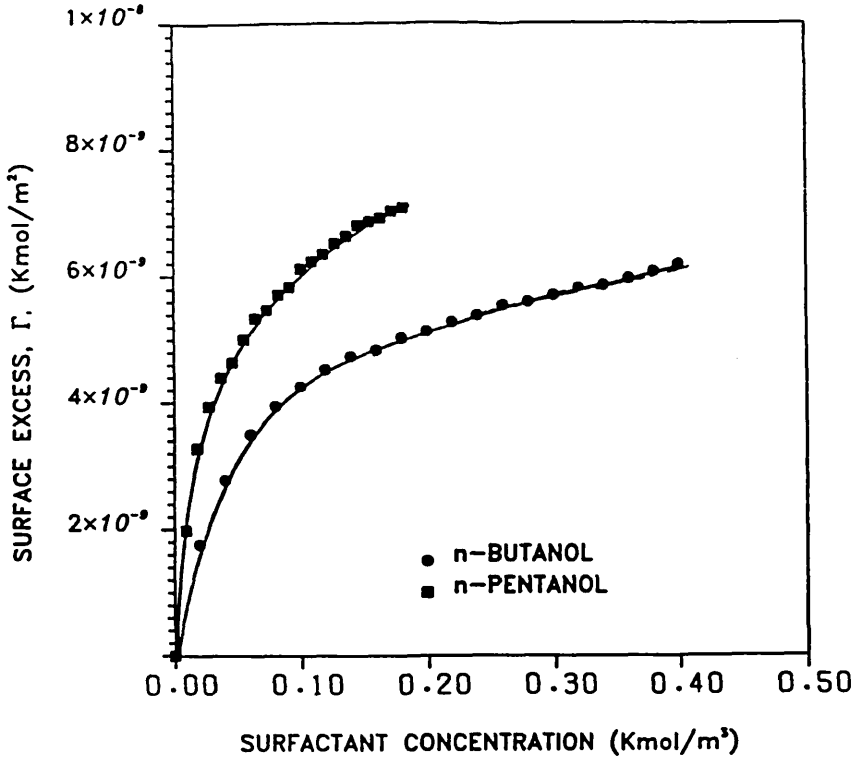

Figure B.1 · Graph of surface excess against solution concentration

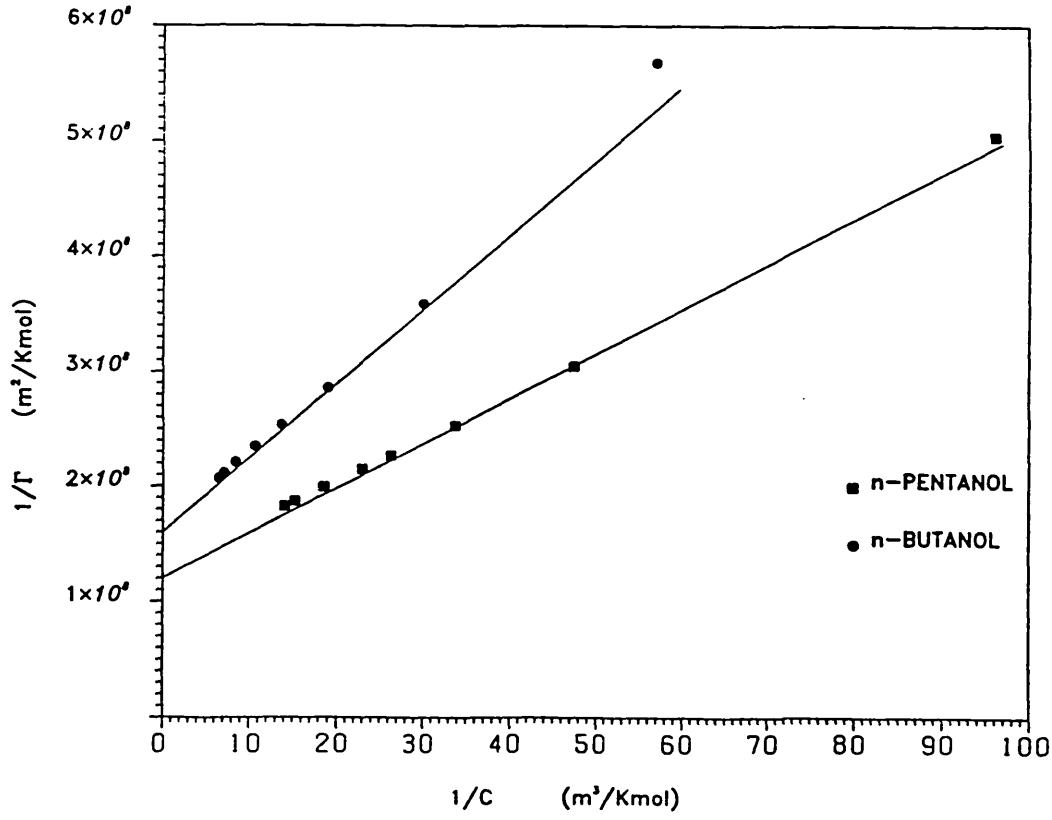

Figure B.2 · Graph of $\frac{1}{\Gamma}$ against $\frac{1}{C}$

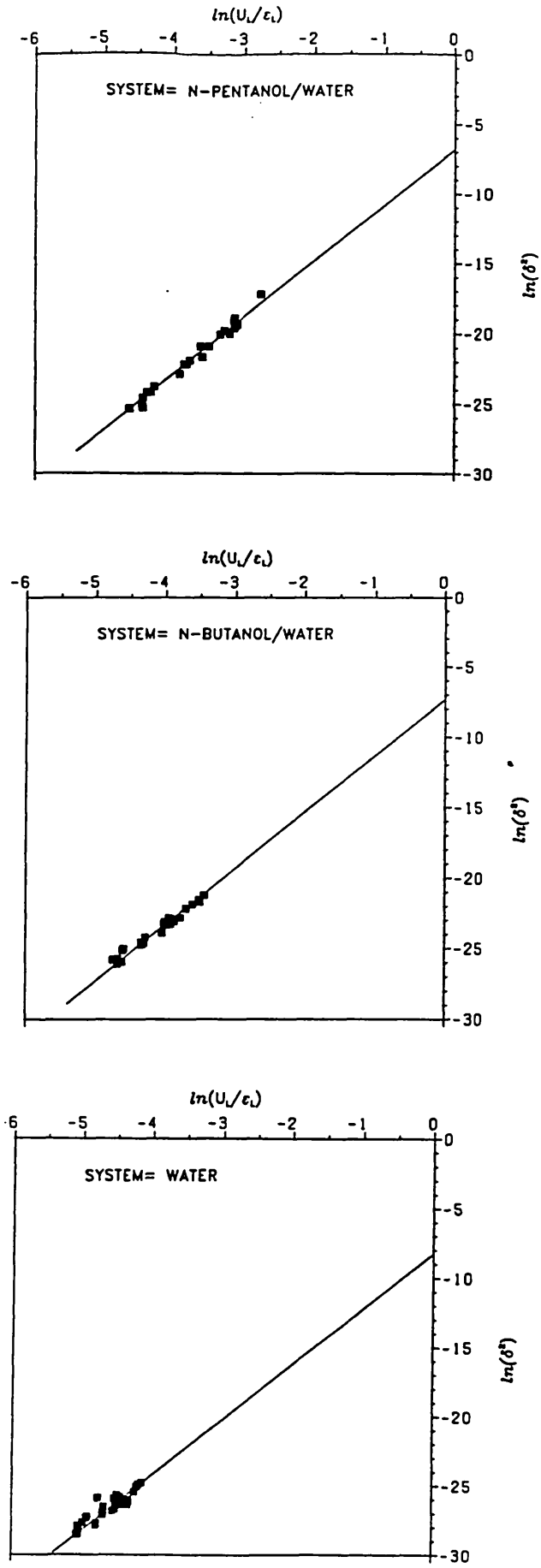

Figure B. 3 :- Graph of film thickness against interstitial liquid velocity

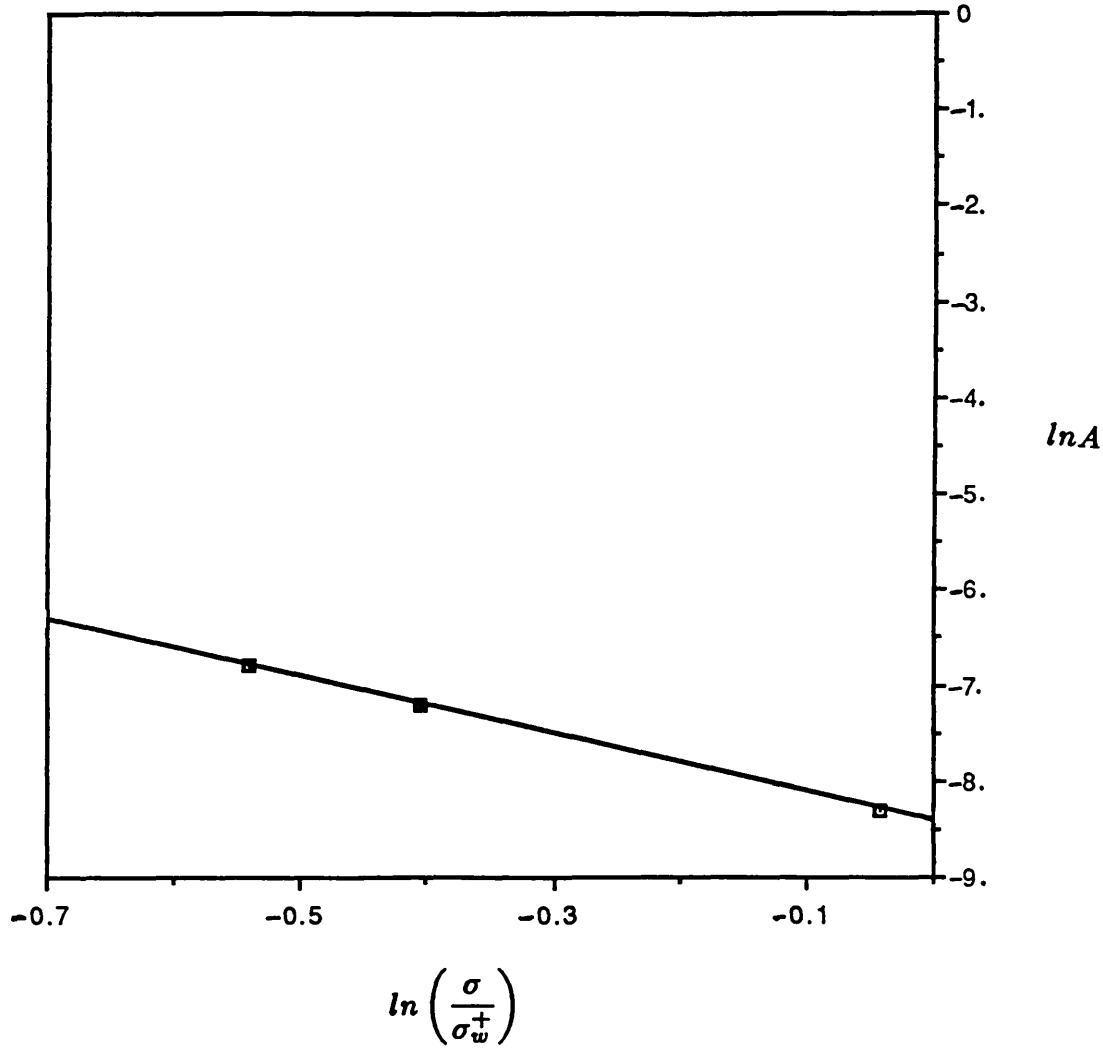

Figure B.4 : Determination of A1 and A2 values

APPENDIX *C*

ERROR IN DISPERSION DENSITY MEASUREMENTS

In chapter 2, it was indicated that the absorption of a parallel monoenergetic beam of gamma radiation by a homogeneous medium of density, ρ, and thickness, x, is governed by the equation

$$I = I_o e^{-\rho\mu x} \qquad (A1)$$

Where

I_o = Intensity of incident radiation

I = Intensity of transmitted radiation

μ = Mass absorption coefficient

x = Thickness of the medium

ρ = Density of the homogeneous medium

In this work, the time, t, taken to record a fixed number of counts, N, was used to interpret the density of the two phase mixture in the downcomer and on the plate. Therefore I, in equation (A1), represents the count rate of the detector output pulses. If these pulses are counted for a time length, t, then the mean number of counts measured in a counting interval will be It, and the root mean square magnitude of the

random variation (standard deviation) in the number of counts measured will be

$$\Delta(It) = \sqrt{It} = \sqrt{N} \tag{A2}$$

This statistical fluctuation arises from the random nature of the radiation and detection processes. This randomness in the count rate will give rise to a random fluctuation in the calculated average density, ρ. the magnitude of this fluctuation is given by

$$| \Delta\rho | = | \frac{\partial \rho}{\partial I} || \Delta I | \tag{A3}$$

From equation (A1),

$$\frac{\partial \rho}{\partial I} = -\frac{1}{\mu x I} \tag{A4}$$

Hence, combining equations (A3) and (A4), the magnitude of the fluctuation in the average density becomes

$$\Delta\rho = \frac{1}{\mu x}\frac{\Delta I}{I} \tag{A5}$$

$$\Rightarrow \Delta\rho = \frac{1}{\mu x}\frac{\Delta(It)}{It}$$

$$= \frac{1}{\mu x}\frac{\sqrt{N}}{N} \tag{A6}$$

$$= \frac{1}{\mu x\sqrt{N}} \tag{A7}$$

The mass absorption coefficient of water is $8.5 \times 10^{-3}\ m^3/Kg$; with density, $\rho = 1000 Kg/m^3$. Normalising this value to the system used in measurements, with the density of water (Clear liquid) equal to unity gives

$$\mu = 8.5$$

Hence for the number of counts fixed at 10000, the error in the liquid fraction measured for a path length, x, equal to 0.15 m is

$$\Delta\rho = \frac{1}{8.5 \times 0.15\sqrt{10000}} = 0.0078$$

Hence the number of counts fixed at 10000 gives a negligible error in the measured value of liquid fraction.